Texas Water Development Board
# Contract Number # 1548301854

Numerical Model Report: Lower Rio Grande Valley Groundwater Transport Model

by:

Sorab Panday, GSI Environmental Inc.
James Rumbaugh, Environmental Simulations, Inc.
William R. Hutchison, Independent Groundwater Consultant
Staffan Schorr, Montgomery & Associates

PROFESSIONAL SEAL
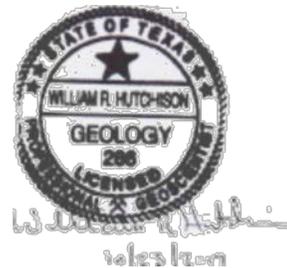
This document is released under the authority of William Hutchison, P.E. 92687, P.G. 286

23 October 2017

This page is intentionally blank.

Table of Contents

List of Figures

List of Tables

Appendices

Executive Summary

Groundwater is a vital resource in the Lower Rio Grande Valley (LRGV). Groundwater pumping in the LRGV is expected to increase in response to increased municipal demands. However, much of the groundwater in the area is brackish with total dissolved solids (TDS) values greater than 1,000 milligrams per liter (mg/L). Brackish groundwater is currently treated at seven desalination plants for municipal use in the LRGV. Additional desalination projects have been recommended in the 2016 Regional Water Plan for Region M.

A numerical groundwater flow and transport model was developed to simulate changes in groundwater levels, TDS concentrations, and surface-water/groundwater interactions within the LRGV due to anticipated increased pumping in the region. The model included density dependent flow considerations to evaluate the impact of salt density on solute migration. Objectives of the model also included evaluating impact of data gaps and faulting within the domain, and estimating the potential for subsidence. Drawdown calculations from the model provide the pore-pressure reductions required to estimate ground subsidence, for known or estimated soil effective stresses.

Challenges to the modeling effort included a large domain (greater than 5,000 square miles); complex geology (deep, multi-layered system with outcrops and pinch-outs); fine resolution to effectively handle groundwater- surface water interaction; accurate depiction of drawdowns in pumping wells; sparse data availability; and a considerable computational effort further burdened by the density coupling of saltwater flow and transport. These challenges were met by selection of a robust and flexible software that can best alleviate the computational burdens and still provide results at the scale of the modeling objectives.

The MODFLOW-USG groundwater flow model (MFUSG) was used for the simulations with the Groundwater Vistas graphic user interface (GUI). The beta version of the code (MFUSG-Beta) includes density dependent flow and transport simulation capabilities. The model consisted of 12 numerical layers to represent the 12 geologic units of interest. A base model grid of 2640 feet on a side was implemented to discretize the domain. Quadpatch refinement was then applied to reduce the cell size to 330 feet around the LRG and irrigation canals for higher resolution of surface-water/groundwater interactions. Wells were represented using vertical conduits that interact with the groundwater using analytical well solutions to provide resolution at the well. Hydraulic conductivity of the geologic units was parameterized using correlations with available sand fraction data. Boundary conditions included inflow to the domain from upland regions and in the LRG from the west, and outflow into the Gulf of Mexico to the east. Simulations were conducted for steady-state 1984 conditions and transient conditions from 1985 through 2013 using annual stress periods for recharge and pumping.

The model was calibrated using all data available. Quantitative and qualitative metrics were implemented in evaluating representativeness of the model. Observed water levels in wells as well as groundwater/surface-water flow estimates were used to constrain the model. The model was well calibrated for the spatial and temporal scales of investigation. Mass balance errors were negligible, and water fluxes at the various boundaries into and out of the domain were reasonable.

Sensitivity analyses were conducted on the calibrated model to evaluate impact of parameter uncertainties and variations in boundary fluxes. Sensitivity to the storage coefficients of the

aquifers indicated similar calibration statistics but smoother water level fluctuations with storage than without. Highest sensitivity to sand conductivity was for model layer 6 (the Upper Lagarto unit) while the highest sensitivity to clay conductivity was for model layer 7 (the Burkeville Confining Unit). The modeled water levels were equally sensitive to the different boundary fluxes that were evaluated.

Correlations between groups of parameters were also evaluated. The largest correlation was between clay hydraulic conductivity (which generally governs the vertical K-values of the layer), and recharge. The maximum ET rate and recharge were inversely correlated with the second highest correlation coefficient.

A sensitivity analysis was also conducted to evaluate the impact of the presence of faults in the domain which may act as barriers to flow. It was noted that barriers that may exist along sections of faults can have a dramatic impact on water levels upstream and downstream of the barrier. These impacts dissipate with distance from the barrier but are also felt across the Burkeville Confining Unit for barriers located below this unit only.

The groundwater flow model was further used to evaluate the movement of Total Dissolved Solids (TDS), representative of salinity within the domain. Density dependent flow and transport simulations were conducted to evaluate the migration of TDS due to historical stresses and pumping conditions from 1984 through 2013. Most of the migration occurred in the geologic units representing the Chicot Aquifer with less migration in the deeper units. Simulations were also conducted to evaluate the impact of pumping versus initial and boundary conditions, and the impact of density on the flow field and resulting concentration changes. Initial and boundary conditions had a significant impact on transport and groundwater chloride levels at current desalination plant locations. Pumping had a lesser impact than initial and boundary conditions, on the redistribution of TDS in the domain. The density effect was significant at some existing desalination plant locations but not at others. Simulations that included density effects of flow were considerably slower than those without density impacts included.

1.0 Introduction and Purpose of the Model

1.1 Introduction

Groundwater use in the Lower Rio Grande Valley (LRGV) is expected to increase in response to increased municipal demands. Much of the groundwater in the area is brackish (total dissolved solids are greater than 1,000 milligrams per liter), and does not meet drinking water quality standards. There are currently seven desalination plants in operation to provide municipal water supply to the valley. The total existing capacity is about 22,300 acre-feet/year (AF/yr) with 14 additional desalination projects being recommended in the 2016 Rio Grande Regional Water Plan (Region M Plan) to meet additional future demands estimated to be about 24,000 AF/yr by the year 2070.

1.2 Purpose of the Model

The Lower Rio Grande Valley groundwater transport model domain is shown in Figure 1.2.1. The model was funded by the Texas Water Development Board (TWDB) for research in support of the Groundwater Availability Modeling Program. The primary objective of the research was to develop a numerical model to simulate the impacts of increased fresh and brackish groundwater pumping in the LRGV as outlined in the 2016 Region M plan. The flow model can be used to evaluate the impact of pumping on groundwater and surface-water flows and levels. The transport model can be used to estimate movement of salinity due to additional desalination plants, and salinity of the extracted water. Drawdown computations from the model for planned future desalination operations further provide estimates of compaction stresses to help evaluate the potential for land subsidence. The model was also applied towards evaluating the impact of data gaps and different conceptualizations (e.g., for faulting) within the basin.

Even though large amounts of data are available over a period of several years, and there is a general conceptual understanding of the hydrogeologic system, large uncertainties still exist including complexities of the faulted aquifer system and associated water level anomalies resulting from localized conditions that can never be fully understood and captured in a regional scale analysis. Therefore, the model should be used to gain understanding of the hydrogeologic behavior, explore alternative model conceptualizations, and evaluate impacts of potential hydrologic changes or resource management options, rather than to make absolute predictions at select points in space and time.

2.0 Numerical Model Development

A conceptual model of the hydrogeologic system of the area of interest in the LRGV was developed by Schorr and others (2017). The conceptual model was the basis of the numerical model described in this report. The groundwater system comprises six eastward-dipping aquifers including (from top to bottom) the Chicot Aquifer, the Evangeline Aquifer, the Burkeville Confining Unit, the Jasper Aquifer, the Catahoula Confining System, and the Yegua-Jackson Aquifer. Each aquifer is further subdivided into its respective geologic units. The numerical model honors this layering including pinch-outs and outcrop of the geologic units. Figure 2.1.1 shows the block diagram of the conceptual geologic framework and the associated numerical model discretization.

The groundwater flow model was first constructed and calibrated to available flow and water level data. The model for density dependent transport of TDS was then developed for the calibrated groundwater flow field. The transport model behavior was then evaluated for historical flow conditions.

Density dependent transport of salts is a slow process. In addition, historical data on transport of salts in the modeled area is sparse. Therefore, the transport model was not calibrated to migration of solutes. Instead, the solute distribution estimated for current conditions was used to initialize simulations of historic conditions to note if there were significant changes that may need further attention. These simulations are also discussed here. Salt transport will then be evaluated in simulations of future conditions to calculate migration of salts and salinity at the desalination plant extraction wells. That will be reported in the model application phase of the project.

The numerical groundwater-flow model was constructed to simulate the conceptualized groundwater-flow system for steady-state, 1984 conditions and transient conditions using annual stress periods from 1985 through 2014. This time period was selected principally based on pumping and groundwater level data availability, and because it includes time before and after the start of brackish groundwater desalination operations in the valley. The three-dimensional modular groundwater-flow model code MODFLOW-USG (Panday and others, 2013) was used for the simulations with the Groundwater Vistas Version 6.93 (Environmental Simulations Inc., 2016) Graphic User Interface (GUI).

Construction of the numerical model required several tasks. The first task was to assess the conceptual model including the hydrogeologic framework, hydrostratigraphy, and assignment of boundaries such as rivers, canals, recharge, evapotranspiration, groundwater pumping and irrigation return flow. This understanding provided the guidelines for discretization of the domain and for selection of relevant packages within MODFLOW-USG to appropriately simulate the required process at the necessary spatial and temporal scales. Spatial resolution requirements were then established and the hydrostratigraphic conceptual model that was developed in Leapfrog was imported into Groundwater Vistas. Other base-maps were also imported into Groundwater Vistas to identify county boundaries, rivers, canals, fractures, coastline and other features that generally orient the model. A grid was subsequently developed for the groundwater model domain; features such as wells and rivers represented by CLNs were then implemented; preliminary model parameter estimates were generated; and boundary conditions (LRG inflow, groundwater pumping rates, diversions, return flows, and prescribed heads or GHBs along coastal and lateral boundaries) were developed for steady-state 1984 conditions as well as for transient conditions from 1985 through 2014 using an annual stress period. Calibration targets were then developed for water levels and fluxes and also imported into Groundwater Vistas. The model was then run in steady-state and transient modes to debug the datasets, establish convergence, and tune solver parameters for optimal simulation performance, before moving on to the model calibration phase.

2.1 MODFLOW-USG Overview and Packages

MODFLOW-USG is an enhanced version of the MODFLOW code released in 2013 by the United States Geological Survey. The code is appropriate for this work as it is capable of meeting all the simulation requirements and challenges for this project. The beta version of MODFLOW-USG (MFUSG-Beta available with Groundwater Vistas) was used for the

simulations as it includes the density dependent flow and transport capabilities. Elements of the code and packages pertinent to the LRGV model flow simulations are discussed here.

The MODFLOW-USG groundwater model (Panday and others, 2013) solves for three-dimensional flow of water in the subsurface using the control volume finite difference (CVFD) approach. The CVFD numerical method "discretizes" the modeled domain into model cells that may have different sizes and shapes. Each model cell represents a part of the domain that is encompassed by that model cell and model inputs and outputs are generated for this discretized system. The CVFD methodology allows for flexible gridding of the subsurface domain including: ability to refine the computational grid locally using nested grids to provide spatial resolution where required; and accurately represent pinch-outs or outcrops of geological layers.

As with the other MODFLOW codes, MODFLOW-USG consists of groups of "modules" or "packages" that perform various functions related to groundwater flow simulations. These packages compartmentalize the model into its various functional elements and includes packages to define the model domain and discretization, parameterize the aquifer and flow processes, and implement various pumping and boundary conditions to the modeled system. MODFLOW-USG uses the formulations for groundwater flow that are available in MODFLOW-2005 (Harbaugh, 2005) and MODFLOW-NWT (Niswonger and others, 2011). Various boundary packages of MODFLOW-2005 are also accommodated.

MODFLOW-USG also includes solution to flow through a network of 1-dimensional conduits which interact with groundwater flow (using the Connected Linear Network or CLN process) fully coupled to the groundwater flow domain. The CLN process can be used to represent surface-water features such as rivers and canals. The 1-dimensional conduits may also be used to represent multi-layer wells coupled to the groundwater domain. Analytical solutions (Thiem equation) are used for the well-to-groundwater coupling to accurately compute well drawdown and flow contribution from each aquifer.

MODFLOW-USG also includes several packages to represent boundary conditions or internal flow barriers, as well as packages to control simulation input/output and numerical solver parameters. Table 2.1.1 shows the various packages of MODFLOW-USG that were used for the LRGV model simulations. Model input files were then developed for each of the packages to represent the conceptual model of the system.

MODFLOW-USG simulation output is contained in several files. The main output listing is written in a run list file (LST), which also includes the mass balance information. Water level output is provided in a file with extension HDS. Modeled flows, storages and boundary flux information is output to a file with extension CBB. Table 2.1.2 shows the various output files generated by MODFLOW-USG. A description of how the LRGV groundwater flow model was developed using these packages is provided in the subsections that follow.

2.2 NAME File

The NAME file of MODFLOW-USG contains the abbreviations of all packages used in developing the model along with a Fortran file "unit number" for each package and a file-name for the input (or output) files that are used in the model.

2.3   Basic Package

The Basic Package (abbreviation BAS) of MODFLOW-USG specifies the general problem dimensions and specifies initial water levels at all groundwater model cells in the domain. Active and inactive cells of the model domain may also be specified by the BAS package; however, the LRGV model was constructed to eliminate any inactive areas and thus all cells were active for this model.

2.4   Discretization Package – Model Domain and Discretization

The DIS Package of MODFLOW-USG contains model discretization information for the 3-dimensional groundwater cells and data related to stress period setup. Discretization of the 1-D processes is performed by the CLN Package which is discussed in a later section.

2.4.1   Domain Discretization

The LRGV model domain and stratigraphy were established during conceptual model development. The domain extends approximately from Rio Grande City at the west, to about 14 miles into the Gulf of Mexico to the east; and from the middle of Kenedy, Brooks, and Jim Hogg counties at the north, to about 14 miles south of the border at the south as seen on Figure 2.4.1 (Figure 1.0.3 of the conceptual model report). The hydrogeologic units and geologic units simulated in the model are shown on Figure 2.4.2. There are 12 geologic units in the model domain which were discretized into 12 numerical layers. The hydrostratigraphic units were subdivided into the geologic units to provide the finer resolution required to evaluate concentration gradients. Figures 2.4.3 through 2.4.20 (Figures 4.1.6 through 4.1.23 of the conceptual model report) show the stratigraphic elevations and thicknesses of the geologic units simulated by the model.

The geologic layers within the model domain dip eastward, with underlying layers outcropping at the surface to the west as discussed in the conceptual model report. The numerical layers were eliminated where a geologic layer pinches out or where the underlying layer outcrops to the surface. MODFLOW-USG accommodates pinch-outs and Groundwater Vistas eliminates pinched-out model cells automatically. This feature honors geologic pinch-out conditions and results in much more efficient and robust simulations.

The domain was discretized using a parent grid-block size of half a mile (2640 feet) on a base grid containing 220 rows and 292 layers. A quad-patch refinement procedure was implemented along the LRG and the network of canals, to provide a finer spatial resolution of 330 feet along these features. Figure 2.4.21 shows the discretization of the groundwater domain. There were 744,324 active groundwater cells in the model. Figure 2.4.22 shows cross-sections of the numerical model along north-south and east-west sections through column 180 and row 100 of the parent grid.

2.4.2   Stress Period Setup

The LRGV model was discretized temporally into 30 stress periods. The first stress-period was simulated as steady-state representing pre-1985 conditions. The remaining stress periods represented transient conditions with each stress-period representing the following year. This temporal discretization using annual stress periods was considered sufficient for the objectives of

the modeling effort – i.e., to evaluate long-term resource availability and impacts of brackish water extraction. Table 2.4.1 shows the stress period details.

2.5   LPF Package – Aquifer Parameters

The LPF Package was used to specify aquifer parameters (hydraulic properties) for the groundwater domain. Aquifer parameters required by the model include horizontal and vertical hydraulic conductivities, specific storage, specific yield, and porosity. The parameter values were established during calibration using the automated parameter estimation software, PEST; that is discussed in a later section. The approach towards parameterization is discussed here.

Hydraulic conductivity values for the aquifers in the domain have previously been estimated at various locations as noted in the conceptual model report; however, it is difficult to partition these values into the various geologic units that comprise each aquifer. Estimated distributions of sand fraction within each of the geologic units were therefore used to parameterize the hydraulic conductivity for each model layer throughout the domain. Figures 2.5.1 through 2.5.10 show the sand fraction distributions for the Beaumont, Lissie, Willis, Upper Goliad, Lower Goliad, Upper Lagarto, Middle Lagarto, Lower Lagarto, Oakville, and Yegua units respectively. The average sand fraction value for a layer was used in locations where this information was not available.

Sand fraction information was not available for model layers 10 and 11 (the Upper Catahoula and the Catahoula Confining System). A uniform value of 0.5 was used to parameterize these units. Also, the sand fraction for the Yegua unit was applied to the Yegua-Jackson Aquifer simulated here.

Hydraulic conductivity parameterization was conducted as follows. A higher hydraulic conductivity value was associated with a sand fraction of unity, and a lower value was associated with a sand fraction of zero for each geologic layer (the assumptions being that each geologic material has its own type of material and that within each unit, less sand implies higher clay content with an associated lower effective hydraulic conductivity). The horizontal hydraulic conductivity for any computational cell in the domain was then computed as an average, weighted by the sand fraction value of the cell; thus providing a linear relationship between the highest and lowest value for each geologic unit. This can be written as:

$$K_h = f_s K_s + (1 - f_s) K_c$$

Where K_h is the horizontal hydraulic conductivity of a cell; f_s is the sand fraction of a cell; K_s is the hydraulic conductivity value for sand for a geologic unit, and K_c is the hydraulic conductivity value for clay for the geologic unit. For vertical hydraulic conductivity, a weighted harmonic mean value was applied. Thus,

$$K_v = \frac{1}{f_s / K_s + (1 - f_s) / K_c}$$

Where K_v is the vertical hydraulic conductivity of a cell.

To understand flow behavior for this parameterization, it is generally noted that the sand hydraulic conductivity would govern horizontal flow in the model since the arithmetic average tends towards the mid-point value for equal fractions of sand and clay. The clay hydraulic

conductivity would generally govern vertical flow in the model since the harmonic average tends to be biased towards the lower (clay) conductivity value for equal fractions of sand and clay.

The sand fraction information is stored in the "Leakance" property within Groundwater Vistas. When the MODFLOW comment-line includes the phrase "Sand Fractions stored as Leakance", Groundwater Vistas performs the computations for K_h and K_v for each cell using the formulas above to create the LPF datasets.

The specific storage and specific yield were maintained as uniform for each geologic unit. There is less data available for these parameters and therefore adding complexity was deemed unwarranted. Instead, the impact of these parameters was tested with a sensitivity analysis to gain a better understanding of system response related to these parameters.

Faults or flow barriers were not implemented in the calibrated model. However, upon evaluation of the data and earlier calibration simulations portions of the Sam Fordyce Fault and the fault cutting through Jim Hogg County, as shown on Figure 2.5.11 (Figure 2.3.1 of the Conceptual Model Report) were implemented as barriers to evaluate alternative possible conceptualizations of the model while conducting sensitivity analyses.

2.6   CLN Package

The CLN Package was used in the LRGV model to represent the LRG and to implement pumping wells in the model. The CLN package contains information on discretization of the 1-dimensional model elements as well as on parameterization of these 1-dimensional segments.

2.6.1   LRG Discretization

The LRG was discretized using the CLN package of MODFLOW-USG. River segment lengths were created independently of the groundwater domain discretization and typically varied between 1000 and 5000 feet. The use of longer CLN segments compared to finer groundwater cell sizes was appropriate considering the generally smaller gradients along the river. There were a total of 202 CLN segments representing the LRG. These segments had a horizontal orientation.

The irrigation canals were not simulated using CLNs since flow in canals is not unhindered; pump-stations, farm ponds and lift-points ultimately govern irrigation flows in the canals. Therefore, the major canals were treated as river boundary conditions to simulate the groundwater interaction component (detailed later in the RIV Package). Diversion amounts were then directly extracted from the LRG; a fraction of which was reapplied to the respective agricultural areas to account for irrigation excess return flow to groundwater (detailed later in the QRT Package).

2.6.2   CLN Parameters for the LRG

The CLN process was used in the model to simulate flow in the LRG. Figure 2.6.1 shows the LRG that was represented in the model by the CLN process. A circular channel geometry was selected with top-widths varying as per data provided for the river (see Figure 2.6.1) and an assumed average depth of 2 feet. Figure 2.6.2 shows the schematic for determining the CLN geometric parameters from this average depth and width consideration.

The Manning's equation was used to simulate flow in the LRG. A Manning's coefficient of roughness value of 0.03 sec/m(1/3) typical for large rivers was used for the entire length of the

River. This parameter is not particularly significant to the current study as the main function of the CLN representing the LRG was to route the flow through the river-channel and to provide a mechanism for groundwater interactions while maintaining mass balance; considering that the evaluation is for annual stress periods and not for flood events.

The interaction of groundwater with the LRG is not a boundary condition, but an internal exchange between the groundwater cells and the CLN segments in the model. The river-bed conductance for CLNs that represent the LRG was uniformly provided a value of 0.01 ft/day with a sediment thickness of 1 foot in the calibrated model. Streamflow gains and losses between gages in the LRG within the domain that were estimated in the conceptual model section, as shown on Figures 2.6.3 and 2.6.4 (Figure 4.4.1 and 4.4.2 of the conceptual model report), were used to develop groundwater interaction calibration targets. Estimated interactions with groundwater help constrain the model through the river-bed conductance.

2.6.3 *Discretization and Parameterization of Pumping Wells*

The CLN process was also used in the model to simulate groundwater wells. Figure 2.6.5 (Figure 4.7.3 of the conceptual model report) indicates the location of groundwater production wells in the study area. Figure 2.6.6 (Figure 1.0.4 of the conceptual model report) shows the location of current desalination plants. There are a total of 3,342 CLN cells representing pumping wells in the model. These segments have a vertical orientation.

The top and bottom screen elevations for the wells were established as per data provided during conceptual model development. Accordingly, the wells may penetrate multiple aquifer or model layers. The CLN cell acts as a conduit that transmits water from all model layers that are penetrated by the well screen, to the pumping location at the bottom of the well. The Thiem analytical solution was used to simulate the interaction of the well with groundwater to provide accurate well drawdowns insensitive to the groundwater grid-block size. Lacking further information, all wells were parameterized with a radius of 1 foot and a well efficiency of 80%.

2.7 Model Boundary Conditions

Flows in and out of the model domain were discussed in the conceptual model sections related to pumping, recharge, the surface-water network, and evapotranspiration. These flows have been translated into the model boundary conditions using the boundary condition packages of MODFLOW-USG. Boundary condition packages essentially allow water to flow into or out of the model domain (i.e., interaction of the model with the "outside world"). The processes that govern this flow determine which package may be used to numerically implement the conceptualized interactions.

Figure 2.7.1 shows the modeled lateral boundary conditions. The CHD condition in offshore regions of the domain in model layer 1 allow flow in and out of the model in the Gulf of Mexico and the inter-coastal waterways. The GHB condition in model layer 12 along the western model boundary allows flow into the domain in the Yegua-Jackson aquifer unit, as this lateral boundary is not a natural aquifer boundary. Similarly, the GHB condition in model layers 8-12 along the northern model boundary allow flow of water into the model domain in the respective aquifers, since this northern boundary is also not a natural aquifer boundary. These and other modeled boundary conditions are discussed in the subsequent sections.

2.8 WEL Package

The WEL package of MODFLOW-USG simulates injection or extraction from any model cell including the groundwater or CLN domain. For the LRGV model, the WEL package was used to provide inflow to the LRG at the easternmost CLN model cell as well as to provide extraction from the bottom of vertically-oriented CLN cells that represent groundwater pumping wells.

2.8.1 Inflow to the LRG

The LRG enters the model domain from the west, near Rio Grande City. Flow of the LRG below Falcon Dam was used (with adjustments for estimated losses between the dam and the western model boundary due to diversions and estimated Mexico contributions from the Rio San Juan Irrigation District) to provide flow into the domain at the eastern boundary. The conceptual model report details the flows from Falcon Dam and estimated gains/losses between the dam and the model western boundary. Figure 2.6.3 (Figure 4.4.1 of the conceptual model report) shows the flow in the LRG below Falcon Dam; Figure 2.8.1 (Figure 4.4.4 of the conceptual model report) shows the diversion along Reach 1 between Falcon Dam and Rio Grande City; and Figure 2.8.2 (Figure 4.4.5 of the conceptual model report) shows the annual contributions to the River from Rio San Juan Irrigation District in Mexico. These net losses and gains between Falcon Dam and the western model boundary in the LRG were noted to be negligible in comparison to the flows below Falcon Dam.

The WEL package of MODFLOW-USG was used to apply a source at the easternmost CLN cell representing this LRG inflow for 1984 conditions and for 1985 through 2013 on an annual stress period. The net inflow was computed as the annual flow at Falcon Dam (Figure 2.6.3) minus estimated losses in reach 1 (Figure 2.6.3) plus estimated contributions from the Rio San Juan Irrigation District between Falcon Dam and Rio Grande City (Figure 2.8.2, also Figure 4.4.5 of the conceptual model report). The estimated contribution to the river from the Rio San Juan Irrigation District in Mexico between Rio Grande City and Anzalduas Dam noted on the lower panel of Figure 2.8.2 was not implemented as a boundary inflow because the Mexico side of the River is included in the model domain and flow to the river from both sides is internal to the model. Also, the amount is orders of magnitude smaller than the River flows and can be neglected.

2.8.2 Groundwater Pumping

Groundwater is pumped in the LRGV for municipal, irrigation, industrial, domestic, and stock uses. Figure 2.6.5 (Figure 4.7.3 of the conceptual model report) indicates locations of groundwater production wells in the study area. There are also desalination plants in the area with planned future expansion of desalination facilities in the region; which is a motivating factor for this study. Figures 2.6.6 and 2.8.3 (Figures 1.0.4 and 1.0.5 of the conceptual model report) show the location of current and planned desalination plants respectively. All pumping locations in the model are shown on Figure 2.8.4 along with the deepest screened/open aquifer unit.

Pumping amounts within the domain are shown in Figure 2.8.5 for 1984 conditions. The highest pumping is noted to occur along the LRG and in the irrigated areas in Starr and Hidalgo Counties. Pumping was generally lower in Jim Hogg, Brooks and Kenedy Counties. The WEL package of MODFLOW-USG was used to apply a sink at the bottommost CLN cell representing

the pumping well. The sink was applied on an annual stress period for 30 stress periods representing 1984-2013 conditions. The planned desalination plant pumping is not in the current calibrated model but will be implemented into scenario simulations using the calibrated model. The CLN cells that represent the wells distribute pumping to the various model layers as part of the model solution and the distribution of extraction among layers is not required a priori.

The WEL Package includes an "AUTOFLOWREDUCE" option that ensures that pumping demand does not draw water levels in the well below the well bottom elevation. This option is turned on for the simulations and any simulated reduction in pumping is reported in a "well flow-reduction" file.

2.9   CHD Package

Flow of the LRG into the Gulf of Mexico was simulated in the model as a constant hydraulic head value of zero, representing outflow at average sea-level conditions for the steady-state (1984) and transient (1985-2013) simulation stress periods. The CHD package of MODFLOW-USG was used at the easternmost CLN cell to provide the constant head condition.

The CHD package was also used to provide a constant hydraulic head value of zero in layer 1, in offshore portions of the domain. The geologic units of the Chicot and Evangeline aquifers (model layers 2-6) also were provided a constant hydraulic head value of zero along the easternmost lateral model boundary.

2.10 GHB Package

Flow into the model domain from upstream lateral model boundaries was simulated using the general head boundary (GHB) package. Along the western model boundary, the Yegua-Jackson aquifer does not have any natural boundary and therefore water enters the domain in the aquifer from further to the west. The head along the western lateral model boundary in layer 12 was set according to interpolated head contours in the region, and ranged from a high of about 550 feet in the upland regions in the north to 150 feet in the LRGV.

Similarly, there is inflow into the model domain in model layers 8-12 (the Lower Lagarto, Oakville, and Upper Catahoula units of the Jasper Aquifer System, the Catahoula Confining System, and the Yegua-Jackson Aquifer) from the northern lateral model boundary. These lateral boundaries were also simulated using the GHB package. The boundary heads ranged from 600 feet in western parts of this boundary, to 300 feet going eastwards into Brooks County.

The GHB condition was only applied partially along the northern boundary and was not applied to the shallower units of model layers 1-7 (where these units exist). This is because flow gradients were generally perpendicular to the northern boundary in eastern portions of the domain with no flow across it thus allowing it to be represented in the model as a no-flow condition. Also, these boundaries are sufficiently far from the current and proposed desalination plants to cause an impact. The locations of the general head boundaries are detailed in Section 2.7 and shown in Figure 2.7.1. Table 2.10.1 shows the GHB head and conductance values and associated model cell number and hydraulic features. Note that the GHB concentration values in the table are only used for inflow cells during transport simulations.

2.11 RIV Package

Major irrigation canals and diversions from the LRG were represented as a river boundary condition in the model using the RIV package of MODFLOW-USG. The RIV package simulates flow in or out of the aquifer to surface-water features such as canals, rivers and streams. Thus, flow within the canals was not simulated, but the groundwater interaction is taken into account. Figure 2.11.1 shows the canals that have been represented by the RIV package in the model. Width, bed thickness and bed conductance (also shown on the figure) were estimated in the conceptual model section and directly imported into the numerical model in Groundwater Vistas. Section 4.3.3 of the conceptual model report discusses the groundwater interaction understanding for these canals. There are 16 major diversions from the LRG represented by the 16 canals shown on Figure 2.11.1. The widths larger than 500 feet represent farm ponds that interact with the canal system. The bed conductance of the RIV Package was adjusted further during calibration by uniformly scaling the values for each canal up or down as needed.

2.12 QRT Package

The QRT Package of MODFLOW-USG simulates extraction from any cell (groundwater or CLN) in a model and applies a portion of that water uniformly over the area that covers the irrigated model cells. This package is used to simulate diversions from the LRG into irrigation canals, with estimated irrigation return flow for each diversion applied appropriately to each irrigation district. Figure 2.12.1 shows the diversion canal section IDs and associated irrigation districts of the model. Diversion amounts were estimated during the conceptual model evaluation and further partitioned into canal losses, M&I usage, and agricultural use as seen on Figure 2.12.2 (Figure 4.4.6 of the conceptual model report). Figure 2.12.3 shows the diversion amounts for each of the canals as input to the model. The largest diversion flows were to canals 7, 8, 4, and 6 with the smallest being to canals 16 and 13 followed by 11 and 10. Diversion amounts peaked and valleyed in tandem with distinctly high diversion amounts to the canals being in 1989, 2006 and 2009, and lower values in 2007 and 2010. For preliminary simulations, a return fraction of 0.2 of the agricultural usage was applied to the associated irrigation districts representing excess return flow to groundwater for each of the diversions, as conceptualized in the Conceptual Model Section. This value was further adjusted during calibration.

2.13 RCH Package

Estimation of recharge as a result of percolation of precipitation was discussed during conceptual model development. Annual average recharge rates were between 0.25% and 2.2% of annual average precipitation as estimated using a chloride mass balance approach (Scanlon and others, 2012). Figure 2.13.1 (Figure 2.1.8 of the conceptual model report) shows the annual average precipitation in the LRGV and Figure 2.13.2 (Figure 4.3.1 of the conceptual model report) provides the annual average distribution of recharge within the domain. This distribution of recharge and annual average precipitation was used to synthesize recharge rates in the model for 1984 through 2013 conditions and that data was directly imported into the Groundwater Vistas. The distributions were noted to be generally similar between years, with locations of higher recharge having higher recharge throughout the simulated years. Therefore, the 1984 recharge distribution was used in the model, with scaling of that recharge by the precipitation ratio between years, obtained from Figure 2.13.1. The scaling factors are provided on Table 2.13.1.

Groundwater Vistas allows import of "multiplication factors" which scale the recharge values for the other years, from that of 1984 conditions.

The recharge data ranged from 0.08 inches/year to 0.7 inches/year. It was noted that these estimates based on chloride data should be considered as a lower bound. Therefore, the recharge distribution was adjusted during calibration by increasing the recharge value where required. The scaling factors for the various years were not changed.

The recharge values were implemented in MODFLOW-USG via the RCH package, with recharge applied to the topmost active cell. The other surface-water bodies within the domain are intermittent and dry especially during drought; therefore, their impact to groundwater was not explicitly modeled but rather is implicit in the recharge distribution provided to the model.

2.14 EVT Package

The EVT package of MODFLOW-USG was used to apply evapotranspiration (ET) to the model. The EVT Package applies an ET flux (in units of length per time) to each associated model cell in the domain. The ET flux depends on a user-defined maximum ET flux rate that occurs when the water table is at or above the "ET surface" for each cell (taken equal to the land surface elevation), and that linearly declines to zero as the water table depth drops down to an "extinction depth".

Potential Evapotranspiration (PET) was estimated by previous studies (Chowdhury and Mace (2007) to be as high as 12.5 inches/year in the upland Mesquite areas, with an extinction depth of 30 feet. This value is about 2 orders of magnitude higher than the estimated recharge rates. This amount of ET tended to dominate the water budget of the model and created an unphysical inland depression of water levels in preliminary model simulations. A further investigation of maximum ET rates for Mesquite from literature (Scanlon et al, 2005; Meader, 2015) indicated that maximum ET rates from groundwater were about 30 to 60% of the PET. Also, Mesquite rooting depths were as high as 30 feet, though most of the roots were shallow with rooting depths that ranged from 6 to 20 feet with complex root processes that may move water to deeper roots (rather than extract from them) during certain time periods (Scanlon et al, 2005).

Thus, for the model, the maximum ET rate was taken as 50% of the PET (6.25 inches/year) with an extinction depth of 10 feet. The distribution of maximum ET rates in the model is shown on Figure 2.14.1. For the EVT package of MODFLOW-USG, ET was applied to the topmost active cell.

2.15 OC Package

The Output Control Package of MODFLOW-USG controls how water levels, fluxes and water budget information is saved during a simulation. The Output Control file was set up to save these results at the end of each stress period. Thus, output was provided for the steady-state 1984 stress-period, and at the end of each year of the 1985-2013 transient simulation period.

2.16 SMS Package

The Sparse Matrix Solver (SMS) package of MODFLOW-USG sets up the solution methodologies and linear solver selection for a simulation. The Newton-Raphson linearization scheme was used for this simulation effort because it affords the most robust of solution schemes

available in MODFLOW-USG and provides convergence to hard problems that arise with drying and rewetting of portions of the simulation domain. The formulation in MODFLOW-USG is the same as that of MODFLOW-NWT (Niswonger and others, 2009). The XMD linear matrix solver was selected from the two linear matrix solvers available.

Nonlinear iterations using the Newton-Raphson linearization scheme were controlled using residual reduction and under-relaxation. The under-relaxation parameters that are a default for MODFLOW-USG (the default parameters in Groundwater Vistas interface reflect these parameter values) are not very sensitive and were not changed for the simulations. The residual reduction parameters are generally tightened when nonlinear convergence difficulties are encountered but are relaxed when convergence eases. Specifically, the residual change tolerance term (BTOL) was varied between 10,000 and 1.2 at various stages of simulation. The final optimal value selected was 110.

The ORTHOMIN scheme of the XMD solver was selected to solve the asymmetric system of linear equations Linear solver parameters that were significant to the simulation included the matrix ordering scheme (NORDER), the level of fill (ILEVEL), and number of orthogonal directions (NORTH). These parameters were varied depending on convergence behavior and ranged from the various ordering schemes available; ILEVEL = 1 to 29; and NORTH = 7 to 21. Final calibrated simulation values were: ILEVEL = 9; the RCM Ordering scheme (NORDER = 1), and NORTH = 21. The "drop tolerance" scheme was used with a drop-tolerance factor (DROPTOL) equal to 1.0x10-5.

Solver parameter tuning was done throughout model development and calibration. This was done to make sure that the simulations progressed as quickly as possible at every stage of the project.

3.0 Calibration Metrics

Groundwater level elevations and groundwater/surface-water interaction flux estimates were used to constrain the model to observed conditions during the simulation period. This section discusses the various qualitative as well as quantitative measures that were used to evaluate model calibration.

3.1 Water Levels

Water level records at 218 well locations within the model domain were available as detailed in the conceptual model report. However, 115 of these wells only have one available annual measurement during the simulation time period. Only 32 of these wells have annual averaged records for over 20 of the 29 simulation years (1984 through 2013), and 26 wells have annual averaged records for between 10 and 20 of the 29 simulation years. Figure 3.1.1 shows the well locations and number of observations at each well. Figures 3.1.2A through 3.1.2D show the water level hydrographs for the 32 wells with greater than 20 available annually averaged records. Data from all 218 wells was used to evaluate calibration and therefore all the data was evaluated for consistency.

Water level information was used qualitatively as well as quantitatively in model calibration. A steady-state stress period for 1984 conditions and transient stress periods beginning 1985 through 2013 were used to evaluate the goodness-of-fit of the model. Statistical evaluations included a comparison between observed and simulated conditions (regression plots and correlation coefficients); error statistics (mean error, absolute error, standard deviation, and the respective

normalized metrics); and spatial bias (residual error map) of simulated results. Transient simulation results were further averaged over all available observation times during the simulation period to evaluate the spatial bias. Transient results were further evaluated qualitatively by visual comparison of observed and simulated hydrographs for wells where sufficient data was available over the calibration period. The simulated water level elevation at the end of a year was used for comparison to observed conditions during PEST simulations and for model evaluation.

Water level elevation data ranged from 66 feet below mean sea level in coastal areas of the model to 553 feet above mean sea level in the upland regions in Jim Hogg County. This range of data was used to scale the modeled statistics to provide normalized calibration metrics. It is generally agreed in the groundwater modeling industry that these scaled statistics should be less than 10% for a good calibration and that the lower the scaled number the better the fit.

Observed water level data was used in a weighted fashion during quantitative evaluation of calibration. This was done to give lower significance to observations that may not be accurate, or that may not fit the conceptual model representation of the system. Annual water level fluctuations at wells were generally noted to be within 10-20 feet over wet and dry years. Thus, annual water level observations that deviated significantly from other observations at the same well were considered suspect and given a lower weighting in evaluation of calibration. Also, some water level measurements were significantly negative (-20 to -66 feet below mean sea level) indicating large drawdowns due to pumping in the area. With a zero hydraulic head in offshore areas, this would further indicate landward pointing gradients of water levels from offshore areas. The conceptual model of the system considers flow being generally from west to east towards the Gulf of Mexico and therefore measurements that had high negative values were also provided a lower weighting during calibration and model evaluation. Finally, some observations were significantly different from observations at nearby wells indicating possible errors or localized anomalies which were not conceptualized to occur (possibly intercepting a faulted system, a locally perched condition or higher recharge causing water levels significantly higher than at surrounding wells). Appendix A lists the water level observations and the weighting that was used for model calibration and evaluation.

3.2   Groundwater/Surface-water Interaction Fluxes

The groundwater / surface-water interaction fluxes were also used during calibration of the model. The estimated canal losses for the major diversion canals to the LRG are shown on Figure 2.11.1. These were evaluated as per the discussions of Sections 4.3.3 and 4.3.4 of the conceptual model report. As noted therein, these are generalized estimates and therefore these flows were considered during calibration but were not given significant weighting.

Figure 3.2.1 shows the measured LRG flow at the three gaging stations in the model area and at the western model boundary. Diversion flows in the model area up to the gage at Brownsville are also shown on the figure. Inflow at the western boundary is almost the same as flow below Falcon Dam – the diversions up to the model western boundary are negligible in comparison. The LRG generally loses about 0 to 50% of its flow between Falcon Dam and Anzalduas Dam – losses before 1995 were closer to 50% of the inflow, and losses after 1995 are noted to be smaller. Flow at Brownsville was only about 10% of flow below Anzalduas Dam at low flow periods and about 60% at high flow periods (losses of 40 to 90% in this reach). Flow losses in the river occur due to diversions and groundwater interaction. Also, flow in 2010 was noted to be

over double of historical flows with very little loss up to Anzalduas Dam and losses of over 60% below Anzalduas Dam up to the gage at Brownsville. Flow patterns at all gages were similar except during 1986, 1987, 1989 and 2004. During these periods, the boundary inflow (which is similar to the flow at Falcon Dam) may be in conflict with the flow signatures at the Anzalduas and Brownsville gages since the reach losses are pretty stable compared to these flow amounts.

Interaction of the LRG with groundwater in the domain was used to evaluate flow calibration of the model. Flow data of Figure 3.2.1 was used to estimate the interaction with groundwater for the river reach from the western model domain near Rio Grande City to Anzalduas Dam, and from the Dam to Brownsville. The groundwater interaction was evaluated as inflow to the reach minus all other outflows that include the reach outflow and all irrigation diversions. Figures 3.2.2 and 3.2.3 show the river reach mass balance between the western model domain and Anzalduas Dam, and between Anzalduas Dam and the river gage near Brownsville, respectively.

As noted on Figure 3.2.2, flow at Anzalduas Dam does not reflect model inflow behavior except for the spikes in 1992 and in 2010. The diversion flows (only canals 1-4 are within this reach of the River) are generally steady and a small percent of the net river inflow. The computed groundwater interaction flow is noted to mimic the general behavior of LRG inflows except for the spikes in 1992 and 2010. Also, the proportion of inflow that is lost to groundwater decreases through time (it is about 50% of the inflow before 1995 and about 10% or less after 2000). These characteristics may be related to data inaccuracies or other processes such as sedimentation or scouring that may have caused the long-term changes in the interaction fluxes and may not be captured by the numerical model. In addition, the conceptualized groundwater level gradients are towards the LRG indicating flow to the River, while the data indicates losses from the River. Therefore, the net groundwater interaction between the Western model boundary and Anzalduas Dam was used only as guidance during model calibration.

As noted on Figures 3.2.3, flow past Anzalduas Dam and the gage near Brownsville have similar patterns through the years. Diversions in this reach of the River consume a large portion of the inflow except during high flow. The resulting groundwater interaction is generally small except for during peak flows in 2010. It is unlikely that flow to groundwater can be that high for only one year and the spike likely results from gaging errors during high flows.

4.0 Model Calibration

The model was constructed as discussed above in Section 3. As discussed earlier, the horizontal and vertical hydraulic conductivities were parameterized in the model using sand fraction data for each of the simulated geologic layers, and estimates of the hydraulic conductivity value for sand, and for the remaining material (assumed clay) for each of the layers. Thus, initial estimates were provided for the hydraulic conductivity value for sand and clay for each geologic unit, and preliminary simulations were conducted to ensure that the model was appropriately assembled and that the simulations perform successfully. Initial estimates were also provided for the specific storage and specific yield values of the units, as required for the transient stress periods. During model calibration, the hydraulic conductivity values for sand and clay were adjusted within reasonable parameter value bounds to provide appropriate flow behavior in the model domain. The specific storage and specific yield values of the units were adjusted within reasonable parameter value bounds to provide appropriate fluctuations of water levels. Solver parameters were initially adjusted for robustness and efficiency and were tuned throughout the calibration process.

The model was calibrated using an interactive expert approach (manual calibration evaluations) in conjunction with automatic model calibration using the parameter estimation code PEST. Preliminary model results were first evaluated to note model behavior and sensitivity. Consistency of the conceptual model was also evaluated, and various adjustments were made to model aquifer parameters or conceptual elements till the model was considered calibrated.

4.1   Calibration of Recharge

Generally, for reasonable parameter values, it was noted that simulated water levels were higher than observed in the irrigated areas and near the LRG, especially upstream of Anzalduas Dam. This caused the canals and LRG to drain more groundwater than was lost from the canals and the LRG, which was generally inconsistent with the observations. Also, the simulated water levels were significantly lower in some wells to the northwest portions of the domain especially in the outcrop regions of the Jasper Aquifer Units and the Catahoula Confining Unit.

Upon further evaluation of the data, it was noted that recharge was applied to the irrigated areas as return flow via diversions using the QRT package as well as via areal recharge of precipitation using the RCH package. An evaluation of the conceptual model indicated that this was likely double-counted in the model and therefore recharge via the RCH package was turned off in the irrigated areas of Figure 2.12.1 to allow the irrigation return flow to control the groundwater interaction. Also the return flow fraction was changed from the conceptualized 20% to 10% during calibration.

The recharge data of the conceptual model was further evaluated in northwest portions of the domain in comparison to other estimates for the region. This is because water levels in this region were severely under-predicted during preliminary model simulations with reasonable parameter values for the aquifers. The GAM model of Chowdhury and Mace (2007) used about 0.11 inches/year in this region. The current conceptual model indicated a value less than half that possibly being underestimated as a result of the chloride method of evaluation (Scanlon et al, 2005). Thus, the current distribution of recharge was changed to a minimum of 0.11 inches/year in Jim Hogg County where the value estimated by the conceptual model was below 0.11 inches/year. The final calibrated recharge distribution in the domain for 1984 conditions is shown on Figure 4.1.1. Table 2.13.1 shows the multiplying factor applied to this recharge distribution, for simulating recharge for years 1985 – 2013.

4.2   Calibration of Aquifer Parameters

The hydraulic conductivity values for sand and clay for all geologic layers were adjusted during calibration, to provide a best fit between observed and simulated groundwater levels. Manual adjustments and automatic calibration using PEST were performed to calibrate the model. Water level results were evaluated layer-by-layer, as well as across layers and PEST was run with different sets of water-level targets to provide focused calibration in different regions and among different layers of the model. The PEST simulations included only steady-state 1984 conditions with limited transient forward model simulations during focused calibration evaluations. The storage terms were noted to be insensitive overall, and mainly affected the nature and magnitude of fluctuations in simulated water levels.

Table 4.2.1 shows the hydraulic conductivity values for sand and clay within the various geologic units in the calibrated model. These estimates along with sand fraction distributions

provide the horizontal and vertical hydraulic conductivity distributions for the various geologic units as shown in Figures 4.2.1 through 4.2.20. For model layers 10 and 11, the sand fraction was assumed to be uniform (equal to 0.5) providing horizontal hydraulic conductivity values of 26 ft/day and 0.105 ft/day respectively, and vertical hydraulic conductivity values of 3.85 ft/day and 0.019 ft/day respectively.

The calibrated hydraulic conductivity values for the Beaumont and Lissie Formations averaged 300-400 ft/day and that of the Willis Formation averaged 10-50 feet/day. The combined effective hydraulic conductivity of these three Formations that comprise the Chicot Aquifer was noted to be relatively high in comparison to field test data. Also, unlike the field test data, the simulated effective hydraulic conductivity of the Chicot Aquifer appears to be high in the north. This is the result of using sand fraction distributions to parameterize the geologic units. Additional work may be needed to further correlate appropriate hydraulic conductivity zones with sand fraction distributions as noted in the Section 7.1 that outlines further suggested research to improve understanding of flow and salt migration in the LRGV.

Once the water levels were reasonably calibrated, the canal and LRG leakance terms were scaled to provide appropriate surface and groundwater interaction fluxes as conceptualized. Table 4.2.2 shows the scaling factors that were applied to each of the canals from the initial leakance values as noted in the conceptual model report. The scaling factors were fairly close to unity indicating that not much tuning was required from the conceptualized model.

4.3 Calibration Results

The various qualitative and quantitative metrics that were used for evaluating model calibration are discussed here.

4.3.1 Simulated versus Observed Heads

Table 4.3.1 shows the summary for head calibration statistics for the steady-state 1984 condition. The residual mean of 0.3 feet is close to zero indicating that there was no overall bias in the calibration. The absolute residual mean was 8.9 feet and the RMS error was 11.8 feet. Table 4.3.2 shows the summary for head calibration statistics for the entire simulation including transient 1985-2013 conditions. The residual mean of -1.38 feet is close to zero indicating that errors in observed and simulated water levels largely cancelled out. The absolute residual mean was 13.4 feet and the RMS error was 20.4 feet. The steady-state and transient error statistics are less than 4% of the range of observations which is generally considered a good calibration. All residuals are computed as observed minus simulated metrics thus positive residuals indicate that simulated water levels are lower than observed, while negative residuals indicate that simulated water levels are higher than observed.

Figure 4.3.1 shows the observed versus simulated water levels for the steady-state 1984 condition, and Figure 4.3.2 shows the observed versus simulated water levels for the entire 1984-2013 simulation period. The results are noted to tightly surround the best-fit line with no noticeable bias throughout the range of observations. The regression coefficient (R2) for both plots was about 0.97 indicating a good match between observed and simulated water levels.

4.3.2   Spatial Distribution of Residuals

The spatial distribution of head residuals for the steady-state 1984 condition and for the 1985-2015 transient time period are shown in Figures 4.3.3 and 4.3.4 respectively. Residuals for the steady-state 1984 condition were generally small and evenly distributed throughout the domain as noted on Figures 4.3.3. The largest errors (positive and negative) were noted to be in the northwestern portions of the model domain, in Jim Hogg County.

Residuals of the transient simulation time period of Figures 4.3.4 indicate larger residuals occurring in Starr County near the Sam Fordyce Fault. Simulated water levels were generally higher on the upstream side of the Fault, and lower on the downstream side of the Fault (note that the fault was not simulated as a hydraulic flow barrier in the calibrated model). It is possible that the Fault acts as a partial barrier at various locations along its length. Also, some of these water levels measurements may be intersecting the complex system of faults that may govern the measured water levels. Simulations that included partial barriers along the Fault indicated that barriers could create such water level conditions; however, it was difficult to pinpoint barrier locations and flow resistance properties that would mimic the observed water level breaks. Short barrier lengths with very low hydraulic conductivity of a barrier in model layers 8-12 created as much as 100 feet of head drop across the barrier. Longer barrier lengths further changed the conceptual model for flow in the system causing flow to be southwards towards the LRG instead of eastward toward the Gulf of Mexico.

4.3.3   Water Level Hydrographs

Figures 4.3.5-A through 4.3.5-D show the observed and simulated hydrographs for wells with more than 10 annual observations. Observed and modeled fluctuations are noted to be similar though some wells indicated larger than observed fluctuations, while others had less simulated fluctuations than observed. Wells in the southwest (Figure 4.3.5A) and southeast (Figure 4.3.5B) seemed to have a better fit to observed conditions than wells in the northwest (Figure 4.3.5C) and northeast (Figure 4.3.5D). An analysis of water levels at pumping wells did not indicate any specific trends in water levels compared to pumping indicating a possible complicated system response rather than at an individual well. Also, it was noted that the water levels used in the calibration effort represent winter conditions and may not reflect conditions of annually averaged pumping rates and recharge/ET stresses – thus, the comparison may not be ideal. Appendix B provides water level hydrographs for all observation wells. It is noted from these hydrographs that the starting heads produced by the 19894 steady-state simulation were reasonable and there were no sudden dips or jumps from starting conditions in the transient simulation.

4.3.4   Simulated Water Levels

Figures 4.3.6 through 4.3.17 show the simulated water levels in the 12 modeled layers respectively, at the end of the simulation in 2013. Water levels are generally similar in model layers 1-6 and then in model layers 8-12 where the units exist. The Burkeville Confining Unit (model layer 7) was noted to have the most impact on the vertical offset of water levels.

Water is noted to generally flow from west to east in the units comprising the Chicot and Evangeline Aquifers (model layers 1-6). Water levels in the Willis Unit at the bottom of the Chicot Aquifer (model layer 3 shown on Figures 4.3.8) compare well with the conceptualized water levels depicted for the Chicot Aquifer in Figure 4.3.18 (Figure 4.2.5 of the conceptual model report). Also, water levels in the Upper Lagarto Unit at the bottom of the Evangeline

Aquifer (model layer 6 shown on Figures 4.3.11) compare well with the respective conceptualized water levels depicted in Figure 4.3.19 (Figure 4.2.6 of the conceptual model report).

In the Burkeville Confining Unit (model layer 7), it was noted that simulated water levels were about 100 feet higher where the overlying units were absent and the unit was unconfined and being direct recharged. This was also noted in the available observed data. The extent of confinement of layer 7, as conceptualized for the model, was therefore sensitive to the water levels in this area. Localized depressions in water levels were also noted around pumping wells in this geologic unit and water levels were highly variable in this layer because of its tight hydraulic conductivity.

In the Jasper and Yegua-Jackson Aquifers (model layers 8-12) below the Burkeville Confining Unit, the simulated water levels were higher than in the shallower units causing an upward direction of flow. In the outcrop areas of model layers 8-12, water flows to the east as well as in the southward direction towards the LRG. Water levels in the Upper Catahoula Unit at the bottom of the Jasper Aquifer (model layer 10) are shown on Figures 4.3.15 and compare well with the conceptualized water levels depicted for the Jasper Aquifer reproduced in Figure 4.3.20 (Figure 4.2.7 of the conceptual model report).

The steep topographic gradients in Starr and western Hidalgo Counties towards the LRG cause simulated water levels to be higher than the land surface elevation in some of the model cells, as the computed hydraulic conductivity (which depended on the sand fraction) could not create the steep water-level gradients that were required here. A separate zone was not implemented in the model near the LRG to provide the additional degree of freedom required to capture these sharp gradients because the number of "flooded" cells was very small. Furthermore, there may be seepage occurring at these steep locations which were not conceptualized in the model. Also, the grid-size may require further refinement in this region for a more accurate depiction of these steep gradient conditions. Finally, the flooded condition occurs in the Jasper and Yegua-Jackson aquifer along the steep topography – a location that is not of significance to this study as the current and planned desalination plants lie closer to the River and not in this area of flooded cells (see Figures 2.6.6 and 2.8.3). Therefore, further refinement of the model (conceptually and numerically) was not done to alleviate this condition.

Figure 4.3.18 shows the simulated and estimated water levels for 1984, 1995, and 2013 in the Chicot Aquifer (water levels in the Lissie Unit in the middle of the Chicot Aquifer are used for the comparison). Simulated water levels compare well with the conceptualized water levels (also shown in Figure 4.2.5 of the conceptual model report). Figure 4.3.19 shows the simulated and estimated water levels for 1984, 1995, and 2013 in the Evangeline Aquifer (water levels in the Lower Goliad Unit in the middle of the Evangeline Aquifer are used for the comparison). Simulated water levels compare well with the respective conceptualized water levels (also shown in Figure 4.2.6 of the conceptual model report), specially near the River where data was most available. Figure 4.3.20 shows the simulated and estimated water levels for 1984, 1995, and 2013 in the Jasper Aquifer (water levels in the Oakville Unit in the middle of the Jasper Aquifer are used for the comparison). The simulated 100 foot contour is more landward than the simulated but otherwise they are a pretty good match.

4.3.5   Simulated Surface-water/Groundwater Interaction Fluxes

Figures 4.3.21-A through 4.3.21-E show the simulated and estimated groundwater interaction fluxes for the various canals and for two reaches of the LRG; between the western model boundary and Anzalduas Dam, and between Anzalduas Dam and the gage near Brownsville. The canal fluxes are noted to be in good agreement with conceptual model estimates with a maximum error of about 10%. Additional refinement was not done on these fluxes as the model is being compared to conceptual estimates and not real data. LRG fluxes between Anzalduas Dam and Brownsville are lower on average by about a factor of 6 than conceptual estimates. The LRG between the western model boundary and Anzalduas Dam is a complex reach with gaining and losing portions as the River flows from the valley towards the coast. This reach also was not calibrated well and additional data would be required to better understand and estimate the interaction with groundwater.

4.3.6   Simulated Water Budgets

The water budget for steady-state 1984 simulation is show in Table 4.3.3. The largest flow in the model occurs within the LRG accounting for 89.3% of all inflow. LRG flow to the Bay accounts for 41.8% of all outflows and diversions from the River comprise almost 41% of the outflow. The largest inflow to the groundwater domain was via return flow followed by areal recharge and canal leakage to groundwater. The largest outflow of groundwater is to the coast followed by evapotranspiration and then groundwater pumping.

The water budget for the transient simulation from 1984 through 2013 is shown in Figure 4.3.22. The largest fluxes were inflow to the LRG at the western model boundary and outflow of the LRG into the Bay. Figure 4.3.23 shows the groundwater budget components of the model. Of the largest inflow components, return flow and areal recharge, it was noted that they generally trended opposite of each other – i.e., when recharge increased, the return flow decreased. The next largest inputs, canal leakage and GHB inflow, were generally stable with little fluctuations. Groundwater flow to the coast, the largest outflow term, also had the largest fluctuations. Fluctuations in evaporation were small. Groundwater pumping was generally stable throughout the calibration period though fluctuations from one year to the next could be as high as 34,000 af/yr.

 The "AUTOFLOWREDUCE" option used with pumping wells reduces the pumping rate when water levels drop to the bottom of the well. Only 8 of the 3,342 pumping wells had flow reduction occur by the end of the simulation. Figure 4.3.24 shows these eight wells. The flow reduction at these wells occurred possibly due to incomplete information on pumping or incorrect localized hydraulic conductivity values.

5.0 Sensitivity Analyses

A sensitivity analysis was conducted on the calibrated model to determine the impact of conceptual or parameter changes to the calibration results. Predictive sensitivity simulations will also be conducted for specific predictions of interest to evaluate uncertainty of the model to the predictions of interest. The current section discusses the sensitivity analyses to calibration.

In general, four sets of sensitivity analyses were performed. A transient sensitivity analysis was first performed on the storage properties of the aquifer to note their overall impact. A steady-state sensitivity analysis was then performed on the hydraulic conductivity parameters of the

aquifers to evaluate those that have a high impact on calibration. Parameters were categorized into high, medium and low sensitivity groups. Parameters that have low sensitivity to calibration but have high impact on model predictions may require further evaluations as the predictive uncertainty of those parameters is high. Steady-state sensitivity analyses were also performed on the model stresses (evapotranspiration, pumping, diversions and return flow). Finally, a conceptual model sensitivity analysis was conducted to note the impact of faults within the domain.

5.1   Sensitivity to Aquifer Storage Properties

The first sensitivity analysis was conducted to note the impact of aquifer storage properties on water level fluctuations in the domain. To evaluate the extreme fluctuation that can be simulated by the model, the specific yield and specific storage values of all modeled aquifer units were set to a negligible value of 1.0 x 10-9. A sensitivity simulation was also conducted using higher specific yield values to evaluate the resulting dampening of simulated fluctuations. The higher storage simulation used a specific yield equal to the porosity that was used for the transport simulations, and generally ranged from 0.05 to 0.25 and averaged about 0.1 in large parts of the domain for all of the simulated geologic units. Note that section 6.3 details the effective porosity evaluations used for transport computations of the model. Figures 5.1.1-A through Figure 5.1.1-D show the hydrographs at select wells for this sensitivity study. Appendix C shows the results for all monitoring wells in the domain. Water level fluctuations are generally higher and sharper for the sensitivity simulation with negligible storage, as compared to the calibrated simulation, while fluctuations are generally more dampened for the simulation with a high storage term. However, the general trends in the hydrographs for all simulations are similar and the storage parameters are not significant to the calibrated simulation. Also, considering the annual time-scale of evaluation for model stress periods, water level fluctuations are generally more dampened due to dampening of peak stresses into average values and therefore a storage term takes on a surrogate role in evaluating fluctuations of a model with annually averaged stress periods.

5.2   Sensitivity to Aquifer Hydraulic Conductivity Parameters

Sensitivity of the model to hydraulic conductivity values of the various geologic units was evaluated through simulations of 1984 steady-state conditions. The transient time periods were not considered as they do not add to the evaluation. This is because it was noted that transient conditions generally follow seasonal behavior and water levels had not indicated long term changes or trends. As noted in Figures 3.1.2, the water levels are generally stable though they may show decline or increase in some of the wells.

The parameter sensitivity study was conducted by running PEST for one iteration with the calibrated model. The linear parameter sensitivity of sand and clay hydraulic conductivity values for each of the units was evaluated. Table 5.2.1 shows the sensitivity of the various parameters. All parameters were generally sensitive with no extreme values noted. Of the sand hydraulic conductivities (which generally controls the horizontal hydraulic conductivity value), layer 6 (Upper Lagarto unit in the Evangeline Aquifer) had the highest sensitivity followed by layer 10 (Upper Catahoula unit in the Jasper Aquifer). Of the clay hydraulic conductivities (which generally controls the vertical hydraulic conductivity value), layer 7 (the Burkeville Confining

Unit) had the most sensitivity with layer 3 (Willis unit of the Chicot Aquifer) having the least sensitivity.

Sensitivity of the model to hydraulic conductivity of the geologic materials was also evaluated by changing the individual value of hydraulic conductivity for sand or clay for each of the geologic units. Thus, 12 sand and 12 clay hydraulic conductivity values were evaluated. For each sensitivity analysis, the property value was increased by a factor and decreased by a factor as deemed appropriate, and the mean head residual and the RMS head error were evaluated to establish model behavior. The mean head residual indicates sensitivity of the residuals to the parameter value showing whether the heads have overall increased or decreased as a result of the parameter change. The RMS head error sensitivity indicates how the spread in observed versus modeled water levels has changed.

Figures 5.2.1 through 5.2.4 show the sensitivity of the model results to the hydraulic conductivity values for sand and clay for the various geological units. The mean head error depicted in Figures 5.2.1 and 5.2.3 shows the change from calibrated conditions while the RMS errors of Figures 5.2.2 and 5.2.4 indicate the variability between simulated and observed conditions. The hydraulic conductivity value for sand for layers 10 and 12, clay for layers 4 and 7, had the highest sensitivity to the mean head error of the results. The lowest sensitivity to mean head error of results was for the hydraulic conductivity value of sand for zones 4, 5, 8 and 9, and of clay for zones 3, 5, 8, and 10. The hydraulic conductivity value for sand for layers 6 and 10, clay for layer 6 had the highest sensitivity to the RMS head error of the results.

Table 5.2.2 categorizes the sensitivity simulations into low, medium and high sensitivity values. The possible "sensitivity types" as defined by ASTM (1994, 2002) are also listed to help with uncertainty evaluations for the predictive analyses. The sensitivity types evaluate the change in calibration versus the change in predictions and are as follows:

Type I sensitivity is defined for parameters that cause insignificant changes to the calibration residuals as well as to model conclusions/predictions of interest. Type I sensitivity is of no concern because regardless of the value of the input, the prediction is also insensitive.

Type II sensitivity is defined for parameters that cause significant changes to the calibration residuals but are not sensitive to model conclusions/predictions of interest. Type II sensitivity is of no concern because the prediction is not sensitive to the calibration.

Type III sensitivity is defined for parameters that cause significant changes to the calibration residuals as well as to the model conclusions/predictions. Type III sensitivity is of no concern because even though the model's predictions change as a result of variation of the input, the calibration residuals are also sensitive and the model becomes uncalibrated as a result. Thus, model calibration ensures that the predictions considered are appropriate for the modeled system.

Type IV sensitivity is defined for parameters that cause insignificant changes to model calibration residuals but significant changes to the model predictions. Type IV sensitivity is of concern because over the range of that parameter in which the model can be considered calibrated, the conclusions/predictions of the model change. Additional data collection for such parameters can help narrow the band of uncertainty in the prediction.

Parameters with low mean and RMS error sensitivities were categorized as possible Sensitivity Type I or IV. These included the sand hydraulic conductivities of layers 4, 5, 8, and 9, and the clay hydraulic conductivities of layers 3, 5, 8, and 10. If predictive sensitivity simulations for

these parameters indicate large prediction changes, they will be classified as Type IV indicating that predictions would be more accurate for better estimates of that parameter even though it may not affect the calibration.

5.3 Sensitivity to Modeled Stresses

The sensitivity of modeled water levels to recharge, evapotranspiration, groundwater pumping and irrigation return flow was evaluated next to note the impact of variations in their values. These sensitivity analyses were also conducted only for 1984 steady-state conditions.

For each sensitivity analysis, the stress values were multiplied by factors of 0.3, 0.7, 1.3 and 1.7 to note the impact on calibration errors. The factors of 0.3 and 1.7 represent a 70% reduction and increase in the respective flux values, while the factors of 0.7 and 1.3 represent a 30% reduction and increase in the respective flux values.

The mean head residual and the RMS head error were evaluated to establish model behavior. The mean head residual indicates sensitivity of the residuals to the parameter value showing whether the heads have overall increased or decreased as a result of the parameter change. The RMS head error sensitivity indicates how the spread in observed versus modeled water levels has changed.

Figure 5.3.1 shows the sensitivity to the mean head residual to recharge, maximum ET rate, groundwater pumping and return flow fraction. Recharge and return flow have the largest impact on the mean head value computed at the target groundwater cells, while the maximum ET rate had the smallest impact.

Figure 5.3.2 shows the sensitivity of recharge, maximum ET rate, groundwater pumping and return flow fraction to the RMS head error. The largest sensitivity again was to recharge followed by return flow. Maximum ET rate did not impact the RMS head error by any appreciable amount.

A sensitivity analysis to model stresses and aquifer hydraulic parameters was also conducted by running PEST for one iteration with the calibrated model. For this analysis, the sand hydraulic conductivity values for all layers were tied with that of model layer 1, and the clay hydraulic conductivity values for all layers were tied with that of model layer 1. Thus, the sensitivity was evaluated for sand and clay hydraulic conductivities of all modeled layers combined. This analysis also evaluated sensitivity to the recharge multiplier, and the maximum ET rate multiplier. Thus, the linear sensitivity of sand and clay hydraulic conductivity values and of scaling the recharge and maximum ET rates was evaluated. Table 5.3.1 shows the sensitivity results for this simulation. All parameters and stresses were sensitive to the results with highest sensitivity to the maximum ET rate multiplier, and lowest to the recharge multiplier. Table 5.3.2 shows the correlation coefficient matrix for these parameters. The largest correlation was between the clay hydraulic conductivity (which generally governs the vertical K-values of the unit), and recharge. The maximum ET rate and recharge were inversely correlated with the second highest correlation coefficient. Sand hydraulic conductivities were directly correlated to the recharge multiplier with the third highest correlation coefficient. Sand and clay conductivity values were correlated the least.

5.4   Conceptual Sensitivity to Presence of Faults

During model calibration, it was noticed that there were some steep gradients in observed water levels that could not be simulated with reasonable aquifer parameter values. Also, as noted on the residual plot of Figure 4.3.4, there were large positive residuals upstream of large negative residuals in the outcrop locations for the Jasper Aquifer units (model layers 8, 9 and 10) in Starr County. These large residuals in the calibrated model generally coincided with the estimated location of the Sam Fordyce Fault suggesting that the fault may impede flow of water along some sections within the domain. A conceptual sensitivity analysis was conducted in this regard, to evaluate the impact of barriers to flow in this region.

For this simulation, the Hydraulic Flow Barrier (HFB) package of MODFLOW-USG was used to create barriers to flow as noted on Figure 5.4.1. The HFBs extended from model layers 8 through 12 creating a barrier to flow in all the units below the Burkeville Confining Unit. The HFB in southern Jim Hogg County was placed to evaluate if the large residuals upstream of the barrier could be reduced without significantly impacting other flow behavior. The HFB in Starr County was placed to evaluate if the large residuals upstream and downstream of it could be reduced as a result. The barrier thickness was taken as 1 foot with a barrier hydraulic conductivity value of 1.0x10-9 feet/day.

Figure 5.4.2 shows the impact of the barriers in model layer 12. The impact in model layers 8-11 is similar (where these units exist). The barrier in Jim Hogg County reduced the residuals in wells upstream of it from over 30 feet to less than 10 feet. The barrier in Starr County also reduced residuals on both sides of it from over 75 feet to less than 35 feet. However, one well (id. 43978) just downstream of the HFB that had good calibrated heads now had a residual of 55 feet. These wells near to faults may have complex interactions from both sides of the fault and therefore such behavior may be difficult to conceptualize and capture in the numerical model.

Figure 5.4.3 shows the impact of the barrier in model layer 6 which is similar to the impact in the shallower layers where they exist. The impact can be as high as 50 feet right next to the outcrop of layer 7 along the Starr and Hidalgo County Line. The impact however drops off rapidly to the east and is less than a foot in most of the domain. Thus, location of the barrier within the deeper units (below layer 7) can have a large impact on the shallower aquifers (layers 6 and above) as well, but the impact diminishes rapidly with distance.

6.0   Transport Simulations

The calibrated model was used further to evaluate transport of salts within the model domain. Transport model was developed primarily to evaluate potential migration of chlorides due to groundwater pumping of future desalination operations; however, test simulations were also conducted over the calibration time period to note behavior of the model. Typically, density dependent transport of salts is a slow process and the model was qualitatively evaluated accordingly.

6.1   Transport Simulation Setup

The calibrated flow model was used to evaluate transport of TDS within the domain for the calibration period from 1984 through 2013. The TDS concentrations of current conditions for all model layers were developed in the Conceptual Model Report using the BRACS database and

observed information. These TDS concentrations are reproduced here in Figure 6.1.1 for the geologic units comprising the Chicot Aquifer; Figure 6.1.2 for the geologic units comprising the Evangeline Aquifer; Figure 6.1.3 for the Burkeville Confining Unit; Figure 6.1.4 for the geologic units comprising the Jasper Aquifer; Figure 6.1.5 for the Catahoula Confining System; and Figure 6.1.6 for the Yegua-Jackson Aquifer model unit. These TDS concentrations were implemented as initial conditions for the simulations discussed here. The base case transport simulation was performed using density dependent flow conditions where fluid density and resulting flow field are affected by the solute concentrations. Since the initial concentrations were categorized into zones, in accordance with the BRACS database it is expected that the sharp zonal boundaries will dissipate through time.

There are impacts of historical pumping within the domain causing migration of the solutes in the base case transport simulation. The initial and boundary conditions also affect solute transport in the model. To isolate the impact of pumping versus other boundary and initial conditions, a second transport simulation was conducted without any groundwater pumping in the domain.

The impact of density on the simulation results was also evaluated by conducting a third transport simulation using historic boundary and pumping conditions but without including density impacts and comparing the results with the base case simulation. This comparison is significant because the density dependent flow and transport simulations took more computational time than simulating transport without density terms; and understanding the approximations can help guide future simulations considering modeling objectives.

Once the transport datasets were developed, simulations were performed to debug the datasets, establish time-stepping considerations, evaluate impact of different transport options, and tune solver parameters for optimal performance of density driven flow and transport simulations.

6.2   Transport Parameters and Packages

The beta version of MODFLOW-USG (MFUSG-Beta available with Groundwater Vistas) includes routines for simulating transport of solutes and density driven flow effects. The Groundwater Vistas GUI accommodates all these features of MFUSG-Beta. These features and capabilities have been tested using analytical example problems and against more complicated numerical solutions.

Transport simulations were conducted by using a CVFD approach and the upstream weighting and Total Variation Diminishing (TVD) schemes. The TVD scheme is a method of solution for the transport equation that minimizes numerical dispersion which would occur with upstream weighting schemes. Early tests indicated that the upstream formulation gave comparable solutions to the TVD scheme and therefore upstream weighting was used for the final transport models due to its lesser computational burden.

The solution sequence between flow and transport is as follows. A flow field was first generated by the flow simulation of MODFLOW-USG. Solute transport was then simulated for that time step followed by updating of the density term with the updated concentrations, before proceeding to solution of flow for the next time step. Thus, the density effect was time-lagged. The transport models indicated very slow change of TDS concentrations during the 30 year simulation period therefore the time-lagged density term was appropriate. For the first stress period which is steady-state, the flow simulation is followed by transport simulations for multiple time-steps of

each 365 day stress period. The buoyancy term was not updated in the flow equation for the first steady-state stress period.

The transport models required additional packages to be used in the simulation. These include the Block Centered Transport (BCT) Package for simulation of solute transport and the Density Dependent Flow (DDF) Package to include the density effects of saltwater in the groundwater flow solution. The transport model also requires that boundary conditions be provided for solutes.

6.3 BCT Package

MFUSG-Beta includes the BCT package to solve for transport of solute species via advection and dispersion in the groundwater flow field. Thus, the BCT package must also be included in the NAME file when transport is simulated. The NAME file further includes filenames for output of resulting concentrations and mass fluxes of solutes.

Transport simulation parameters include an effective transport porosity; longitudinal and transverse dispersivity; diffusion coefficient; decay coefficient; and adsorption coefficient. Parameter values were selected as follows:

A longitudinal dispersivity of 100 feet and transverse dispersivity of 10 feet was selected for the simulations. The impact of dispersivity was not significant as noted in preliminary simulations.

A diffusion coefficient value of zero was used for the transport simulations. Diffusion is generally a small transport mechanism in advection dominated systems and is usually neglected.

Adsorption coefficient and decay coefficient values were zero for the transport simulations. Chlorides which constitute most of the TDS may be considered to have no adsorption and zero decay. Geochemical interactions of calcium and sodium with chlorides is therefore neglected.

The effective porosity was computed using sand fraction information with the conceptualization that transport occurs within the sand portions and that the remaining (clay) portions of the domain do not contribute to flow and transport. The effective porosity for each CVFD cell was computed as:

$$\phi = f_s \phi_s + (1 - f_s)\phi_c$$

Where ϕ is the effective porosity of a cell; f_s is the sand fraction of a cell; ϕ_s is the effective porosity value for sand for a geologic unit, and ϕ_c is the effective porosity value for clay for the geologic unit. A sand effective porosity value of 0.3 was selected for all geologic units. A clay effective porosity value of 0 was used to exclude clay from the transport pore spaces. These values have been entered into Groundwater Vistas which uses the sand fractions to compute the effective porosity for each model cell. Figures 6.3.1 through 6.3.10 show the resulting porosity distribution for the Beaumont, Lissie, Willis, Upper Goliad, Lower Goliad, Upper Lagarto, Middle Lagarto, Lower Lagarto, Oakville, and Yegua units respectively. The effective porosity value for model layers 10 and 11 (the Upper Catahoula and the Catahoula Confining System) was 0.15. Abrupt changes in the porosity values across county boundaries reflect the abrupt changes in sand fraction data that was provided for the numerical model.

When the MODFLOW comment-line includes the phrase "Sand Fractions stored as Leakance", Groundwater Vistas performs the computations for effective porosity of each cell using the formula above to create the BCT datasets.

Initial conditions for all transport simulations in this report are the current conditions depicted in Figures 6.1.1 through 6.1.6 as noted earlier. Generally, the higher TDS water underlies water with lower TDS; however, it was noticed that fresher water sits under higher salinity water in the Chicot Aquifer in eastern Brooks/western Kenedy Counties.

When transport of solutes is simulated, the main output listing file (LST) also includes information and mass balance results for the transport simulation. Concentration output is provided in a binary file with extension CON. Flux of solutes is output to a binary file with extension CBT.

6.4   DDF Package

MFUSG-Beta also includes the DDF package to provide a coupling of solute transport (with associated density changes) to the flow solution. This is required when solute concentrations are high enough to where the salt concentrations significantly affect the density of water which in turn impacts the driving forces for flow.

When the DDF package is included in the NAME-file, it indicates that the simulation should include density effects. Input for the density driven flow simulation includes a freshwater density (1000 kg/m3), a saltwater density (1025 kg/m3), and a reference saltwater concentration (40,000 mg/L of TDS). The saltwater density and concentrations reflect seawater conditions.

The DDF package has been formulated using the hydraulic head formulation. Thus, there is no need to convert any of the boundary conditions or initial water level conditions to other variables as is required by the equivalent freshwater head formulation. Furthermore, all Newton Raphson schemes related to unconfined water level conditions are naturally accommodated.

6.5   Transport Boundary Conditions

Each boundary condition that has inflow to the model for flow simulations also requires that a concentration be provided for the inflowing water. This is done in the respective boundary condition packages (WEL, CHD, GHB, RIV, RCH) by including an AUXILLIARY variable named "C01" indicating that there will be additional input for concentration of solute component 1. MODFLOW-USG then applies a mass flux boundary condition whereby the mass flux of solutes is the concentration of inflow times the flow rate. For outflow conditions, the concentration of outflow times the flow rate provides the mass flux rate at the boundary – thus, the concentration provided at an outflow boundary is ignored assuming mass flux due to advection out of the domain. The mass exchange for QRT and CLN packages is internal to the simulation and therefore no additional input is provided for transport simulations for these packages. Finally, ET is a process which removes water from the domain but leaves behind salts.

Concentration at the boundary for the various packages was applied as follows:

The coastal boundary is typically an outflow boundary and does not require that a concentration be prescribed. However, since it is a CHD condition, there could be inflow occurring locally depending on water level gradients and therefore, a seawater TDS concentration of 40,000 mg/L was provided along the coastal CHD boundary.

Inflow to the LRG was provided a TDS concentration of 1,000 mg/L. The conceptual model report indicated that average concentrations at the LRG below Falcon Dam were around 500 mg/L, and at the LRG at Rio Grande City were around 1,500 mg/L. The western model boundary is about half-way between these two gages and thus the average TDS concentration of these two locations was selected for the model.

Concentrations of inflow at all RIV boundary conditions representing irrigation canals was set at 1,500 mg/L to represent concentrations in the LRG that were diverted into the canals. This value is the average concentration of TDS in the LRG within the model domain as noted in the conceptual model report.

Concentrations at lateral GHB boundaries to the west and to the north were taken from the initial concentration distribution at that location (shown on Figures 6.1.1 through 6.1.6). Thus, inflow occurs at the same concentration as is currently noted at the boundary.

Concentration in groundwater recharge water was taken as 300 mg/L. This generally reflects the lower of TDS values that have been noted in the domain and represents salts present in precipitation water as well as that which would be leached from above the water table.

The EVT package removes water without removing solutes.

6.6   Transport Simulation Results

The base-case transport simulation evaluates the density dependent flow and transport of TDS within the domain over the model calibration period that included a 1-year steady-state flow-field for 1984 conditions followed by 29 stress periods (1985-2013) of transient flow and pumping conditions on an annual stress-period basis. The density coupling caused difficulties in convergence, specifically in time-step 3 of stress period 7, time-steps 2-5 of stress period 21 and time-step 1 of stress period 22 of the simulation. An evaluation of the mass balance and convergence behavior during these times indicated that the results were still meaningful.

The concentration distribution after 30 years of simulation with historic pumping and boundary stresses is shown on Figure 6.6.1 for the geologic units comprising the Chicot Aquifer; Figure 6.6.2 for the geologic units comprising the Evangeline Aquifer; Figure 6.6.3 for the Burkeville Confining Unit; Figure 6.6.4 for the geologic units comprising the Jasper Aquifer; Figure 6.6.5 for the Catahoula Confining System; and Figure 6.6.6 for the Yegua-Jackson Aquifer model unit. The concentration distributions generally look similar to those of the initial conditions depicted on Figures 6.1.1 through 6.1.6 for the respective geologic units. The most significant changes are noted in eastern Brooks/western Kenedy Counties in the Chicot Aquifer, where the lower concentration water of the lower geological layers is noted to increase, while the higher concentrations of TDS in the upper geological layers are noted to decrease.

The change in concentration from initial conditions over the 30 year simulation is shown on Figure 6.6.7 for the geologic units comprising the Chicot Aquifer; Figure 6.6.8 for the geologic units comprising the Evangeline Aquifer; Figure 6.6.9 for the Burkeville Confining Unit; Figure 6.6.10 for the geologic units comprising the Jasper Aquifer; Figure 6.6.11 for the Catahoula Confining System; and Figure 6.6.12 for the Yegua-Jackson Aquifer model unit. The largest changes are noted to occur in the Chicot Aquifer with diminishing changes in the deeper aquifers. Changes of greater than 10,000 mg/L were noted in the Chicot Aquifer in coastal regions. Along the LRG within the Chicot Aquifer, there were increases and decreases in

concentration. Decreases of 100 to 1000 mg/L were noted in coastal regions along the LRG and increases of 100 to 1000 mg/L were noted in more western portions along the LRG. Large changes are also noted along eastern Brooks/western Kenedy Counties where higher concentration water overlies lower TDS water in the Chicot Aquifer. Large changes were also noted in the Upper Catahoula unit of the Jasper Aquifer (model layer 10) which has a higher conductivity than the adjacent units.

A density dependent flow and transport situation can impact the hydraulic head and therefore, the calibrated head of the groundwater flow model may be different from the actual head that would include density effects. To note the impact on hydraulic head, Figures 6.6.13 through 6.6.24 which depict the hydraulic head from the density dependent case at the end of the simulation in 2013, can be compared with the calibrated groundwater flow model results for the respective layers (Figures 4.3.6 through 4.3.17). It is noted that the hydraulic heads are generally similar to those of the groundwater flow model, though there is also a marked impact from the concentration distributions in the model. The sharp concentration zones of Figures 6.1.1 through 6.1.6 produced sharp horizontal gradients or breaks in the hydraulic head most notable in the deeper layers. For instance, sharp hydraulic head differences of up to 30 feet are noted across zones of TDS concentrations in layers 8 through 12. Also, in the deeper layers, the hydraulic head was significantly lower near the coast, than for the non-density dependent flow simulation.

Tables 6.6.1 and 6.6.2 show the calibration statistics for the simulation with density effects, for 1984 steady-state conditions, and for the entire simulation period from 1984 through 2013 respectively. Comparing these statistics to their counterparts in the flow model (Tables 4.3.1 and 4.3.2), it is noted that the calibration statistics are similar. For steady-state 1984 conditions, the average simulated heads were about four feet higher for the density dependent simulation as compared to the groundwater flow model. For the entire simulation period, the average simulated heads were about five feet higher for the density dependent simulation as compared to the groundwater flow model. The scaled statistics for both transient and steady-state conditions were well below 5% indicting that the model is generally well calibrated even when evaluated against density dependent flow conditions. It is noted here that due to lack of historical total dissolved solid (TDS) data, calibration was not performed for the transport part of the model in consultation with GAM and BRACS staff at the TWDB.

6.7   Additional Transport Evaluations

Two additional transport simulations were conducted with the model aside from the density dependent simulation discussed above. The first of these was identical to the density dependent simulation of Section 6.6 but without any pumping wells in the domain. The second of these was also identical to the density dependent simulation of Section 6.6 but without including the density impact in the simulation. These additional simulations are discussed here.

Another transport simulation was conducted following the base-case simulation but without any of the pumping wells, to note the impact of initial and boundary conditions, on migration of TDS over the simulation period, in isolation from the impact of pumping and the presence of wells. The difference in 2013 concentrations between the base-case transport simulation, and the current simulation without wells gives the impact of pumping for 30 years. This difference is shown on Figure 6.7.1 for the geologic units comprising the Chicot Aquifer; Figure 6.7.2 for the geologic units comprising the Evangeline Aquifer; Figure 6.7.3 for the Burkeville Confining Unit; Figure 6.7.4 for the geologic units comprising the Jasper Aquifer; Figure 6.7.5 for the

Catahoula Confining System; and Figure 6.7.6 for the Yegua-Jackson Aquifer model unit. These plots indicate smaller differences than the changes that occurred over 30 years noted in Figures 6.6.1 through 6.6.6 for the case with pumping. Therefore, initial and boundary conditions had a considerable impact and that of pumping was smaller. The largest differences between the pumping and non-pumping simulations (the impact of pumping) are noted on Figure 6.7.1 for the Chicot Aquifer. Pumping impacts on TDS were noted to be small near the LRG and most of the changes noted in the base-case simulation were a result of the initial and boundary conditions applied to the system.

The next transport simulation was conducted following the base-case simulation but without the density effect on flow. The difference in concentrations between the base-case transport simulation, and the current simulation without density effects is shown on Figure 6.7.7 for the geologic units comprising the Chicot Aquifer; Figure 6.7.8 for the geologic units comprising the Evangeline Aquifer; Figure 6.7.9 for the Burkeville Confining Unit; Figure 6.7.10 for the geologic units comprising the Jasper Aquifer; Figure 6.7.11 for the Catahoula Confining System; and Figure 6.7.12 for the Yegua-Jackson Aquifer model unit. There is a comparatively small impact noted due to density effects with the largest impacts noted in the geologic units comprising the Chicot Aquifer. Therefore, the non-density version of the model may be used without incurring much error for faster evaluations of the impact of pumping, in deeper aquifers where the differences are small. However, in parts of Cameron County where current desalination plants are located, the differences can be as large as 5,000 mg/L in the Chicot Aquifer and therefore analyses of chloride migration using a non-density version of the model may have larger errors in that area.

Figure 6.7.13 shows the TDS Concentrations in groundwater at Existing Desalination Plant Wells for the 1984-2013 Simulation Period (see Figure 2.6.6 for Desalination Plant locations) for the Base Case, No Pumping, and No Density transport simulations. The wells show increasing as well as decreasing trends depending on initial salt concentrations. Also, the impact of no pumping or no density effects varied depending on local conditions. For instance, concentrations in groundwater at Plant 2 were increasing, while those at Plant 4 which is just to the south showed decreasing concentration trends; similar to Plant 1 slightly east-southeast from Plant 4. All three simulations showed similar concentration behavior at these locations. Plants 6 and 7 which are nearer to the coast showed stable to slightly increasing concentrations. The no-density case deviated significantly from the base-case and no-pumping cases for these locations indicating that the density term had a considerable impact on the flow-field an associated concentration changes. Plants 3 and 5 show similar results for the no-pumping and no-density case which are different than the base case results. This behavior may be attributed to complex migration behavior depending on initial salt concentrations and flow patterns. Just east of Plant 3, for instance, it is noted that there is an inversion in concentrations between layers 3 and 4 (layer 3 is absent as the Evangeline Aquifer outcrops just above Plant 3. The initial lowering of concentrations can be attributed to the flow-field in layer 4 causing freshening activities for all three simulations. The density dependent simulation however, causes additional migration of the salts down from layer 3 which are attracted towards the Plant 3 pumping well in the base-case scenario causing the related increase in concentrations. Thus, it is noted that migration of salts is a complex process and wells may behave differently depending on the nature of the simulation and the initial concentrations of TDS in the model.

Table 6.7.1 shows the execution times for the various transport simulations and the calibrated flow model simulation. The groundwater flow model takes almost 4 hours to complete the 30-year simulation. Running the simulation for transport of TDS without density effects adds about 45 minutes. Including density coupling in the simulations increased the computational burden significantly, taking almost 14 hours to complete the 30-year simulation. Thus, simulations may be faster if concentration differences are small at study locations. Also, if only flow impacts are significant to a simulation, predictive simulations may be performed using only the groundwater flow version of the model. Furthermore, since the concentration changes in most of the domain were small, the density effect would generally cancel out in these locations for drawdown computations.

The simulation of density dependent flow and transport without any wells took 5 hours and 15 minutes to complete the 30-year simulation run. Thus, it seems that the difficulties encountered in the density dependent simulations were largely in the CLN domain representing the pumping wells. Alternate representations of wells or adjustments on the well conductance term may yet help speed up the density dependent flow and transport simulations.

7.0 Modeling Assumptions and Limitations

Several simplifications, assumptions and approximations have been made in developing the LRGV flow and transport model. Representation of the domain by discrete finite-volumes; approximation of groundwater flow by the continuity equation and Darcy's Law; and of the various boundary conditions and stresses by steady-state or annual average conditions, create an idealized representation of the flow system enabling regional evaluations at long time-scales (of years to decades). Errors are also associated with mesh design, aquifer or boundary geometry or areal extent, and the configuration of hydrologic components (conceptualization errors). These errors were minimized during model development and further evaluated and reduced during model calibration.

Data that is incorporated into a model may be incomplete, may contain errors, or may be incompatible with the modeled spatial and temporal scale. Measurement errors were estimated and their impacts were considered by using a lower calibration weighting when these errors were obvious. Pumping information, diversion amounts, return-flow estimates, and data on groundwater interactions of the LRG and irrigation canals were not complete or were only rough estimates. This also affects the model calibration and therefore sensitivity analyses to these stresses were conducted to evaluate their significance.

A groundwater flow model requires that the entire domain be appropriately parameterized. Although information exists on general aquifer characteristics, and more detailed sand fraction distributions were available for the geologic units, detailed hydrologic characterization is not possible except by extrapolating information from areas where data is available. This lack of information can introduce uncertainty and errors in model results, especially in complex faulted systems such as the LRG Basin. Sensitivity analyses helped to quantify the impact of these errors for the various parameters and conceptual model elements.

The LRGV model has been developed to evaluate the long-term impacts of planned future desalination plant operations on water levels, groundwater/surface-water interactions, and TDS concentrations within the domain. Therefore, appropriate assumptions have been made to develop a model that is consistent with these objectives. General modeling assumptions have

been noted in the model development and calibration process. Some significant assumptions include:

The spatial resolution of the model was set to provide a regional evaluation of groundwater flow with refined discretization around surface-water features to capture the groundwater/surface-water interaction in a detailed manner.

The temporal resolution of the model was set to annual stress periods for recharge, pumping and boundary flows for long-term planning purposes.

It was assumed that the kriged sand fractions of the geologic units correlated with the horizontal and vertical hydraulic conductivity values at any given location. Also, the horizontal hydraulic conductivity was assumed to be the weighted arithmetic mean of sand and clay conductivities, while the vertical hydraulic conductivity was assumed to be the weighted harmonic mean of the sand and clay conductivities.

Annually average stresses were used for the simulations which were calibrated to water levels averaged annually for winter conditions. It is therefore assumed that the calibration is representative considering the averaging of data.

The effective transport porosity was assumed to be correlated to sand fractions. The conceptual transport model considered the effective transport domain to be in the sand and that the clay did not participate in the active flow and transport domain. Net transport of salts was noted to be relatively small in the 30-year simulation period especially in the deeper layers.

The model limitations further include uncertainty in predictions. Predictive sensitivity analyses should also be conducted with predictions of significance, to evaluate the impact of parameter variations on the prediction. Categorizing the predictive sensitivities along with calibration sensitivities as per ASTM (1994, 2000) provides further information on the significance of data to the predictions.

7.1   Further Research

A groundwater flow and transport model of the LRGV was developed in this project using the MODFLOW-USG software. The hydrogeologic units were subdivided into multiple numerical layers coincident with the geologic units to provide finer vertical resolution within each hydrogeologic unit for the TDS transport computations. Use of nested grids facilitated providing finer resolution to the numerical discretization near surface-water features to accurately capture the interactions. Pinch-outs and outcrops were handled in a geologically consistent manner. The Groundwater Vistas GUI was used to develop the model. Multiple calibration metrics were used to constrain the model. The groundwater flow model generally depicts conditions within the domain during the 1984-2013 simulation period for annually averaged stress conditions.

A groundwater transport model was also developed for the LRGV domain. Transport with and without density effects was evaluated. Also, the impact of initial and boundary conditions was evaluated. The model will be used for evaluating the impact of additional desalination plant pumping from the domain.

There were several challenges overcome by this study. A regional domain was simulated with sufficient resolution of the solution near surface-water features by use of quadpatch grid refinement. Wells were depicted appropriately as multi-aquifer conduits with analytical solutions providing accurate drawdown computations at the well. Density dependent flow conditions were

also evaluated; however, these simulations were slower and exhibited convergence difficulties. Transport of salts was also evaluated for non-pumping conditions and where density impacts on flow are neglected to better understand the driving forces and how initial concentration estimates play into them. Further research suggested by this work includes:

A further evaluation of sand fraction distributions along with hydraulic conductivity data for the Chicot Aquifer will help constrain hydraulic conductivity values for the Beaumont, Lissie and Willis Formations that comprise the modeled Chicot Aquifer. Currently modeled hydraulic conductivity distributions do not match field distributions or conceptual understanding of the geologic setting. Chicot Aquifer hydraulic conductivity values are generally higher in the River Valley than in the counties further north; however, that was not depicted by the model because the sand fraction distributions that were used to parameterize the hydraulic conductivity of the model did not follow that trend. The raw sand fraction data should be reviewed along with estimated hydraulic conductivity variations to improve the sand fraction distribution representation. The data may also show differences in material types between regions which can be used to further categorize the hydraulic conductivity correlations – i.e., have different sand types for the geologic units comprising the Chicot Aquifer in the different areal locations, with each sand type having its own hydraulic conductivity correlation. Also, field measurements of hydraulic conductivity are at a different scale than model grid sizes and there may be other considerations in field estimates of hydraulic conductivity that may cause differences.

Adding a more refined grid in the west of the domain where the topography steeply dips towards the LRG. A more refined grid with additional calibration zones or adjustments to sand fractions within this region would help to depict water levels here more accurately. Currently there is no specific objective affected by this area but this adjustment would help improve water level gradients in the area and avoid flooded cells in the model altogether.

Improvement of convergence and efficiency on density dependent transport simulations. The density dependent transport simulations took significantly longer to run than the flow model or the flow and transport model without density impacts. Also, the density dependent simulation did not converge during six of the time-steps in the simulation. An investigation of why this is the case at the model's matrix level should help understand the situation and improve simulation performance. Difficulties that were encountered with density dependent flow in the CLN package may also benefit from further investigations at the matrix level or use of alternate representations of flow to CLN wells. The SAMG multi-grid parallel solver may further help to speed up computations – SAMG is a proprietary solver that is hooked up to MFUSG-Beta through the Groundwater Vistas Interface.

The density dependent simulations also depict hydraulic head distributions throughout the model domain, which are different from groundwater flow hydraulic heads without the density impacts of salts. The initial distributions of TDS implemented into the model were noted to significantly impact the density-driven hydraulic heads. The BRACS database should be revisited in an iterative manner along with the density dependent model, to better understand the distribution of salts within and among the geologic units by evaluating the hydraulic head distributions and smoothening out sharp concentration gradients in areas of sparse data.

The density dependent model indicated that there was inversion of salts during the 30 year simulation period in the Chicot Aquifer in eastern Brooks and western Kenedy Counties. This occurred mostly because initial TDS concentrations were higher in shallower layers than in

deeper layers of the Chicot Aquifer. Unless these higher TDS concentrations were trapped in or above lower conductivity units, the model indicates that they will move downward due to density effects in 30 years. The BRACS database should be further evaluated for correlations with sand fractions to note if there may be geologic controls to salinity distributions. There may be higher concentrations of older water trapped in finer materials; alternatively, there may be brackish conditions that are transported rapidly through the higher conductivity sands; or it may be neither. Understanding these controls will help with establishing improved TDS concentration distributions within and among the various geologic units.

8.0 References

ASTM, 1994 (reapproved 2000). Standard Guide for Conducting a Sensitivity Analysis for a Ground-Water Flow Model Application, ASTM D 5611-94. ASTM International, West Conshohocken, PA 19428-2959.

Chowdhury, A., and Mace, R.E., 2007, Groundwater resource evaluation and availability model of the Gulf Coast Aquifer in the Lower Rio Grande Valley of Texas: Texas Water Development Board Report 368, June 2007, 119 p.

Environmental Simulations Inc., 2016. Groundwater Vistas Version 6.93, available from www.groundwatermodels.com.

Harbaugh, A.W., 2005, MODFLOW-2005, the U.S. Geological Survey modular ground-water model -- the Ground-Water Flow Process: U.S. Geological Survey Techniques and Methods 6-A16, variously p.

Meader, N., 2015. A Review of Riparian Mesquite and Crop Water Use, Lower San Pedro Watershed Alliance, and Cascabel Conservation Association, Arizona.

Montgomery and Associates, 2017. Conceptual Model Report: Lower Rio Grande Valley Groundwater Transport Model, Prepared for Texas Water Development Board, January 31, 2017.

Niswonger, R.G., Panday, Sorab, and Ibaraki, Motomu, 2011, MODFLOW-NWT, A Newton formulation for MODFLOW-2005: U.S. Geological Survey Techniques and Methods 6–A37, 44p.

Scanlon, B., K. Keese, N. Bonal, N. Deeds, V. Kelley, and M. Litvak, 2005. Evapotranspiration estimates with emphasis on groundwater evapotranspiration in Texas, Prepared for Texas Water Development Board.

Schorr, S., W. R. Hutchison, S. Panday, J. Rumbaugh, 2017. Conceptual Model Report: Lower Rio Grande Valley Groundwater Transport Model, Final Report prepared for Texas Water Development Board.

Table 2.1.1 Summary of model input packages.

Package type	Abbreviation	Description
Namefile	NAM	Controls all other model files and names
Basic	BAS	Sets up basic model and stress periods
Discretization	DIS	Discretizes groundwater domain
Layer Property Flow	LPF	Provides aquifer properties
Connected Linear Network	CLN	Discretize 1-D domain
	WEL	Implement sources/sinks
Prescribed Head	CHD	Implement constant head boundary
General Head Boundary	GHB	Implement head-dependent flux boundary
	RIV	Implement river boundary
Sink with return flow	QRT	Implement sink with return flow
Recharge	RCH	Implement recharge
Evaportanspiration	EVT	Implement evaportanspiration
Output Control	OC	Control simulation output
Solver	SMS	Implement solver parameters
Hydraulic Flow Barrier	HFB[1]	Implement barriers to flow within domain
Block Centered Transport	BCT[2]	Solves for transport of solute
Density Dependent Flow	DDF[2]	Couples density term to transport

Notes:

1. Package was used in sensitivity simulations to occurrence of faults

2. Packages used for density dependent flow and transport simulations

Table 2.1.2 Summary of model output packages.

Output Type	Abbreviation	Description
Listfile	LST	Lists model input, simulation summary, and mass balance
GWF Head output	HDS	Contains head output for all GWF cells at all stress periods
CLN Head output	_cln.HDS	Contains head output for all CLN cells at all stress periods
Cell-by-cell flows	CBB	Contains CBB output for all cells at all stress periods
GWF Concentration output	CON	Contains TDS output for all GWF cells at all stress periods
Cell-by-cell TDS transport	CCB	Contains CCB output for all cells at all stress periods

Table 2.4.1 Stress period setup.

Stress period	Length (days)	Representative year	Type
1	365	1984	Steady state
2	365	1985	Transient
3	365	1986	Transient
4	365	1987	Transient
5	365	1988	Transient
6	365	1989	Transient
7	365	1990	Transient
8	365	1991	Transient
9	365	1992	Transient
10	365	1993	Transient
11	365	1994	Transient
12	365	1995	Transient
13	365	1996	Transient
14	365	1997	Transient
15	365	1998	Transient
16	365	1999	Transient
17	365	2000	Transient
18	365	2001	Transient
19	365	2002	Transient
20	365	2003	Transient
21	365	2004	Transient
22	365	2005	Transient
23	365	2006	Transient
24	365	2007	Transient
25	365	2008	Transient
26	365	2009	Transient
27	365	2010	Transient
28	365	2011	Transient
29	365	2012	Transient
30	365	2013	Transient

Table 2.10.1 General head boundary conditions.

Cell Number	GHB Head (feet)	GHB Conductance (feet^3/day)	GHB Concentration (mg/L)	Hydraulic Feature
681170	397.612312	10000	6500	Lateral boundary
681405	393.31727	10000	6500	Lateral boundary
681640	389.022228	10000	6500	Lateral boundary
681875	384.727186	10000	6500	Lateral boundary
682110	380.432144	10000	6500	Lateral boundary
682345	376.137102	10000	6500	Lateral boundary
682580	371.84206	10000	6500	Lateral boundary
682815	367.547018	10000	6500	Lateral boundary
683050	363.251976	10000	6500	Lateral boundary
683286	358.956934	10000	6500	Lateral boundary
683522	354.661892	10000	6500	Lateral boundary
683758	350.36685	10000	6500	Lateral boundary
683995	346.071808	10000	6500	Lateral boundary
684232	341.776766	10000	6500	Lateral boundary
684470	337.481723	10000	6500	Lateral boundary
684708	333.186681	10000	6500	Lateral boundary
684946	328.891639	10000	6500	Lateral boundary
685185	324.596597	10000	6500	Lateral boundary
685424	320.301555	10000	6500	Lateral boundary
685664	316.006513	10000	6500	Lateral boundary
685904	311.711471	10000	6500	Lateral boundary
686144	307.416429	10000	6500	Lateral boundary
686385	303.121387	10000	6500	Lateral boundary
686626	298.826345	10000	6500	Lateral boundary
686868	294.531303	10000	6500	Lateral boundary
687110	290.236261	10000	6500	Lateral boundary
687352	285.941219	10000	6500	Lateral boundary
687595	281.646176	10000	6500	Lateral boundary
687838	277.351134	10000	6500	Lateral boundary
688082	273.056092	10000	6500	Lateral boundary
688326	268.76105	10000	6500	Lateral boundary
688570	264.466008	10000	6500	Lateral boundary
688814	260.170966	10000	6500	Lateral boundary
689059	255.875924	10000	6500	Lateral boundary
689304	251.580882	10000	6500	Lateral boundary
689549	247.28584	10000	6500	Lateral boundary
689794	242.990798	10000	6500	Lateral boundary
690040	238.695756	10000	6500	Lateral boundary
690286	234.400714	10000	6500	Lateral boundary
690532	230.105672	10000	6500	Lateral boundary

Cell Number	GHB Head (feet)	GHB Conductance (feet^3/day)	GHB Concentration (mg/L)	Hydraulic Feature
690779	225.81063	10000	6500	Lateral boundary
691026	221.515587	10000	6500	Lateral boundary
691282	217.220545	10000	6500	Lateral boundary
691550	212.925503	10000	6500	Lateral boundary
691819	208.630461	10000	6500	Lateral boundary
692097	204.335419	10000	6500	Lateral boundary
692390	200.040377	10000	6500	Lateral boundary
692704	195.745335	10000	6500	Lateral boundary
693076	191.450293	10000	6500	Lateral boundary
693544	187.155251	10000	6500	Lateral boundary
693898	182.860209	10000	6500	Lateral boundary
694223	178.565167	10000	6500	Lateral boundary
694584	174.270125	10000	6500	Lateral boundary
694924	169.975083	10000	6500	Lateral boundary
695267	165.68004	10000	6500	Lateral boundary
695623	161.384998	10000	6500	Lateral boundary
695973	157.089956	10000	6500	Lateral boundary
696311	152.794914	10000	6500	Lateral boundary
696659	150.323872	10000	6500	Lateral boundary
697058	150	10000	6500	Lateral boundary
697062	150	10000	6500	Lateral boundary
697066	150	10000	6500	Lateral boundary
697070	150	10000	6500	Lateral boundary
697616	150	10000	6500	Lateral boundary
697618	150	10000	6500	Lateral boundary
698285	150	10000	6500	Lateral boundary
698287	150	10000	6500	Lateral boundary
698835	150	10000	6500	Lateral boundary
699502	150	10000	6500	Lateral boundary
700226	150	10000	6500	Lateral boundary
700980	150	10000	6500	Lateral boundary
701612	150	10000	6500	Lateral boundary
702181	150	10000	6500	Lateral boundary
702756	150	10000	6500	Lateral boundary
703392	150	10000	6500	Lateral boundary
703959	150	10000	6500	Lateral boundary
704538	150	10000	6500	Lateral boundary
705171	150	10000	6500	Lateral boundary
705871	150	10000	6500	Lateral boundary
706619	150	10000	6500	Lateral boundary
707310	150	10000	6500	Lateral boundary
708013	150	10000	6500	Lateral boundary

Cell Number	GHB Head (feet)	GHB Conductance (feet^3/day)	GHB Concentration (mg/L)	Hydraulic Feature
708765	150	10000	6500	Lateral boundary
670238	600	26410000	35000	Lateral boundary
670239	600	26400000	35000	Lateral boundary
670240	600	26400000	35000	Lateral boundary
670241	600	26400000	35000	Lateral boundary
670242	600	26400000	35000	Lateral boundary
670243	600	26400000	35000	Lateral boundary
670244	600	26400000	35000	Lateral boundary
670245	600	26400000	35000	Lateral boundary
670246	600	26400000	35000	Lateral boundary
670247	600	26400000	35000	Lateral boundary
670248	600	26400000	35000	Lateral boundary
670249	600	26400000	35000	Lateral boundary
670250	600	26400000	35000	Lateral boundary
670251	600	26400000	35000	Lateral boundary
670252	600	15590000	35000	Lateral boundary
670253	596.824078	22880000	35000	Lateral boundary
670254	594.991977	26400000	35000	Lateral boundary
670255	591.327777	26400000	35000	Lateral boundary
670256	587.663577	26400000	35000	Lateral boundary
670257	583.999376	26400000	35000	Lateral boundary
670258	580.335176	26400000	35000	Lateral boundary
670259	576.670975	26400000	35000	Lateral boundary
670260	573.006775	26400000	35000	Lateral boundary
670261	569.342575	26400000	35000	Lateral boundary
670262	565.678374	26400000	35000	Lateral boundary
670263	562.014174	26400000	35000	Lateral boundary
670264	558.349974	26400000	35000	Lateral boundary
670265	554.685773	26400000	35000	Lateral boundary
670266	551.021573	26400000	35000	Lateral boundary
670267	547.357372	26400000	35000	Lateral boundary
670268	543.693172	26410000	35000	Lateral boundary
670269	540.028972	26400000	35000	Lateral boundary
670270	536.364771	26400000	35000	Lateral boundary
670271	532.700571	26400000	35000	Lateral boundary
670272	529.03637	26400000	40000	Lateral boundary
670273	525.37217	26400000	40000	Lateral boundary
670274	521.770035	25500000	40000	Lateral boundary
670275	515.917273	23710000	40000	Lateral boundary
670276	513.64472	26400000	40000	Lateral boundary
670277	509.099614	26400000	40000	Lateral boundary
670278	504.554507	26400000	40000	Lateral boundary

Cell Number	GHB Head (feet)	GHB Conductance (feet^3/day)	GHB Concentration (mg/L)	Hydraulic Feature
670279	500.009401	26400000	40000	Lateral boundary
670280	495.464294	26400000	40000	Lateral boundary
670281	490.919188	26400000	40000	Lateral boundary
670282	486.374082	26400000	40000	Lateral boundary
670283	481.828975	26400000	40000	Lateral boundary
670284	477.283869	26400000	40000	Lateral boundary
670285	472.738762	26400000	40000	Lateral boundary
670286	468.193656	26400000	40000	Lateral boundary
670287	463.648549	26400000	40000	Lateral boundary
670288	459.103443	26400000	40000	Lateral boundary
670289	454.558337	26400000	40000	Lateral boundary
670290	450.01323	26400000	40000	Lateral boundary
670291	445.468124	26400000	40000	Lateral boundary
670292	440.923017	26400000	40000	Lateral boundary
670293	436.377911	26400000	40000	Lateral boundary
670294	431.832804	26400000	40000	Lateral boundary
670295	427.287698	26400000	40000	Lateral boundary
670296	423.507572	17520000	40000	Lateral boundary
670297	417.072472	20960000	40000	Lateral boundary
670298	413.970221	26400000	40000	Lateral boundary
670299	407.765719	26400000	40000	Lateral boundary
670300	401.561217	26400000	40000	Lateral boundary
670301	395.356715	26400000	40000	Lateral boundary
670302	389.152213	26400000	40000	Lateral boundary
670303	382.947711	26400000	40000	Lateral boundary
670304	376.743209	26400000	40000	Lateral boundary
670305	370.538707	26400000	40000	Lateral boundary
670306	364.334205	26400000	40000	Lateral boundary
670307	358.129703	26400000	40000	Lateral boundary
670308	351.925201	26400000	40000	Lateral boundary
670309	345.720699	26400000	40000	Lateral boundary
670310	339.516197	26400000	40000	Lateral boundary
670311	333.311694	26400000	40000	Lateral boundary
670312	327.107192	26400000	40000	Lateral boundary
670313	320.90269	26400000	40000	Lateral boundary
670314	314.698188	26400000	40000	Lateral boundary
670315	308.493686	26400000	40000	Lateral boundary
670316	302.695718	22950000	40000	Lateral boundary
393576	551.021573	26400000	6500	Lateral boundary
393577	547.357372	26400000	6500	Lateral boundary
393578	543.693172	26410000	6500	Lateral boundary
393579	540.028972	26400000	6500	Lateral boundary

Cell Number	GHB Head (feet)	GHB Conductance (feet^3/day)	GHB Concentration (mg/L)	Hydraulic Feature
393580	536.364771	26400000	6500	Lateral boundary
393581	532.700571	26400000	6500	Lateral boundary
393582	529.03637	26400000	6500	Lateral boundary
393583	525.37217	26400000	500	Lateral boundary
393584	521.770035	25500000	500	Lateral boundary
393585	515.917273	23710000	500	Lateral boundary
393586	513.64472	26400000	500	Lateral boundary
393587	509.099614	26400000	500	Lateral boundary
393588	504.554507	26400000	500	Lateral boundary
393589	500.009401	26400000	500	Lateral boundary
393590	495.464294	26400000	500	Lateral boundary
393591	490.919188	26400000	500	Lateral boundary
393592	486.374082	26400000	500	Lateral boundary
393593	481.828975	26400000	500	Lateral boundary
393594	477.283869	26400000	500	Lateral boundary
393595	472.738762	26400000	500	Lateral boundary
393596	468.193656	26400000	6500	Lateral boundary
393597	463.648549	26400000	6500	Lateral boundary
393598	459.103443	26400000	6500	Lateral boundary
393599	454.558337	26400000	6500	Lateral boundary
393600	450.01323	26400000	6500	Lateral boundary
393601	445.468124	26400000	6500	Lateral boundary
393602	440.923017	26400000	6500	Lateral boundary
393603	436.377911	26400000	6500	Lateral boundary
393604	431.832804	26400000	6500	Lateral boundary
393605	427.287698	26400000	6500	Lateral boundary
393606	423.507572	17520000	6500	Lateral boundary
393607	417.072472	20960000	22500	Lateral boundary
393608	413.970221	26400000	22500	Lateral boundary
393609	407.765719	26400000	22500	Lateral boundary
393610	401.561217	26400000	22500	Lateral boundary
393611	395.356715	26400000	22500	Lateral boundary
393612	389.152213	26400000	22500	Lateral boundary
393613	382.947711	26400000	22500	Lateral boundary
393614	376.743209	26400000	22500	Lateral boundary
393615	370.538707	26400000	22500	Lateral boundary
393616	364.334205	26400000	22500	Lateral boundary
393617	358.129703	26400000	22500	Lateral boundary
393618	351.925201	26400000	22500	Lateral boundary
393619	345.720699	26400000	22500	Lateral boundary
393620	339.516197	26400000	22500	Lateral boundary
393621	333.311694	26400000	22500	Lateral boundary

Cell Number	GHB Head (feet)	GHB Conductance (feet^3/day)	GHB Concentration (mg/L)	Hydraulic Feature
393622	327.107192	26400000	22500	Lateral boundary
393623	320.90269	26400000	22500	Lateral boundary
393624	314.698188	26400000	22500	Lateral boundary
393625	308.493686	26400000	22500	Lateral boundary
393626	302.695718	22950000	22500	Lateral boundary
459944	600	26400000	1500	Lateral boundary
459945	600	15590000	1500	Lateral boundary
459946	596.824078	22880000	1500	Lateral boundary
459947	594.991977	26400000	1500	Lateral boundary
459948	591.327777	26400000	1500	Lateral boundary
459949	587.663577	26400000	1500	Lateral boundary
459950	583.999376	26400000	1500	Lateral boundary
459951	580.335176	26400000	1500	Lateral boundary
459952	576.670975	26400000	1500	Lateral boundary
459953	573.006775	26400000	1500	Lateral boundary
459954	569.342575	26400000	1500	Lateral boundary
459955	565.678374	26400000	1500	Lateral boundary
459956	562.014174	26400000	1500	Lateral boundary
459957	558.349974	26400000	1500	Lateral boundary
459958	554.685773	26400000	1500	Lateral boundary
459959	551.021573	26400000	1500	Lateral boundary
459960	547.357372	26400000	1500	Lateral boundary
459961	543.693172	26410000	1500	Lateral boundary
459962	540.028972	26400000	1500	Lateral boundary
459963	536.364771	26400000	1500	Lateral boundary
459964	532.700571	26400000	1500	Lateral boundary
459965	529.03637	26400000	1500	Lateral boundary
459966	525.37217	26400000	6500	Lateral boundary
459967	521.770035	25500000	6500	Lateral boundary
459968	515.917273	23710000	6500	Lateral boundary
459969	513.64472	26400000	6500	Lateral boundary
459970	509.099614	26400000	6500	Lateral boundary
459971	504.554507	26400000	6500	Lateral boundary
459972	500.009401	26400000	6500	Lateral boundary
459973	495.464294	26400000	6500	Lateral boundary
459974	490.919188	26400000	6500	Lateral boundary
459975	486.374082	26400000	6500	Lateral boundary
459976	481.828975	26400000	6500	Lateral boundary
459977	477.283869	26400000	6500	Lateral boundary
459978	472.738762	26400000	6500	Lateral boundary
459979	468.193656	26400000	6500	Lateral boundary
459980	463.648549	26400000	6500	Lateral boundary

Cell Number	GHB Head (feet)	GHB Conductance (feet^3/day)	GHB Concentration (mg/L)	Hydraulic Feature
459981	459.103443	26400000	6500	Lateral boundary
459982	454.558337	26400000	6500	Lateral boundary
459983	450.01323	26400000	6500	Lateral boundary
459984	445.468124	26400000	6500	Lateral boundary
459985	440.923017	26400000	6500	Lateral boundary
459986	436.377911	26400000	6500	Lateral boundary
459987	431.832804	26400000	6500	Lateral boundary
459988	427.287698	26400000	6500	Lateral boundary
459989	423.507572	17520000	6500	Lateral boundary
459990	417.072472	20960000	22500	Lateral boundary
459991	413.970221	26400000	22500	Lateral boundary
459992	407.765719	26400000	22500	Lateral boundary
459993	401.561217	26400000	22500	Lateral boundary
459994	395.356715	26400000	22500	Lateral boundary
459995	389.152213	26400000	22500	Lateral boundary
459996	382.947711	26400000	22500	Lateral boundary
459997	376.743209	26400000	22500	Lateral boundary
459998	370.538707	26400000	22500	Lateral boundary
459999	364.334205	26400000	22500	Lateral boundary
460000	358.129703	26400000	22500	Lateral boundary
460001	351.925201	26400000	22500	Lateral boundary
460002	345.720699	26400000	22500	Lateral boundary
460003	339.516197	26400000	22500	Lateral boundary
460004	333.311694	26400000	22500	Lateral boundary
460005	327.107192	26400000	22500	Lateral boundary
460006	320.90269	26400000	22500	Lateral boundary
460007	314.698188	26400000	22500	Lateral boundary
460008	308.493686	26400000	22500	Lateral boundary
460009	302.695718	22950000	22500	Lateral boundary
528218	600	26400000	3888.8	Lateral boundary
528219	600	26400000	3888.8	Lateral boundary
528220	600	26400000	3888.8	Lateral boundary
528221	600	26400000	3888.8	Lateral boundary
528222	600	26400000	3888.8	Lateral boundary
528223	600	26400000	3888.8	Lateral boundary
528224	600	26400000	3888.8	Lateral boundary
528225	600	26400000	3888.8	Lateral boundary
528226	600	26400000	3888.8	Lateral boundary
528227	600	26400000	3888.8	Lateral boundary
528228	600	26400000	3888.8	Lateral boundary
528229	600	26400000	3888.8	Lateral boundary
528230	600	15590000	3888.8	Lateral boundary

Cell Number	GHB Head (feet)	GHB Conductance (feet^3/day)	GHB Concentration (mg/L)	Hydraulic Feature
528231	596.824078	22880000	3888.8	Lateral boundary
528232	594.991977	26400000	3888.8	Lateral boundary
528233	591.327777	26400000	3888.8	Lateral boundary
528234	587.663577	26400000	3888.8	Lateral boundary
528235	583.999376	26400000	3888.8	Lateral boundary
528236	580.335176	26400000	3888.8	Lateral boundary
528237	576.670975	26400000	3888.8	Lateral boundary
528238	573.006775	26400000	3888.8	Lateral boundary
528239	569.342575	26400000	6500	Lateral boundary
528240	565.678374	26400000	6500	Lateral boundary
528241	562.014174	26400000	6500	Lateral boundary
528242	558.349974	26400000	6500	Lateral boundary
528243	554.685773	26400000	6500	Lateral boundary
528244	551.021573	26400000	6500	Lateral boundary
528245	547.357372	26400000	6500	Lateral boundary
528246	543.693172	26410000	6500	Lateral boundary
528247	540.028972	26400000	6500	Lateral boundary
528248	536.364771	26400000	6500	Lateral boundary
528249	532.700571	26400000	6500	Lateral boundary
528250	529.03637	26400000	6500	Lateral boundary
528251	525.37217	26400000	6500	Lateral boundary
528252	521.770035	25500000	6500	Lateral boundary
528253	515.917273	23710000	6500	Lateral boundary
528254	513.64472	26400000	6500	Lateral boundary
528255	509.099614	26400000	6500	Lateral boundary
528256	504.554507	26400000	6500	Lateral boundary
528257	500.009401	26400000	6500	Lateral boundary
528258	495.464294	26400000	6500	Lateral boundary
528259	490.919188	26400000	6500	Lateral boundary
528260	486.374082	26400000	6500	Lateral boundary
528261	481.828975	26400000	6500	Lateral boundary
528262	477.283869	26400000	6500	Lateral boundary
528263	472.738762	26400000	6500	Lateral boundary
528264	468.193656	26400000	6500	Lateral boundary
528265	463.648549	26400000	6500	Lateral boundary
528266	459.103443	26400000	6500	Lateral boundary
528267	454.558337	26400000	6500	Lateral boundary
528268	450.01323	26400000	6500	Lateral boundary
528269	445.468124	26400000	6500	Lateral boundary
528270	440.923017	26400000	6500	Lateral boundary
528271	436.377911	26400000	6500	Lateral boundary
528272	431.832804	26400000	6500	Lateral boundary

Cell Number	GHB Head (feet)	GHB Conductance (feet^3/day)	GHB Concentration (mg/L)	Hydraulic Feature
528273	427.287698	26400000	6500	Lateral boundary
528274	423.507572	17520000	22500	Lateral boundary
528275	417.072472	20960000	22500	Lateral boundary
528276	413.970221	26400000	22500	Lateral boundary
528277	407.765719	26400000	22500	Lateral boundary
528278	401.561217	26400000	22500	Lateral boundary
528279	395.356715	26400000	22500	Lateral boundary
528280	389.152213	26400000	22500	Lateral boundary
528281	382.947711	26400000	22500	Lateral boundary
528282	376.743209	26400000	22500	Lateral boundary
528283	370.538707	26400000	22500	Lateral boundary
528284	364.334205	26400000	22500	Lateral boundary
528285	358.129703	26400000	22500	Lateral boundary
528286	351.925201	26400000	22500	Lateral boundary
528287	345.720699	26400000	22500	Lateral boundary
528288	339.516197	26400000	22500	Lateral boundary
528289	333.311694	26400000	22500	Lateral boundary
528290	327.107192	26400000	22500	Lateral boundary
528291	320.90269	26400000	22500	Lateral boundary
528292	314.698188	26400000	22500	Lateral boundary
528293	308.493686	26400000	22500	Lateral boundary
528294	302.695718	22950000	22500	Lateral boundary
598611	600	26400000	6500	Lateral boundary
598612	600	26400000	6500	Lateral boundary
598613	600	26400000	6500	Lateral boundary
598614	600	26400000	6500	Lateral boundary
598615	600	26400000	6500	Lateral boundary
598616	600	26400000	6500	Lateral boundary
598617	600	26400000	6500	Lateral boundary
598618	600	26400000	6500	Lateral boundary
598619	600	26400000	6500	Lateral boundary
598620	600	26400000	6500	Lateral boundary
598621	600	26400000	6500	Lateral boundary
598622	600	26400000	6500	Lateral boundary
598623	600	26400000	6500	Lateral boundary
598624	600	15590000	6500	Lateral boundary
598625	596.824078	22880000	6500	Lateral boundary
598626	594.991977	26400000	6500	Lateral boundary
598627	591.327777	26400000	6500	Lateral boundary
598628	587.663577	26400000	6500	Lateral boundary
598629	583.999376	26400000	6500	Lateral boundary
598630	580.335176	26400000	22500	Lateral boundary

Cell Number	GHB Head (feet)	GHB Conductance (feet^3/day)	GHB Concentration (mg/L)	Hydraulic Feature
598631	576.670975	26400000	22500	Lateral boundary
598632	573.006775	26400000	22500	Lateral boundary
598633	569.342575	26400000	22500	Lateral boundary
598634	565.678374	26400000	22500	Lateral boundary
598635	562.014174	26400000	22500	Lateral boundary
598636	558.349974	26400000	22500	Lateral boundary
598637	554.685773	26400000	22500	Lateral boundary
598638	551.021573	26400000	22500	Lateral boundary
598639	547.357372	26400000	22500	Lateral boundary
598640	543.693172	26410000	22500	Lateral boundary
598641	540.028972	26400000	22500	Lateral boundary
598642	536.364771	26400000	22500	Lateral boundary
598643	532.700571	26400000	22500	Lateral boundary
598644	529.03637	26400000	22500	Lateral boundary
598645	525.37217	26400000	22500	Lateral boundary
598646	521.770035	25500000	22500	Lateral boundary
598647	515.917273	23710000	22500	Lateral boundary
598648	513.64472	26400000	22500	Lateral boundary
598649	509.099614	26400000	22500	Lateral boundary
598650	504.554507	26400000	22500	Lateral boundary
598651	500.009401	26400000	22500	Lateral boundary
598652	495.464294	26400000	22500	Lateral boundary
598653	490.919188	26400000	22500	Lateral boundary
598654	486.374082	26400000	22500	Lateral boundary
598655	481.828975	26400000	22500	Lateral boundary
598656	477.283869	26400000	22500	Lateral boundary
598657	472.738762	26400000	22500	Lateral boundary
598658	468.193656	26400000	22500	Lateral boundary
598659	463.648549	26400000	22500	Lateral boundary
598660	459.103443	26400000	22500	Lateral boundary
598661	454.558337	26400000	22500	Lateral boundary
598662	450.01323	26400000	22500	Lateral boundary
598663	445.468124	26400000	22500	Lateral boundary
598664	440.923017	26400000	22500	Lateral boundary
598665	436.377911	26400000	22500	Lateral boundary
598666	431.832804	26400000	40000	Lateral boundary
598667	427.287698	26400000	40000	Lateral boundary
598668	423.507572	17520000	40000	Lateral boundary
598669	417.072472	20960000	40000	Lateral boundary
598670	413.970221	26400000	40000	Lateral boundary
598671	407.765719	26400000	40000	Lateral boundary
598672	401.561217	26400000	40000	Lateral boundary

Cell Number	GHB Head (feet)	GHB Conductance (feet^3/day)	GHB Concentration (mg/L)	Hydraulic Feature
598673	395.356715	26400000	40000	Lateral boundary
598674	389.152213	26400000	40000	Lateral boundary
598675	382.947711	26400000	40000	Lateral boundary
598676	376.743209	26400000	40000	Lateral boundary
598677	370.538707	26400000	40000	Lateral boundary
598678	364.334205	26400000	40000	Lateral boundary
598679	358.129703	26400000	40000	Lateral boundary
598680	351.925201	26400000	40000	Lateral boundary
598681	345.720699	26400000	40000	Lateral boundary
598682	339.516197	26400000	40000	Lateral boundary
598683	333.311694	26400000	40000	Lateral boundary
598684	327.107192	26400000	40000	Lateral boundary
598685	320.90269	26400000	40000	Lateral boundary
598686	314.698188	26400000	40000	Lateral boundary
598687	308.493686	26400000	40000	Lateral boundary
598688	302.695718	22950000	40000	Lateral boundary
670232	554.432582	26090000	6500	Lateral boundary
670233	563.351214	26400000	6500	Lateral boundary
670234	572.323312	26410000	6500	Lateral boundary
670235	581.29541	26410000	6500	Lateral boundary
670236	590.267509	26400000	6500	Lateral boundary
670237	594.753558	15440000	35000	Lateral boundary
670464	547.582074	1928000	6500	Lateral boundary
670696	545.927383	2640000	6500	Lateral boundary
670928	542.618003	2640000	6500	Lateral boundary
671160	539.308622	2640000	6500	Lateral boundary
671392	535.999242	2640000	6500	Lateral boundary
671624	532.689861	2640000	6500	Lateral boundary
671856	529.380481	2640000	6500	Lateral boundary
672088	526.0711	2640000	6500	Lateral boundary
672320	522.761719	2640000	6500	Lateral boundary
672552	519.452339	2640000	6500	Lateral boundary
672784	516.142958	2640000	6500	Lateral boundary
673016	512.833578	2640000	6500	Lateral boundary
673248	509.524197	2640000	6500	Lateral boundary
673480	506.214817	2640000	6500	Lateral boundary
673712	502.905436	2641000	6500	Lateral boundary
673944	499.596056	2640000	6500	Lateral boundary
674176	496.286675	2640000	6500	Lateral boundary
674408	492.977294	2640000	6500	Lateral boundary
674640	489.667914	2640000	6500	Lateral boundary
674872	486.358533	2640000	6500	Lateral boundary

Cell Number	GHB Head (feet)	GHB Conductance (feet^3/day)	GHB Concentration (mg/L)	Hydraulic Feature
675104	483.049153	2640000	6500	Lateral boundary
675337	479.739772	2640000	6500	Lateral boundary
675570	476.430392	2640000	6500	Lateral boundary
675803	473.121011	2640000	6500	Lateral boundary
676036	469.811631	2640000	6500	Lateral boundary
676269	466.50225	2640000	6500	Lateral boundary
676502	463.192869	2640000	6500	Lateral boundary
676735	459.883489	2640000	6500	Lateral boundary
676968	456.574108	2640000	6500	Lateral boundary
677201	453.264728	2640000	6500	Lateral boundary
677434	449.955347	2640000	6500	Lateral boundary
677667	446.645967	2640000	6500	Lateral boundary
677900	443.336586	2640000	6500	Lateral boundary
678133	440.027205	2640000	6500	Lateral boundary
678366	436.717825	2640000	6500	Lateral boundary
678599	433.408444	2640000	6500	Lateral boundary
678832	430.099064	2640000	6500	Lateral boundary
679065	426.789683	2640000	6500	Lateral boundary
679298	423.480303	2640000	6500	Lateral boundary
679532	420.170922	2640000	6500	Lateral boundary
679766	416.861542	2640000	6500	Lateral boundary
680000	413.552161	2640000	6500	Lateral boundary
680234	410.24278	2640000	6500	Lateral boundary
680468	406.9334	2640000	6500	Lateral boundary
680702	403.624019	2640000	6500	Lateral boundary
680936	400.984665	1571000	6500	Lateral boundary

Notes:

feet^3/day - square-feet per day

mg/L = milligrams per liter

Table 2.13.1 Recharge multiplier for 1984 - 2013 conditions.

Stress Period	Representative Year	Recharge Multiplier
1	1984	1
2	1985	1.19
3	1986	1.02
4	1987	1.23
5	1988	0.85
6	1989	0.65
7	1990	0.74
8	1991	1.28
9	1992	1.35
10	1993	1.25
11	1994	0.95
12	1995	1.12
13	1996	0.65
14	1997	1.29
15	1998	1.15
16	1999	0.97
17	2000	0.71
18	2001	0.86
19	2002	1.34
20	2003	1.58
21	2004	1.28
22	2005	0.82
23	2006	1.17
24	2007	1.39
25	2008	1.38
26	2009	0.92
27	2010	1.48
28	2011	0.55
29	2012	0.76
30	2013	1.13

Table 4.2.1 Calibrated hydraulic conductivity for sand and clay for modeled geologic units.

Model layer	Hydraulic conductivity (feet per day)	
	Sand	Clay
1	700	100
2	700	100
3	100	1.46
4	1.04	0.0042
5	1.00	1.07
6	8.25	5.82
7	0.0093	0.00012
8	0.59	0.01
9	0.507	0.0066
10	50	2.00
11	0.20	0.01
12	10	0.10

Table 4.2.2 Scaling factors for calibrating canal leakance.

Canal	Factor
Canal-1	1.274
Canal-2	1.021
Canal-3	0.713
Canal-4	0.819
Canal-5	1.969
Canal-6	0.798
Canal-7	0.614
Canal-8	0.588
Canal-9	0.598
Canal-10	0.566
Canal-11	0.486
Canal-12	0.462
Canal-13	0.066
Canal-14	0.502
Canal-15	0.967
Canal-16	1.248

Table 4.3.1 Calibration statistics for steady-state 1984 simulation conditions.

Number of Targets	83
Range in Observed Values	483.35
Minimum Residual	-33.82
Maximum Residual	39.69
Sum of Squared Residuals	1.16E+04
RMS Error	11.82
Residual Mean	0.29
Absolute Residual Mean	8.94
Standard Deviation	11.81
Scaled Residual Mean	0.00060
Scaled Absolute Residual Mean	0.018
Scaled Standard Deviation	0.024
Scaled RMS Error	0.024

Table 4.3.2 Calibration statistics for transient 1984-2013 simulation conditions.

Number of Targets	1483
Range in Observed Values	619.5
Minimum Residual	-98.52
Maximum Residual	118.42
Sum of Squared Residuals	6.18E+05
RMS Error	20.41
Residual Mean	-1.38
Absolute Residual Mean	13.38
Standard Deviation	20.36
Scaled Residual Mean	-0.0022
Scaled Absolute Residual Mean	0.022
Scaled Standard Deviation	0.033
Scaled RMS Error	0.033

Table 4.3.3 Water budget for steady-state 1984 conditions.

In:	Af/yr	Percent total	Percent GW
Coastal Constant head	0.80	0.00	0.00
LRG River	2066360.64	89.30	
Canal Leakage to GW	54261.15	2.35	21.92
GHB Inflow	38530.25	1.67	15.57
Recharge	68859.84	2.98	27.82
Return Flow	85889.21	3.71	34.70
Total in	**2313901.89**	**100.00**	**100.00**

Out:	Af/yr	Percent total	Percent GW
Coastal Constant head	296992.61	12.83	74.61
LRG River Outflow into Bay	967911.37	41.82	
Wells	20106.51	0.87	5.05
Baseflow to Canals	745.81	0.03	0.19
Evapotranspiration	75785.35	3.27	19.04
GHB Outflow	4423.90	0.19	1.11
Diversions from LRG River	948545.97	40.98	
Total out	**2314511.52**	**100.00**	**100.00**

In-out	**-609.63**
Percent discrepancy	**-0.013**

Table 5.2.1 Sensitivity of calibrated model to aquifer hydraulic conductivity.

Parameter	Value (ft/d)	Sensitivity
Sand Layer 1	700	1.03
Sand Layer 2	700	1.14
Sand Layer 3	100	0.37
Sand Layer 4	1.04	0.21
Sand Layer 5	1.00	0.15
Sand Layer 6	8.25	1.57
Sand Layer 7	0.01	7.62E-02
Sand Layer 8	0.59	7.74E-02
Sand Layer 9	0.51	5.67E-02
Sand Layer 10	50.00	1.35
Sand Layer 11	0.20	9.39E-02
Sand Layer 12	10.00	0.61
Clay Layer 1	100.00	0.20
Clay Layer 2	100.00	0.35
Clay Layer 3	1.46	7.00E-03
Clay Layer 4	4.22E-03	0.33
Clay Layer 5	1.07	0.12
Clay Layer 6	5.82	0.99
Clay Layer 7	1.23E-04	1.37
Clay Layer 8	1.02E-02	4.66E-02
Clay Layer 9	6.55E-03	0.17
Clay Layer 10	2.00	5.39E-02
Clay Layer 11	1.00E-02	0.22
Clay Layer 12	0.10	7.81E-02

Table 5.2.2 Sensitivity categories for sand and clay hydraulic conductivities.

Material	Model Layer	Mean Head Error Sensitivity	RMS Head Error Sensitivity	Possible ASTM (1994) Sensitivity Type
Sand	1	High	Low	II or III
Clay	1	Medium	Low	II or III
Sand	2	High	Low	II or III
Clay	2	Medium	Low	II or III
Sand	3	Medium	Low	II or III
Clay	3	Low	Low	I or IV
Sand	4	Low	Low	I or IV
Clay	4	High	Low	II or III
Sand	5	Low	Low	I or IV
Clay	5	Low	Low	I or IV
Sand	6	High	High	II or III
Clay	6	Medium	High	II or III
Sand	7	Medium	Low	II or III
Clay	7	High	Low	II or III
Sand	8	Low	Low	I or IV
Clay	8	Low	Low	I or IV
Sand	9	Low	Low	I or IV
Clay	9	Medium	Low	II or III
Sand	10	High	High	II or III
Clay	10	Low	Low	I or IV
Sand	11	Medium	Low	II or III
Clay	11	Medium	Low	II or III
Sand	12	High	Low	II or III
Clay	12	Medium	Low	II or III

Table 5.3.1 Sensitivity of calibrated model to hydraulic conductivities and stresses.

Parameter	Value	Sensitivity
Sand hydraulic conductivity	700	2.65
Recharge multiplier	1	1.34
Maximum ET multiplier	1	2.86
Clay hydraulic conductivity	100	1.89

Note: Hydraulic conductivity values are in feet per day.

Table 5.3.2 Correlation matrix between hydraulic conductivities and stresses.

	Sand Hydraulic Conductivity	Recharge Multiplier	Maximum ET Multiplier	Clay Hydraulic Conductivity
Sand Hydraulic Conductivity	1	0.385	-0.1422	3.02E-02
Recharge Multiplier	0.385	1	-0.6547	0.6727
Maximum ET Multiplier	-0.1422	-0.6547	1	-0.2662
Clay Hydraulic Conductivity	3.02E-02	0.6727	-0.2662	1

Note: Hydraulic conductivity values are in feet per day.

Table 6.6.1 Calibration statistics for steady-state 1984 simulation conditions for density dependent flow.

Number of Targets	**83**
Range in Observed Values	483.35
Minimum Residual	-37.60
Maximum Residual	34.54
Sum of Squared Residuals	1.38E+04
RMS Error	12.89
Residual Mean	-4.27
Absolute Residual Mean	9.57
Standard Deviation	12.16
Scaled Residual Mean	-0.0088
Scaled Absolute Residual Mean	0.020
Scaled Standard Deviation	0.025
Scaled RMS Error	0.027

Table 6.6.2 Calibration statistics for transient 1984-2013 simulation conditions for density dependent flow.

Number of Targets	1483
Range in Observed Values	619.5
Minimum Residual	-98.85
Maximum Residual	108.62
Sum of Squared Residuals	6.95E+05
RMS Error	21.66
Residual Mean	-6.40
Absolute Residual Mean	14.74
Standard Deviation	20.69
Scaled Residual Mean	-0.010
Scaled Absolute Residual Mean	0.024
Scaled Standard Deviation	0.033
Scaled RMS Error	0.035

Table 6.7.1 Simulation times for flow and transport simulations.

Simulation	Clock Time[1]
Calibrated Flow Model	3 Hours, 51 Minutes
Density Dependent Flow and Transport	13 Hours, 58 Minutes
Flow and Transport without Density	4 Hours, 35 Minutes
Density Dependent Flow and Transport without wells	5 Hours, 15 Minutes

Note:

[1] Simulations were conducted on an Intel 17 laptop.
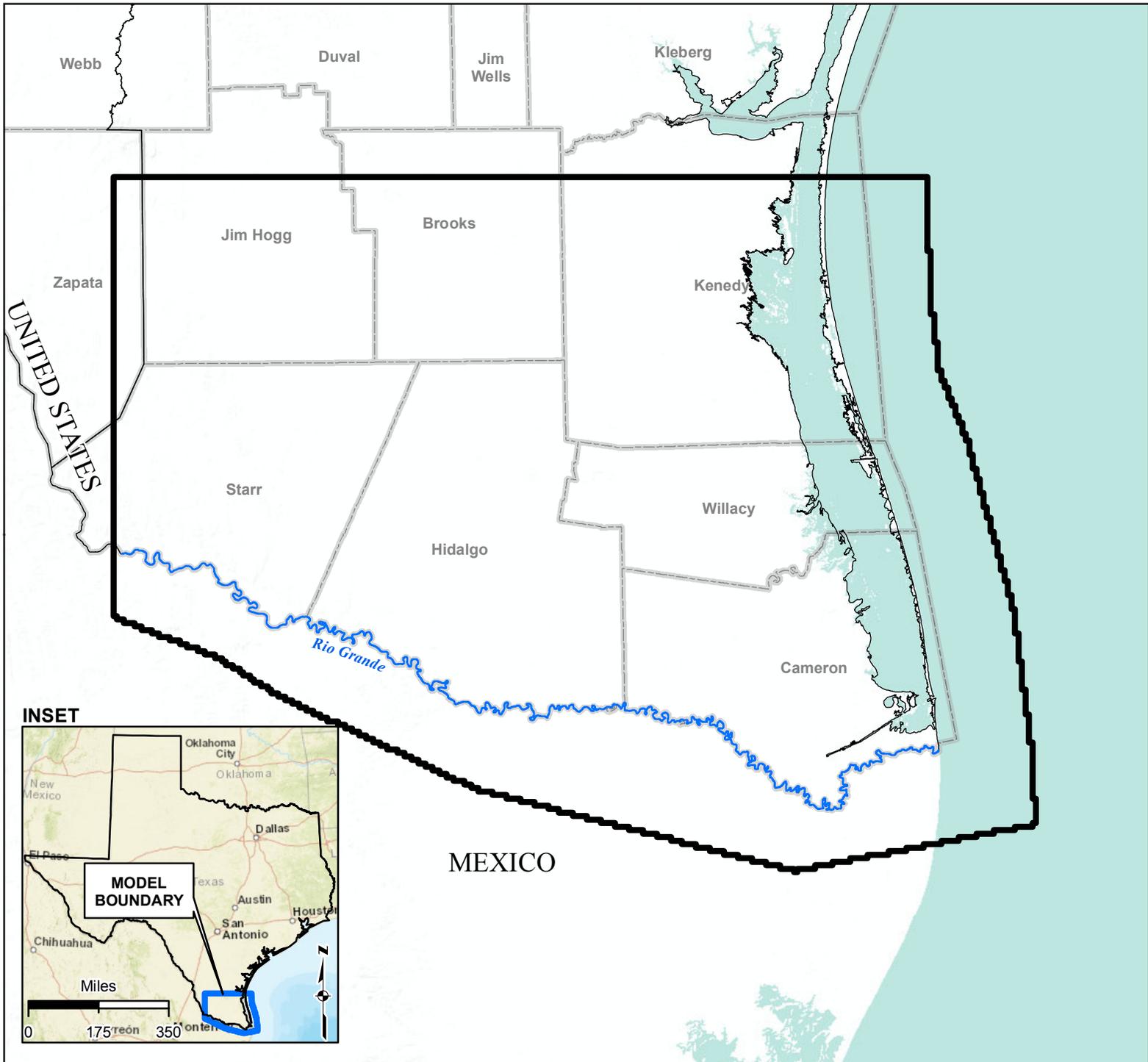
LEGEND

— Rio Grande
☐ Texas County
▢ Model Boundary

Note:

Basemap provided by Montgomery & Associates, December 2016.

Scale in Miles

0   10   20

Projected Coordinate System Datum: NAD 1983 Albers Equal Area

GSI
ENVIRONMENTAL
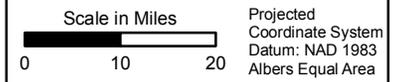
SITE LOCATION MAP

Lower Rio Grande Valley

GSI Job No. 4276	Drawn By: AV
Issued: 19-Jun-2017	Chk'd By: KER
Map ID: LRGV_SLM	Appv'd By: SP

FIGURE 1.2.1

a) Conceptual Model Layers

b) Numerical Model Layers

Vertical exaggeration: 10x

EXPLANATION

Aquifer (Hydrostratigraphic Unit)

Chicot (Beaumont)
Chicot (Lissie)
Chicot (Willis)
Evangeline (Upper Goliad)

Evangeline (Lower Goliad)
Evangeline (Upper Lagarto)
Burkeville Confining Unit (Middle Lagarto)
Jasper (Lower Lagarto)

Jasper (Oakville)
Jasper (Upper Catahoula)
Catahoula Confining System
Yegua-Jackson Aquifer

GSI
ENVIRONMENTAL

COMPARISON OF AQUIFER LAYERING BETWEEN CONCEPTUAL AND NUMERICAL MODEL FOR LOWER RIO GRANDE VALLEY

Lower Rio Grande Valley

GSI Job No. 4276	Drawn By: AV
Issued: 23-Jun-2017	Chk'd By: KER
Map ID: LRGV_Xsection	Appv'd By: SP

FIGURE 2.1.1
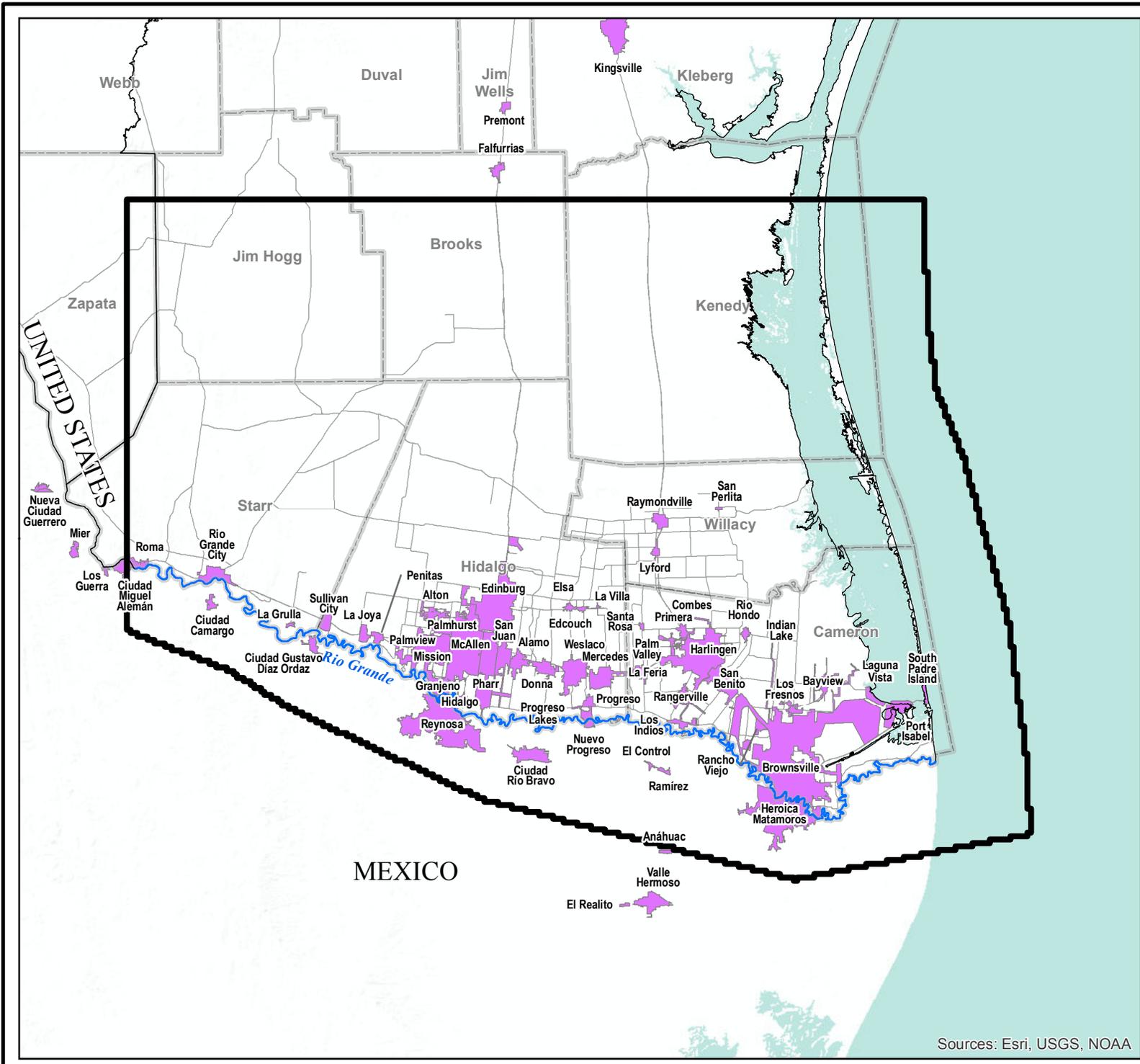
LEGEND

— Rio Grande

☐ Texas County

◻ Model Boundary

▨ Urban Area, as defined by USGS Border Environmental Health Initiative

Note:

Presented in the "Conceptual Model Report: Lower Rio Grande Valley Groundwater Transport Model" prepared by Montgomery & Associates, January 2017 as Figure 1.0.3.

Scale in Miles

0   10   20

Projected Coordinate System Datum: NAD 1983 Albers Equal Area

GSI ENVIRONMENTAL

LOWER RIO GRANDE VALLEY STUDY AREA

Lower Rio Grande Valley

GSI Job No. 4276	Drawn By: AV
Issued: 19-Jun-2017	Chk'd By: KER
Map ID: LRGV_Fig_1_0_3	Appv'd By: SP

FIGURE 2.4.1

Sources: Esri, USGS, NOAA

Model Layer	Geologic Formation	Hydrogeologic Unit	
Layer 1	Beaumont	Chicot Aquifer	Gulf Coast Aquifer
Layer 2	Lissie		
Layer 3	Willis		
Layer 4	Upper Goliad	Evangeline Aquifer	
Layer 5	Lower Goliad		
Layer 6	Upper Lagarto		
Layer 7	Middle Lagarto	Burkeville Confining Unit	
Layer 8	Lower Lagarto	Jasper Aquifer	
Layer 9	Oakville		
Layer 10	(Upper) Catahoula		
Layer 11	Catahoula Confining System		
Layer 12	Yegua-Jackson Aquifer		

Map labels:

Webb, Duval, Jim Wells, Kleberg, Jim Hogg, Brooks, Zapata, Kenedy, UNITED STATES, Starr, Willacy, Hidalgo, Rio Grande, Cameron, MEXICO

Contour labels: 0, 0, 0, 0, -500, -1000, -1500, -2000, -2500, -3000, -3500
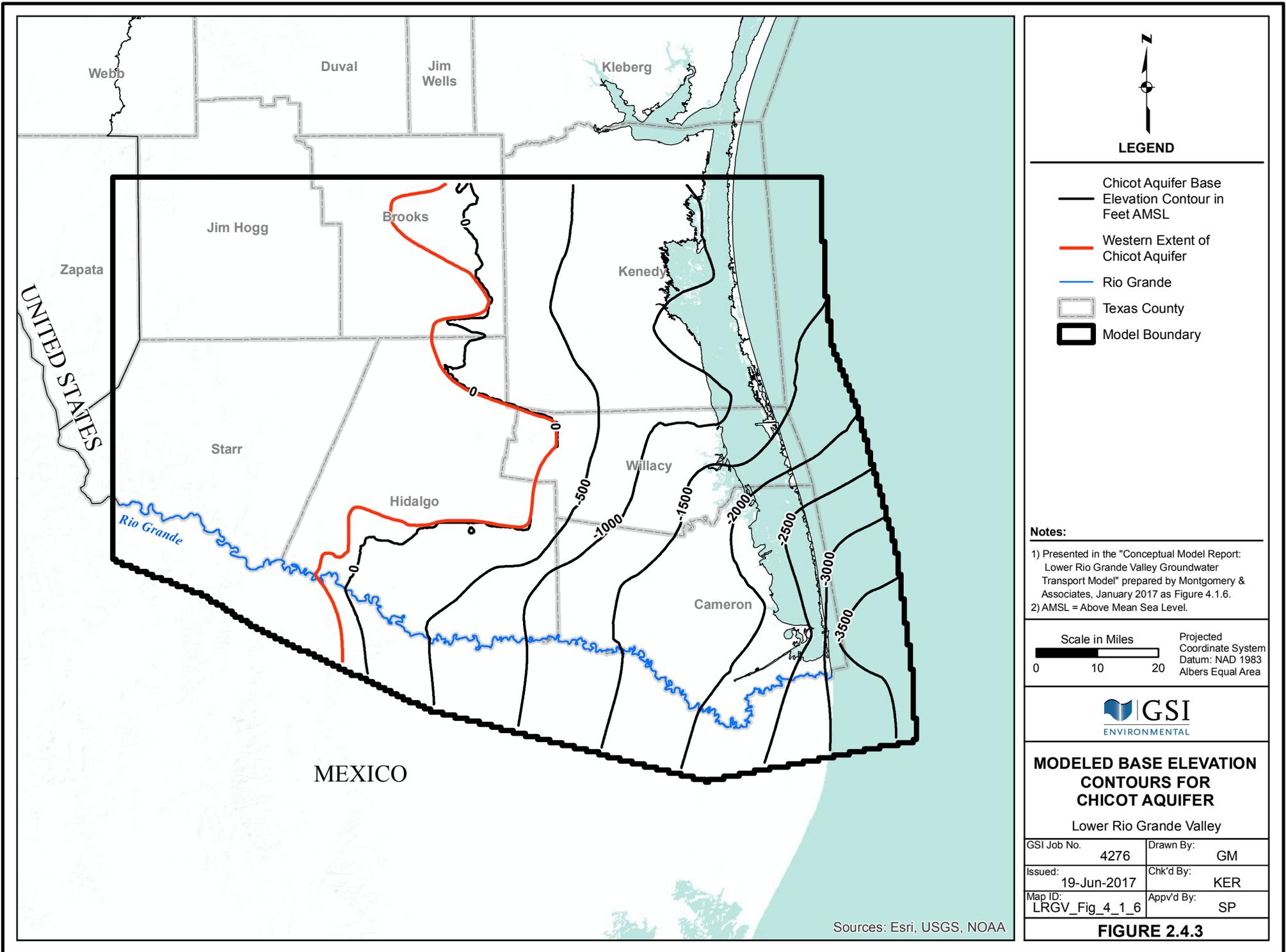
LEGEND

— Chicot Aquifer Base Elevation Contour in Feet AMSL

— Western Extent of Chicot Aquifer

— Rio Grande

☐ Texas County

☐ Model Boundary

Notes:

1) Presented in the "Conceptual Model Report: Lower Rio Grande Valley Groundwater Transport Model" prepared by Montgomery & Associates, January 2017 as Figure 4.1.6.

2) AMSL = Above Mean Sea Level.

Scale in Miles

0   10   20

Projected Coordinate System Datum: NAD 1983 Albers Equal Area

GSI ENVIRONMENTAL

MODELED BASE ELEVATION CONTOURS FOR CHICOT AQUIFER

Lower Rio Grande Valley

GSI Job No. 4276	Drawn By: GM
Issued: 19-Jun-2017	Chk'd By: KER
Map ID: LRGV_Fig_4_1_6	Appv'd By: SP

FIGURE 2.4.3
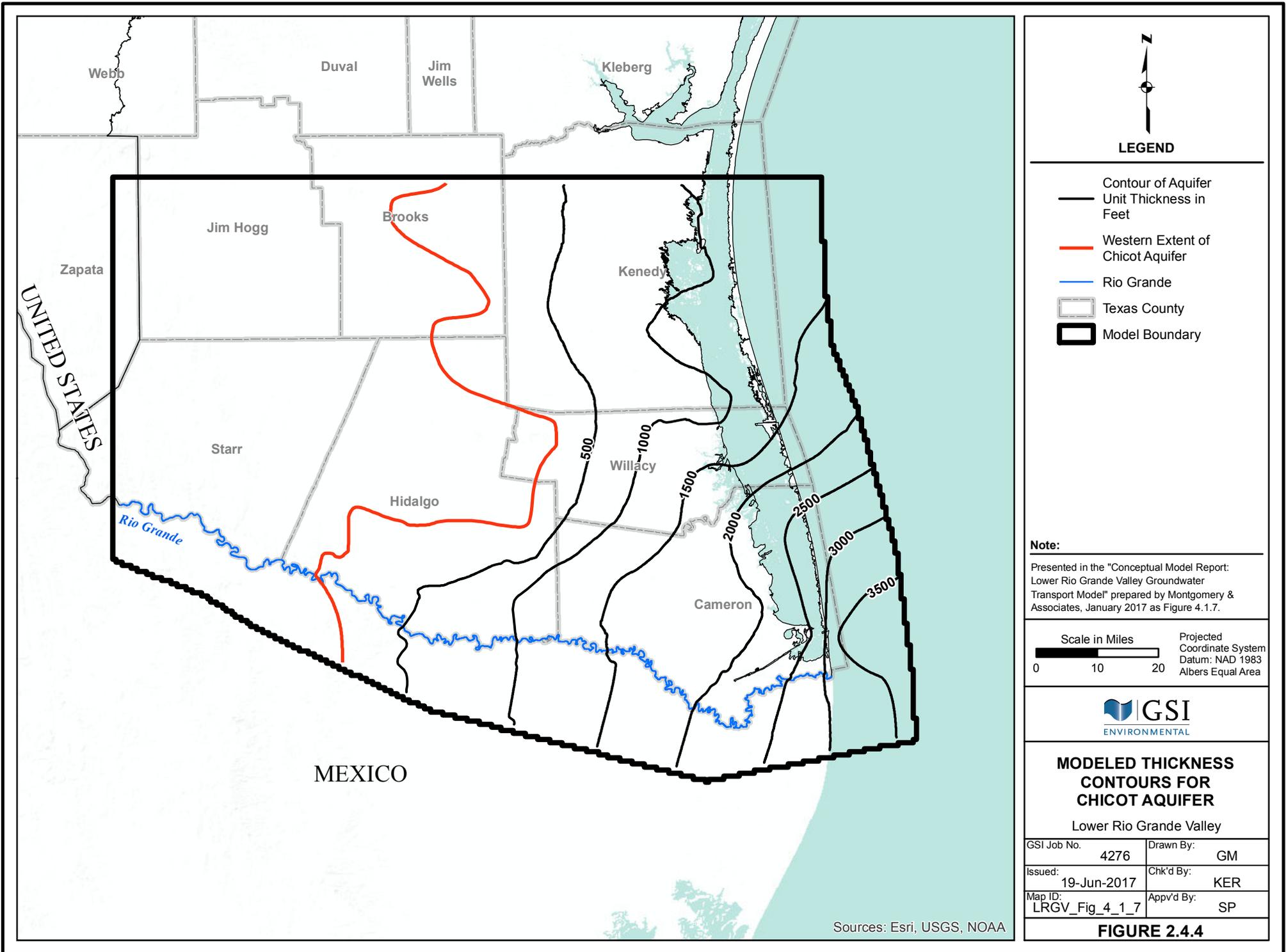
LEGEND

— Contour of Aquifer Unit Thickness in Feet

— Western Extent of Chicot Aquifer

— Rio Grande

Texas County

Model Boundary

Note:

Presented in the "Conceptual Model Report: Lower Rio Grande Valley Groundwater Transport Model" prepared by Montgomery & Associates, January 2017 as Figure 4.1.7.

Scale in Miles

0   10   20

Projected Coordinate System Datum: NAD 1983 Albers Equal Area

GSI ENVIRONMENTAL

MODELED THICKNESS CONTOURS FOR CHICOT AQUIFER

Lower Rio Grande Valley

GSI Job No. 4276	Drawn By: GM
Issued: 19-Jun-2017	Chk'd By: KER
Map ID: LRGV_Fig_4_1_7	Appv'd By: SP

FIGURE 2.4.4

Sources: Esri, USGS, NOAA
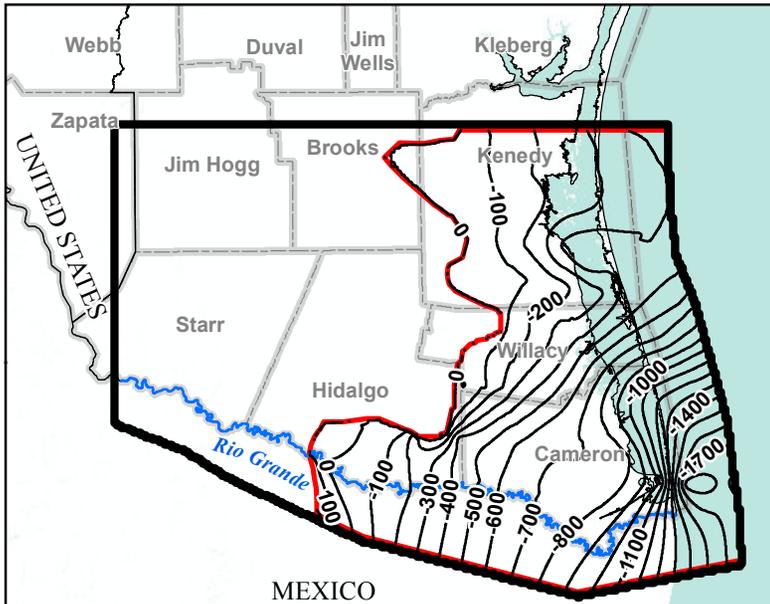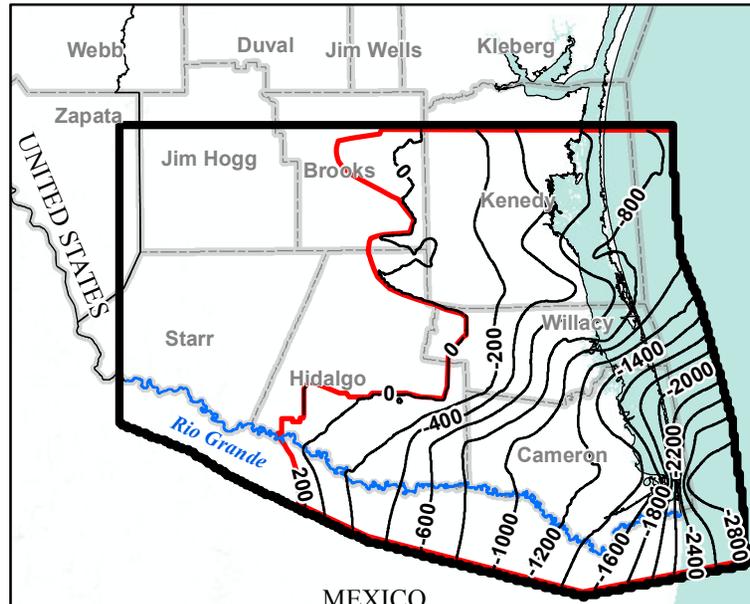
Webb
Duval
Jim Wells
Kleberg
Brooks
Jim Hogg
Zapata
Kenedy
UNITED STATES
Starr
Willacy
Hidalgo
Rio Grande
Cameron
MEXICO

500
1000
1500
2000
2500
3000
3500

Beaumont Formation (Chicot Aquifer)

Sources: Esri, USGS, NOAA

Lissie Formation (Chicot Aquifer)

Sources: Esri, USGS, NOAA
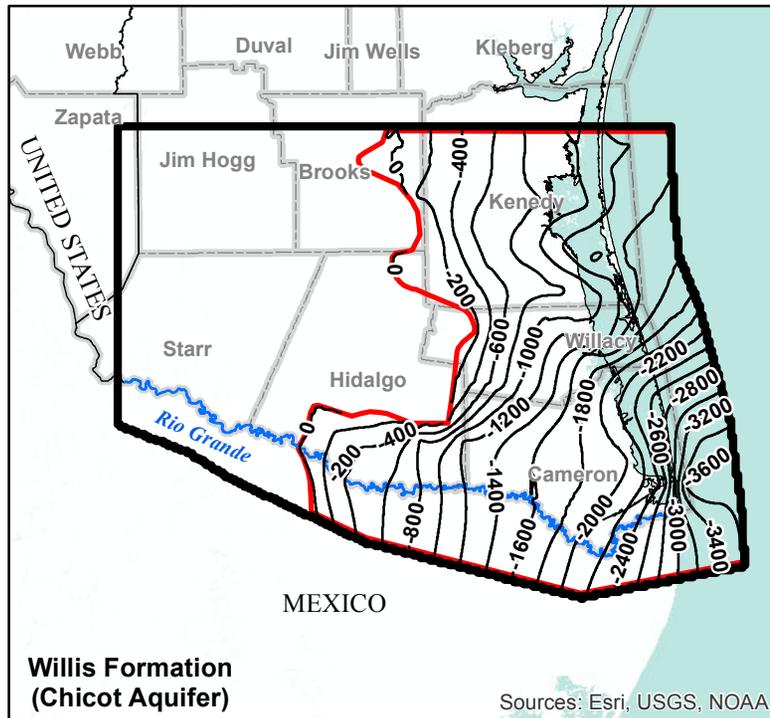
Willis Formation (Chicot Aquifer)

Sources: Esri, USGS, NOAA

LEGEND

— Hydrostratigraphic Unit Extent
Base Elevation Contour in Feet AMSL

— Rio Grande

Texas County

Model Boundary

Hydrostratigraphic Unit Extent

Notes:

1) Presented in the "Conceptual Model Report: Lower Rio Grande Valley Groundwater Transport Model" prepared by Montgomery & Associates, January 2017 as Figure 4.1.8.

2) AMSL = Above Mean Sea Level.
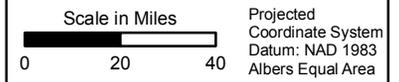
Scale in Miles

0   20   40

Projected Coordinate System Datum: NAD 1983 Albers Equal Area

GSI ENVIRONMENTAL

MODELED BASE ELEVATION CONTOURS FOR HYDROSTRATIGRAPHIC UNITS IN CHICOT AQUIFER
Lower Rio Grande Valley

GSI Job No.	Drawn By:
4276	AV
Issued:	Chk'd By:
22-Jun-2017	KER
Map ID:	Appv'd By:
LRGV_Fig_4_1_8	SP

FIGURE 2.4.5

**Beaumont Formation
(Chicot Aquifer)**

Sources: Esri, USGS, NOAA

**Lissie Formation
(Chicot Aquifer)**

Sources: Esri, USGS, NOAA

**Willis Formation
(Chicot Aquifer)**

Sources: Esri, USGS, NOAA

LEGEND

— Hydrostratigraphic Unit Extent
Thickness Contour in Feet

— Rio Grande

Texas County

Model Boundary

Hydrostratigraphic Unit Extent

Note:

Presented in the "Conceptual Model Report:
Lower Rio Grande Valley Groundwater
Transport Model" prepared by Montgomery &
Associates, January 2017 as Figure 4.1.9.
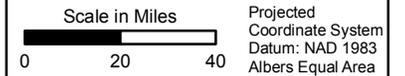
Scale in Miles

0   20   40

Projected
Coordinate System
Datum: NAD 1983
Albers Equal Area

GSI
ENVIRONMENTAL

**MODELED THICKNESS
CONTOURS FOR
HYDROSTRATIGRAPHIC
UNITS IN CHICOT AQUIFER**
Lower Rio Grande Valley

GSI Job No. 4276	Drawn By: AV
Issued: 23-Jun-2017	Chk'd By: KER
Map ID: LRGV_Fig_4_1_9	Appv'd By: SP

FIGURE 2.4.6

LEGEND

— Evangeline Aquifer Base Elevation Contour in Feet AMSL

— Western Extent of Evangeline Aquifer

— Rio Grande

Texas County

Model Boundary

Notes:

1) Presented in the "Conceptual Model Report: Lower Rio Grande Valley Groundwater Transport Model" prepared by Montgomery & Associates, January 2017 as Figure 4.1.10.

2) AMSL = Above Mean Sea Level.
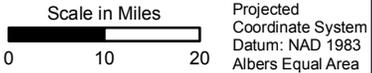
Scale in Miles

0   10   20

Projected Coordinate System Datum: NAD 1983 Albers Equal Area

GSI ENVIRONMENTAL

MODELED BASE ELEVATION CONTOURS FOR EVANGELINE AQUIFER

Lower Rio Grande Valley

GSI Job No. 4276	Drawn By: GM
Issued: 19-Jun-2017	Chk'd By: KER
Map ID: LRGV_Fig_4_1_10	Appv'd By: SP

FIGURE 2.4.7

Sources: Esri, USGS, NOAA
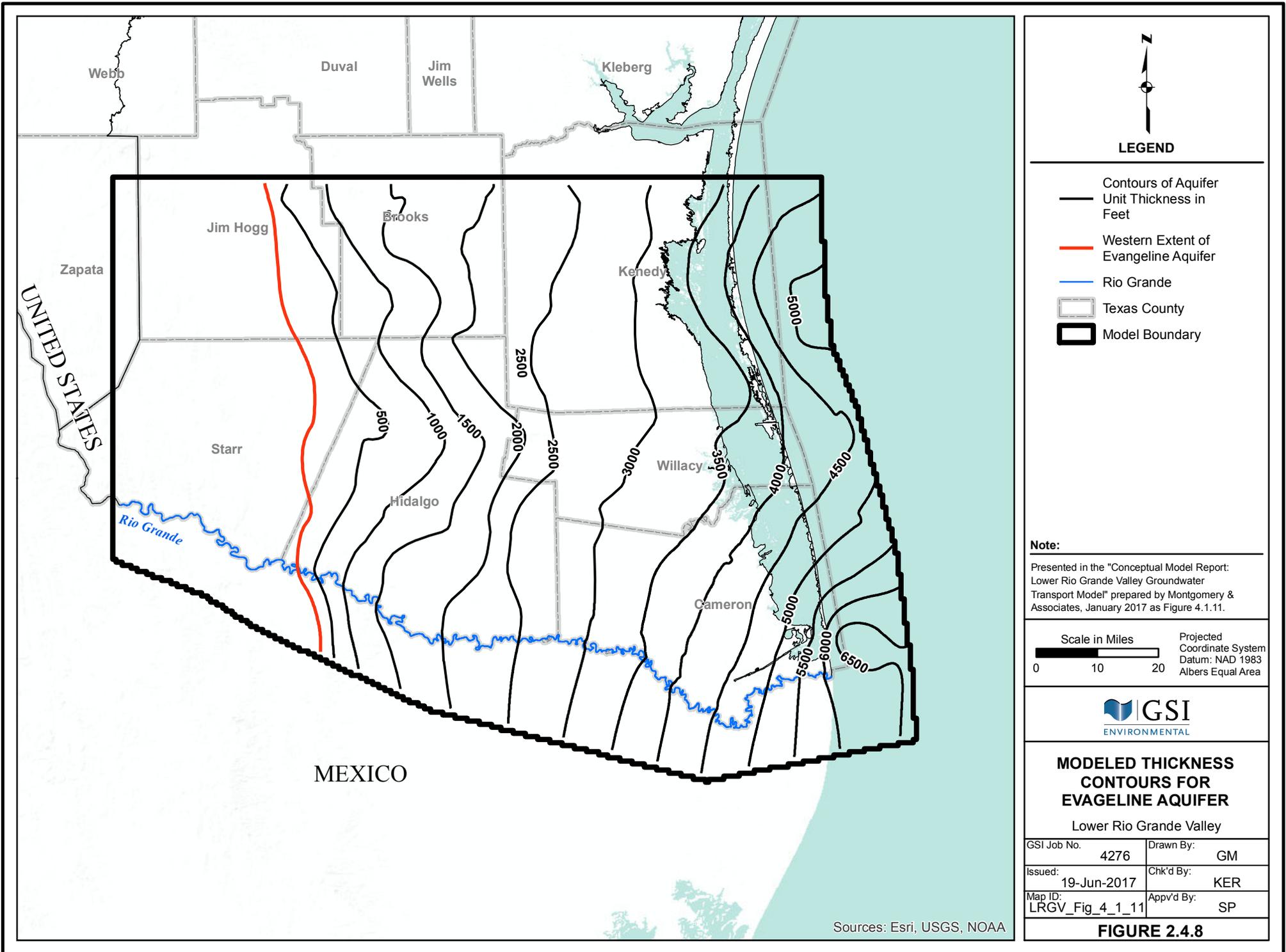
LEGEND

▬	Contours of Aquifer Unit Thickness in Feet
▬	Western Extent of Evangeline Aquifer
▬	Rio Grande
▭	Texas County
▬	Model Boundary

Note:

Presented in the "Conceptual Model Report: Lower Rio Grande Valley Groundwater Transport Model" prepared by Montgomery & Associates, January 2017 as Figure 4.1.11.

Scale in Miles

0   10   20

Projected Coordinate System Datum: NAD 1983 Albers Equal Area

GSI ENVIRONMENTAL

MODELED THICKNESS CONTOURS FOR EVAGELINE AQUIFER

Lower Rio Grande Valley

GSI Job No. 4276	Drawn By: GM
Issued: 19-Jun-2017	Chk'd By: KER
Map ID: LRGV_Fig_4_1_11	Appv'd By: SP

FIGURE 2.4.8

Sources: Esri, USGS, NOAA
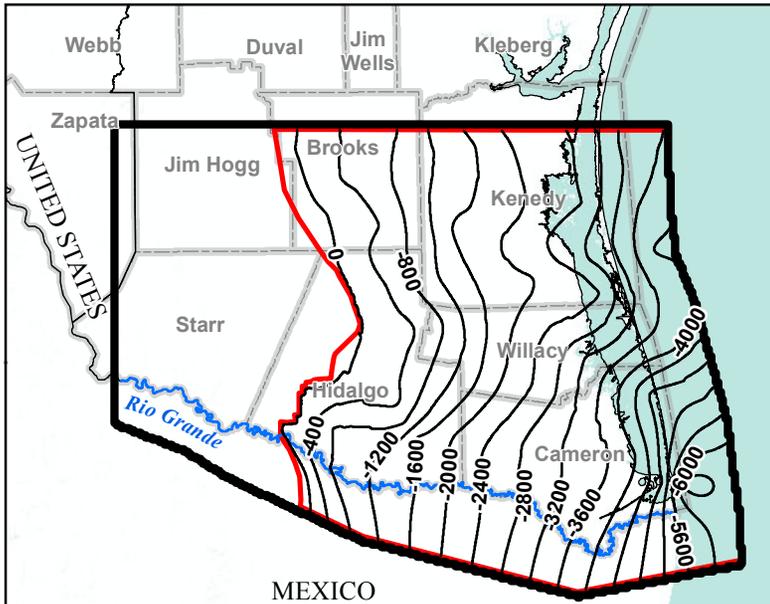
Upper Goliad Formation
(Evangeline Aquifer)
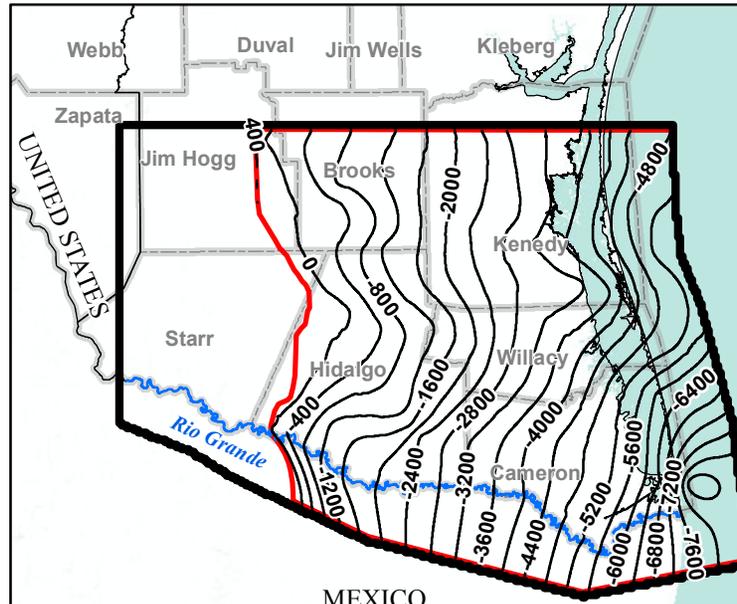
Sources: Esri, USGS, NOAA

Lower Goliad Formation
(Evangeline Aquifer)

Sources: Esri, USGS, NOAA

Upper Lagarto Formation
(Evangeline Aquifer)

Sources: Esri, USGS, NOAA

LEGEND

— Hydrostratigraphic Unit Extent
Base Elevation Contour in
Feet AMSL

— Rio Grande

Texas County

Model Boundary

Hydrostratigraphic Unit Extent

Notes:

1) Presented in the "Conceptual Model Report:
Lower Rio Grande Valley Groundwater
Transport Model" prepared by Montgomery &
Associates, January 2017 as Figure 4.1.12.
2) AMSL = Above Mean Sea Level.
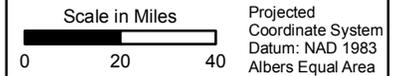
Scale in Miles

0   20   40

Projected
Coordinate System
Datum: NAD 1983
Albers Equal Area

GSI
ENVIRONMENTAL

**MODELED BASE ELEVATION
CONTOURS FOR
HYDROSTRATIGRAPHIC UNITS
IN EVANGELINE AQUIFER**

Lower Rio Grande Valley

GSI Job No. 4276	Drawn By: AV
Issued: 22-Jun-2017	Chk'd By: KER
Map ID: LRGV_Fig_4_1_12	Appv'd By: SP

FIGURE 2.4.9

**Upper Goliad Formation
(Evangeline Aquifer)**

Sources: Esri, USGS, NOAA

**Lower Goliad Formation
(Evangeline Aquifer)**

Sources: Esri, USGS, NOAA

**Upper Lagarto Formation
(Evangeline Aquifer)**

Sources: Esri, USGS, NOAA

LEGEND

—— Hydrostratigraphic Unit Extent
Thickness Contour in Feet

—— Rio Grande

Texas County

Model Boundary

Hydrostratigraphic Unit Extent

Note:

Presented in the "Conceptual Model Report: Lower Rio Grande Valley Groundwater Transport Model" prepared by Montgomery & Associates, January 2017 as Figure 4.1.13.
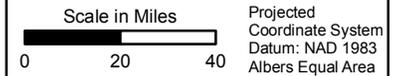
Scale in Miles

0   20   40

Projected Coordinate System Datum: NAD 1983 Albers Equal Area

GSI ENVIRONMENTAL

**MODELED THICKNESS
CONTOURS FOR
HYDROSTRATIGRAPHIC UNITS
IN EVANGELINE AQUIFER**

Lower Rio Grande Valley

GSI Job No. 4276	Drawn By: AV
Issued: 22-Jun-2017	Chk'd By: KER
Map ID: LRGV_Fig_4_1_13	Appv'd By: SP

FIGURE 2.4.10
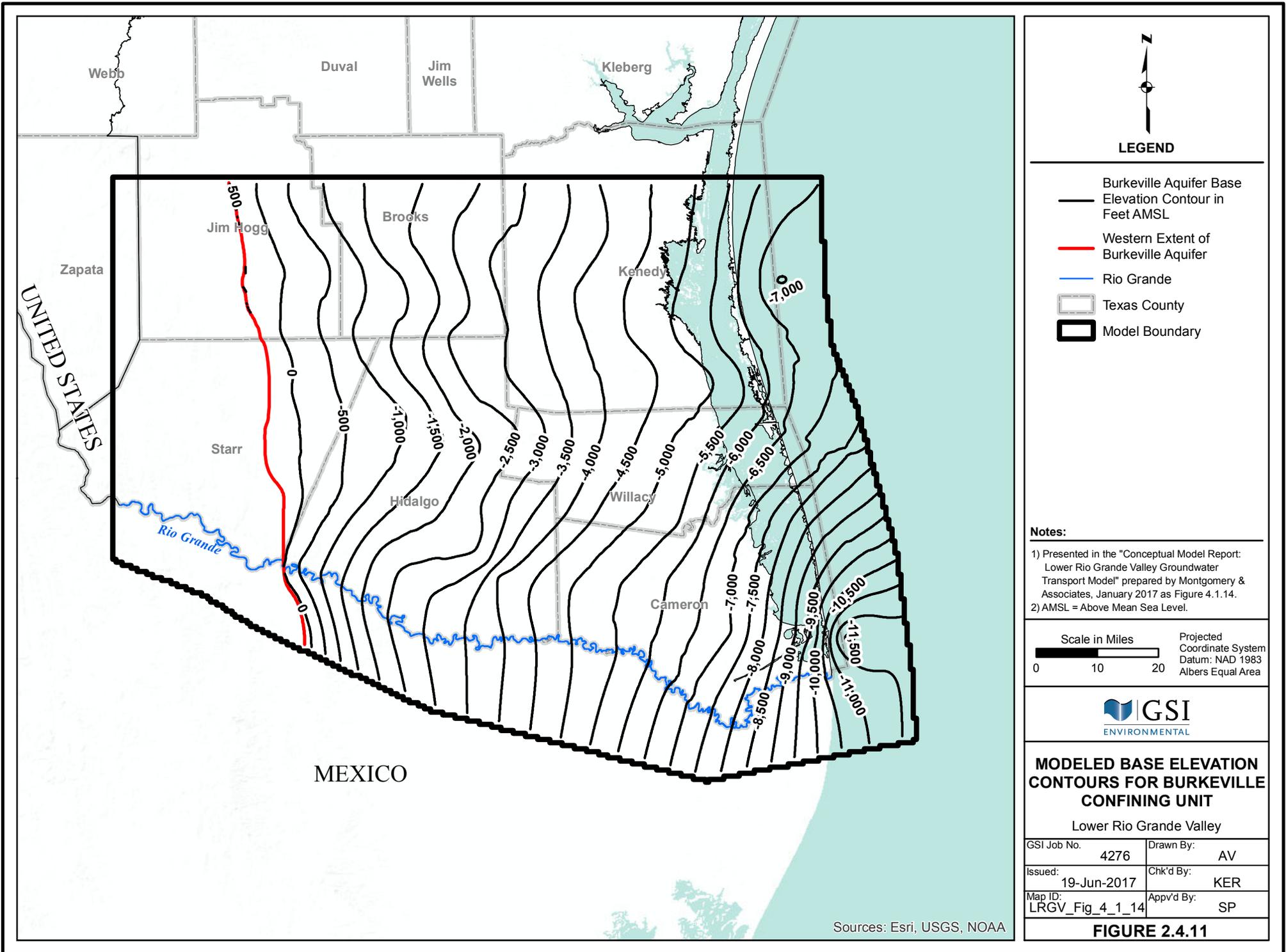
Burkeville Aquifer Base Elevation Contour in Feet AMSL

Western Extent of Burkeville Aquifer

Rio Grande

Texas County

Model Boundary

Notes:

1) Presented in the "Conceptual Model Report: Lower Rio Grande Valley Groundwater Transport Model" prepared by Montgomery & Associates, January 2017 as Figure 4.1.14.

2) AMSL = Above Mean Sea Level.
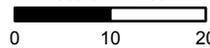
Scale in Miles

0   10   20

Projected Coordinate System Datum: NAD 1983 Albers Equal Area

GSI ENVIRONMENTAL

MODELED BASE ELEVATION CONTOURS FOR BURKEVILLE CONFINING UNIT

Lower Rio Grande Valley

GSI Job No. 4276	Drawn By: AV
Issued: 19-Jun-2017	Chk'd By: KER
Map ID: LRGV_Fig_4_1_14	Appv'd By: SP

FIGURE 2.4.11

Sources: Esri, USGS, NOAA
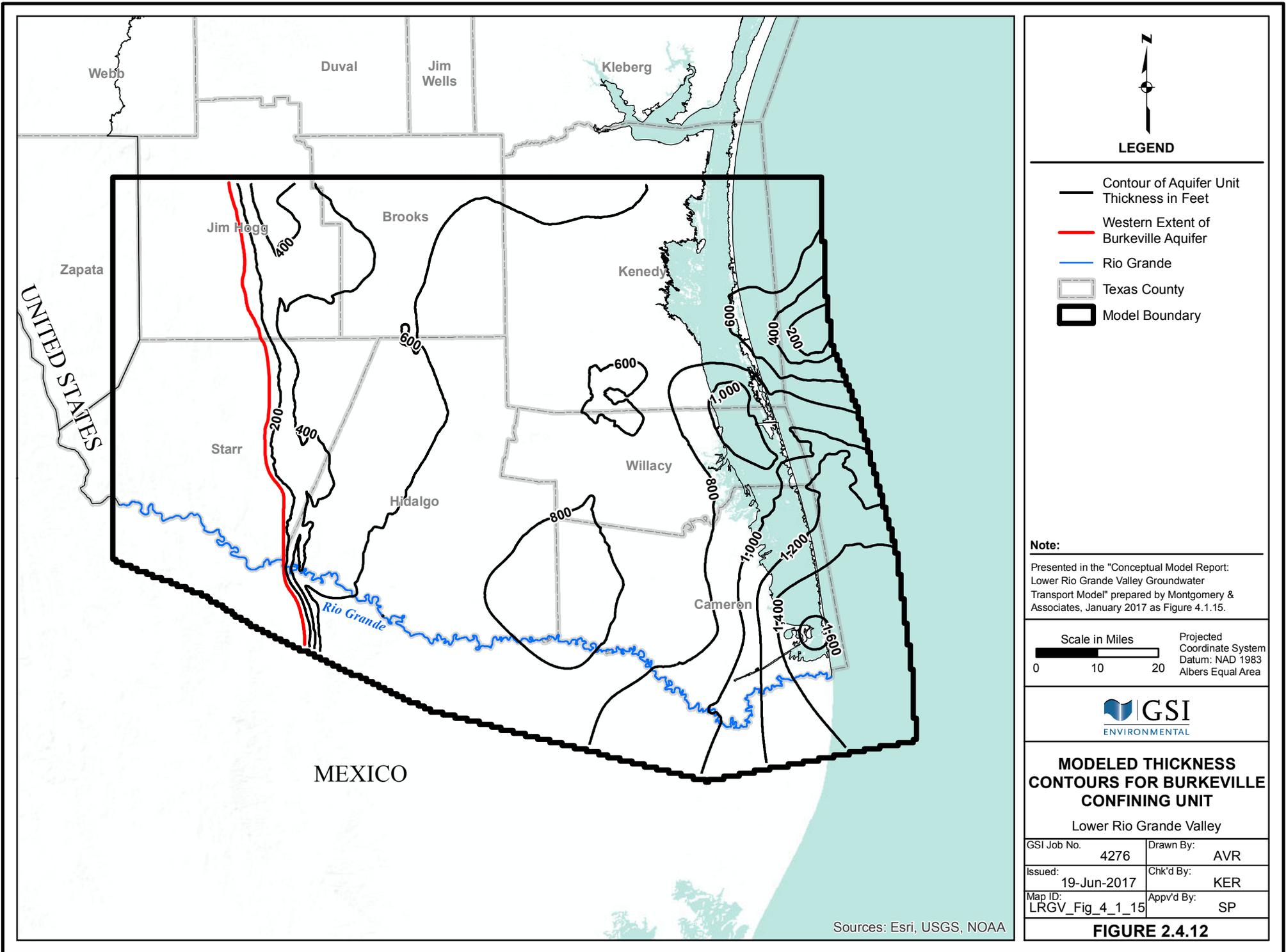
LEGEND

— Contour of Aquifer Unit Thickness in Feet

— Western Extent of Burkeville Aquifer

— Rio Grande

Texas County

Model Boundary

Note:

Presented in the "Conceptual Model Report: Lower Rio Grande Valley Groundwater Transport Model" prepared by Montgomery & Associates, January 2017 as Figure 4.1.15.

Scale in Miles

0   10   20

Projected Coordinate System Datum: NAD 1983 Albers Equal Area

GSI ENVIRONMENTAL

MODELED THICKNESS CONTOURS FOR BURKEVILLE CONFINING UNIT

Lower Rio Grande Valley

GSI Job No. 4276	Drawn By: AVR
Issued: 19-Jun-2017	Chk'd By: KER
Map ID: LRGV_Fig_4_1_15	Appv'd By: SP

FIGURE 2.4.12

Sources: Esri, USGS, NOAA
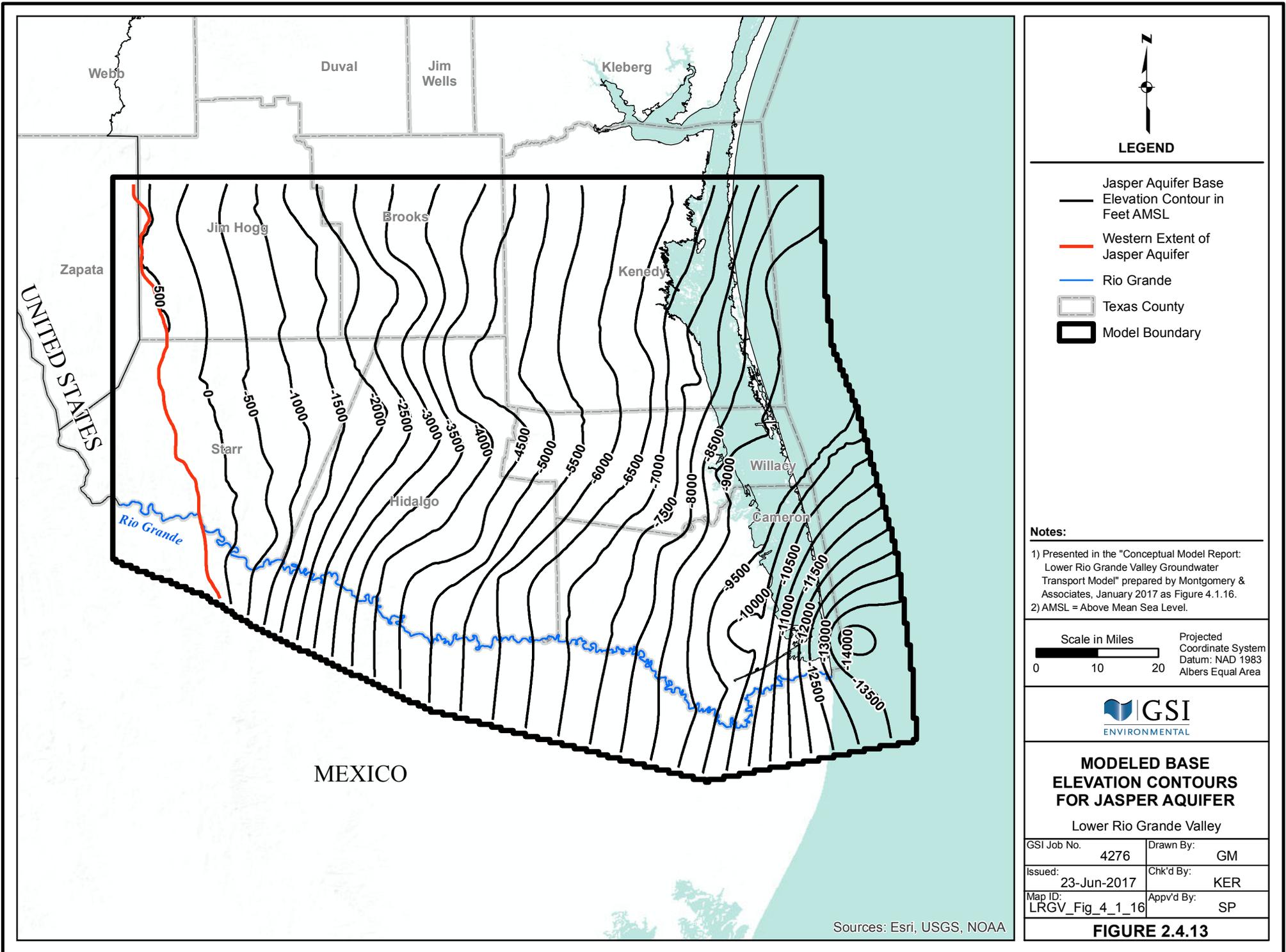
LEGEND

— Jasper Aquifer Base Elevation Contour in Feet AMSL

— Western Extent of Jasper Aquifer

— Rio Grande

Texas County

Model Boundary

Notes:

1) Presented in the "Conceptual Model Report: Lower Rio Grande Valley Groundwater Transport Model" prepared by Montgomery & Associates, January 2017 as Figure 4.1.16.

2) AMSL = Above Mean Sea Level.
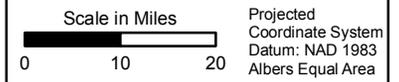
Scale in Miles

0   10   20

Projected Coordinate System Datum: NAD 1983 Albers Equal Area

GSI ENVIRONMENTAL

MODELED BASE ELEVATION CONTOURS FOR JASPER AQUIFER

Lower Rio Grande Valley

GSI Job No. 4276	Drawn By: GM
Issued: 23-Jun-2017	Chk'd By: KER
Map ID: LRGV_Fig_4_1_16	Appv'd By: SP

FIGURE 2.4.13

Sources: Esri, USGS, NOAA
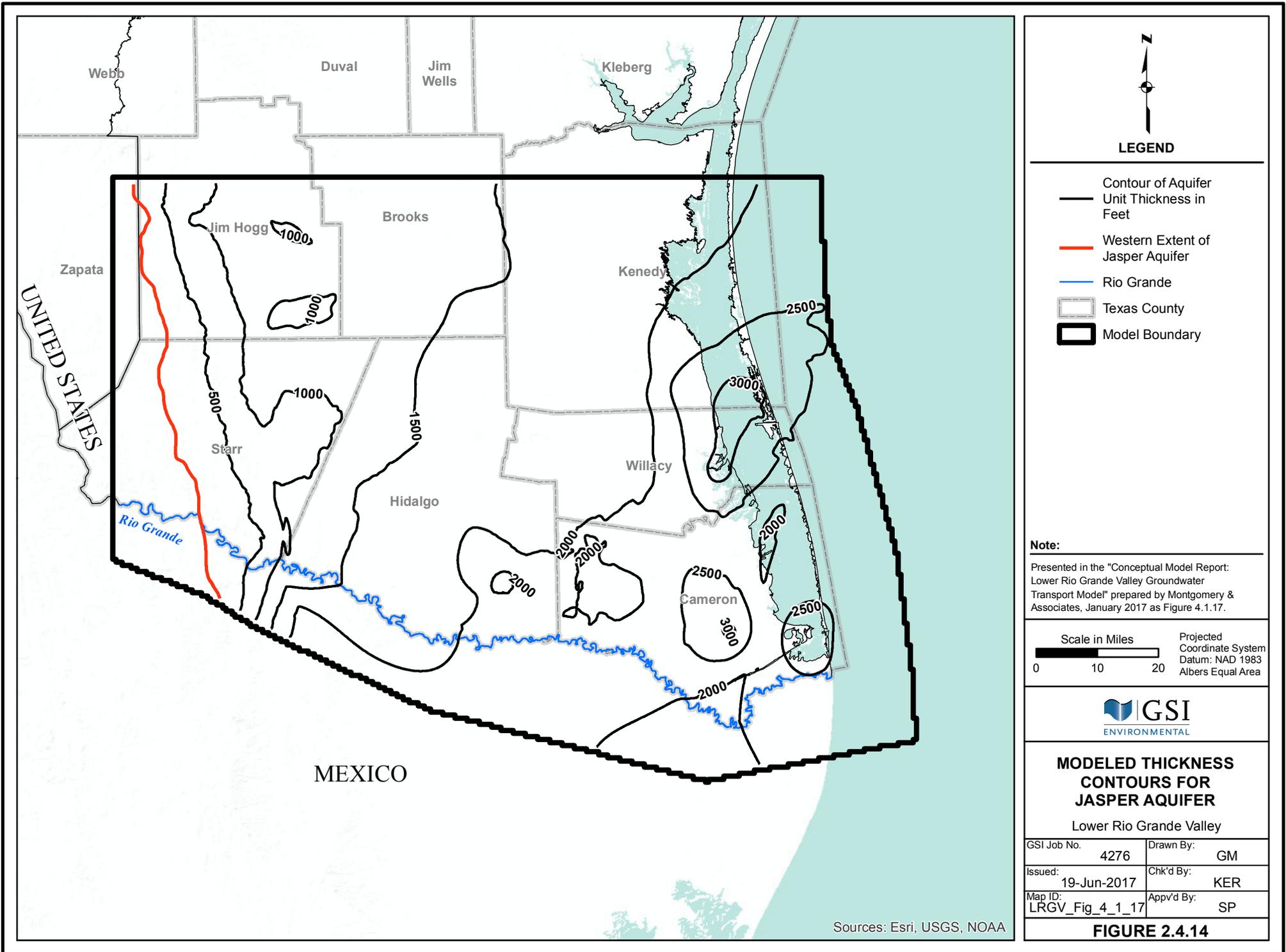
LEGEND

— Contour of Aquifer Unit Thickness in Feet

— Western Extent of Jasper Aquifer

— Rio Grande

Texas County

Model Boundary

Note:

Presented in the "Conceptual Model Report: Lower Rio Grande Valley Groundwater Transport Model" prepared by Montgomery & Associates, January 2017 as Figure 4.1.17.

Scale in Miles

0   10   20

Projected Coordinate System Datum: NAD 1983 Albers Equal Area

GSI ENVIRONMENTAL

MODELED THICKNESS CONTOURS FOR JASPER AQUIFER

Lower Rio Grande Valley

GSI Job No. 4276	Drawn By: GM
Issued: 19-Jun-2017	Chk'd By: KER
Map ID: LRGV_Fig_4_1_17	Appv'd By: SP

FIGURE 2.4.14

Sources: Esri, USGS, NOAA
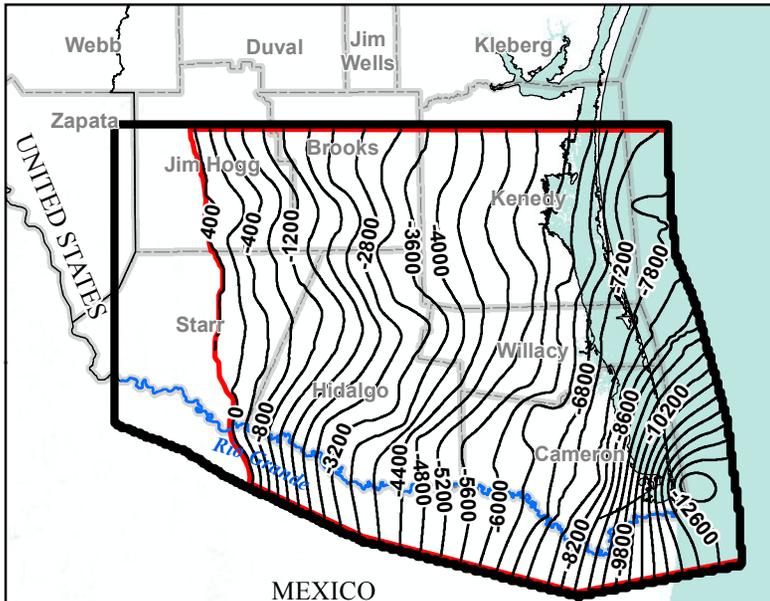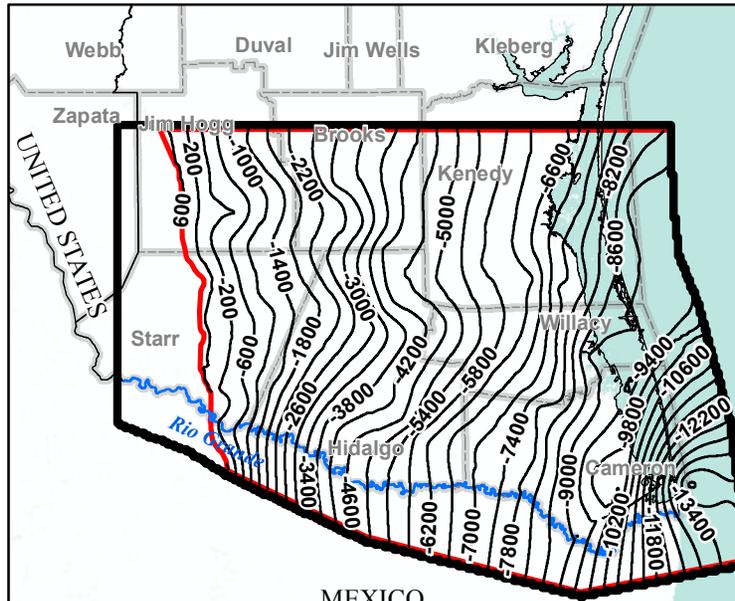
**Lower Lagarto Formation
(Jasper Aquifer)**

Sources: Esri, USGS, NOAA

**Oakville Formation
(Jasper Aquifer)**

Sources: Esri, USGS, NOAA

**Upper Catahoula Formation
(Jasper Aquifer)**

Sources: Esri, USGS, NOAA

LEGEND

Hydrostratigraphic Unit Extent
Base Elevation Contour in
Feet AMSL

Rio Grande

Texas County

Model Boundary

Hydrostratigraphic Unit Extent

Notes:

1) Presented in the "Conceptual Model Report:
Lower Rio Grande Valley Groundwater
Transport Model" prepared by Montgomery &
Associates, January 2017 as Figure 4.1.18.
2) AMSL = Above Mean Sea Level.
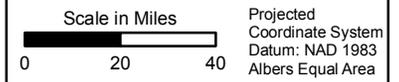
Scale in Miles

Projected
Coordinate System
Datum: NAD 1983
Albers Equal Area

0   20   40

GSI | ENVIRONMENTAL

**MODELED BASE ELEVATION
CONTOURS FOR
HYDROSTRATIGRAPHIC
UNITS IN JASPER AQUIFER**

Lower Rio Grande Valley

GSI Job No. 4276	Drawn By: AV
Issued: 22-Jun-2017	Chk'd By: KER
Map ID: LRGV_Fig_4_1_18	Appv'd By: SP

FIGURE 2.4.15
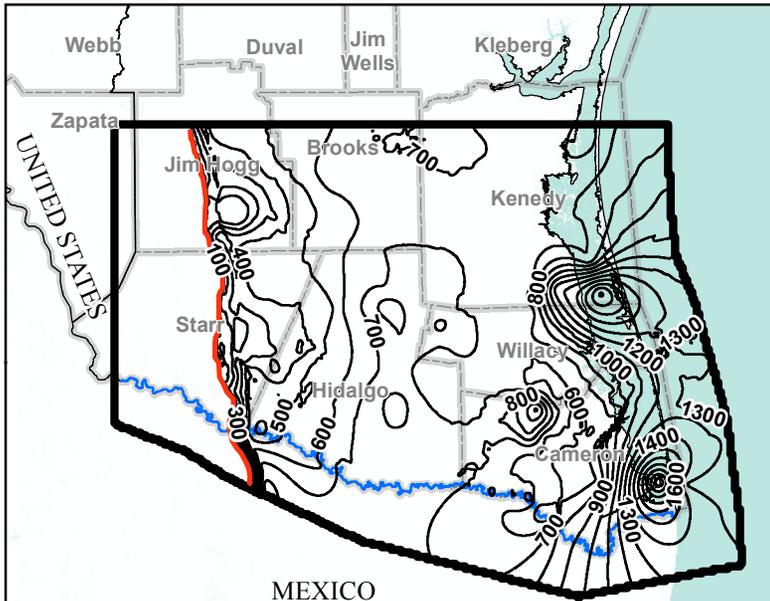
**Lower Lagarto Formation
(Jasper Aquifer)**
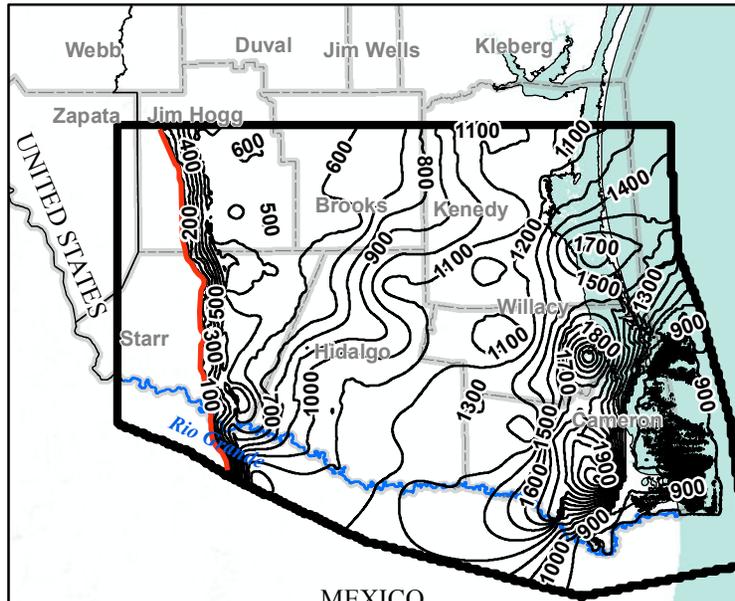
Sources: Esri, USGS, NOAA

**Oakville Formation
(Jasper Aquifer)**

Sources: Esri, USGS, NOAA
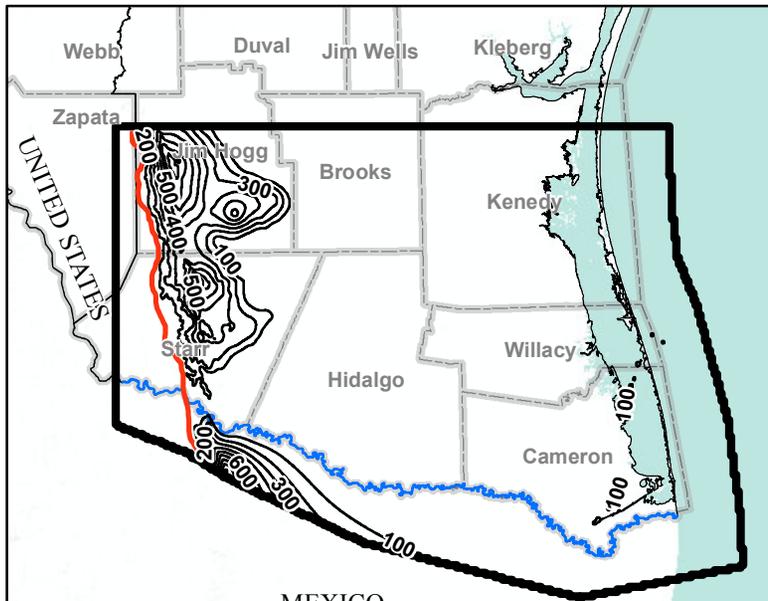
**Upper Catahoula Formation
(Jasper Aquifer)**

Sources: Esri, USGS, NOAA

LEGEND

Hydrostratigraphic Unit
Thickness Contour in
Feet

Hydrostratigraphic Unit
Extent

Rio Grande

Texas County

Model Boundary

Note:

Presented in the "Conceptual Model Report:
Lower Rio Grande Valley Groundwater
Transport Model" prepared by Montgomery &
Associates, January 2017 as Figure 4.1.19.
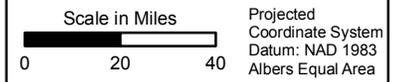
Scale in Miles

0   20   40

Projected
Coordinate System
Datum: NAD 1983
Albers Equal Area

GSI ENVIRONMENTAL

**MODELED THICKNESS
CONTOURS FOR
HYDROSTRATIGRAPHIC
UNITS IN JASPER AQUIFER**
Lower Rio Grande Valley

GSI Job No. 4276	Drawn By: GM
Issued: 22-Jun-2017	Chk'd By: KER
Map ID: LRGV_Fig_4_1_19	Appv'd By: SP

FIGURE 2.4.16
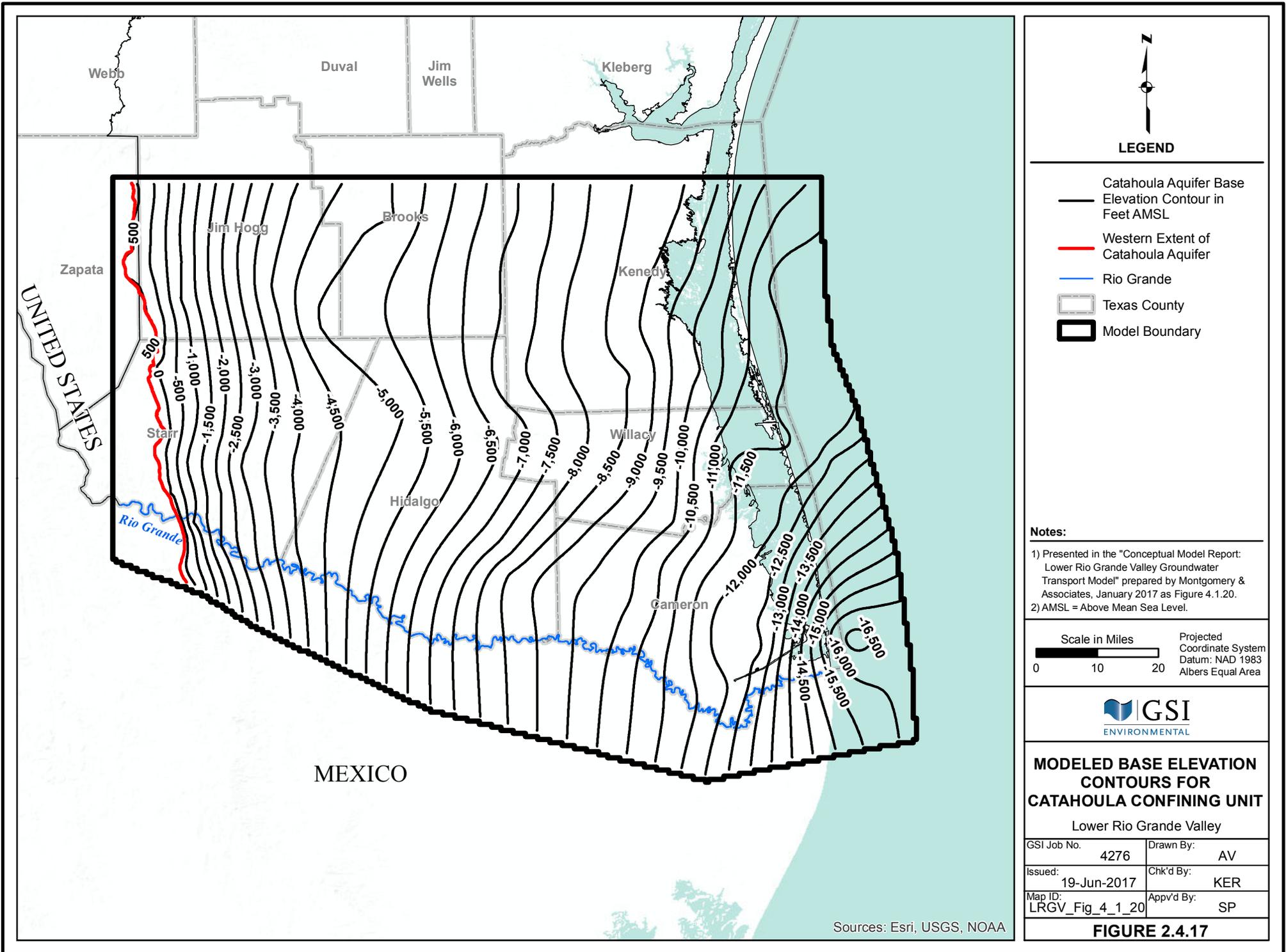
LEGEND

—— Catahoula Aquifer Base Elevation Contour in Feet AMSL

—— Western Extent of Catahoula Aquifer

—— Rio Grande

Texas County

Model Boundary

Notes:

1) Presented in the "Conceptual Model Report: Lower Rio Grande Valley Groundwater Transport Model" prepared by Montgomery & Associates, January 2017 as Figure 4.1.20.
2) AMSL = Above Mean Sea Level.

Scale in Miles

0   10   20

Projected Coordinate System Datum: NAD 1983 Albers Equal Area

GSI ENVIRONMENTAL
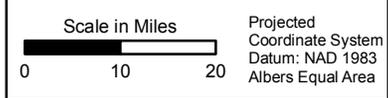
MODELED BASE ELEVATION CONTOURS FOR CATAHOULA CONFINING UNIT

Lower Rio Grande Valley

GSI Job No. 4276	Drawn By: AV
Issued: 19-Jun-2017	Chk'd By: KER
Map ID: LRGV_Fig_4_1_20	Appv'd By: SP

FIGURE 2.4.17

Sources: Esri, USGS, NOAA
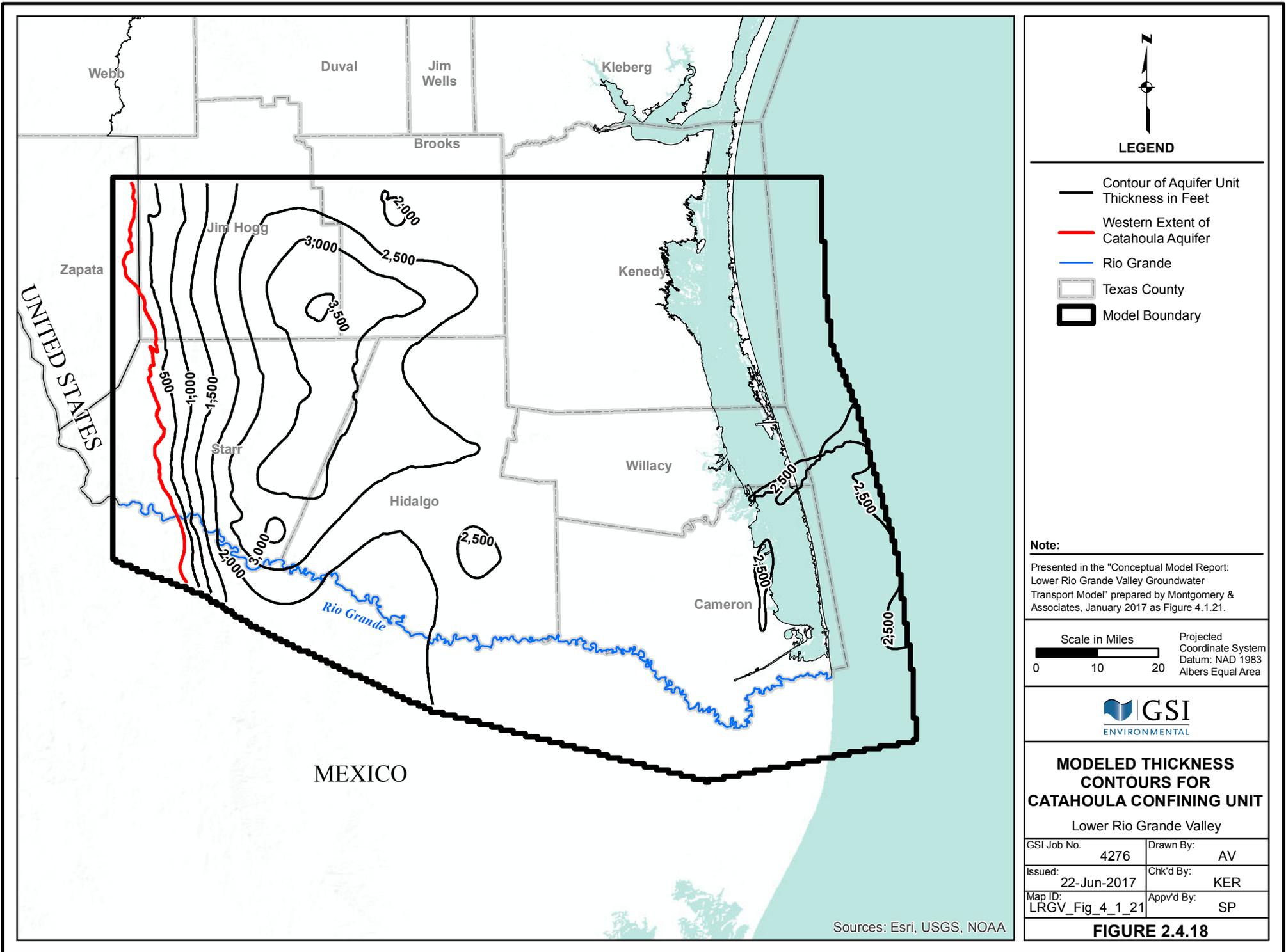
LEGEND

— Contour of Aquifer Unit Thickness in Feet

— Western Extent of Catahoula Aquifer

— Rio Grande

Texas County

Model Boundary

Note:

Presented in the "Conceptual Model Report: Lower Rio Grande Valley Groundwater Transport Model" prepared by Montgomery & Associates, January 2017 as Figure 4.1.21.

Scale in Miles

0   10   20

Projected Coordinate System Datum: NAD 1983 Albers Equal Area

GSI ENVIRONMENTAL

MODELED THICKNESS CONTOURS FOR CATAHOULA CONFINING UNIT

Lower Rio Grande Valley

GSI Job No. 4276	Drawn By: AV
Issued: 22-Jun-2017	Chk'd By: KER
Map ID: LRGV_Fig_4_1_21	Appv'd By: SP

FIGURE 2.4.18

Sources: Esri, USGS, NOAA

Webb Duval Jim Wells Kleberg Brooks Jim Hogg Zapata Kenedy UNITED STATES Starr Willacy Hidalgo Cameron Rio Grande MEXICO

2,000 3,000 2,500 3,500 500 1,000 1,500 2,000 3,000 2,500 2,500
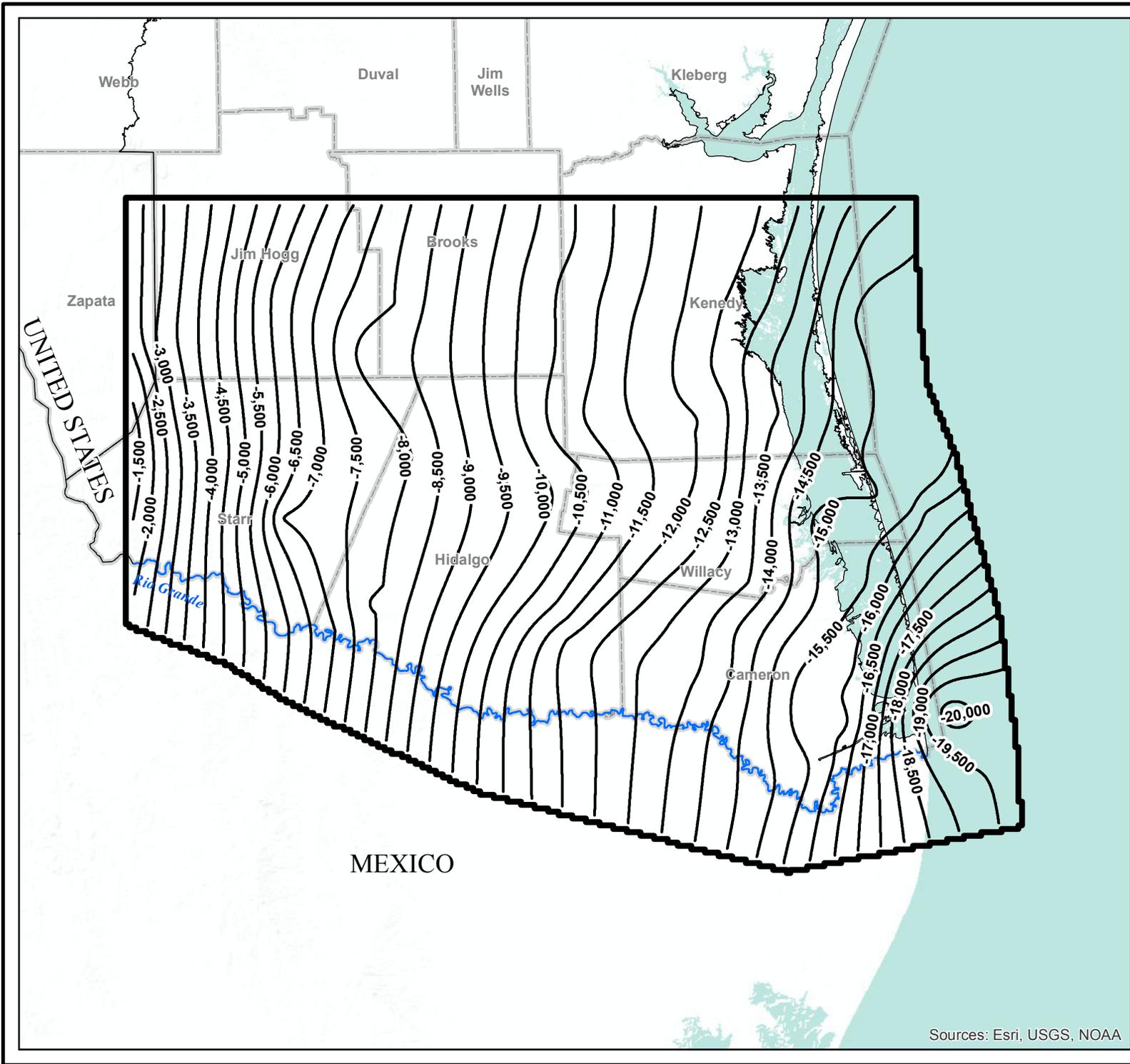
LEGEND

—— Yegua-Jackson Aquifer Base Elevation Contour in Feet AMSL

—— Rio Grande

☐ Texas County

☐ Model Boundary

Notes:

1) Presented in the "Conceptual Model Report: Lower Rio Grande Valley Groundwater Transport Model" prepared by Montgomery & Associates, January 2017 as Figure 4.1.22.

2) AMSL = Above Mean Sea Level.

Scale in Miles

0   10   20

Projected Coordinate System Datum: NAD 1983 Albers Equal Area

GSI ENVIRONMENTAL
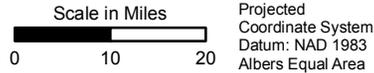
MODELED BASE ELEVATION CONTOURS FOR YEGUA-JACKSON AQUIFER

Lower Rio Grande Valley

GSI Job No. 4276	Drawn By: AV
Issued: 19-Jun-2017	Chk'd By: KER
Map ID: LRGV_Fig_4_1_22	Appv'd By: SP

FIGURE 2.4.19

Sources: Esri, USGS, NOAA
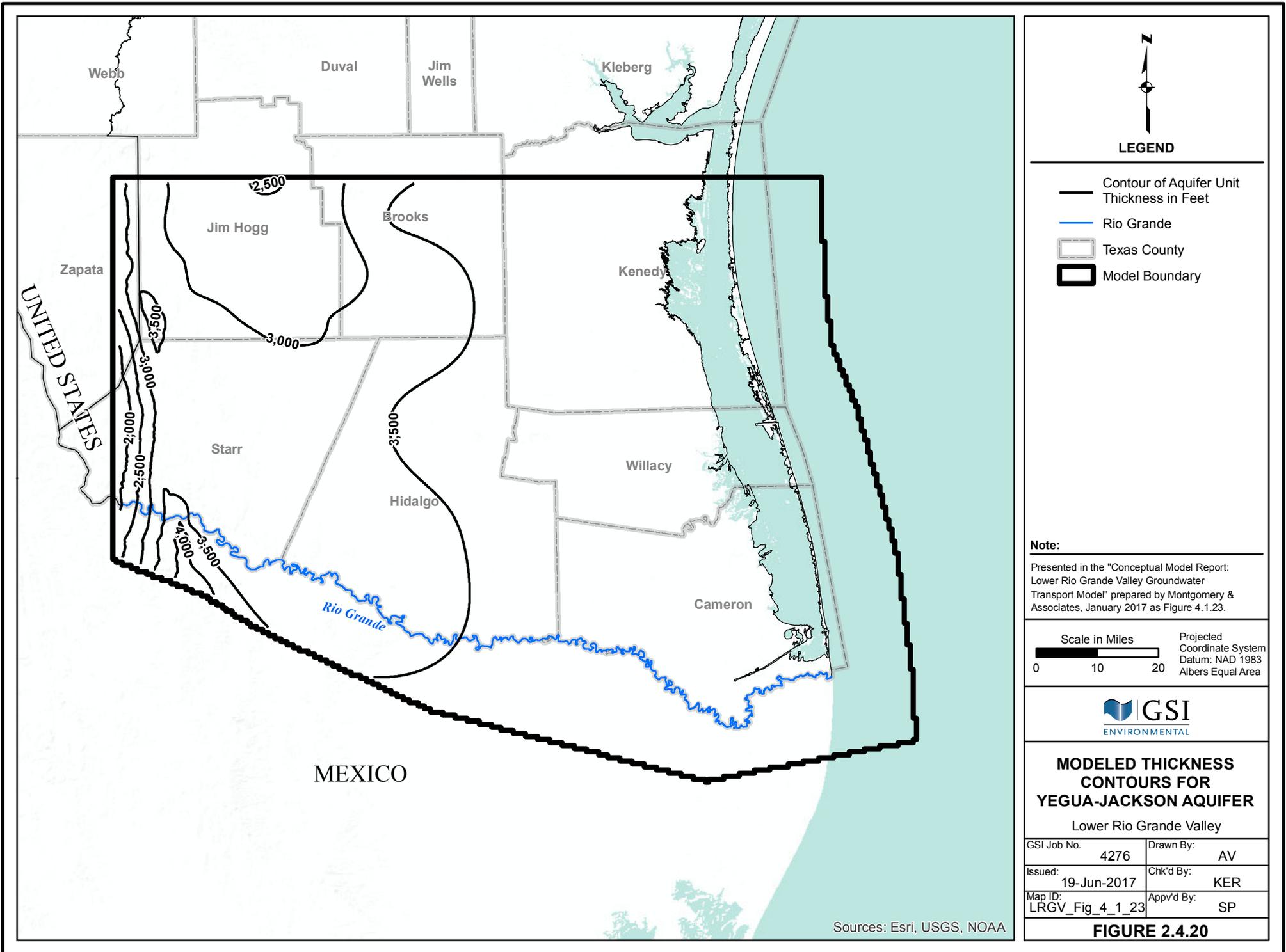
LEGEND

— Contour of Aquifer Unit Thickness in Feet

— Rio Grande

☐ Texas County

☐ Model Boundary

Note:

Presented in the "Conceptual Model Report: Lower Rio Grande Valley Groundwater Transport Model" prepared by Montgomery & Associates, January 2017 as Figure 4.1.23.

Scale in Miles

0   10   20

Projected Coordinate System Datum: NAD 1983 Albers Equal Area

GSI
ENVIRONMENTAL

MODELED THICKNESS CONTOURS FOR YEGUA-JACKSON AQUIFER

Lower Rio Grande Valley

GSI Job No. 4276	Drawn By: AV
Issued: 19-Jun-2017	Chk'd By: KER
Map ID: LRGV_Fig_4_1_23	Appv'd By: SP

FIGURE 2.4.20

Sources: Esri, USGS, NOAA

Webb

Duval

Jim Wells

Kleberg

Zapata

UNITED STATES

Jim Hogg

Brooks

Kenedy

Starr

Hidalgo

Willacy

Cameron

INSET

INSET

MEXICO

N

Miles

0 2 4

Sources: Esri, USGS, NOAA

West | **East**

L10

ELEVATION (feet amsl)

MODEL LAYERS — L1, L2, L3, L4, L5, L6, L7, L8, L9, L11, L12

Units Not Included in Model

a) Section Row 100

DISTANCE (feet)

South | **North**

MODEL LAYERS — L1-3, L4, L5, L6, L7, L8, L9, L10, L11, L12

ELEVATION (feet amsl)

Units Not Included in Model

b) Section Column 180

DISTANCE (feet)

Vertical exaggeration: 10x

Inset map: Zapata, Jim Hogg, Brooks, Kenedy, Gulf of Mexico, Starr, Model Column 180, Model Row 100, W, E, Hidalgo, Willacy, Cameron, Rio Grande, N, S

EXPLANATION
- Lines of Hydrogeologic Sections
- Study Area
- County
- State
- Rio Grande

0 20 Miles

EXPLANATION

Aquifer (Hydrostratigraphic Unit)

- Chicot (Beaumont)
- Chicot (Lissie)
- Chicot (Willis)
- Evangeline (Upper Goliad)
- Evangeline (Lower Goliad)
- Evangeline (Upper Lagarto)
- Burkeville Confining Unit (Middle Lagarto)
- Jasper (Lower Lagarto)
- Jasper (Oakville)
- Jasper (Upper Catahoula)
- Catahoula Confining System
- Yegua-Jackson Aquifer

GSI ENVIRONMENTAL

CROSS SECTIONS OF GRIDDED MODEL LAYERS IN THE GROUNDWATER FLOW MODEL

Lower Rio Grande Valley

GSI Job No.	Drawn By:
4276	AV
Issued:	Chk'd By:
19-Jun-2017	KER
Map ID:	Appv'd By:
LRGV_Xsection2	SP

FIGURE 2.4.22

LEGEND

Texas County

Model Boundary

Estimated Sand Fraction

0 - 0.2

0.2 - 0.4

0.4 - 0.6

0.6 - 0.8

0.8 - 1

Layer Pinchout

Note:

Basemap provided by Montgomery & Associates December 2016.

Scale in Miles

0   10   20

Projected Coordinate System Datum: NAD 1983 Albers Equal Area

GSI ENVIRONMENTAL
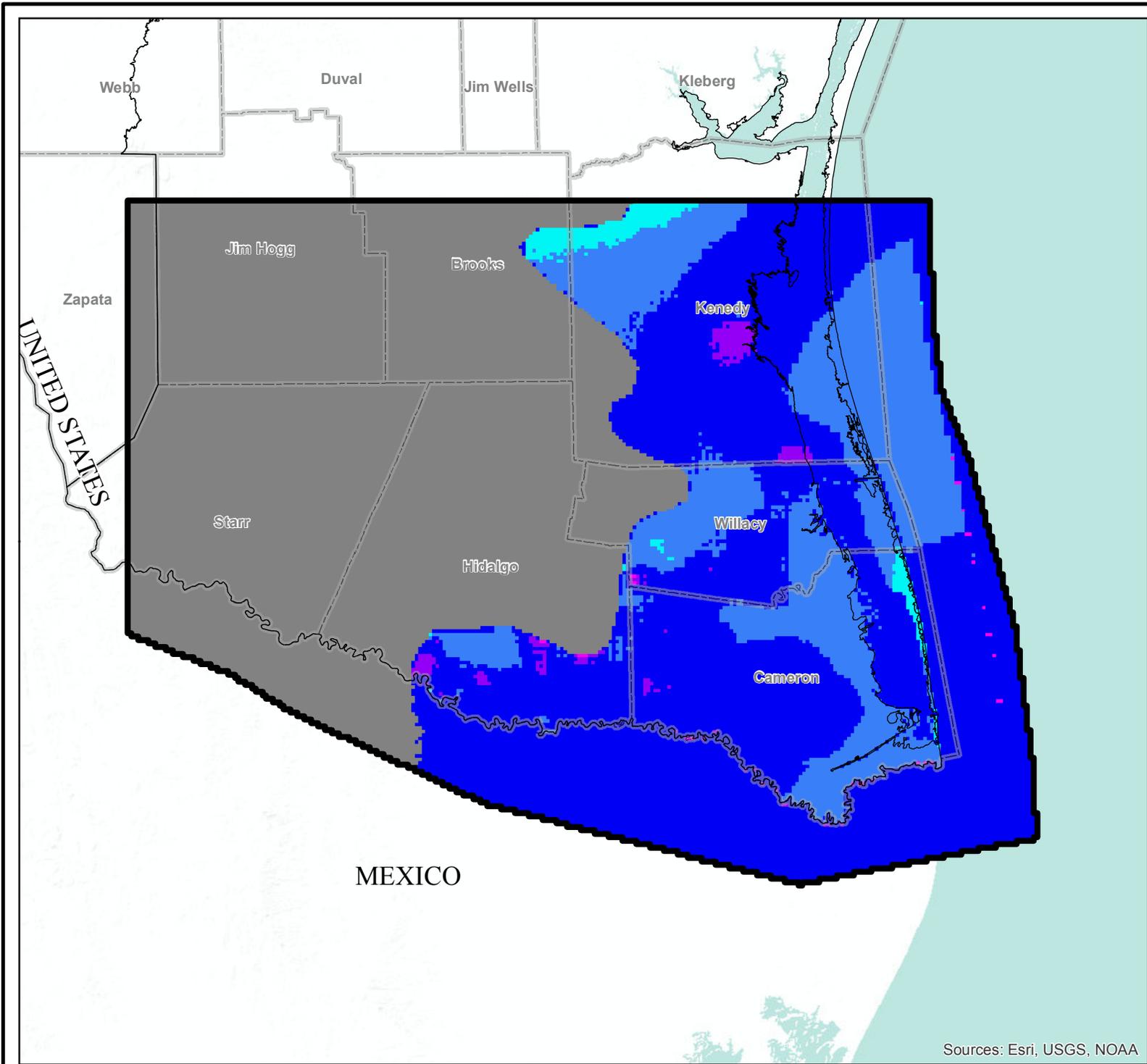
ESTIMATED SAND FRACTION DISTRIBUTION FOR BEAUMONT FORMATION OF CHICOT AQUIFER
Lower Rio Grande Valley

GSI Job No. 4276	Drawn By: AV
Issued: 22-Jun-2017	Chk'd By: KER
Map ID: LRGV_SF_B_L1	Appv'd By: SP

FIGURE 2.5.1
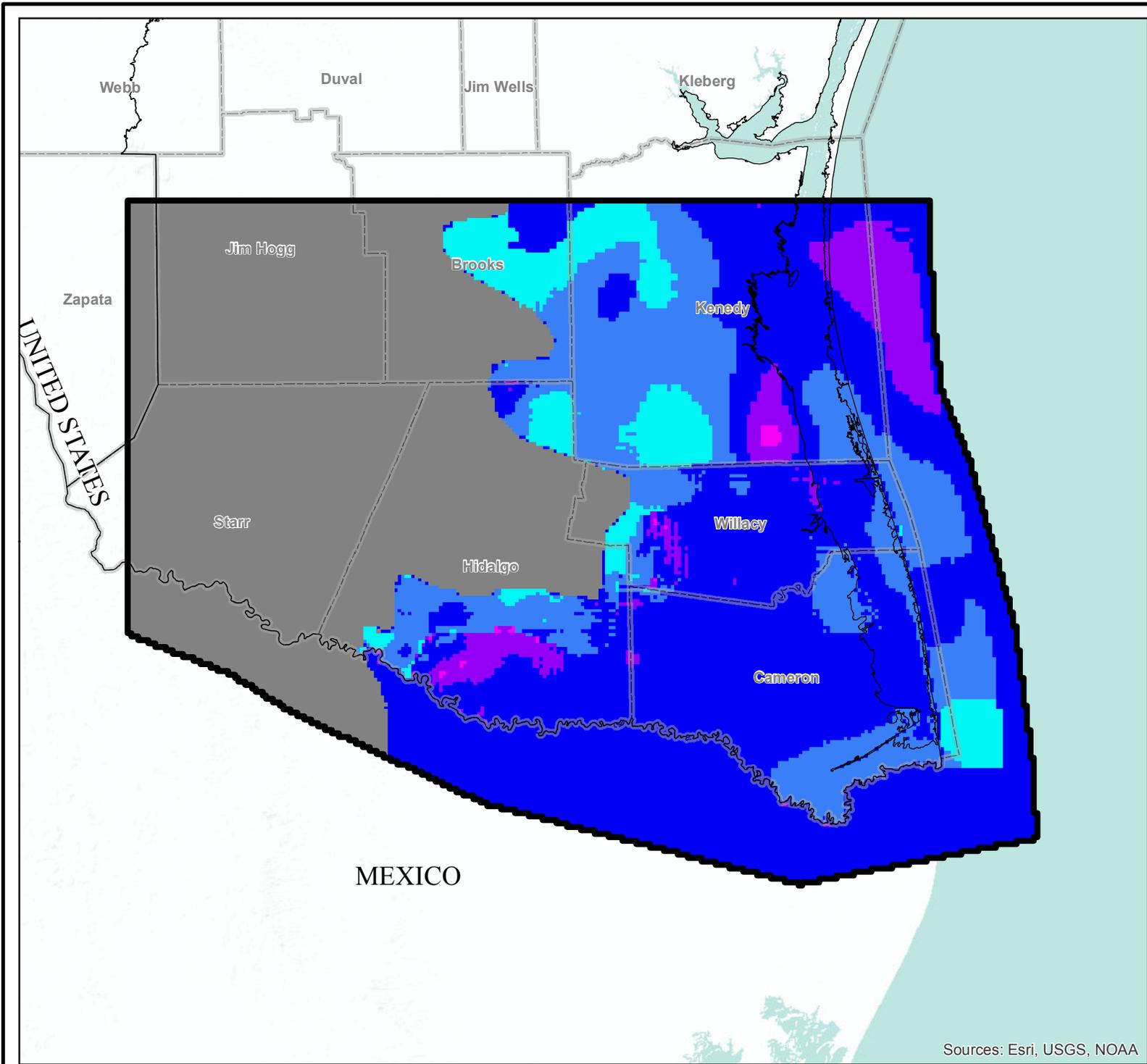
Sources: Esri, USGS, NOAA

LEGEND

Texas County
Model Boundary

Estimated Sand Fraction

	0 - 0.2
	0.2 - 0.4
	0.4 - 0.6
	0.6 - 0.8
	0.8 - 1
	Layer Pinchout

Note:

Basemap provided by Montgomery & Associates December 2016.

Scale in Miles

0   10   20

Projected Coordinate System Datum: NAD 1983 Albers Equal Area

GSI
ENVIRONMENTAL
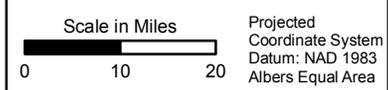
ESTIMATED SAND FRACTION DISTRIBUTION FOR LISSIE FORMATION OF CHICOT AQUIFER
Lower Rio Grande Valley

GSI Job No. 4276	Drawn By: AV
Issued: 22-Jun-2017	Chk'd By: KER
Map ID: LRGV_SF_L_L2	Appv'd By: SP

FIGURE 2.5.2

Sources: Esri, USGS, NOAA
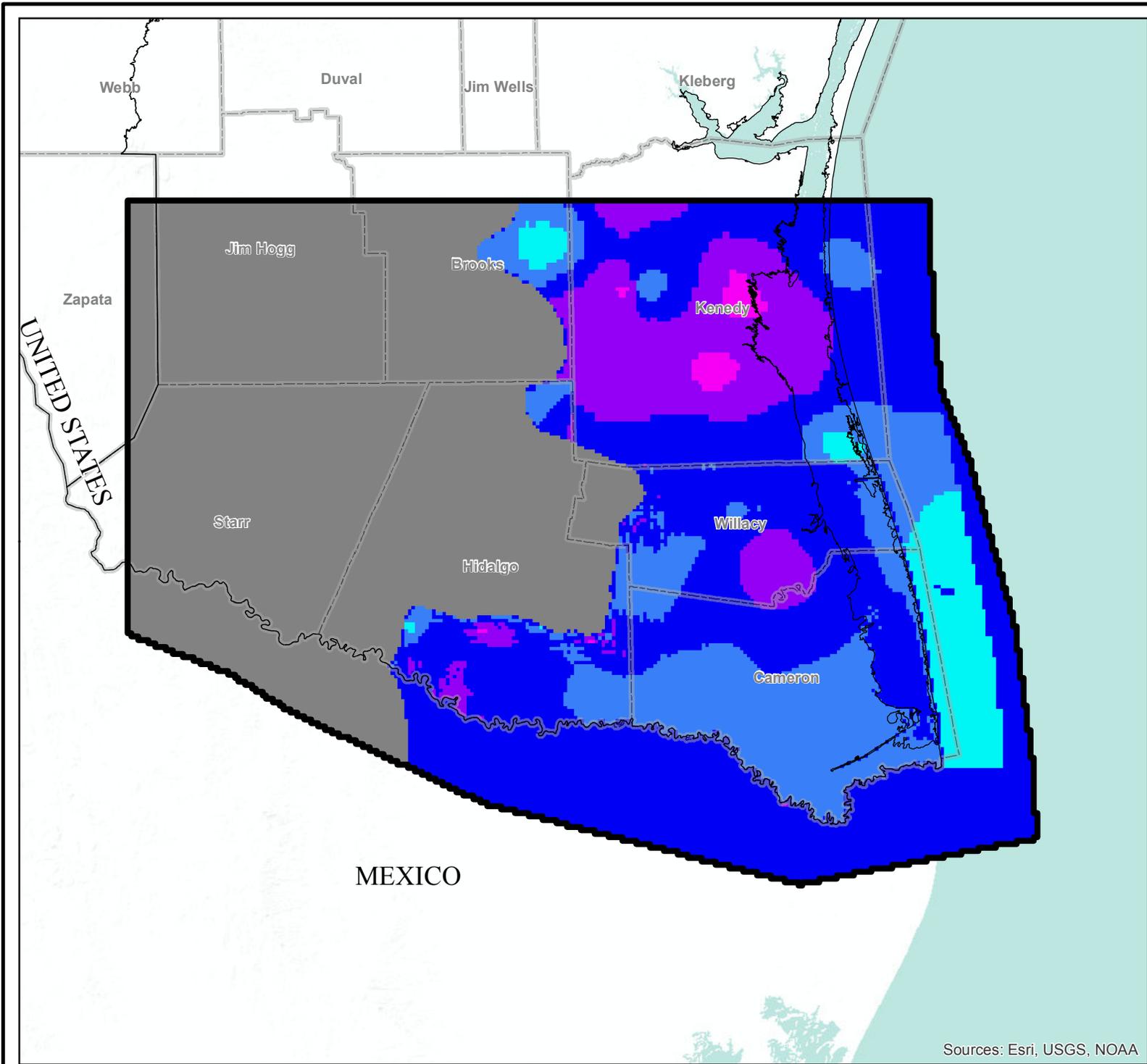
LEGEND

- ☐ Texas County
- ☐ Model Boundary

Estimated Sand Fraction
- 0 - 0.2
- 0.2 - 0.4
- 0.4 - 0.6
- 0.6 - 0.8
- 0.8 - 1
- Layer Pinchout

Note:

Basemap provided by Montgomery & Associates December 2016.

Scale in Miles

0   10   20

Projected Coordinate System
Datum: NAD 1983
Albers Equal Area

GSI ENVIRONMENTAL

ESTIMATED SAND FRACTION DISTRIBUTION FOR WILLIS FORMATION OF CHICOT AQUIFER
Lower Rio Grande Valley

GSI Job No. 4276	Drawn By: AV
Issued: 22-Jun-2017	Chk'd By: KER
Map ID: LRGV_SF_W_L3	Appv'd By: SP

FIGURE 2.5.3
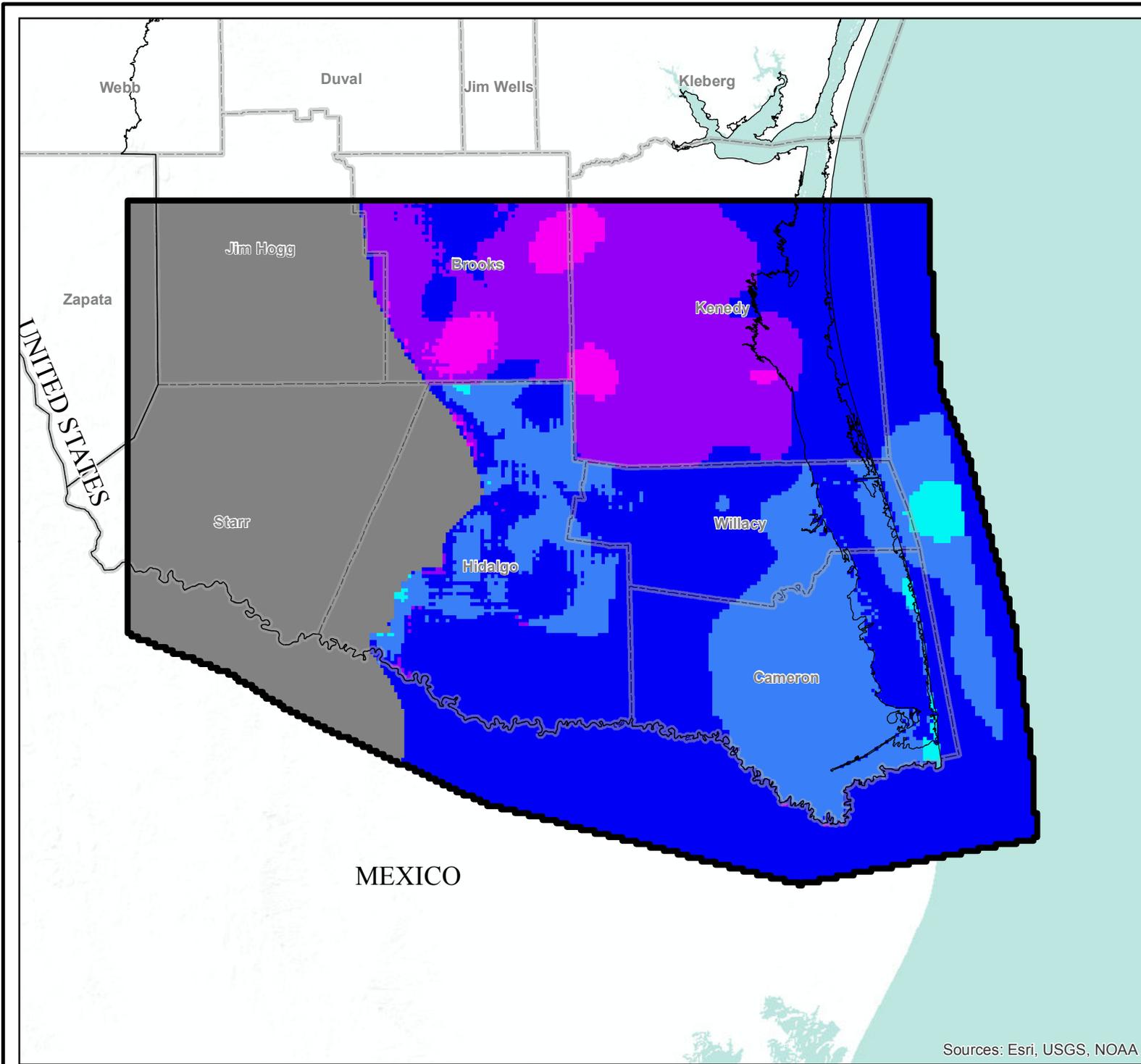
Sources: Esri, USGS, NOAA

LEGEND

Texas County

Model Boundary

Estimated Sand Fraction

	0 - 0.2
	0.2 - 0.4
	0.4 - 0.6
	0.6 - 0.8
	0.8 - 1
	Layer Pinchout

Note:

Basemap provided by Montgomery & Associates December 2016.

Scale in Miles

0   10   20

Projected Coordinate System Datum: NAD 1983 Albers Equal Area

GSI ENVIRONMENTAL

ESTIMATED SAND FRACTION DISTRIBUTION FOR UPPER GOLIAD FORMATION OF EVANGELINE AQUIFER
Lower Rio Grande Valley

GSI Job No.	Drawn By:
4276	AV
Issued:	Chk'd By:
22-Jun-2017	KER
Map ID:	Appv'd By:
LRGV_SF_UG_L4	SP

FIGURE 2.5.4

County labels on map: Webb, Duval, Jim Wells, Kleberg, Jim Hogg, Zapata, Brooks, Kenedy, Starr, Hidalgo, Willacy, Cameron

UNITED STATES

MEXICO

Sources: Esri, USGS, NOAA

LEGEND

Texas County

Model Boundary

Estimated Sand Fraction

- 0 - 0.2
- 0.2 - 0.4
- 0.4 - 0.6
- 0.6 - 0.8
- 0.8 - 1
- Layer Pinchout

Note:

Basemap provided by Montgomery & Associates December 2016.

Scale in Miles

0   10   20

Projected Coordinate System Datum: NAD 1983 Albers Equal Area

GSI ENVIRONMENTAL
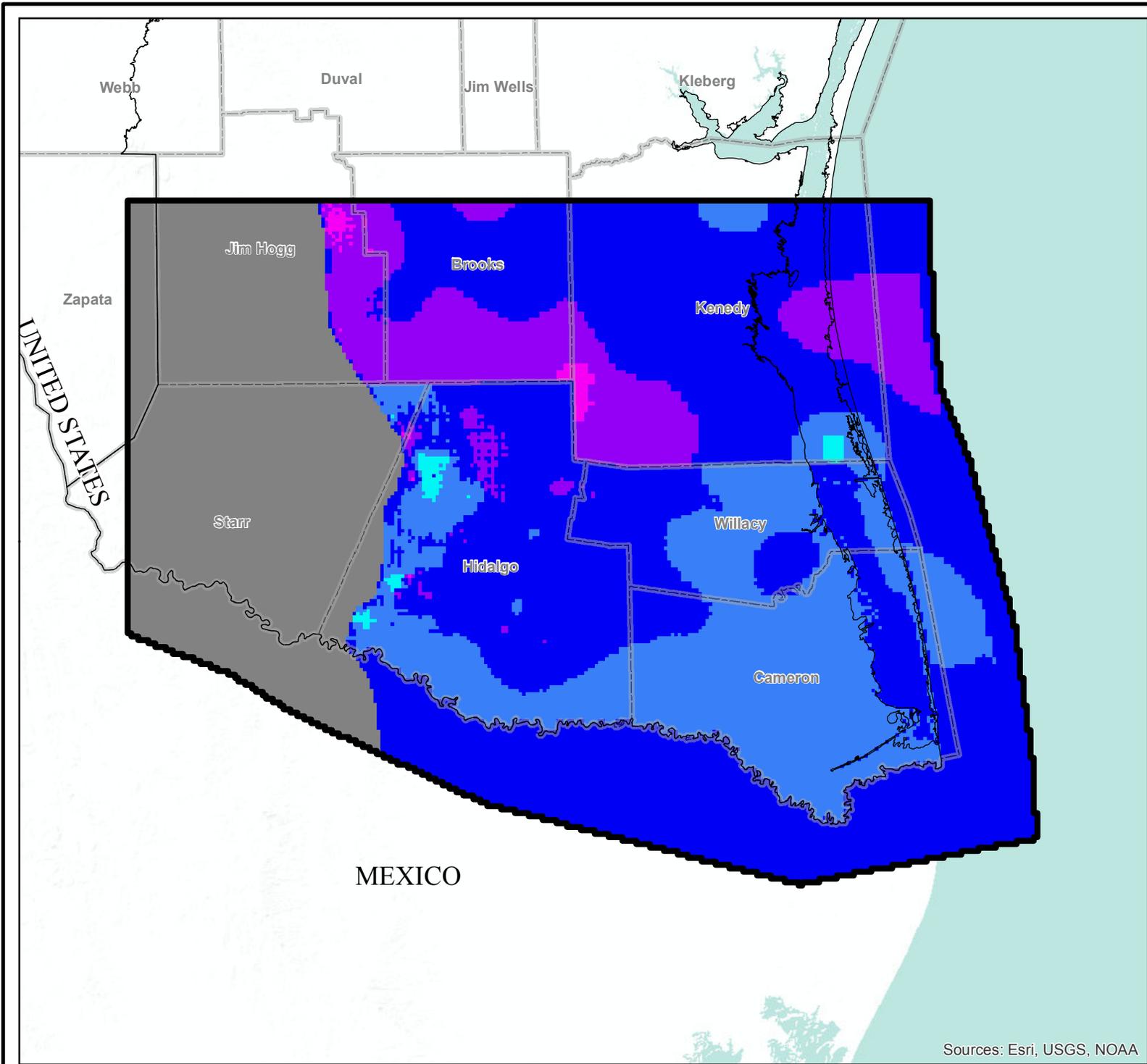
ESTIMATED SAND FRACTION DISTRIBUTION FOR LOWER GOLIAD FORMATION OF EVANGELINE AQUIFER
Lower Rio Grande Valley

GSI Job No. 4276	Drawn By: AV
Issued: 22-Jun-2017	Chk'd By: KER
Map ID: LRGV_SF_LG_L5	Appv'd By: SP

FIGURE 2.5.5

Sources: Esri, USGS, NOAA
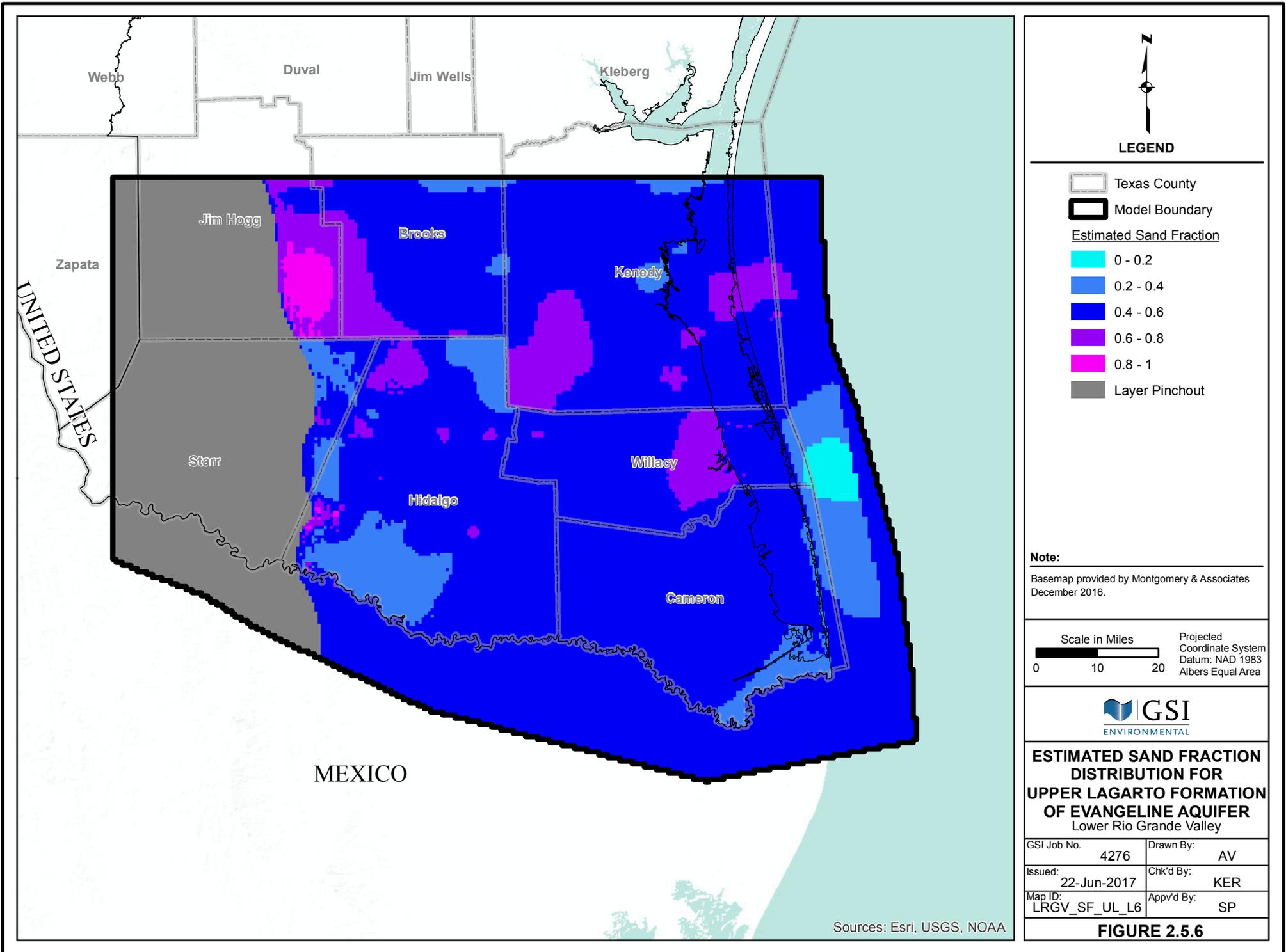
LEGEND

☐	Texas County
▢	Model Boundary

Estimated Sand Fraction

■	0 - 0.2
■	0.2 - 0.4
■	0.4 - 0.6
■	0.6 - 0.8
■	0.8 - 1
■	Layer Pinchout

Note:

Basemap provided by Montgomery & Associates December 2016.

Scale in Miles

0   10   20

Projected Coordinate System Datum: NAD 1983 Albers Equal Area

GSI ENVIRONMENTAL
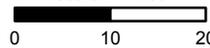
ESTIMATED SAND FRACTION DISTRIBUTION FOR UPPER LAGARTO FORMATION OF EVANGELINE AQUIFER

Lower Rio Grande Valley

GSI Job No. 4276	Drawn By: AV
Issued: 22-Jun-2017	Chk'd By: KER
Map ID: LRGV_SF_UL_L6	Appv'd By: SP

FIGURE 2.5.6

Sources: Esri, USGS, NOAA

LEGEND

Texas County
Model Boundary

Estimated Sand Fraction
- 0 - 0.2
- 0.2 - 0.4
- 0.4 - 0.6
- 0.6 - 0.8
- 0.8 - 1
- Layer Pinchout

Note:

Basemap provided by Montgomery & Associates December 2016.

Scale in Miles

0   10   20

Projected Coordinate System Datum: NAD 1983 Albers Equal Area

GSI ENVIRONMENTAL

ESTIMATED SAND FRACTION DISTRIBUTION FOR MIDDLE LAGARTO FORMATION OF BURKEVILLE CONFINING UNIT
Lower Rio Grande Valley

GSI Job No.	Drawn By:
4276	AV
Issued:	Chk'd By:
22-Jun-2017	KER
Map ID:	Appv'd By:
LRGV_SF_ML_L7	SP

FIGURE 2.5.7

Webb
Duval
Jim Wells
Kleberg
Jim Hogg
Brooks
Kenedy
Zapata
UNITED STATES
Starr
Willacy
Hidalgo
Cameron
MEXICO

Sources: Esri, USGS, NOAA

LEGEND

Texas County
Model Boundary

Estimated Sand Fraction

- 0 -0.2
- 0.2 - 0.4
- 0.4 - 0.6
- 0.6 - 0.8
- 0.8 - 1
- Layer Pinchout

Note:

Basemap provided by Montgomery & Associates December 2016.

Scale in Miles

0   10   20

Projected Coordinate System Datum: NAD 1983 Albers Equal Area

GSI
ENVIRONMENTAL

ESTIMATED SAND FRACTION DISTRIBUTION FOR LOWER LAGARTO FORMATION OF JASPER AQUIFER
Lower Rio Grande Valley

GSI Job No. 4276	Drawn By: AV
Issued: 22-Jun-2017	Chk'd By: KER
Map ID: LRGV_SF_LL_L8	Appv'd By: SP

FIGURE 2.5.8
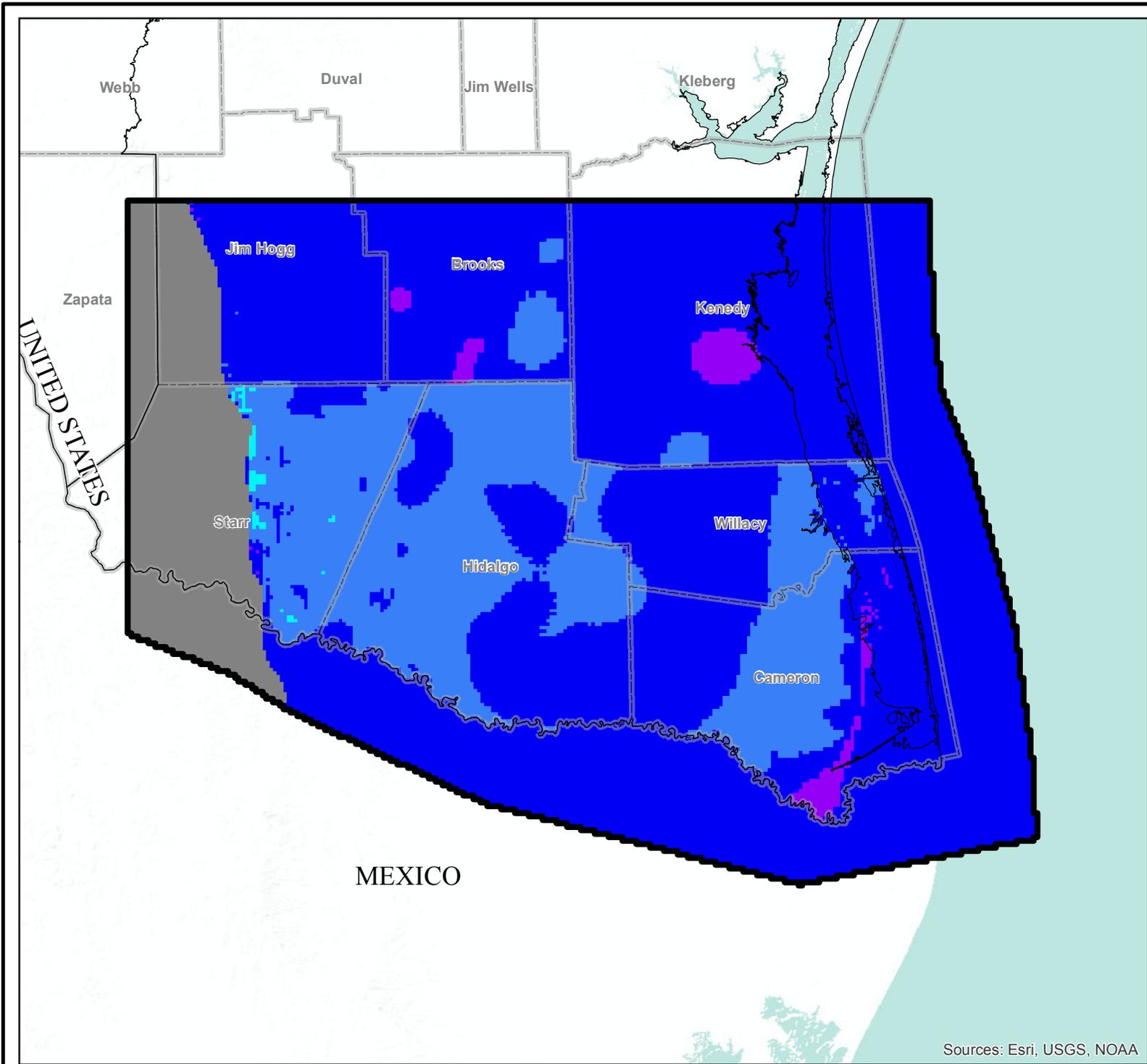
Sources: Esri, USGS, NOAA

LEGEND

Texas County

Model Boundary

Estimated Sand Fraction

0 - 0.2

0.2 - 0.4

0.4 - 0.6

0.6 - 0.8

0.8 - 1

Layer Pinchout

Note:

Basemap provided by Montgomery & Associates December 2016.

Scale in Miles

0   10   20

Projected Coordinate System
Datum: NAD 1983
Albers Equal Area

GSI ENVIRONMENTAL

ESTIMATED SAND FRACTION DISTRIBUTION FOR OAKVILLE FORMATION OF JASPER AQUIFER
Lower Rio Grande Valley

GSI Job No. 4276	Drawn By: AV
Issued: 22-Jun-2017	Chk'd By: KER
Map ID: LRGV_SF_Ok_L9	Appv'd By: SP

FIGURE 2.5.9

Sources: Esri, USGS, NOAA
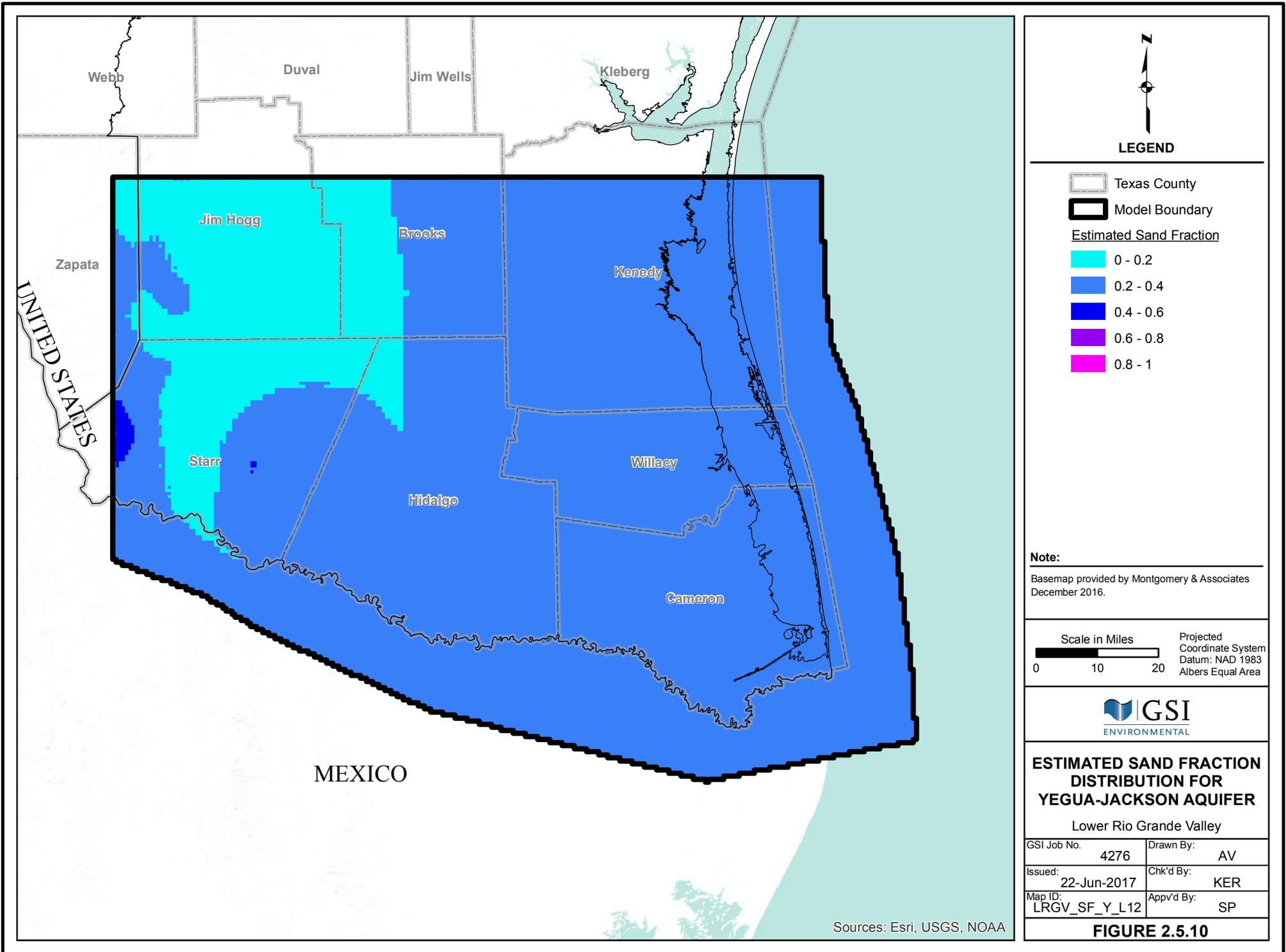
LEGEND

- ☐ Texas County
- ▬ Model Boundary

Estimated Sand Fraction

- ☐ 0 - 0.2
- ☐ 0.2 - 0.4
- ☐ 0.4 - 0.6
- ☐ 0.6 - 0.8
- ☐ 0.8 - 1

Note:

Basemap provided by Montgomery & Associates December 2016.

Scale in Miles

0   10   20

Projected Coordinate System
Datum: NAD 1983
Albers Equal Area

GSI
ENVIRONMENTAL

ESTIMATED SAND FRACTION DISTRIBUTION FOR YEGUA-JACKSON AQUIFER

Lower Rio Grande Valley

GSI Job No. 4276	Drawn By: AV
Issued: 22-Jun-2017	Chk'd By: KER
Map ID: LRGV_SF_Y_L12	Appv'd By: SP

FIGURE 2.5.10

Sources: Esri, USGS, NOAA
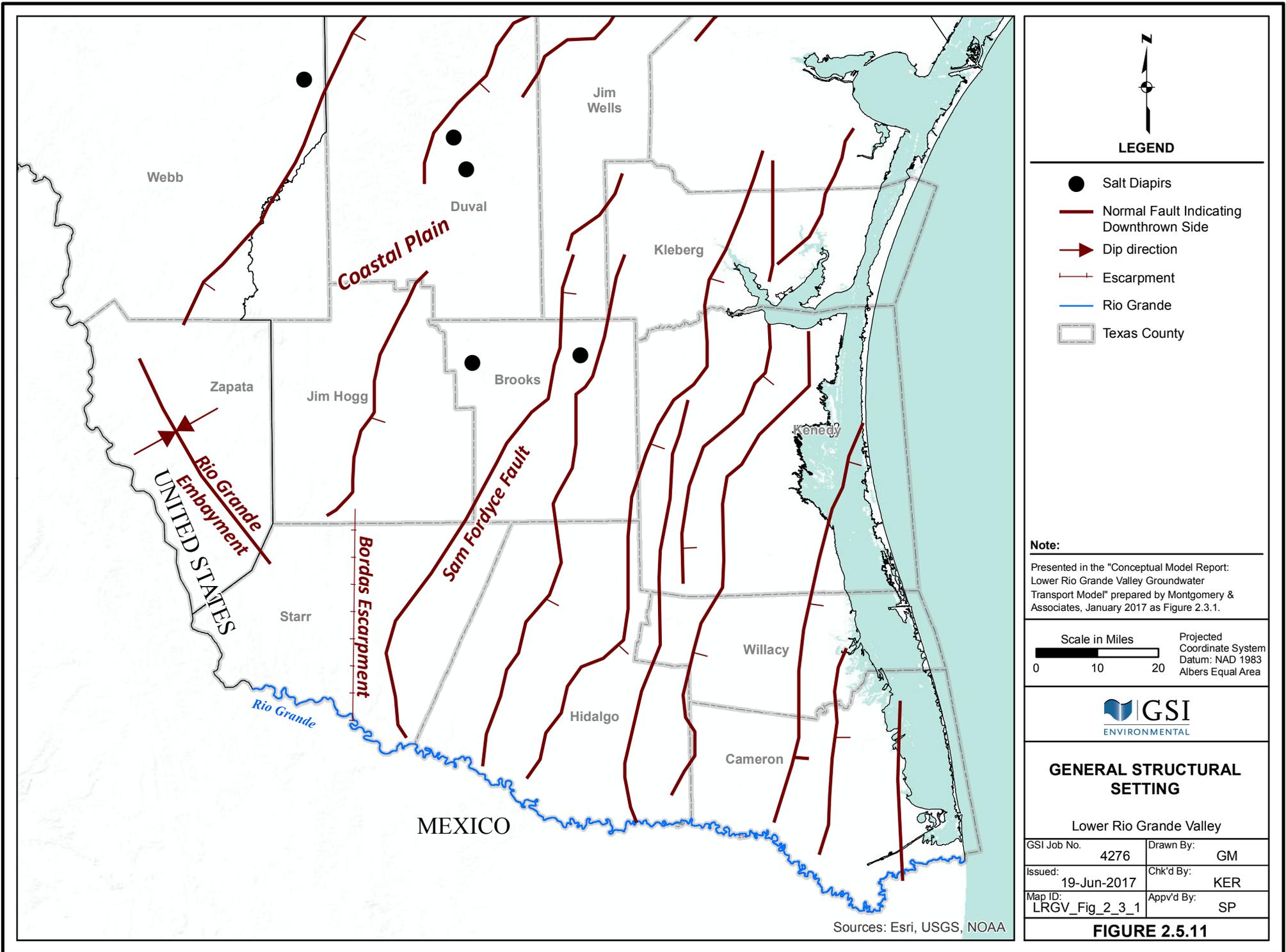
LEGEND

- ● Salt Diapirs
- ▬ Normal Fault Indicating Downthrown Side
- ➤ Dip direction
- ┼ Escarpment
- ▬ Rio Grande
- ☐ Texas County

Note:

Presented in the "Conceptual Model Report: Lower Rio Grande Valley Groundwater Transport Model" prepared by Montgomery & Associates, January 2017 as Figure 2.3.1.

Scale in Miles

0   10   20

Projected Coordinate System Datum: NAD 1983 Albers Equal Area

GSI ENVIRONMENTAL

GENERAL STRUCTURAL SETTING

Lower Rio Grande Valley

GSI Job No. 4276	Drawn By: GM
Issued: 19-Jun-2017	Chk'd By: KER
Map ID: LRGV_Fig_2_3_1	Appv'd By: SP

FIGURE 2.5.11

Sources: Esri, USGS, NOAA
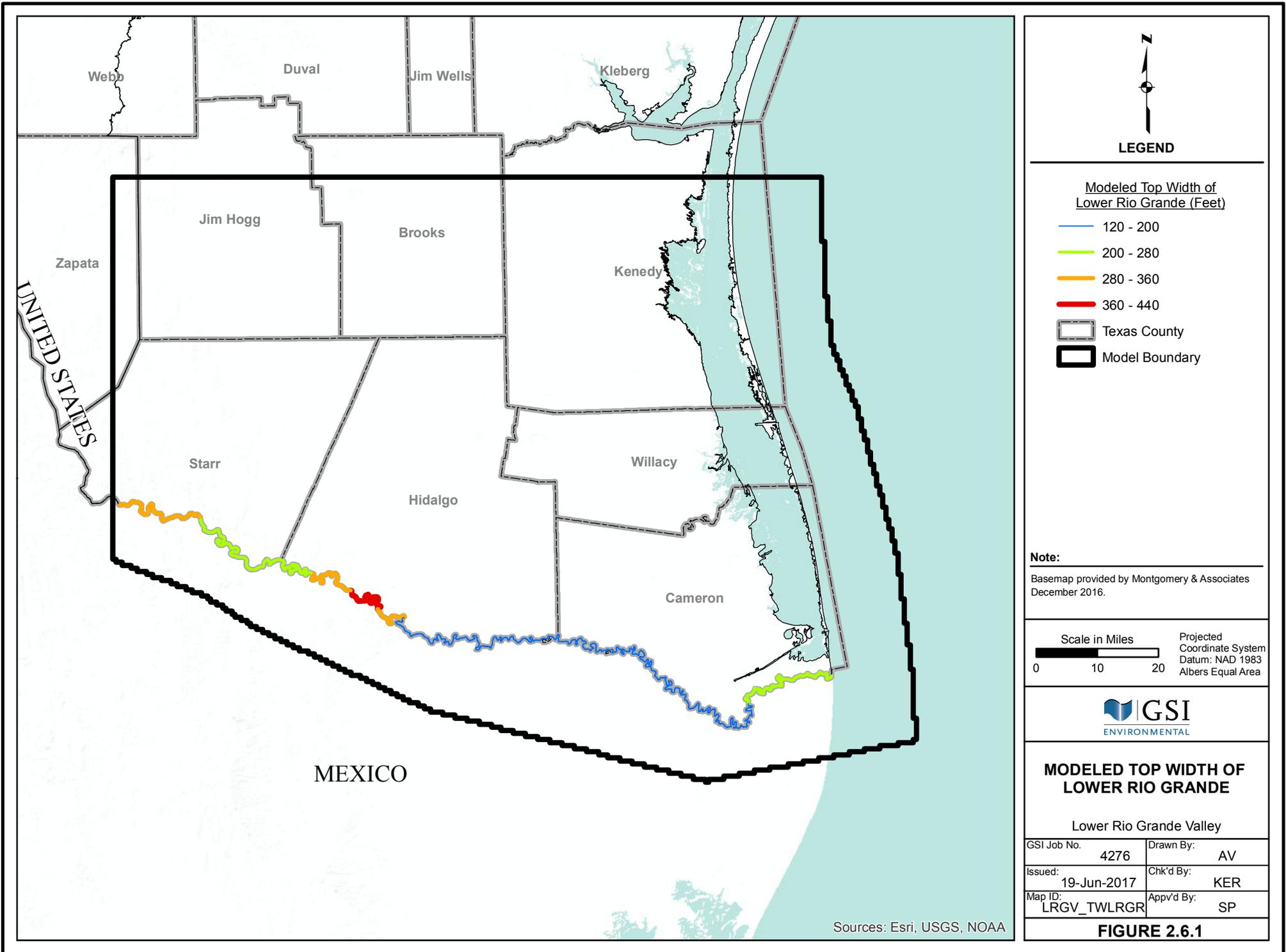
LEGEND

Modeled Top Width of Lower Rio Grande (Feet)

— 120 - 200
— 200 - 280
— 280 - 360
— 360 - 440

Texas County

Model Boundary

Note:

Basemap provided by Montgomery & Associates December 2016.

Scale in Miles

0   10   20

Projected Coordinate System Datum: NAD 1983 Albers Equal Area

GSI
ENVIRONMENTAL

MODELED TOP WIDTH OF LOWER RIO GRANDE

Lower Rio Grande Valley

GSI Job No. 4276	Drawn By: AV
Issued: 19-Jun-2017	Chk'd By: KER
Map ID: LRGV_TWLRGR	Appv'd By: SP

FIGURE 2.6.1

Webb
Duval
Jim Wells
Kleberg
Jim Hogg
Brooks
Zapata
Kenedy
UNITED STATES
Starr
Willacy
Hidalgo
Cameron
MEXICO

Sources: Esri, USGS, NOAA

$$R = h/2 + w^2/(8h)$$
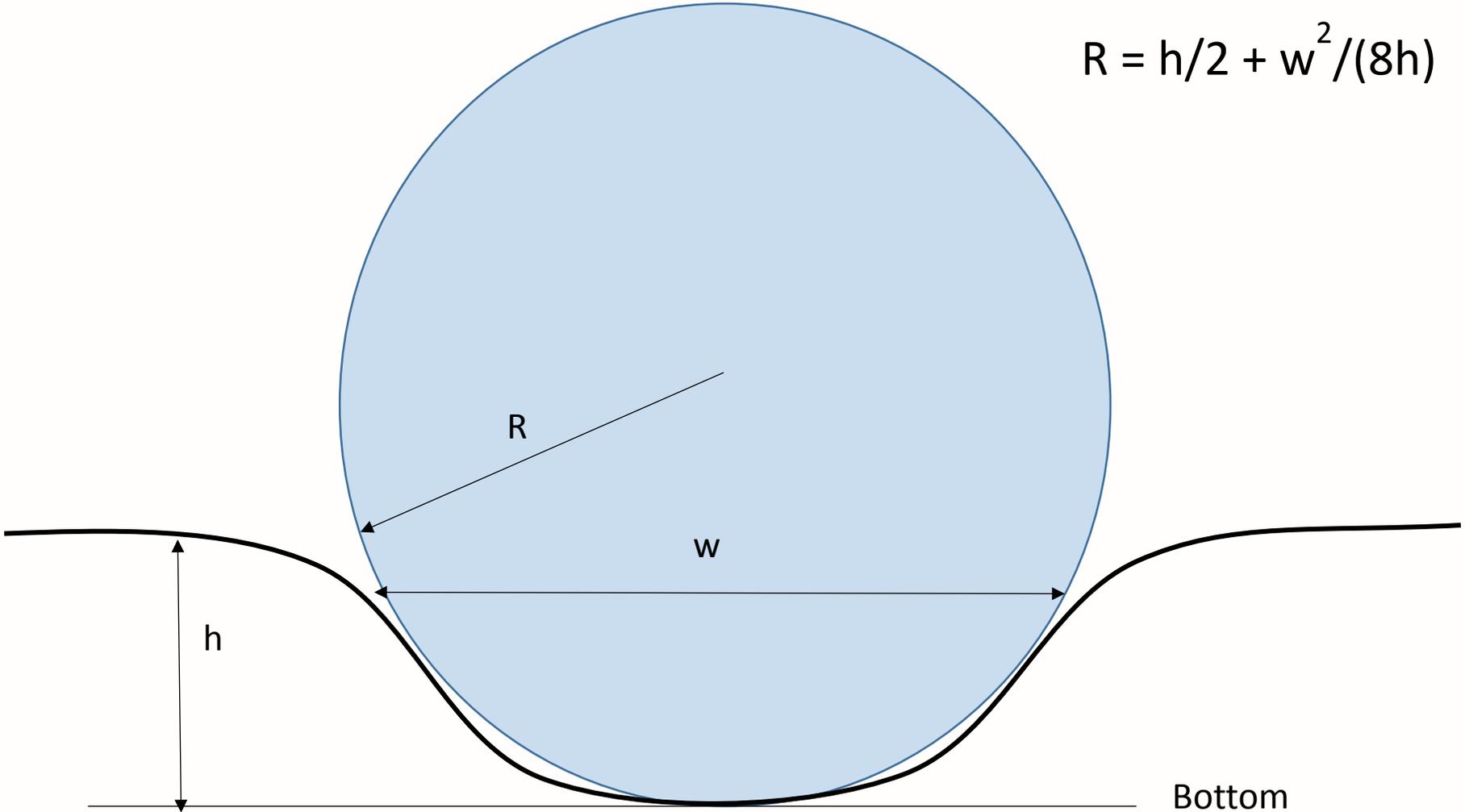
h

w

R

Bottom
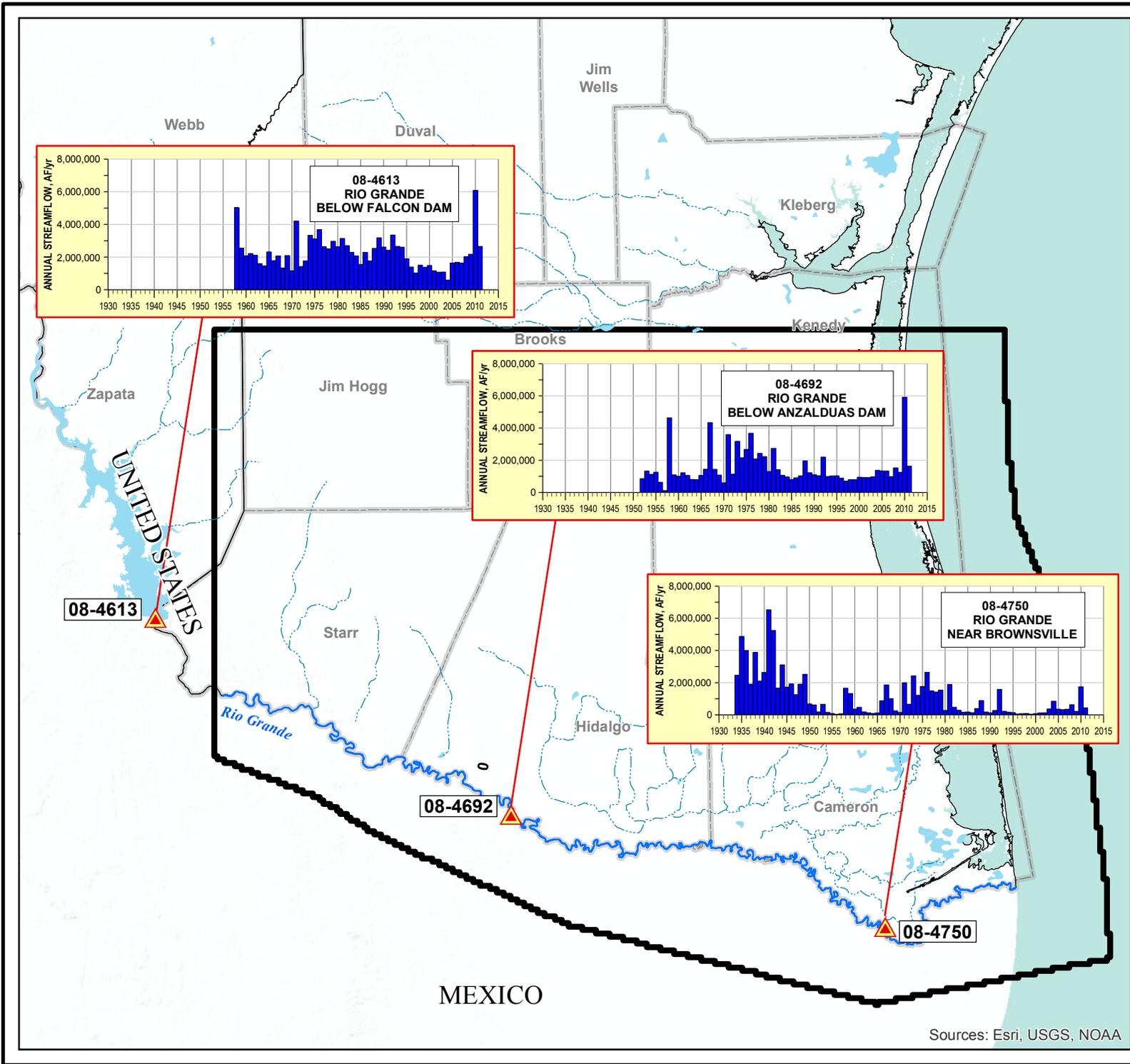
ESTIMATED ANNUAL STREAMFLOWS
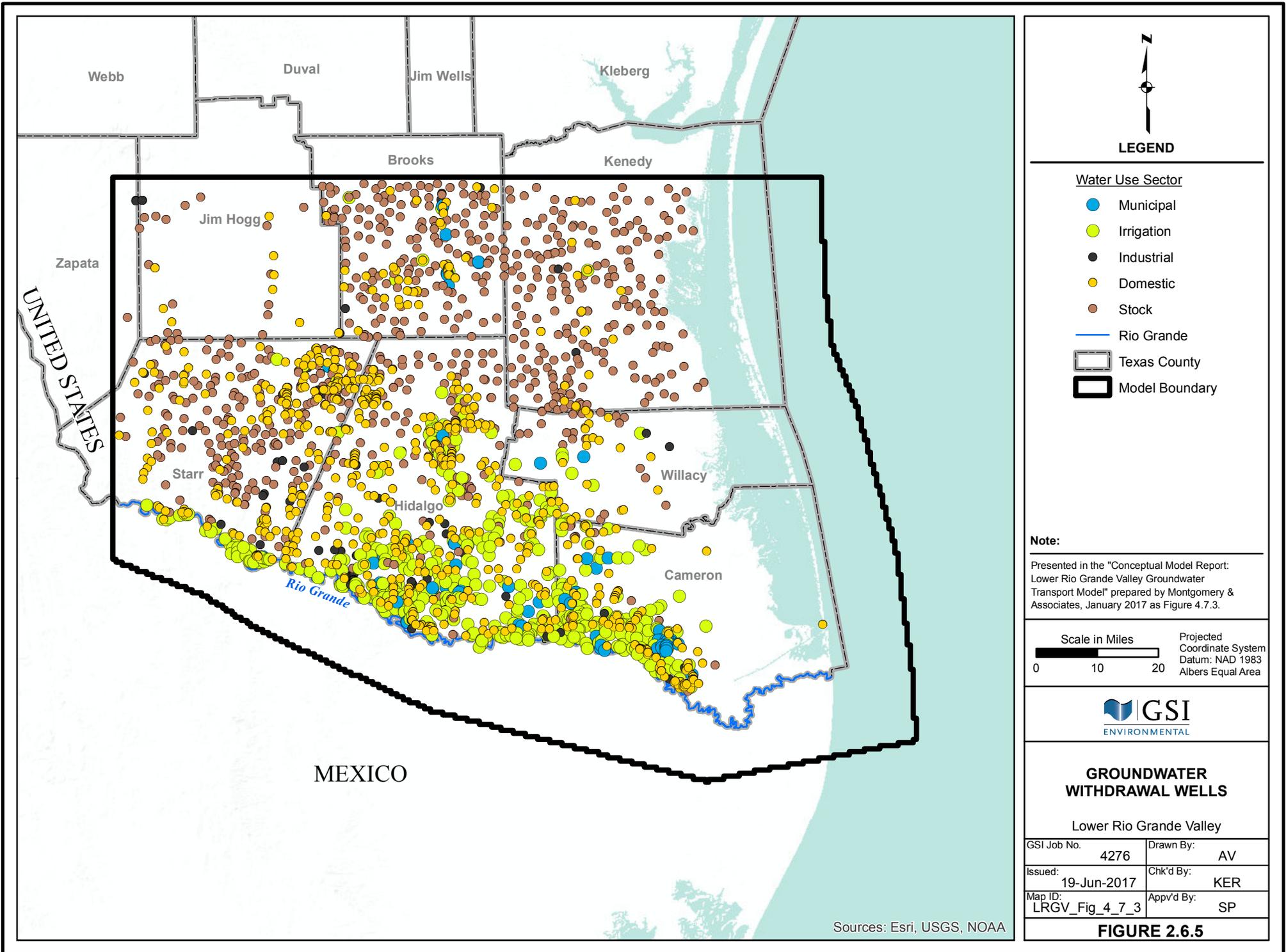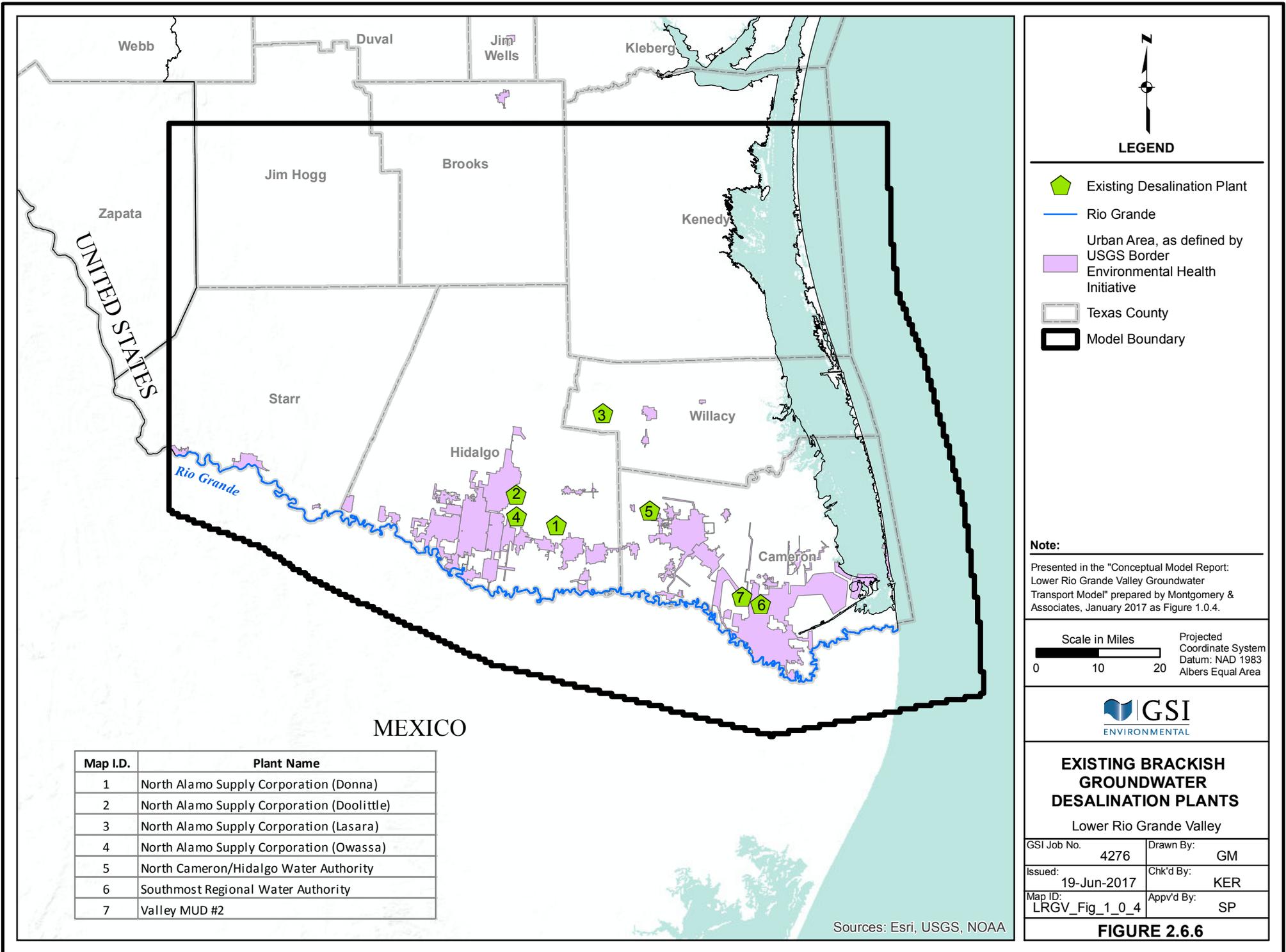
Lower Rio Grande Valley

GSI Job No. 4276	Drawn By: GM
Issued: 23-Jun-2017	Chk'd By: KER
Map ID: LRGV_Fig_4_4_1	Appv'd By: SP

FIGURE 2.6.3

Falcon Dam to Anzalduas Dam

Anzalduas Dam to Brownsville, TX

Notes:

Positive values indicate gains; negative values indicate losses.

Source: IBWC streamflow data

Presented in the "Conceptual Model Report: Lower Rio Grande Valley Groundwater Transport Model" prepared by Montgomery & Associates, January 2017 as Figure 4.4.2

Sources: Esri, USGS, NOAA

LEGEND

⬠ Existing Desalination Plant

— Rio Grande

▢ Urban Area, as defined by USGS Border Environmental Health Initiative

▢ Texas County

▢ Model Boundary

Note:

Presented in the "Conceptual Model Report: Lower Rio Grande Valley Groundwater Transport Model" prepared by Montgomery & Associates, January 2017 as Figure 1.0.4.

Scale in Miles

0   10   20

Projected Coordinate System Datum: NAD 1983 Albers Equal Area

GSI
ENVIRONMENTAL
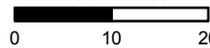
EXISTING BRACKISH GROUNDWATER DESALINATION PLANTS

Lower Rio Grande Valley

GSI Job No. 4276	Drawn By: GM
Issued: 19-Jun-2017	Chk'd By: KER
Map ID: LRGV_Fig_1_0_4	Appv'd By: SP

FIGURE 2.6.6

Map I.D.	Plant Name
1	North Alamo Supply Corporation (Donna)
2	North Alamo Supply Corporation (Doolittle)
3	North Alamo Supply Corporation (Lasara)
4	North Alamo Supply Corporation (Owassa)
5	North Cameron/Hidalgo Water Authority
6	Southmost Regional Water Authority
7	Valley MUD #2
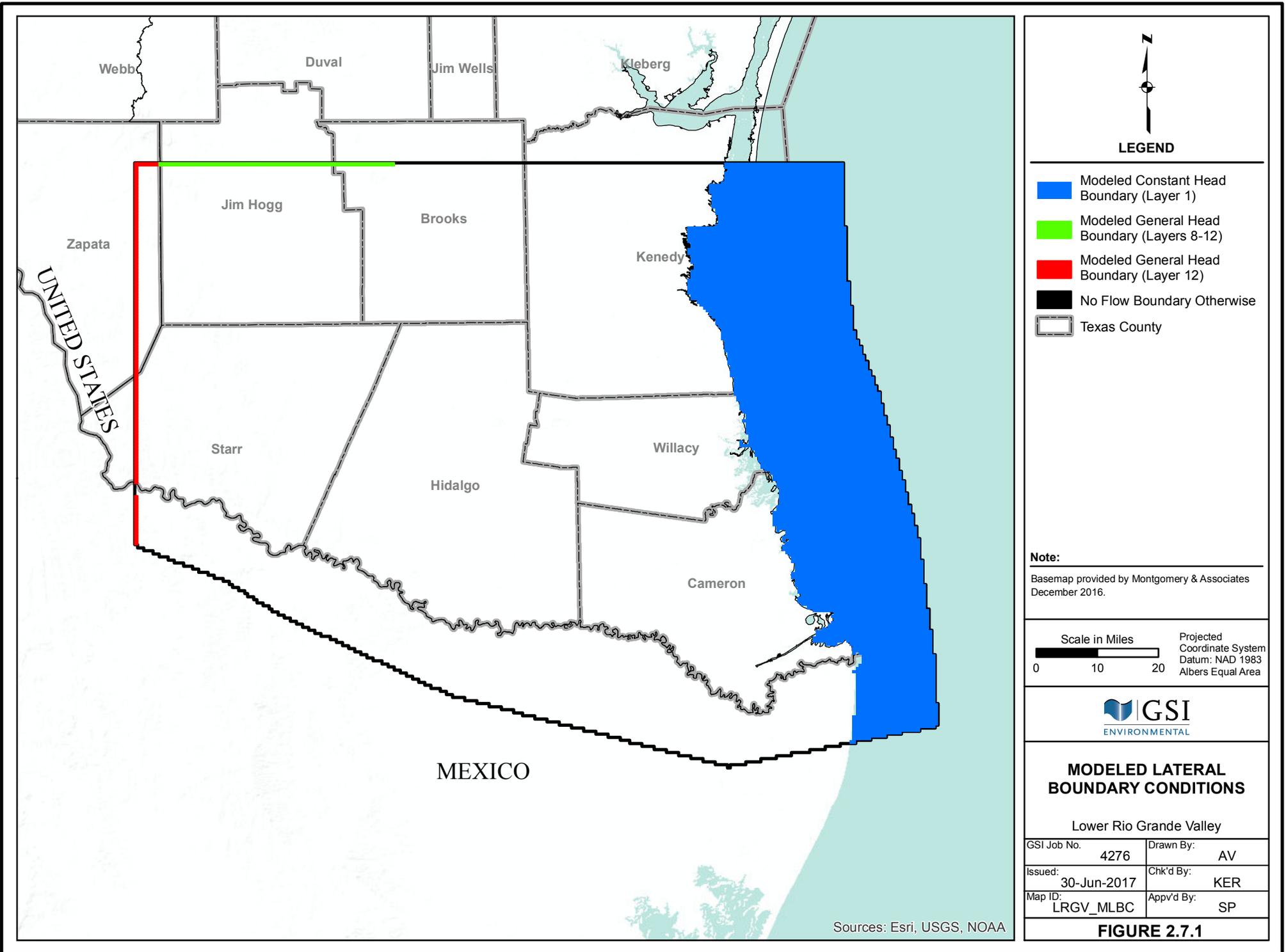
LEGEND

- ▇ Modeled Constant Head Boundary (Layer 1)
- ▇ Modeled General Head Boundary (Layers 8-12)
- ▇ Modeled General Head Boundary (Layer 12)
- ▇ No Flow Boundary Otherwise
- ▢ Texas County

Note:

Basemap provided by Montgomery & Associates December 2016.

Scale in Miles

0   10   20

Projected Coordinate System Datum: NAD 1983 Albers Equal Area

GSI ENVIRONMENTAL

MODELED LATERAL BOUNDARY CONDITIONS

Lower Rio Grande Valley

GSI Job No. 4276	Drawn By: AV
Issued: 30-Jun-2017	Chk'd By: KER
Map ID: LRGV_MLBC	Appv'd By: SP
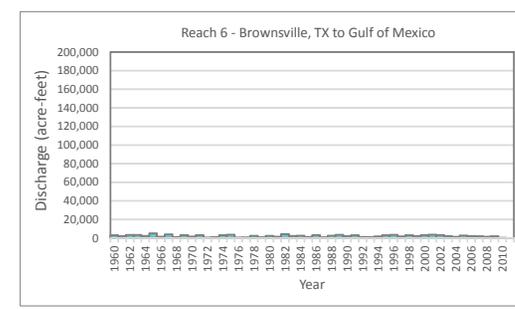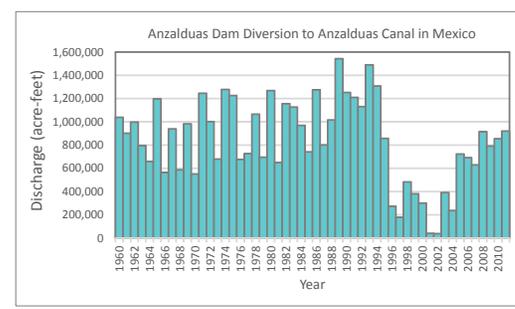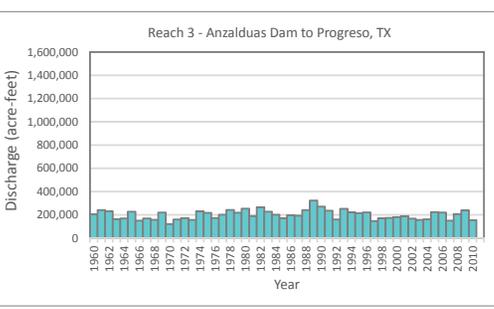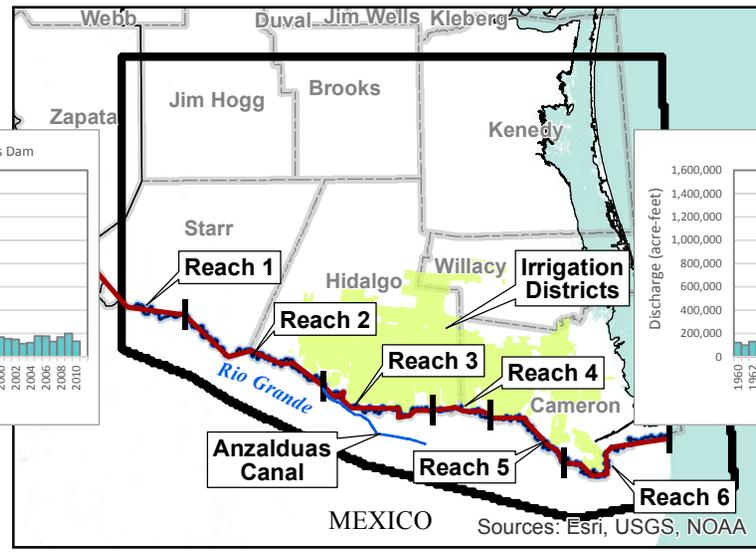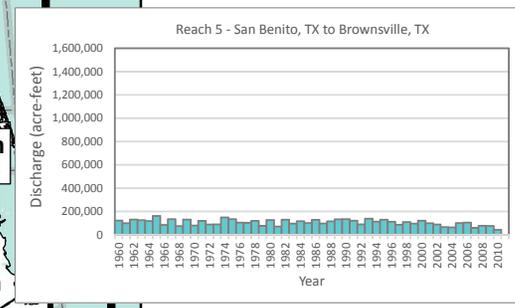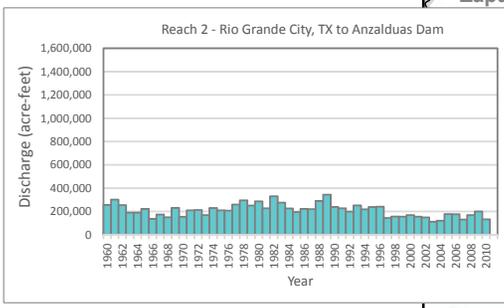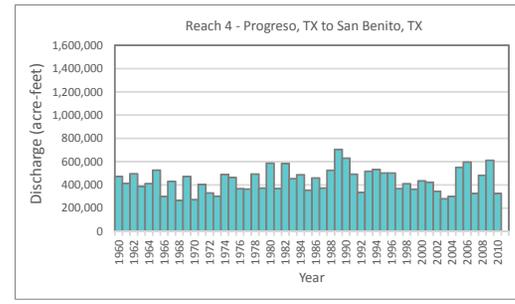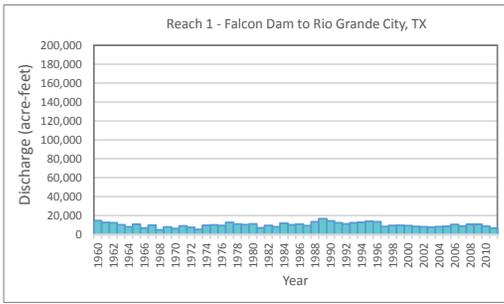
Sources: Esri, USGS, NOAA

FIGURE 2.7.1

ESTIMATED ANNUAL DIVERSIONS FROM THE RIO GRANDE

Lower Rio Grande Valley

FIGURE 2.8.1

Contribution to Rio Grande River - Falcon Dam to Rio Grande City, TX

Contribution to Rio Grande River - Rio Grande City, TX to Anzalduas Dam
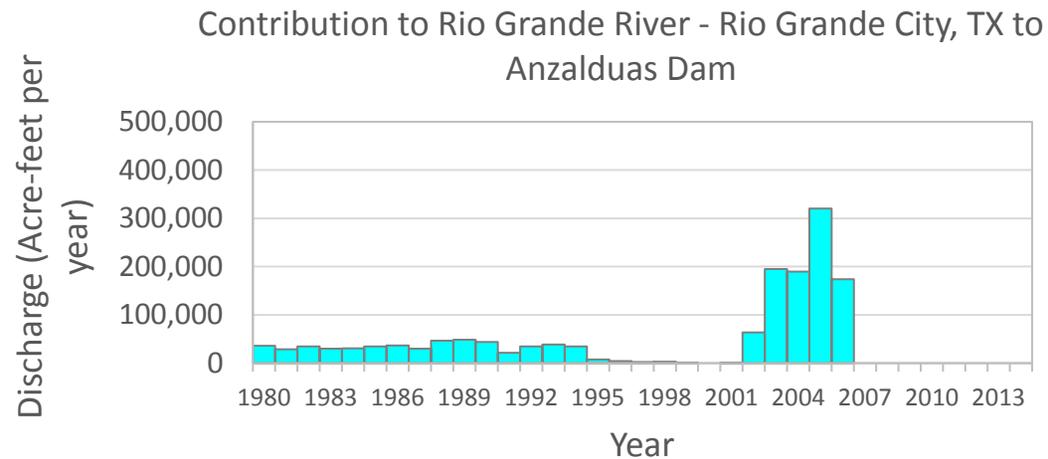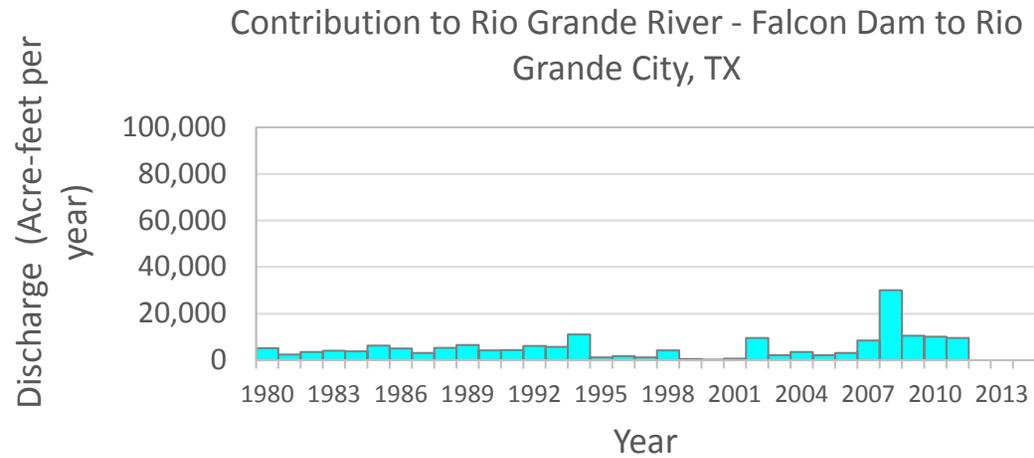
Notes:

Source: US International Boundary and Water Commission. Data for contributions along Rio Grande City, TX to Anzalduas Dam from 2007 to 2011 were not reported. Presented in the "Conceptual Model Report: Lower Rio Grande Valley Groundwater Transport Model" prepared by Montgomery & Associates, January 2017 as Figure 4.4.5.

GSI Job No. 4276	Drawn By: KER	**ESTIMATED ANNUAL CONTRIBUTIONS TO RIO GRANDE FROM RIO SAN JUAN IRRIGATION DISTRICT IN MEXICO**	
Issued: 19-Jun-2017	Chk'd By: GM		
Revised:	Aprv'd By: SP	Lower Rio Grande Valley	
Figure No. 2.8.2			

GSI ENVIRONMENTAL

LEGEND

- Recommended Desalination Plant
- Rio Grande
- Urban Area, as defined by USGS Border Environmental Health Initiative
- Texas County
- Model Boundary

Note:

Presented in the "Conceptual Model Report: Lower Rio Grande Valley Groundwater Transport Model" prepared by Montgomery & Associates, January 2017 as Figure 1.0.5.

Scale in Miles
0   10   20

Projected Coordinate System Datum: NAD 1983 Albers Equal Area

GSI ENVIRONMENTAL

RECOMMENDED BRACKISH GROUNDWATER DESALINATION PLANTS

Lower Rio Grande Valley

GSI Job No. 4276	Drawn By: GM
Issued: 19-Jun-2017	Chk'd By: KER
Map ID: LRGV_Fig_1_0_5	Appv'd By: SP

FIGURE 2.8.3
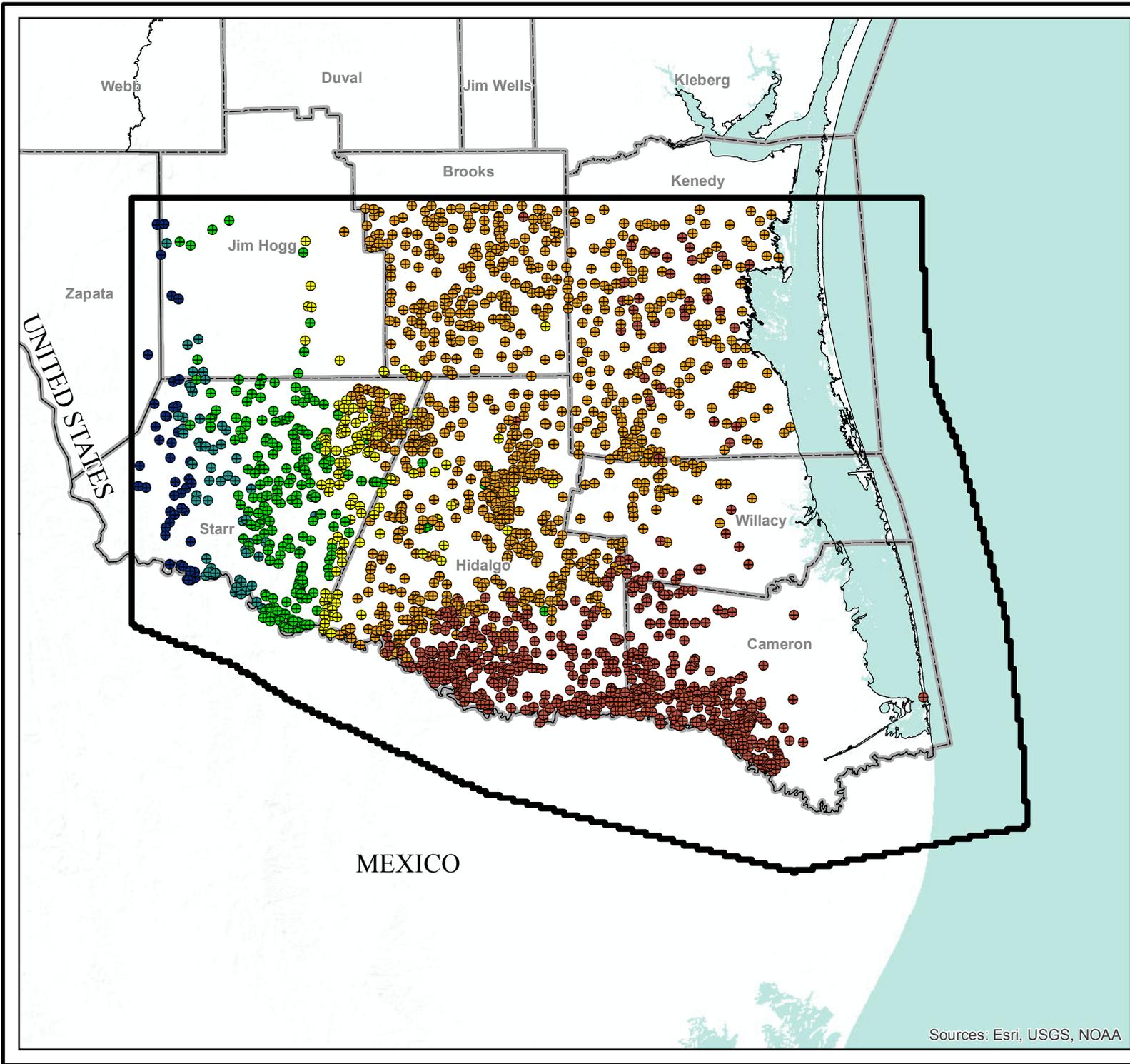
Map I.D.	Plant Name
8	Alamo
9	East Rio Hondo WSC & North Alamo WSC
10	El Jardin WSC
11	La Feria
12	Lagune Madre WD
13	Lyford
14	McAllen
15	Mission
16	North Alamo WSC (Delta Area)
17	North Alamo WSC (La Sara)
18	Primera
19	Sharyland WSC (WTP 2)
20	Sharyland WSC (WTP 3)
21	Union WSC (Rio Grande City)

Sources: Esri, USGS, NOAA

LEGEND

Modeled Pumping Well Screen Depth Hydrogeologic Unit Extent

- Chicot Aquifer
- Evageline Aquifer
- Burkeville Confining Unit
- Jasper Aquifer
- Catahoula Confining System
- Yegua-Jackson Aquifer
- Texas County
- Model Boundary

Notes:

1) Basemap provided by Montgomery & Associates December 2016.
2) Pumping wells are screened across multiple mode layers. Layer shown is the lowest layer the pumping will is screened across.

Scale in Miles

0   10   20

Projected Coordinate System
Datum: NAD 1983
Albers Equal Area

GSI ENVIRONMENTAL
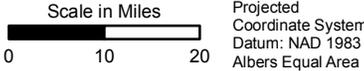
LOCATION OF MODELED GROUNDWATER PUMPING WELLS

Lower Rio Grande Valley

GSI Job No. 4276	Drawn By: AV
Issued: 23-Jun-2017	Chk'd By: KER
Map ID: LRGV_LMGWPW	Appv'd By: SP

FIGURE 2.8.4

Sources: Esri, USGS, NOAA
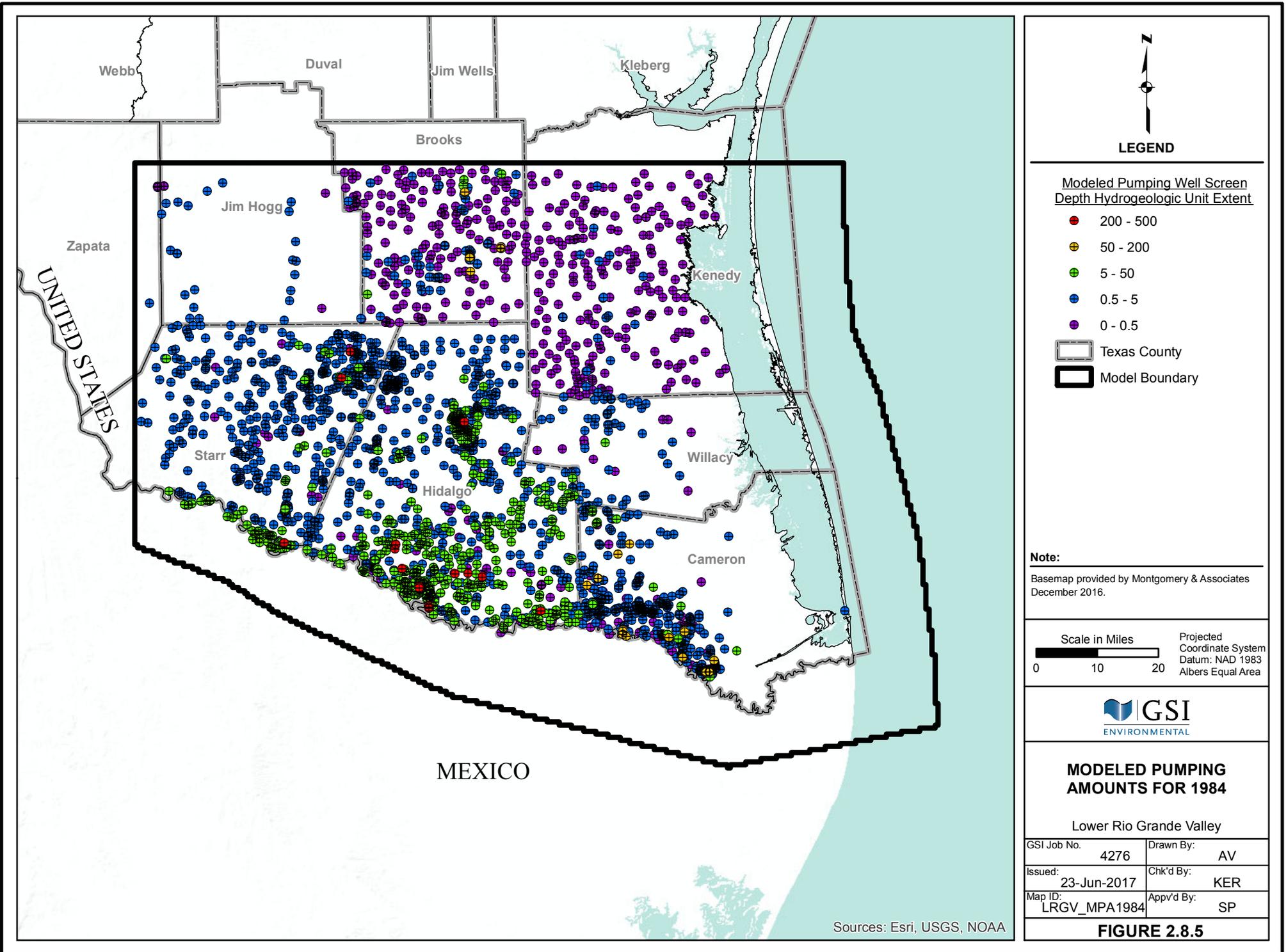
LEGEND

Modeled Pumping Well Screen Depth Hydrogeologic Unit Extent

- 🔴 200 - 500
- 🟡 50 - 200
- 🟢 5 - 50
- 🔵 0.5 - 5
- 🟣 0 - 0.5

▢ Texas County

▢ Model Boundary

Note:

Basemap provided by Montgomery & Associates December 2016.

Scale in Miles

0 — 10 — 20

Projected Coordinate System
Datum: NAD 1983
Albers Equal Area

GSI ENVIRONMENTAL

MODELED PUMPING AMOUNTS FOR 1984

Lower Rio Grande Valley

GSI Job No. 4276	Drawn By: AV
Issued: 23-Jun-2017	Chk'd By: KER
Map ID: LRGV_MPA1984	Appv'd By: SP

FIGURE 2.8.5

Sources: Esri, USGS, NOAA

Map labels: Webb, Duval, Jim Wells, Kleberg, Brooks, Jim Hogg, Zapata, UNITED STATES, Kenedy, Starr, Hidalgo, Willacy, Cameron, MEXICO

LEGEND
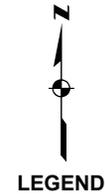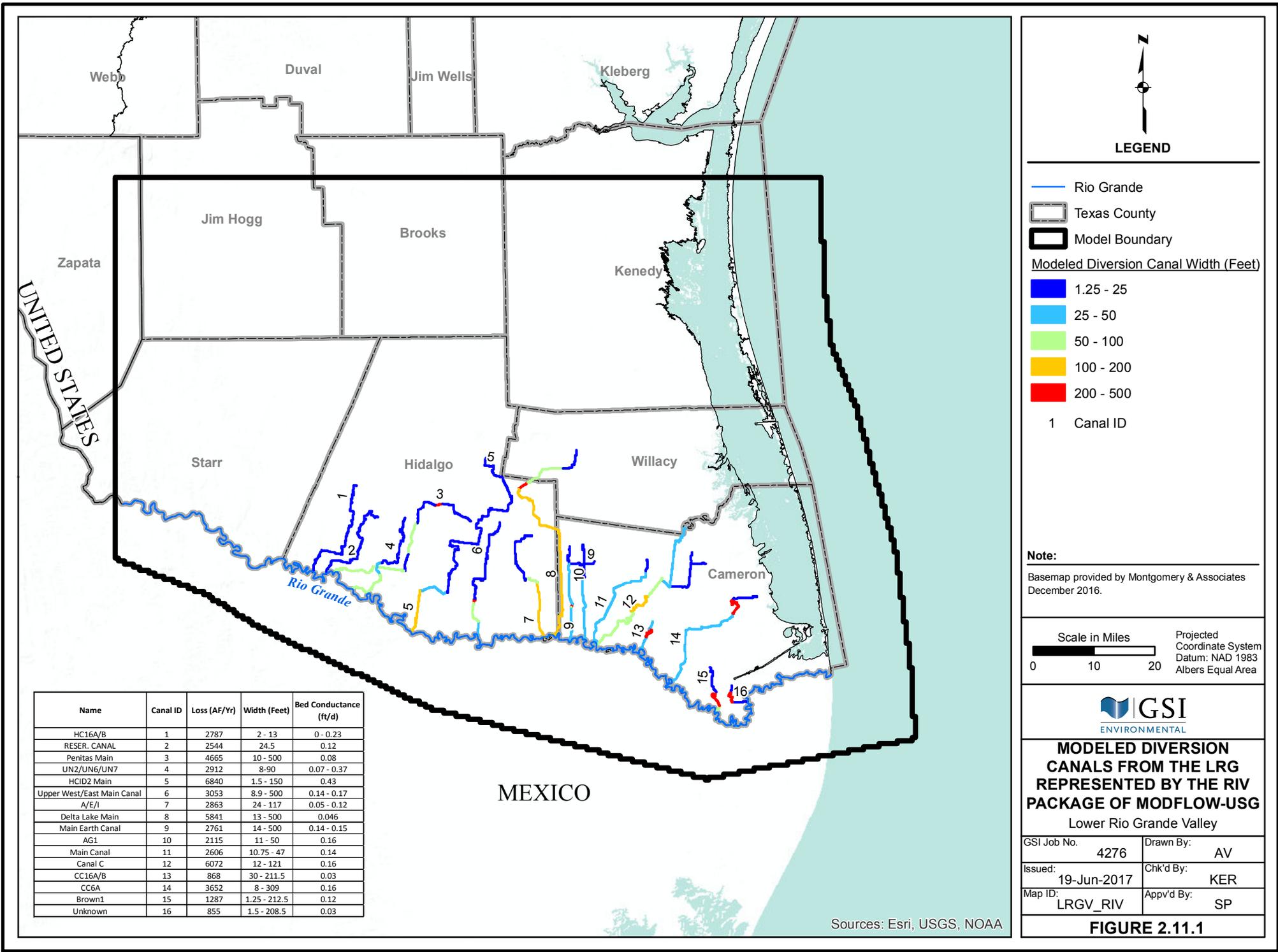
——	Rio Grande
▢	Texas County
▢	Model Boundary

Modeled Diversion Canal Width (Feet)

■	1.25 - 25
■	25 - 50
■	50 - 100
■	100 - 200
■	200 - 500
1	Canal ID

Note:

Basemap provided by Montgomery & Associates December 2016.

Scale in Miles
0   10   20

Projected Coordinate System
Datum: NAD 1983
Albers Equal Area

GSI ENVIRONMENTAL

MODELED DIVERSION CANALS FROM THE LRG REPRESENTED BY THE RIV PACKAGE OF MODFLOW-USG

Lower Rio Grande Valley

GSI Job No.	Drawn By:
4276	AV
Issued:	Chk'd By:
19-Jun-2017	KER
Map ID:	Appv'd By:
LRGV_RIV	SP

FIGURE 2.11.1

Sources: Esri, USGS, NOAA

Name	Canal ID	Loss (AF/Yr)	Width (Feet)	Bed Conductance (ft/d)
HC16A/B	1	2787	2 - 13	0 - 0.23
RESER. CANAL	2	2544	24.5	0.12
Penitas Main	3	4665	10 - 500	0.08
UN2/UN6/UN7	4	2912	8-90	0.07 - 0.37
HCID2 Main	5	6840	1.5 - 150	0.43
Upper West/East Main Canal	6	3053	8.9 - 500	0.14 - 0.17
A/E/I	7	2863	24 - 117	0.05 - 0.12
Delta Lake Main	8	5841	13 - 500	0.046
Main Earth Canal	9	2761	14 - 500	0.14 - 0.15
AG1	10	2115	11 - 50	0.16
Main Canal	11	2606	10.75 - 47	0.14
Canal C	12	6072	12 - 121	0.16
CC16A/B	13	868	30 - 211.5	0.03
CC6A	14	3652	8 - 309	0.16
Brown1	15	1287	1.25 - 212.5	0.12
Unknown	16	855	1.5 - 208.5	0.03

ESTIMATED SURFACE WATER USE IN
LOWER RIO GRANDE VALLEY

Lower Rio Grande Valley

Note:
Source: US International Boundary and Water Commission and Texas Water Development Board.

GSI Job No. 4276	Drawn By: KER
Issued: 23-Jun-2017	Chk'd By: GM
Revised:	Aprv'd By: SP
Figure No. 2.12.2	

Diversion Flows (Acre-feet per Year) vs **Year**

Legend:
Canal 1, Canal 2, Canal 3, Canal 4, Canal 5, Canal 6, Canal 7, Canal 8, Canal 9, Canal 10, Canal 11, Canal 12, Canal 13, Canal 14, Canal 15, Canal 16

GSI Job No.	4276	Drawn By:	AV	**MODELED DIVERSION FLOWS EXTRACTED**
Issued:	19-Jun-2017	Chk'd By:	KER	**FROM THE LRG USING THE QRT PACKAGE OF**
Revised:		Aprv'd By:	SP	**MODFLOW-USG**
Figure No.	2.12.3			Lower Rio Grande Valley

GSI ENVIRONMENTAL

Y-axis: Precipitation (inches)

X-axis: Year (1981 through 2013)

Note:
Source: Data obtained from PRISM Climate Group.

GSI Job No. 4276	Drawn By: AV	**ESTIMATED ANNUAL PRECIPITATION FROM 1981 THROUGH 2013**
Issued: 23-Jun-2017	Chk'd By: KER	
Revised:	Aprv'd By: SP	Lower Rio Grande Valley
Figure No. 2.13.1		

GSI ENVIRONMENTAL

Rio Grande
Texas County
Model Boundary

Estimated Recharge (Inches/Year)

<0.2
0.2 - 0.4
>0.4

Note:

Presented in the "Conceptual Model Report:
Lower Rio Grande Valley Groundwater
Transport Model" prepared by Montgomery &
Associates, January 2017 as Figure 4.3.1.

Scale in Miles

Projected
Coordinate System
Datum: NAD 1983
0   10   20   Albers Equal Area

GSI
ENVIRONMENTAL

**DISTRIBUTION OF AVERAGE
ESTIMATED ANNUAL
RECHARGE RATES
FOR 1984**
Lower Rio Grande Valley

GSI Job No. 4276	Drawn By: AV
Issued: 23-Jun-2017	Chk'd By: KER
Map ID: LRGV_Fig_4_3_1	Appv'd By: SP

FIGURE 2.13.2

Webb
Duval
Jim Wells
Kleberg
Jim Hogg
Brooks
Zapata
Kenedy
Starr
Willacy
Hidalgo
Cameron
UNITED STATES
Rio Grande
MEXICO

Sources: Esri, USGS, NOAA

Webb

Duval

Jim Wells

Kleberg

Jim Hogg

Brooks

Kenedy

Zapata

Starr

Willacy

Hidalgo

Cameron

UNITED STATES

Rio Grande

MEXICO

Sources: Esri, USGS, NOAA
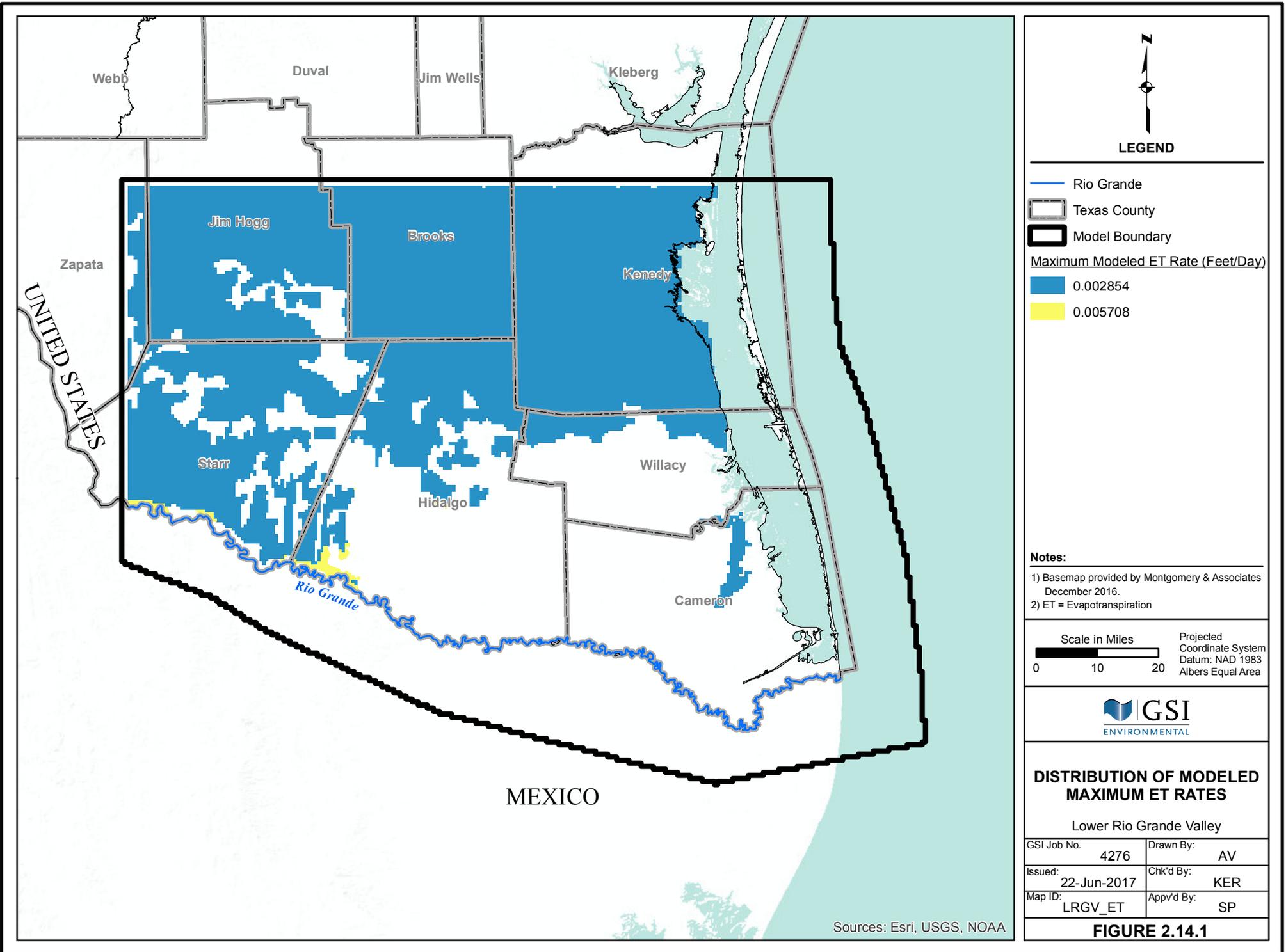
LEGEND

— Rio Grande

☐ Texas County

☐ Model Boundary

Maximum Modeled ET Rate (Feet/Day)

■ 0.002854

■ 0.005708

Notes:

1) Basemap provided by Montgomery & Associates December 2016.
2) ET = Evapotranspiration

Scale in Miles
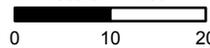
0   10   20

Projected
Coordinate System
Datum: NAD 1983
Albers Equal Area

GSI
ENVIRONMENTAL

**DISTRIBUTION OF MODELED
MAXIMUM ET RATES**

Lower Rio Grande Valley

GSI Job No. 4276	Drawn By: AV
Issued: 22-Jun-2017	Chk'd By: KER
Map ID: LRGV_ET	Appv'd By: SP

FIGURE 2.14.1
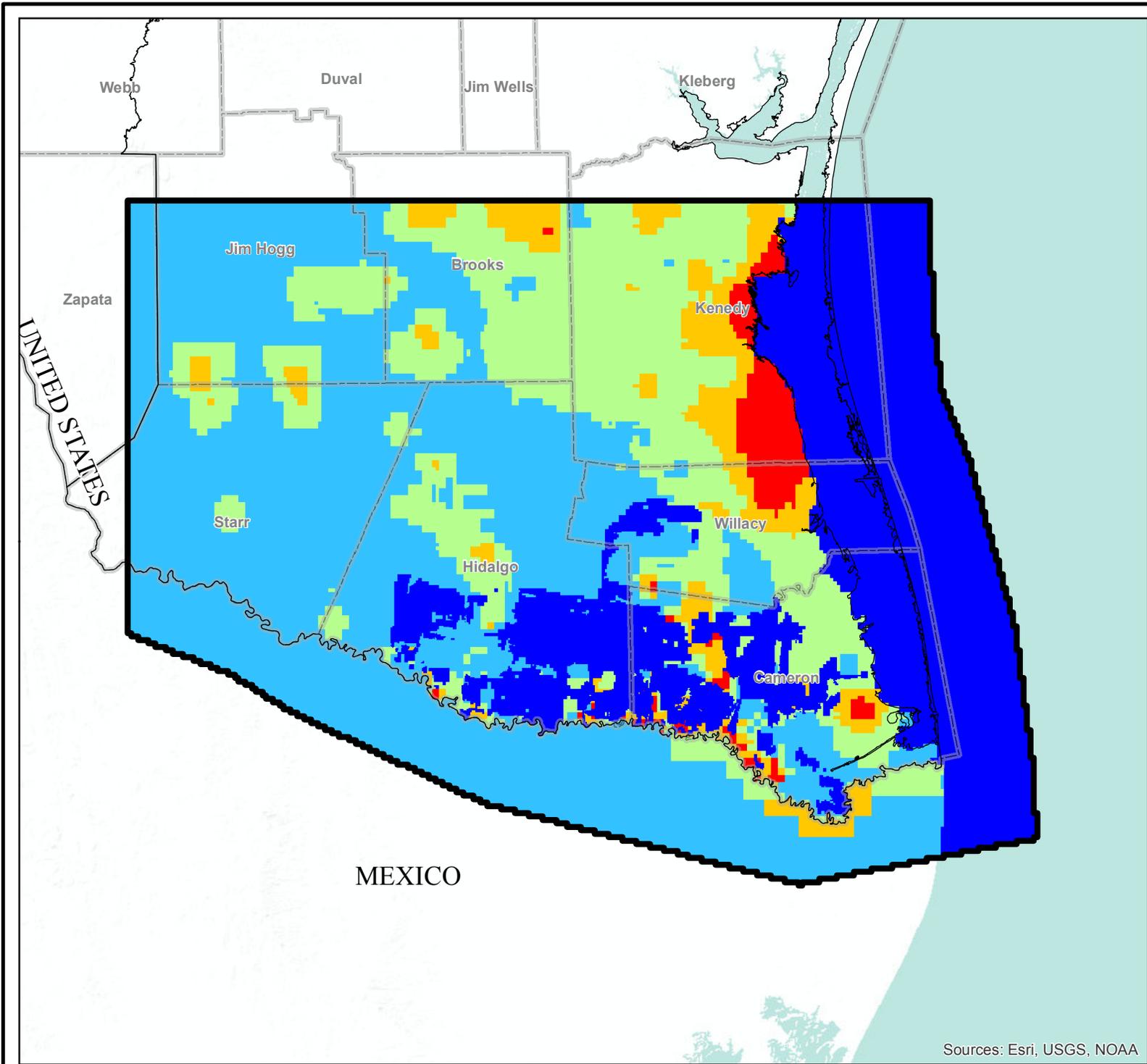
LEGEND

Texas County
Model Boundary

Modeled Recharge (Inch/Year)
- 0
- 0 - 0.15
- 0.15 - 0.25
- 0.25 - 0.35
- 0.35 - 0.66

Note:

Basemap provided by Montgomery & Associates December 2016.

Scale in Miles
0   10   20

Projected Coordinate System
Datum: NAD 1983
Albers Equal Area

GSI ENVIRONMENTAL
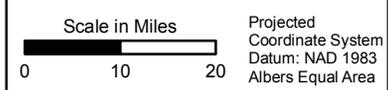
RECHARGE DISTRIBUTION OF CALIBRATED MODEL FOR 1984 CONDITIONS

Lower Rio Grande Valley

GSI Job No. 4276	Drawn By: AV
Issued: 20-Jun-2017	Chk'd By: KER
Map ID: LRGV_RDCM_1984	Appv'd By: SP

Sources: Esri, USGS, NOAA

FIGURE 4.1.1
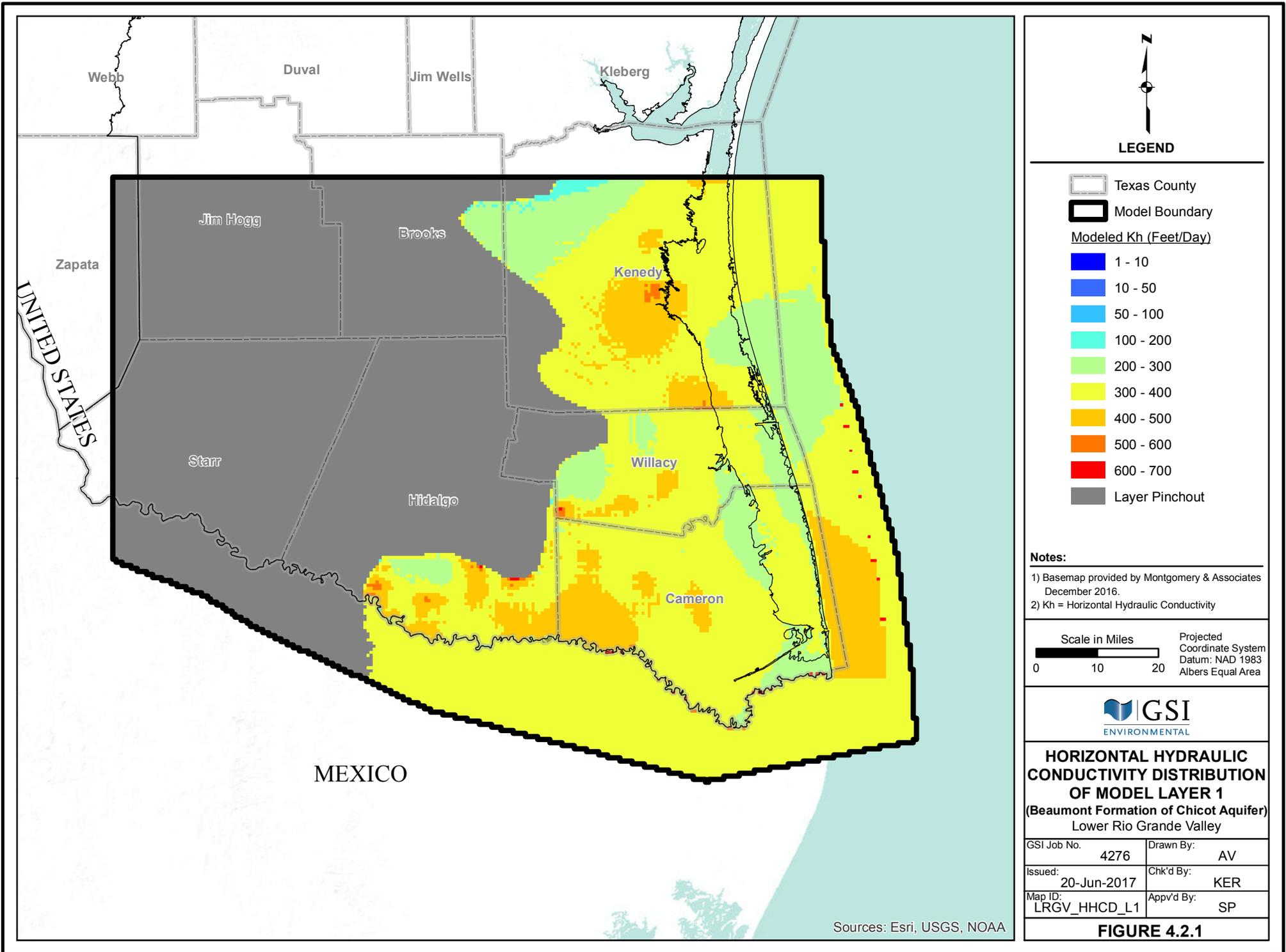
LEGEND

Texas County

Model Boundary

Modeled Kh (Feet/Day)

- 1 - 10
- 10 - 50
- 50 - 100
- 100 - 200
- 200 - 300
- 300 - 400
- 400 - 500
- 500 - 600
- 600 - 700
- Layer Pinchout

Notes:

1) Basemap provided by Montgomery & Associates December 2016.
2) Kh = Horizontal Hydraulic Conductivity

Scale in Miles

0   10   20

Projected Coordinate System Datum: NAD 1983 Albers Equal Area

GSI ENVIRONMENTAL

HORIZONTAL HYDRAULIC CONDUCTIVITY DISTRIBUTION OF MODEL LAYER 1
(Beaumont Formation of Chicot Aquifer)
Lower Rio Grande Valley

GSI Job No. 4276	Drawn By: AV
Issued: 20-Jun-2017	Chk'd By: KER
Map ID: LRGV_HHCD_L1	Appv'd By: SP

FIGURE 4.2.1

Sources: Esri, USGS, NOAA

LEGEND

☐	Texas County
☐	Model Boundary

Modeled Kh (Feet/Day)

■ (blue)	1 - 10
■ (blue)	10 - 50
■ (light blue)	50 - 100
■ (teal)	100 - 200
■ (light green)	200 - 300
■ (yellow)	300 - 400
■ (orange)	400 - 500
■ (dark orange)	500 - 600
■ (red)	600 - 700
■ (gray)	Layer Pinchout

Notes:

1) Basemap provided by Montgomery & Associates December 2016.
2) Kh = Horizontal Hydraulic Conductivity

Scale in Miles

0   10   20

Projected Coordinate System Datum: NAD 1983 Albers Equal Area

GSI ENVIRONMENTAL

HORIZONTAL HYDRAULIC CONDUCTIVITY DISTRIBUTION OF MODEL LAYER 2
(Lissie Formation of Chicot Aquifer)
Lower Rio Grande Valley

GSI Job No. 4276	Drawn By: AV
Issued: 20-Jun-2017	Chk'd By: KER
Map ID: LRGV_HHCD_L2	Appv'd By: SP

FIGURE 4.2.2

Sources: Esri, USGS, NOAA

LEGEND

☐	Texas County
▢	Model Boundary

Modeled Kh (Feet/Day)

■ (dark blue)	1 - 10
■ (blue)	10 - 50
■ (light blue)	50 - 100
■ (cyan)	100 - 200
■ (light green)	200 - 300
■ (yellow-green)	300 - 400
■ (yellow)	400 - 500
■ (orange)	500 - 600
■ (red)	600 - 700
■ (gray)	Layer Pinchout

Notes:

1) Basemap provided by Montgomery & Associates December 2016.
2) Kh = Horizontal Hydraulic Conductivity

Scale in Miles

0   10   20

Projected Coordinate System
Datum: NAD 1983
Albers Equal Area

GSI
ENVIRONMENTAL

HORIZONTAL HYDRAULIC CONDUCTIVITY DISTRIBUTION OF MODEL LAYER 3
(Willis Formation of Chicot Aquifer)
Lower Rio Grande Valley

GSI Job No. 4276	Drawn By: AV
Issued: 20-Jun-2017	Chk'd By: KER
Map ID: LRGV_HHCD_L3	Appv'd By: SP

FIGURE 4.2.3

Sources: Esri, USGS, NOAA

LEGEND

Texas County

Model Boundary

Modeled Kh (Feet/Day)

- 0.0001 - 0.001
- 0.001 - 0.01
- 0.01 - 0.1
- 0.1 - 1
- 1 - 5
- 5 - 10

Layer Pinchout

Notes:

1) Basemap provided by Montgomery & Associates December 2016.
2) Kh = Horizontal Hydraulic Conductivity

Scale in Miles

0   10   20

Projected Coordinate System
Datum: NAD 1983
Albers Equal Area

GSI ENVIRONMENTAL

HORIZONTAL HYDRAULIC CONDUCTIVITY DISTRIBUTION OF MODEL LAYER 4
(Upper Goliad Formation of Evangeline Aquifer)
Lower Rio Grande Valley

GSI Job No. 4276	Drawn By: AV
Issued: 20-Jun-2017	Chk'd By: KER
Map ID: LRGV_HHCD_L4	Appv'd By: SP

FIGURE 4.2.4

Sources: Esri, USGS, NOAA

LEGEND

Texas County

Model Boundary

Modeled Kh (Feet/Day)

0.0001 - 0.001
0.001 - 0.01
0.01 - 0.1
0.1 - 1
1 - 5
5 - 10
Layer Pinchout

Notes:

1) Basemap provided by Montgomery & Associates December 2016.
2) Kh = Horizontal Hydraulic Conductivity

Scale in Miles

0   10   20

Projected Coordinate System Datum: NAD 1983 Albers Equal Area

GSI ENVIRONMENTAL

HORIZONTAL HYDRAULIC CONDUCTIVITY DISTRIBUTION OF MODEL LAYER 5
(Lower Goliad Formation of Evangeline Aquifer)
Lower Rio Grande Valley

GSI Job No. 4276	Drawn By: AV
Issued: 20-Jun-2017	Chk'd By: KER
Map ID: LRGV_HHCD_L5	Appv'd By: SP

FIGURE 4.2.5

Webb
Duval
Jim Wells
Kleberg
Jim Hogg
Brooks
Zapata
Kenedy
UNITED STATES
Starr
Willacy
Hidalgo
Cameron
MEXICO

Sources: Esri, USGS, NOAA

LEGEND

Texas County

Model Boundary

Modeled Kh (Feet/Day)
- 0.0001 - 0.001
- 0.001 - 0.01
- 0.01 - 0.1
- 0.1 - 1
- 1 - 5
- 5 - 10
- Layer Pinchout

Notes:

1) Basemap provided by Montgomery & Associates December 2016.
2) Kh = Horizontal Hydraulic Conductivity

Scale in Miles

0   10   20

Projected Coordinate System
Datum: NAD 1983
Albers Equal Area

GSI
ENVIRONMENTAL

HORIZONTAL HYDRAULIC CONDUCTIVITY DISTRIBUTION OF MODEL LAYER 6
(Upper Lagarto Formation of Evangeline Aquifer)
Lower Rio Grande Valley

GSI Job No.		Drawn By:	
4276		AV	
Issued:		Chk'd By:	
20-Jun-2017		KER	
Map ID:		Appv'd By:	
LRGV_HHCD_L6		SP	

FIGURE 4.2.6

LEGEND

☐ (white)	Texas County
☐ (black)	Model Boundary

Modeled Kh (Feet/Day)

■ (blue)	0.0001 - 0.001
■ (light blue)	0.001 - 0.01
■ (teal)	0.01 - 0.1
■ (yellow)	0.1 - 1
■ (orange)	1 - 5
■ (red)	5 - 10
■ (gray)	Layer Pinchout

Notes:

1) Basemap provided by Montgomery & Associates December 2016.
2) Kh = Horizontal Hydraulic Conductivity

Scale in Miles

0   10   20

Projected Coordinate System Datum: NAD 1983 Albers Equal Area

GSI
ENVIRONMENTAL

HORIZONTAL HYDRAULIC CONDUCTIVITY DISTRIBUTION OF MODEL LAYER 7
(Middle Lagarto Formation of Burkeville Confining Unit)
Lower Rio Grande Valley

GSI Job No. 4276	Drawn By: AV
Issued: 20-Jun-2017	Chk'd By: KER
Map ID: LRGV_HHCD_L7	Appv'd By: SP

FIGURE 4.2.7

Sources: Esri, USGS, NOAA

Map labels: Webb, Duval, Jim Wells, Kleberg, Jim Hogg, Brooks, Kenedy, Zapata, UNITED STATES, Starr, Hidalgo, Willacy, Cameron, MEXICO

LEGEND

☐	Texas County
▢	Model Boundary

Modeled Kh (Feet/Day)

■	0.0001 - 0.001
■	0.001 - 0.01
■	0.01 - 0.1
■	0.1 - 1
■	1 - 5
■	5 - 10
■	Layer Pinchout

Notes:

1) Basemap provided by Montgomery & Associates December 2016.
2) Kh = Horizontal Hydraulic Conductivity

Scale in Miles

0   10   20

Projected Coordinate System
Datum: NAD 1983
Albers Equal Area

GSI ENVIRONMENTAL

HORIZONTAL HYDRAULIC CONDUCTIVITY DISTRIBUTION OF MODEL LAYER 8
(Lower Lagarto Formation of Jasper Aquifer)
Lower Rio Grande Valley

GSI Job No. 4276	Drawn By: AV
Issued: 20-Jun-2017	Chk'd By: KER
Map ID: LRGV_HHCD_L8	Appv'd By: SP

FIGURE 4.2.8

Sources: Esri, USGS, NOAA

LEGEND

☐	Texas County
▬	Model Boundary

Modeled Kh (Feet/Day)

■ (blue)	0.0001 - 0.001
■ (light blue)	0.001 - 0.01
■ (teal)	0.01 - 0.1
■ (yellow-green)	0.1 - 1
■ (orange)	1 - 5
■ (red)	5 - 10
■ (gray)	Layer Pinchout

Notes:

1) Basemap provided by Montgomery & Associates December 2016.
2) Kh = Horizontal Hydraulic Conductivity

Scale in Miles

0   10   20

Projected Coordinate System Datum: NAD 1983 Albers Equal Area

GSI ENVIRONMENTAL

HORIZONTAL HYDRAULIC CONDUCTIVITY DISTRIBUTION OF MODEL LAYER 9
(Oakville Formation of Jasper Aquifer)
Lower Rio Grande Valley

GSI Job No. 4276	Drawn By: AV
Issued: 20-Jun-2017	Chk'd By: KER
Map ID: LRGV_HHCD_L9	Appv'd By: SP

FIGURE 4.2.9

Sources: Esri, USGS, NOAA

Sources: Esri, USGS, NOAA

LEGEND

Texas County

Model Boundary

Modeled Kv (Feet/Day)

- 1 - 10
- 10 - 50
- 50 - 100
- 100 - 200
- 200 - 300
- 300 - 400
- 400 - 500
- Layer Pinchout

Notes:

1) Basemap provided by Montgomery & Associates December 2016.
2) Kv = Vertical Hydraulic Conductivity

Scale in Miles

0   10   20

Projected Coordinate System Datum: NAD 1983 Albers Equal Area

GSI ENVIRONMENTAL

VERTICAL HYDRAULIC CONDUCTIVITY DISTRIBUTION OF MODEL LAYER 1
(Beaumont Formation of Chicot Aquifer)
Lower Rio Grande Valley

GSI Job No.	Drawn By:
4276	AV
Issued:	Chk'd By:
20-Jun-2017	KER
Map ID:	Appv'd By:
LRGV_VHCD_L1	SP

FIGURE 4.2.11

Jim Hogg

Brooks

Zapata

Kenedy

UNITED STATES

Starr

Willacy

Hidalgo

Cameron

MEXICO

Sources: Esri, USGS, NOAA

LEGEND

Texas County

Model Boundary

Modeled Kv (Feet/Day)

1 - 10

10 - 50

50 - 100

100 - 200

200 - 300

300 - 400

400 - 500

Layer Pinchout

Notes:

1) Basemap provided by Montgomery & Associates December 2016.
2) Kv = Vertical Hydraulic Conductivity

Scale in Miles

0   10   20

Projected Coordinate System Datum: NAD 1983 Albers Equal Area

GSI ENVIRONMENTAL

VERTICAL HYDRAULIC CONDUCTIVITY DISTRIBUTION OF MODEL LAYER 2
(Lissie Formation of Chicot Aquifer)
Lower Rio Grande Valley

GSI Job No. 4276	Drawn By: AV
Issued: 20-Jun-2017	Chk'd By: KER
Map ID: LRGV_VHCD_L2	Appv'd By: SP

FIGURE 4.2.12
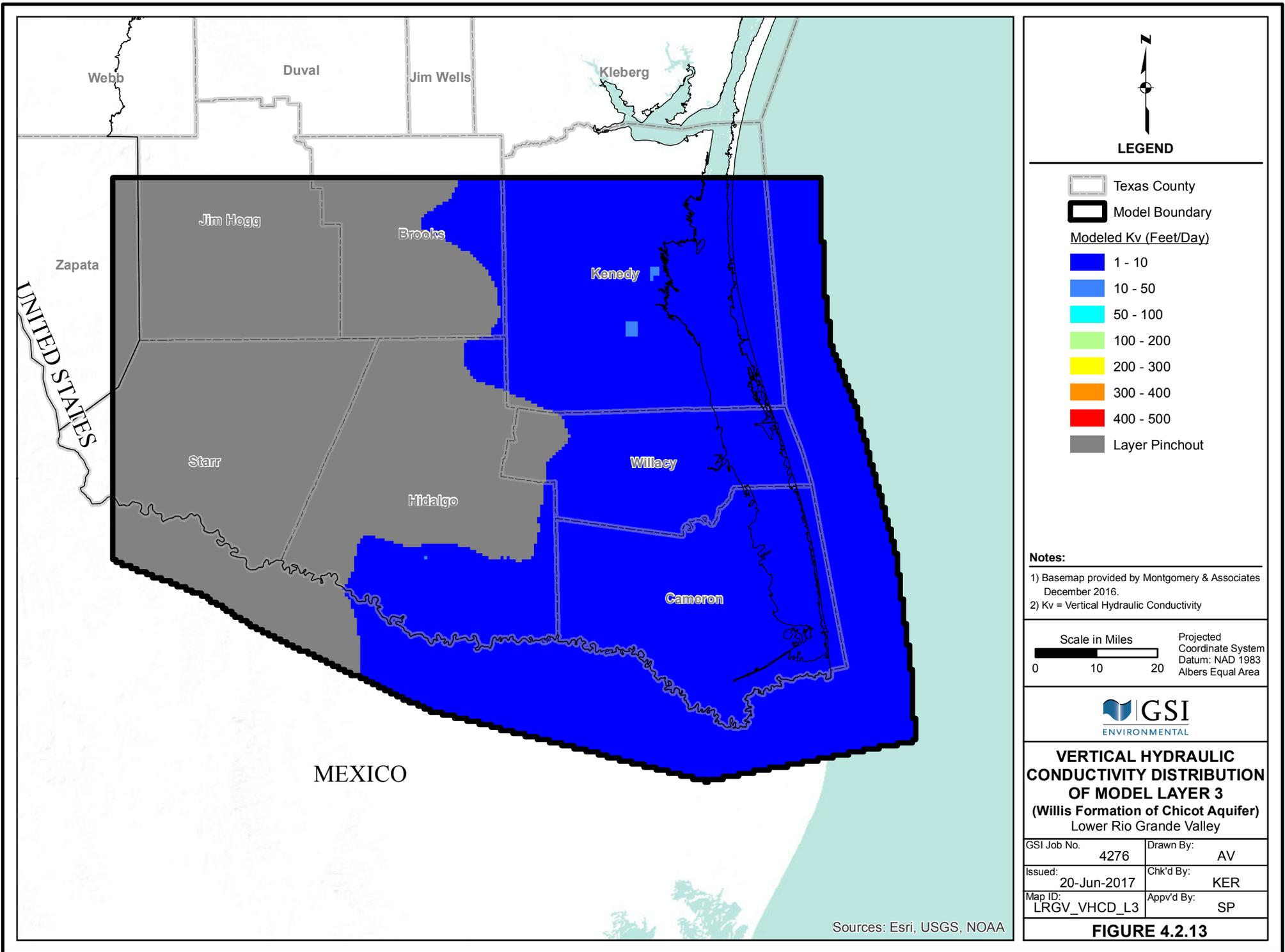
LEGEND

- Texas County
- Model Boundary

Modeled Kv (Feet/Day)

- 1 - 10
- 10 - 50
- 50 - 100
- 100 - 200
- 200 - 300
- 300 - 400
- 400 - 500
- Layer Pinchout

Notes:

1) Basemap provided by Montgomery & Associates December 2016.
2) Kv = Vertical Hydraulic Conductivity

Scale in Miles

0   10   20

Projected Coordinate System Datum: NAD 1983 Albers Equal Area

GSI ENVIRONMENTAL
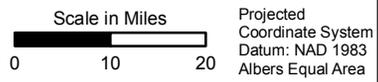
VERTICAL HYDRAULIC CONDUCTIVITY DISTRIBUTION OF MODEL LAYER 3
(Willis Formation of Chicot Aquifer)
Lower Rio Grande Valley

GSI Job No. 4276	Drawn By: AV
Issued: 20-Jun-2017	Chk'd By: KER
Map ID: LRGV_VHCD_L3	Appv'd By: SP

FIGURE 4.2.13

Sources: Esri, USGS, NOAA

LEGEND

☐	Texas County
■	Model Boundary

Modeled Kv (Feet/Day)

■	0.0001 - 0.001
■	0.001 - 0.01
■	0.01 - 0.1
■	0.1 - 1
■	1 - 5
■	5 - 10
■	Layer Pinchout

Notes:

1) Basemap provided by Montgomery & Associates December 2016.
2) Kv = Vertical Hydraulic Conductivity

Scale in Miles

0   10   20

Projected
Coordinate System
Datum: NAD 1983
Albers Equal Area

GSI ENVIRONMENTAL

VERTICAL HYDRAULIC CONDUCTIVITY DISTRIBUTION OF MODEL LAYER 4
(Upper Goliad Formation of Evangeline Aquifer)
Lower Rio Grande Valley

GSI Job No. 4276	Drawn By: AV
Issued: 20-Jun-2017	Chk'd By: KER
Map ID: LRGV_VHCD_L4	Appv'd By: SP

FIGURE 4.2.14

Sources: Esri, USGS, NOAA

LEGEND

Texas County

Model Boundary

Modeled Kv (Feet/Day)

0.0001 - 0.001

0.001 - 0.01

0.01 - 0.1

0.1 - 1

1 - 5

5 - 10

Layer Pinchout

Notes:

1) Basemap provided by Montgomery & Associates December 2016.

2) Kv = Vertical Hydraulic Conductivity

Scale in Miles

0   10   20

Projected Coordinate System Datum: NAD 1983 Albers Equal Area

GSI ENVIRONMENTAL

VERTICAL HYDRAULIC CONDUCTIVITY DISTRIBUTION OF MODEL LAYER 5
(Lower Goliad Formation of Evangeline Aquifer)
Lower Rio Grande Valley

GSI Job No.	Drawn By:
4276	AV
Issued:	Chk'd By:
20-Jun-2017	KER
Map ID:	Appv'd By:
LRGV_VHCD_L5	SP

FIGURE 4.2.15

Webb · Duval · Jim Wells · Kleberg

Jim Hogg · Brooks · Kenedy

Zapata

UNITED STATES

Starr · Hidalgo · Willacy · Cameron

MEXICO

Sources: Esri, USGS, NOAA

LEGEND

▢	Texas County
▮	Model Boundary

Modeled Kv (Feet/Day)

■	0.0001 - 0.001
■	0.001 - 0.01
■	0.01 - 0.1
■	0.1 - 1
■	1 - 5
■	5 - 10
■	Layer Pinchout

Notes:

1) Basemap provided by Montgomery & Associates December 2016.
2) Kv = Vertical Hydraulic Conductivity

Scale in Miles

0   10   20

Projected Coordinate System
Datum: NAD 1983
Albers Equal Area

GSI ENVIRONMENTAL

VERTICAL HYDRAULIC CONDUCTIVITY DISTRIBUTION OF MODEL LAYER 6
(Upper Lagarto Formation of Evangeline Aquifer)
Lower Rio Grande Valley

GSI Job No.	4276	Drawn By:	AV
Issued:	20-Jun-2017	Chk'd By:	KER
Map ID:	LRGV_VHCD_L6	Appv'd By:	SP
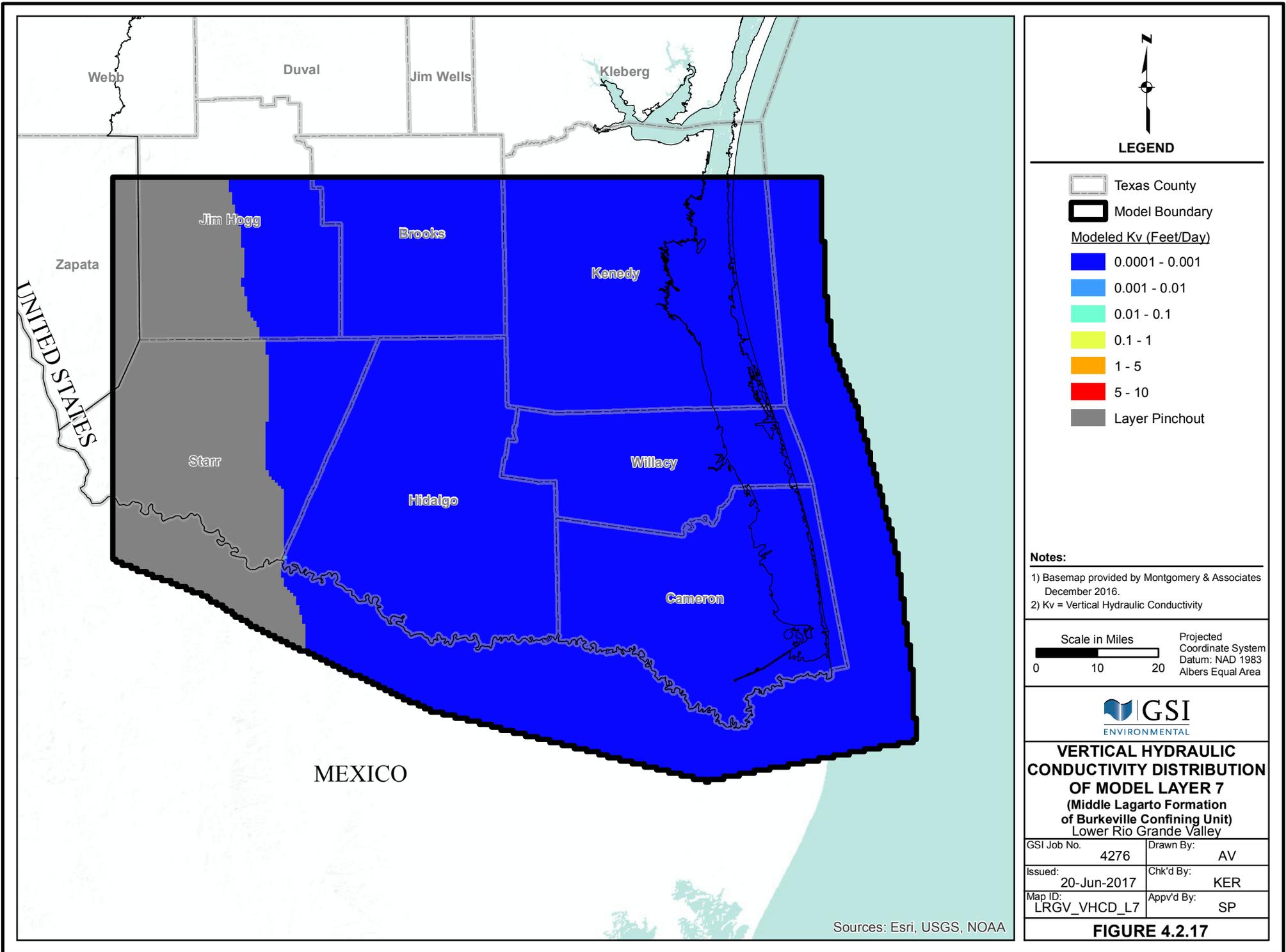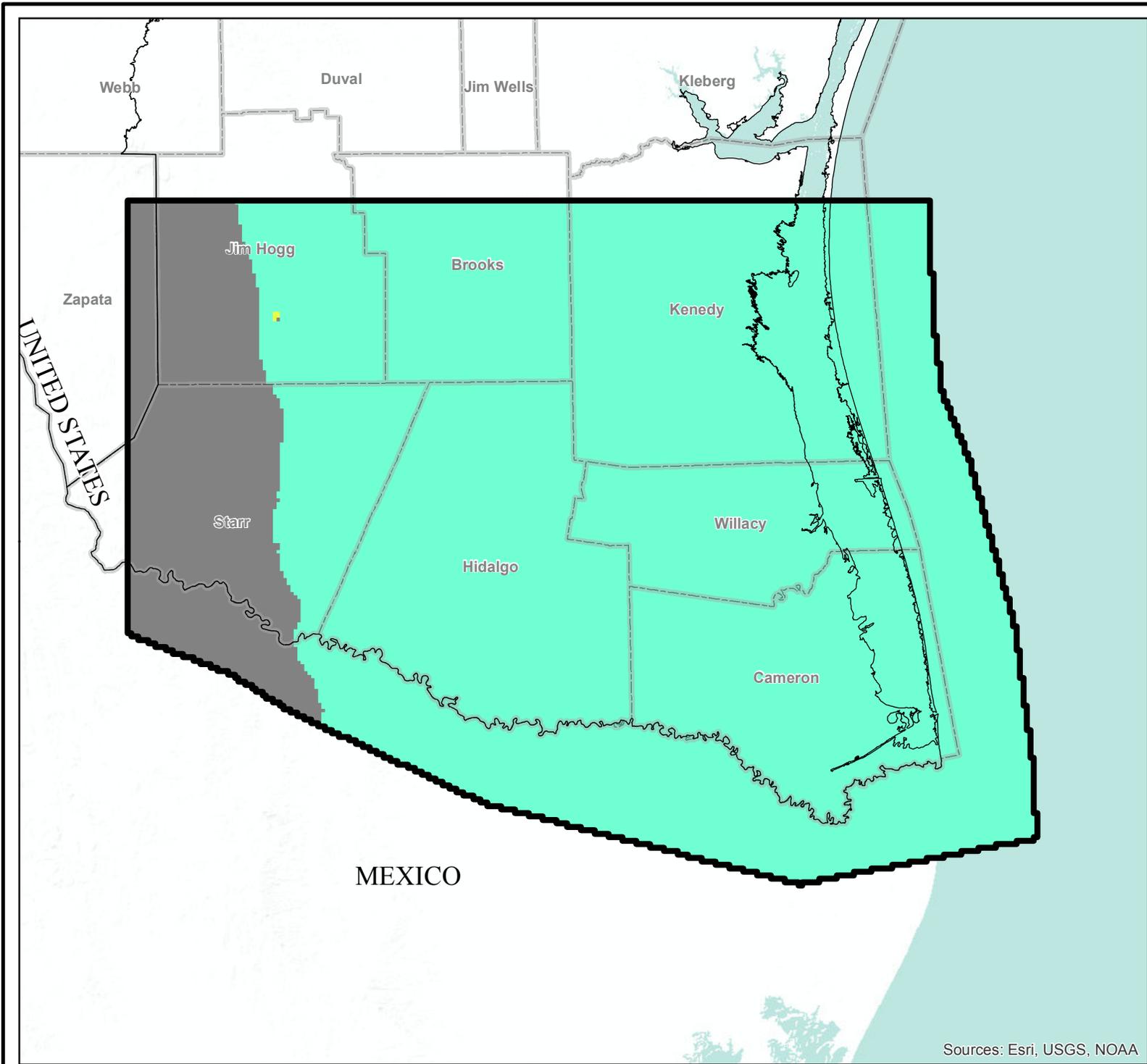
Sources: Esri, USGS, NOAA

FIGURE 4.2.16

Map labels: Webb, Duval, Jim Wells, Kleberg, Zapata, Jim Hogg, Brooks, Kenedy, UNITED STATES, Starr, Hidalgo, Willacy, Cameron, MEXICO

LEGEND

Texas County

Model Boundary

Modeled Kv (Feet/Day)

0.0001 - 0.001

0.001 - 0.01

0.01 - 0.1

0.1 - 1

1 - 5

5 - 10

Layer Pinchout

Notes:

1) Basemap provided by Montgomery & Associates December 2016.

2) Kv = Vertical Hydraulic Conductivity

Scale in Miles

0   10   20

Projected Coordinate System Datum: NAD 1983 Albers Equal Area

GSI ENVIRONMENTAL

VERTICAL HYDRAULIC CONDUCTIVITY DISTRIBUTION OF MODEL LAYER 7
(Middle Lagarto Formation of Burkeville Confining Unit)
Lower Rio Grande Valley

GSI Job No. 4276	Drawn By: AV
Issued: 20-Jun-2017	Chk'd By: KER
Map ID: LRGV_VHCD_L7	Appv'd By: SP

FIGURE 4.2.17

LEGEND

Texas County
Model Boundary

Modeled Kv (Feet/Day)
- 0.0001 - 0.001
- 0.001 - 0.01
- 0.01 - 0.1
- 0.1 - 1
- 1 - 5
- 5 - 10
- Layer Pinchout

Notes:

1) Basemap provided by Montgomery & Associates December 2016.
2) Kv = Vertical Hydraulic Conductivity

Scale in Miles

0   10   20

Projected Coordinate System Datum: NAD 1983 Albers Equal Area

GSI ENVIRONMENTAL

VERTICAL HYDRAULIC CONDUCTIVITY DISTRIBUTION OF MODEL LAYER 8
(Lower Lagarto Formation of Jasper Aquifer)
Lower Rio Grande Valley

GSI Job No.	Drawn By:
4276	AV
Issued:	Chk'd By:
20-Jun-2017	KER
Map ID:	Appv'd By:
LRGV_VHCD_L8	SP

FIGURE 4.2.18

Sources: Esri, USGS, NOAA

Texas County

Model Boundary

Modeled Kv (Feet/Day)

- 0.0001 - 0.001
- 0.001 - 0.01
- 0.01 - 0.1
- 0.1 - 1
- 1 - 5
- 5 - 10
- Layer Pinchout

Notes:

1) Basemap provided by Montgomery & Associates December 2016.
2) Kv = Vertical Hydraulic Conductivity

Scale in Miles

0   10   20

Projected Coordinate System
Datum: NAD 1983
Albers Equal Area

GSI ENVIRONMENTAL

VERTICAL HYDRAULIC CONDUCTIVITY DISTRIBUTION OF MODEL LAYER 9
(Oakville Formation of Jasper Aquifer)
Lower Rio Grande Valley

GSI Job No. 4276	Drawn By: AV
Issued: 20-Jun-2017	Chk'd By: KER
Map ID: LRGV_VHCD_L9	Appv'd By: SP

FIGURE 4.2.19

Sources: Esri, USGS, NOAA

$y = 0.9795x + 1.191$
$R^2 = 0.9758$

Legend:
- Layer 1 - Beaumont Formation of Chicot Aquifer
- Layer 2 - Lissie Formation of Chicot Aquifer
- Layer 3 - Willis Formation of Chicot Aquifer
- Layer 4 - Upper Goliad Formation of Evangeline Aquifer
- Layer 6 - Upper Lagarto Formation of Evangeline Aquifer
- Layer 7 - Middle Lagarto Formation of Burkeville Confining Unit
- Layer 8 - Lower Lagarto Formation of Jasper Aquifer
- Layer 9 - Oakville Formation of Jasper Aquifer
- Layer 10 - Upper Catahoula Formation of Jasper Aquifer
- Layer 11 - Catahoula Confining System
- Trendline

X-axis: Observed Water Levels (feet above mean sea level)
Y-axis: Simulated Water Levels (feet above mean sea level)

GSI Job No. 4276	Drawn By: AV	OBSERVED vs SIMULATED WATER LEVELS FOR CALIBRATED 1984 CONDITIONS
Issued: 20-Jun-2017	Chk'd By: KER	
Revised:	Aprv'd By: SP	Lower Rio Grande Valley
Figure No. 4.3.1		

GSI ENVIRONMENTAL

$y = 0.9677x + 4.7252$
$R^2 = 0.9681$

- Layer 1 - Beaumont Formation of Chicot Aquifer
- Layer 2 - Lissie Formation of Chicot Aquifer
- Layer 3 - Willis Formation of Chicot Aquifer
- Layer 4 - Upper Goliad Formation of Evangeline Aquifer
- Layer 5 - Lower Goliad Formation Evangeline Aquifer
- Layer 6 - Upper Lagarto Formation of Evangeline Aquifer
- Layer 7 - Middle Lagarto Formation of Burkeville Confining Unit
- Layer 8 - Lower Lagarto Formation of Jasper Aquifer
- Layer 9 - Oakville Formation of Jasper Aquifer
- Layer 10 - Upper Catahoula Formation of Jasper Aquifer
- Layer 11 - Catahoula Confining System
- .... Trendline

Observed Water Levels (feet above mean sea level)

Simulated Water Levels (feet above mean sea level)

GSI Job No.	4276	Drawn By:	AV	OBSERVED vs SIMULATED WATER LEVELS FOR CALIBRATED 1984-2013 SIMULATIONS
Issued:	20-Jun-2017	Chk'd By:	KER	
Revised:		Aprv'd By:	SP	Lower Rio Grande Valley
Figure No.	4.3.2-A			

GSI ENVIRONMENTAL

$y = 0.9677x + 4.7252$
$R^2 = 0.9681$

- ● Layer 1 - Beaumont Formation of Chicot Aquifer
- ● Layer 2 - Lissie Formation of Chicot Aquifer
- ● Layer 3 - Willis Formation of Chicot Aquifer
- ⋯⋯ Trendline

Simulated Water Levels (feet above mean sea level) (y-axis)

600
500
400
300
200
100
0
-100

Observed Water Levels (feet above mean sea level) (x-axis)

-100   0   100   200   300   400   500   600

GSI Job No. 4276	Drawn By: AV	**OBSERVED vs SIMULATED WATER LEVELS FOR**
Issued: 23-Jun-2017	Chk'd By: KER	**CALIBRATED 1984-2013 SIMULATIONS**
Revised:	Aprv'd By: SP	Lower Rio Grande Valley
Figure No. 4.3.2-B		

GSI ENVIRONMENTAL

OBSERVED vs SIMULATED WATER LEVELS FOR CALIBRATED 1984-2013 SIMULATIONS

Lower Rio Grande Valley

GSI Job No.	4276	Drawn By:	AV
Issued:	23-Jun-2017	Chk'd By:	KER
Revised:		Aprv'd By:	SP
Figure No.	4.3.2-C		

Figure 4.3.2-D — Observed vs Simulated Water Levels for Calibrated 1984-2013 Simulations, Lower Rio Grande Valley

Chart annotations:

$y = 0.9677x + 4.7252$
$R^2 = 0.9681$

Y-axis: Simulated Water Levels (feet above mean sea level)
X-axis: Observed Water Levels (feet above mean sea level)

Legend:
- Layer 7 - Middle Lagarto Formation of Burkeville Confining Unit
- Layer 8 - Lower Lagarto Formation of Jasper Aquifer
- Layer 9 - Oakville Formation of Jasper Aquifer
- Layer 10 - Upper Catahoula Formation of Jasper Aquifer
- Layer 11 - Catahoula Confining System
- Trendline

GSI Job No.	4276	Drawn By:	AV	OBSERVED vs SIMULATED WATER LEVELS FOR CALIBRATED 1984-2013 SIMULATIONS
Issued:	23-Jun-2017	Chk'd By:	KER	
Revised:		Aprv'd By:	SP	Lower Rio Grande Valley
Figure No.	4.3.2-D			

GSI ENVIRONMENTAL

LEGEND

Calculated Steady State Residuals per Well

Symbol	Range
● (large red)	-40 - -30
● (red)	-30 - -20
● (red)	-20 - -10
• (small red)	-10 - 0
• (small blue)	0 - 10
● (blue)	10 - 20
● (blue)	20 - 30
● (large blue)	30 - 40

— Rio Grande

⬚ Texas County

⬛ Model Boundary

Note:

Basemap provided by Montgomery & Associates December 2016.

Scale in Miles
0   10   20

Projected Coordinate System
Datum: NAD 1983
Albers Equal Area

GSI
ENVIRONMENTAL

DISTRIBUTION OF WATER LEVEL ERRORS FOR CALIBRATED 1984 CONDITIONS

Lower Rio Grande Valley

GSI Job No. 4276	Drawn By: AV
Issued: 20-Jun-2017	Chk'd By: KER
Map ID: LRGV_WLErrors1984	Appv'd By: SP

FIGURE 4.3.3

Sources: Esri, USGS, NOAA
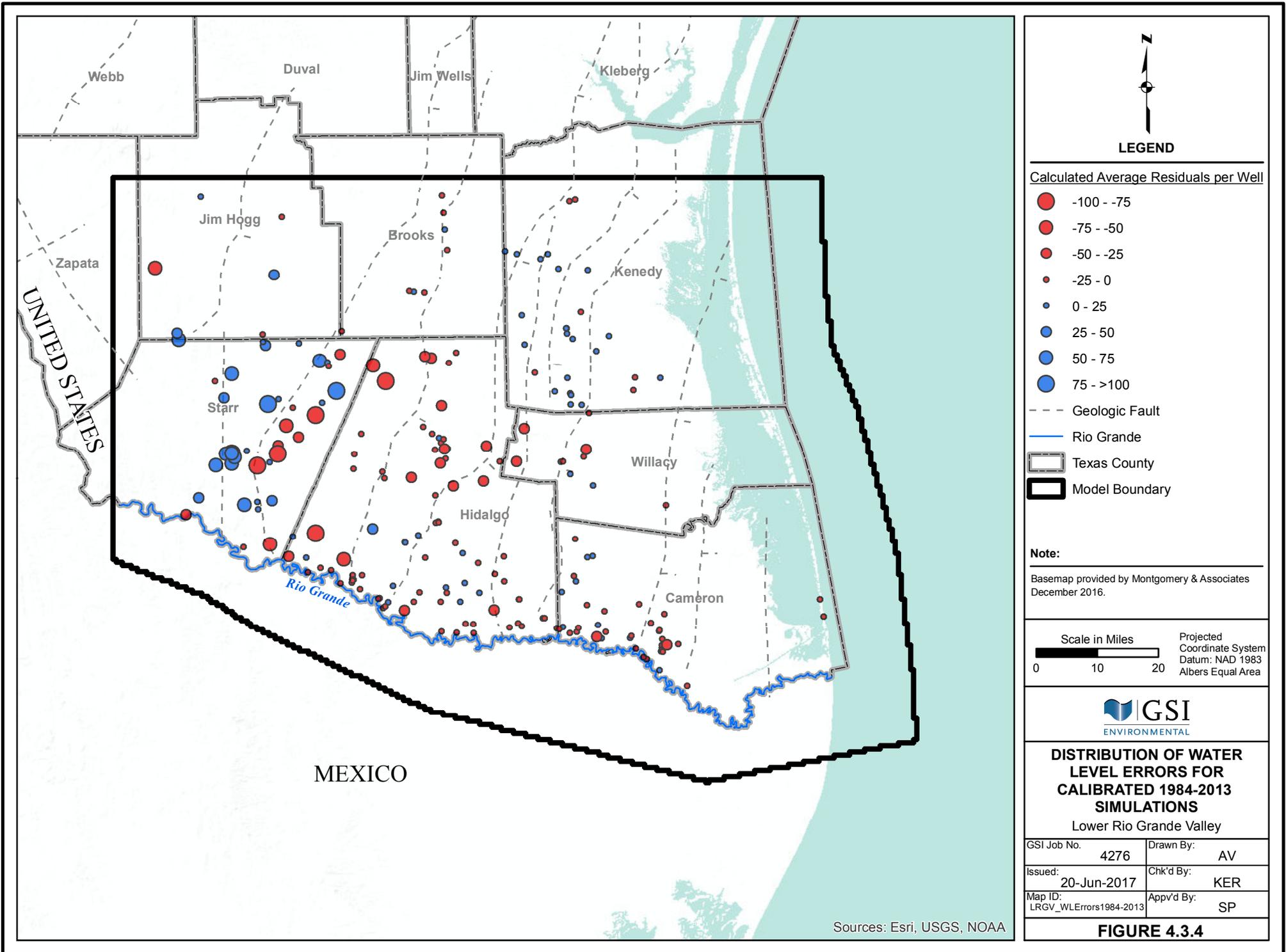
LEGEND

Calculated Average Residuals per Well

- ⬤ -100 - -75
- ⬤ -75 - -50
- ● -50 - -25
- • -25 - 0
- • 0 - 25
- ● 25 - 50
- ⬤ 50 - 75
- ⬤ 75 - >100

- - - Geologic Fault

—— Rio Grande

Texas County

Model Boundary

Note:

Basemap provided by Montgomery & Associates December 2016.

Scale in Miles

0   10   20

Projected Coordinate System Datum: NAD 1983 Albers Equal Area

GSI ENVIRONMENTAL

DISTRIBUTION OF WATER LEVEL ERRORS FOR CALIBRATED 1984-2013 SIMULATIONS

Lower Rio Grande Valley

GSI Job No. 4276	Drawn By: AV
Issued: 20-Jun-2017	Chk'd By: KER
Map ID: LRGV_WLErrors1984-2013	Appv'd By: SP

FIGURE 4.3.4
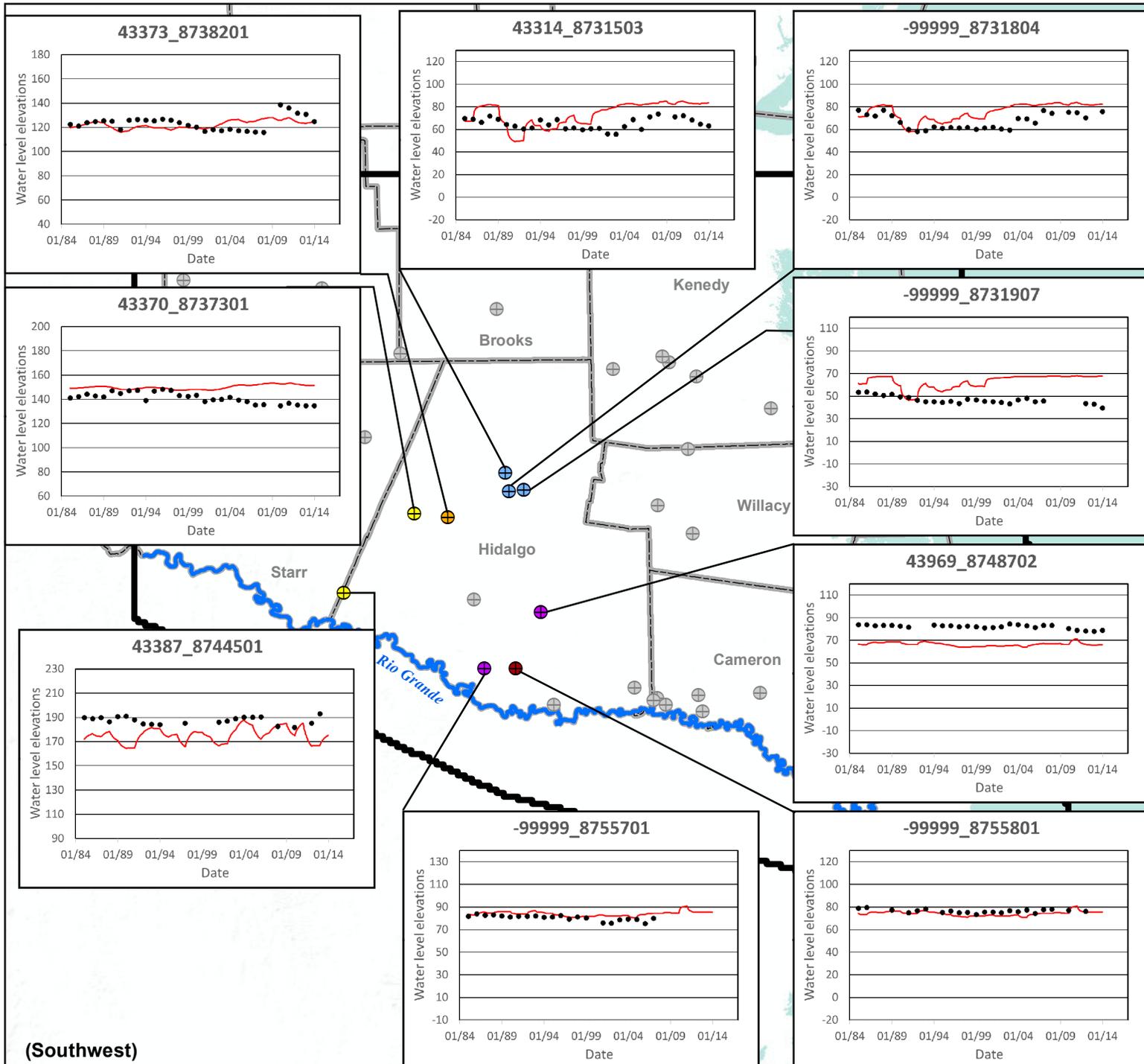
Webb

Duval

Jim Wells

Kleberg

Jim Hogg

Brooks

Zapata

Kenedy

UNITED STATES

Starr

Willacy

Hidalgo

Rio Grande

Cameron

MEXICO

Sources: Esri, USGS, NOAA

MEASURED AND SIMULATED ANNUAL WATER LEVEL HYDROGRAPHS FOR WELLS WITH MOST AVAILABLE DATA

Lower Rio Grande Valley

LEGEND

- Observed Water Level Elevation (Feet AMSL)
- Simulated Water Level Elevation (Feet AMSL)

Well with 20 or More Years of Data Shown

- Lissie Formation of Chicot Aquifer (Model Layer 2)
- Willis Formation of Chicot Aquifer (Model Layer 3)
- Upper Goliad Formation of Evangeline Aquifer (Model Layer 4)
- Upper Lagarto Formation of Evangeline Aquifer (Model Layer 6)
- Middle Lagarto Formation of Burkeville Confining Unit (Model Layer 7)
- Not Shown
- Texas County
- Rio Grande
- Model Boundary

Notes:
1) Basemap provided by Montgomery & Associates, December 2016.
2) AMSL = Above Mean Sea Level.
3) Observed water level elevations shown are yearly averages of measured values.
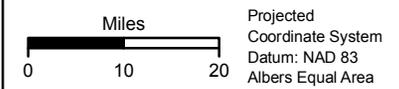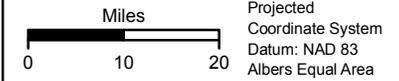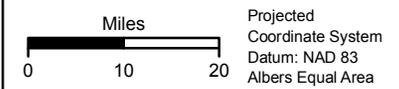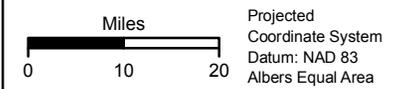
Projected Coordinate System Datum: NAD 83 Albers Equal Area

Miles
0   10   20

GSI Job No. 4276-103
Drawn By: AV
Issued: 23-Jun-2017
Chk'd By: KER
Map ID: LRGV_GraphsOS_SW
Appv'd By: SP

FIGURE 4.3.5-A

(Southwest)

MEASURED AND SIMULATED ANNUAL WATER LEVEL HYDROGRAPHS FOR WELLS WITH MOST AVAILABLE DATA

Lower Rio Grande Valley

FIGURE 4.3.5-B

MEASURED AND SIMULATED ANNUAL WATER LEVEL HYDROGRAPHS FOR WELLS WITH MOST AVAILABLE DATA

Lower Rio Grande Valley

(Northwest)

FIGURE 4.3.5-C

MEASURED AND SIMULATED ANNUAL WATER LEVEL HYDROGRAPHS FOR WELLS WITH MOST AVAILABLE DATA

Lower Rio Grande Valley

GSI Job No.	Drawn By:
4276-103	AV
Issued: 23-Jun-2017	Chk'd By: KER
Map ID: LRGV_GraphsOS_NE	Appv'd By: SP

FIGURE 4.3.5-D
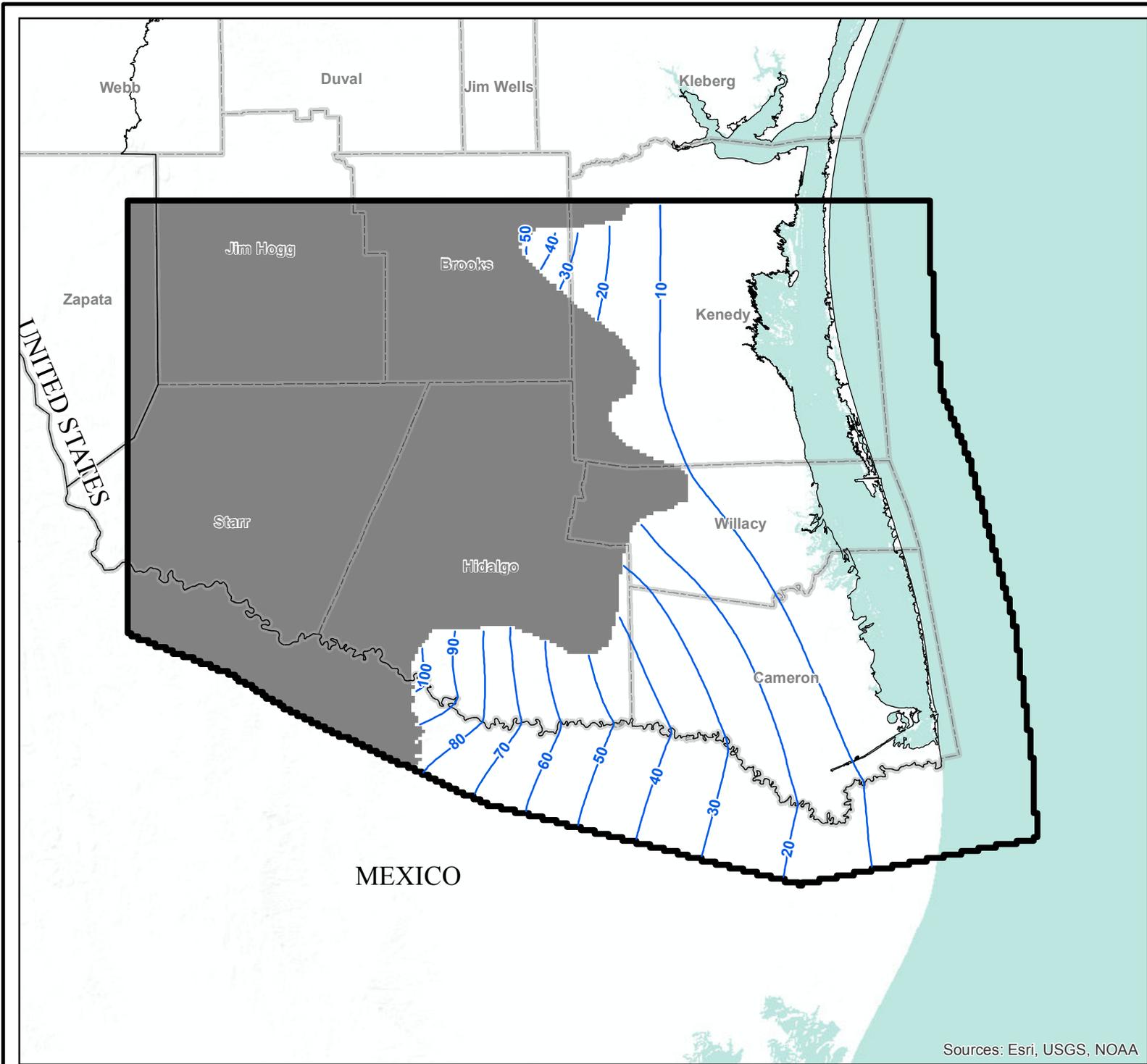
LEGEND

———	Modeled Water Level Contour (Feet AMSL)
▭	Texas County
▬	Model Boundary
■	Layer Pinchout

Notes:

1) Basemap provided by Montgomery & Associates December 2016.
2) AMSL = Above Mean Sea Level.

Scale in Miles

0   10   20

Projected Coordinate System Datum: NAD 1983 Albers Equal Area

GSI
ENVIRONMENTAL
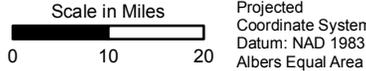
SIMULATED WATER LEVELS IN MODEL LAYER 1 (BEAUMONT FORMATION OF CHICOT AQUIFER) FOR 2013
Lower Rio Grande Valley

| GSI Job No. 4276	Drawn By: AV
Issued: 21-Jun-2017	Chk'd By: KER
Map ID: LRGV_SWLML1_2013	Appv'd By: SP

FIGURE 4.3.6

Sources: Esri, USGS, NOAA

Map labels:

Webb · Duval · Jim Wells · Kleberg

Jim Hogg

Zapata

Brooks

Kenedy

Starr

Willacy

Hidalgo

Cameron

UNITED STATES

MEXICO

LEGEND

Modeled Water Level Contour (Feet AMSL)
Texas County
Model Boundary
Layer Pinchout

Notes:

1) Basemap provided by Montgomery & Associates December 2016.
2) AMSL = Above Mean Sea Level.

Scale in Miles
0   10   20

Projected Coordinate System Datum: NAD 1983 Albers Equal Area

GSI ENVIRONMENTAL

SIMULATED WATER LEVELS IN MODEL LAYER 2 (LISSIE FORMATION OF CHICOT AQUIFER) FOR 2013
Lower Rio Grande Valley

GSI Job No. 4276	Drawn By: AV
Issued: 21-Jun-2017	Chk'd By: KER
Map ID: LRGV_SWLML2_2013	Appv'd By: SP
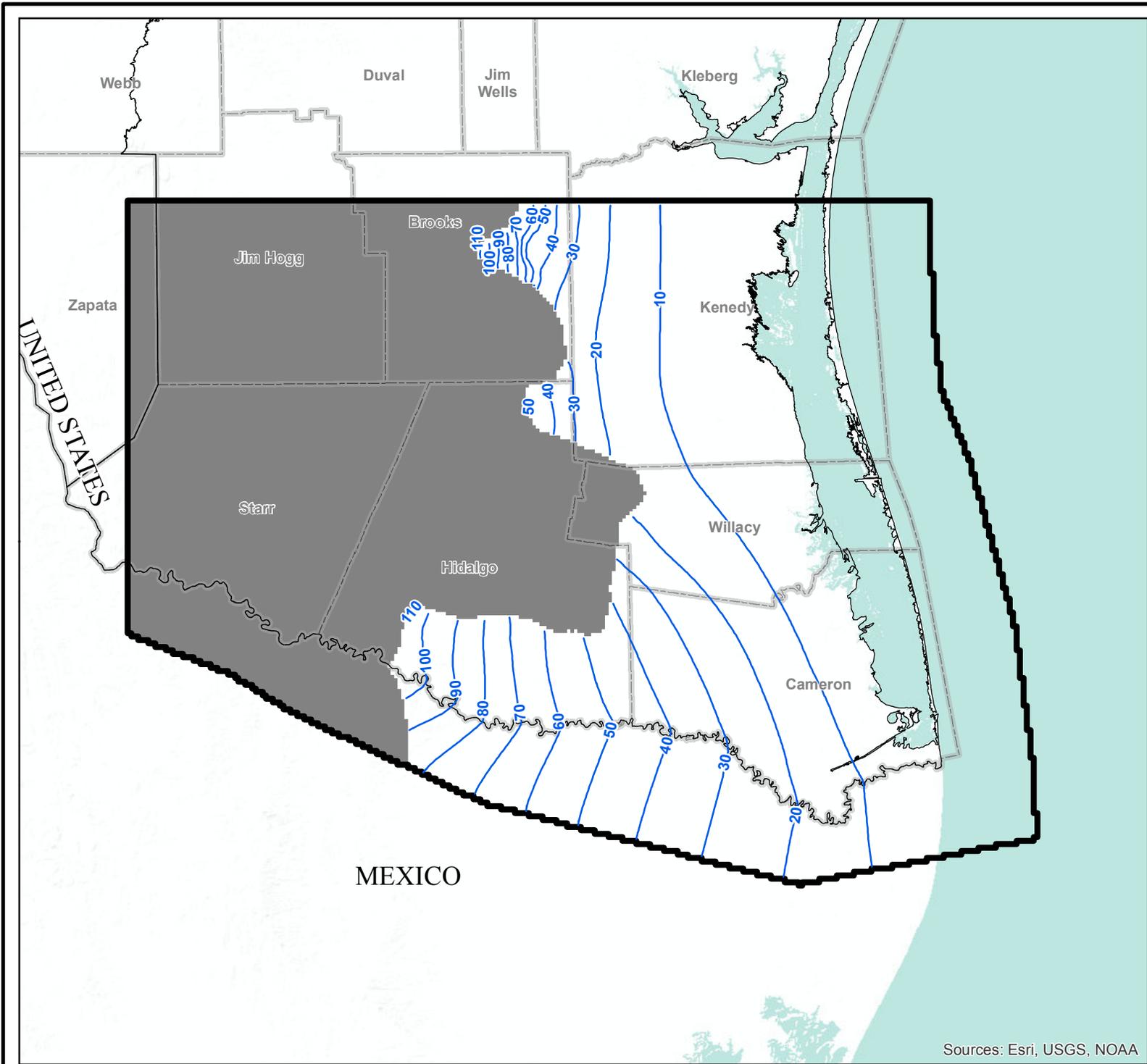
Sources: Esri, USGS, NOAA

FIGURE 4.3.7

LEGEND

Modeled Water Level Contour (Feet AMSL)

Texas County

Model Boundary

Layer Pinchout

Notes:

1) Basemap provided by Montgomery & Associates December 2016.
2) AMSL = Above Mean Sea Level.

Scale in Miles

0   10   20

Projected Coordinate System Datum: NAD 1983 Albers Equal Area

GSI ENVIRONMENTAL

SIMULATED WATER LEVELS IN MODEL LAYER 3 (WILLIS FORMATION OF CHICOT AQUIFER) FOR 2013
Lower Rio Grande Valley

GSI Job No. 4276	Drawn By: AV
Issued: 21-Jun-2017	Chk'd By: KER
Map ID: LRGV_SWLML3_2013	Appv'd By: SP

FIGURE 4.3.8
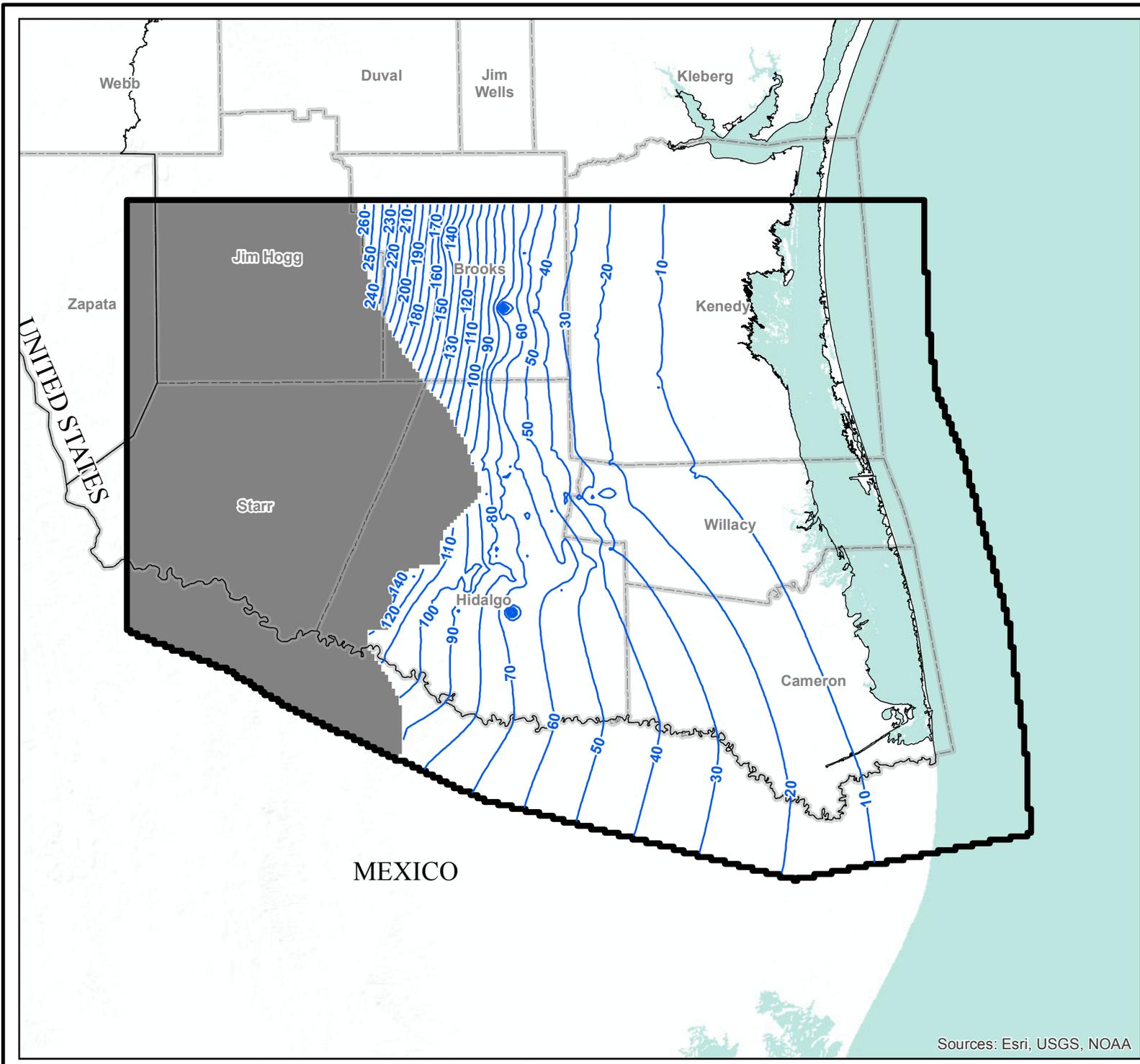
Sources: Esri, USGS, NOAA

LEGEND

— Modeled Water Level Contour (Feet AMSL)

Texas County

Model Boundary

Layer Pinchout

Notes:

1) Basemap provided by Montgomery & Associates December 2016.
2) AMSL = Above Mean Sea Level.

Scale in Miles

0   10   20

Projected Coordinate System
Datum: NAD 1983
Albers Equal Area

GSI
ENVIRONMENTAL
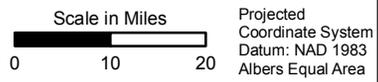
SIMULATED WATER LEVELS IN MODEL LAYER 4 (UPPER GOLIAD FORMATION OF EVANGELINE AQUIFER) FOR 2013

Lower Rio Grande Valley

GSI Job No. 4276	Drawn By: AV
Issued: 21-Jun-2017	Chk'd By: KER
Map ID: LRGV_SWLML4_2013	Appv'd By: SP

FIGURE 4.3.9

Sources: Esri, USGS, NOAA
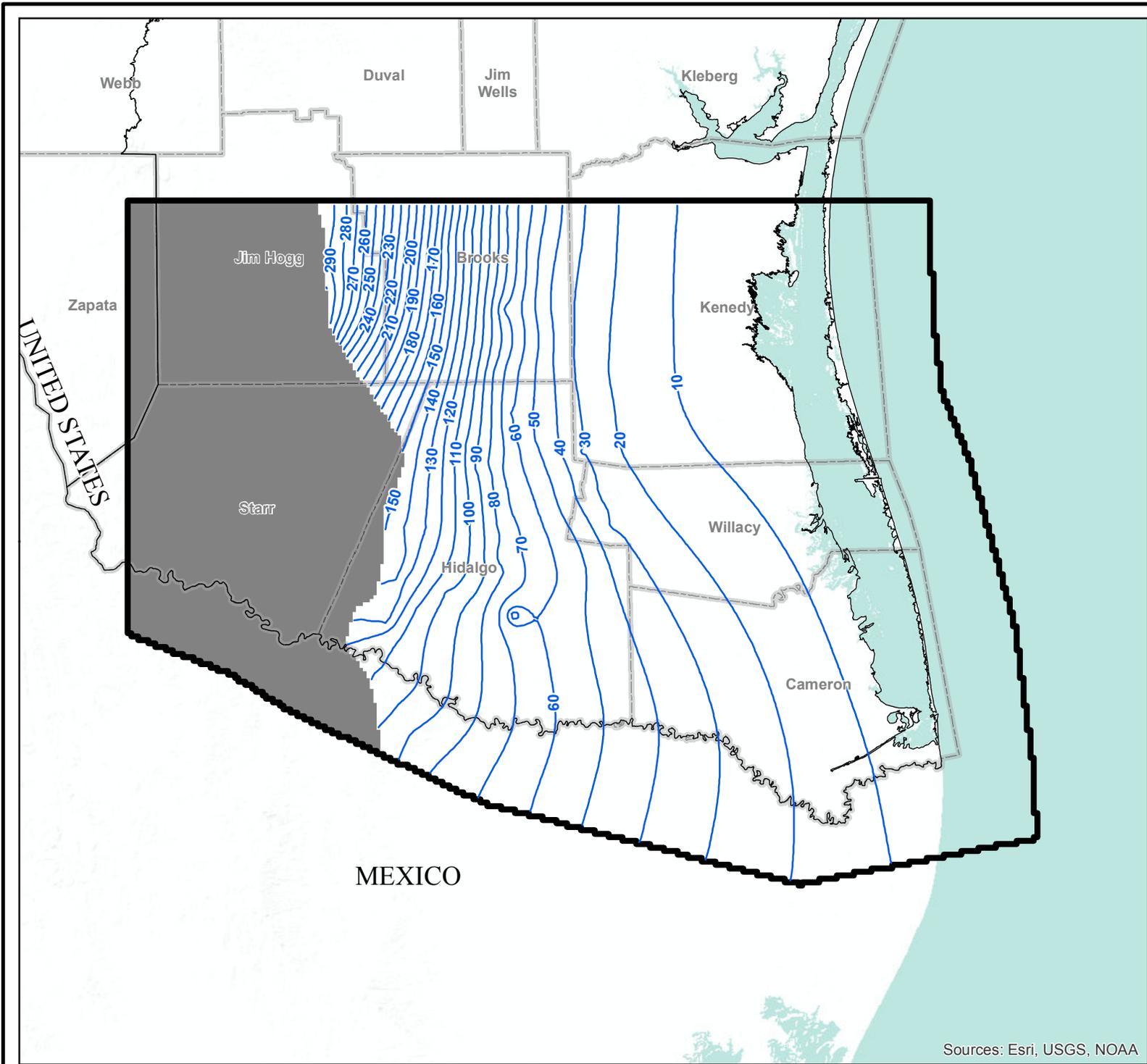
LEGEND

— Modeled Water Level Contour (Feet AMSL)

Texas County

Model Boundary

Layer Pinchout

Notes:

1) Basemap provided by Montgomery & Associates December 2016.
2) AMSL = Above Mean Sea Level.

Scale in Miles

0   10   20

Projected Coordinate System Datum: NAD 1983 Albers Equal Area

GSI ENVIRONMENTAL
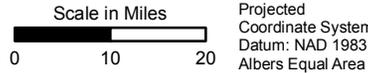
SIMULATED WATER LEVELS IN MODEL LAYER 5 (LOWER GOLIAD FORMATION OF EVANGELINE AQUIFER) FOR 2013

Lower Rio Grande Valley

GSI Job No. 4276	Drawn By: AV
Issued: 21-Jun-2017	Chk'd By: KER
Map ID: LRGV_SWLML5_2013	Appv'd By: SP

FIGURE 4.3.10
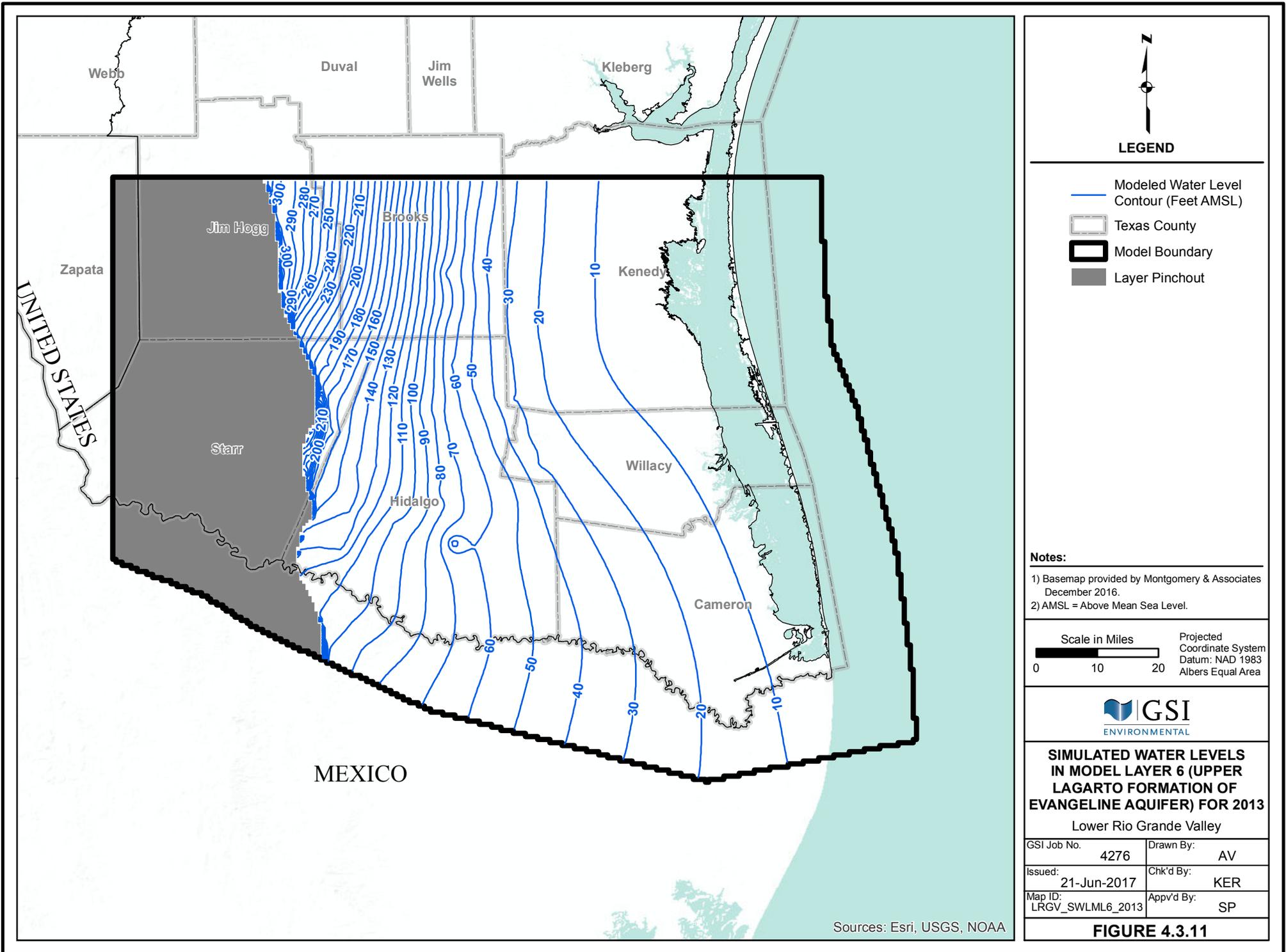
LEGEND

— Modeled Water Level Contour (Feet AMSL)

☐ Texas County

■ Model Boundary

▨ Layer Pinchout

Notes:

1) Basemap provided by Montgomery & Associates December 2016.
2) AMSL = Above Mean Sea Level.

Scale in Miles

0   10   20

Projected Coordinate System
Datum: NAD 1983
Albers Equal Area

GSI ENVIRONMENTAL

SIMULATED WATER LEVELS IN MODEL LAYER 6 (UPPER LAGARTO FORMATION OF EVANGELINE AQUIFER) FOR 2013

Lower Rio Grande Valley

GSI Job No. 4276	Drawn By: AV
Issued: 21-Jun-2017	Chk'd By: KER
Map ID: LRGV_SWLML6_2013	Appv'd By: SP

FIGURE 4.3.11

Sources: Esri, USGS, NOAA
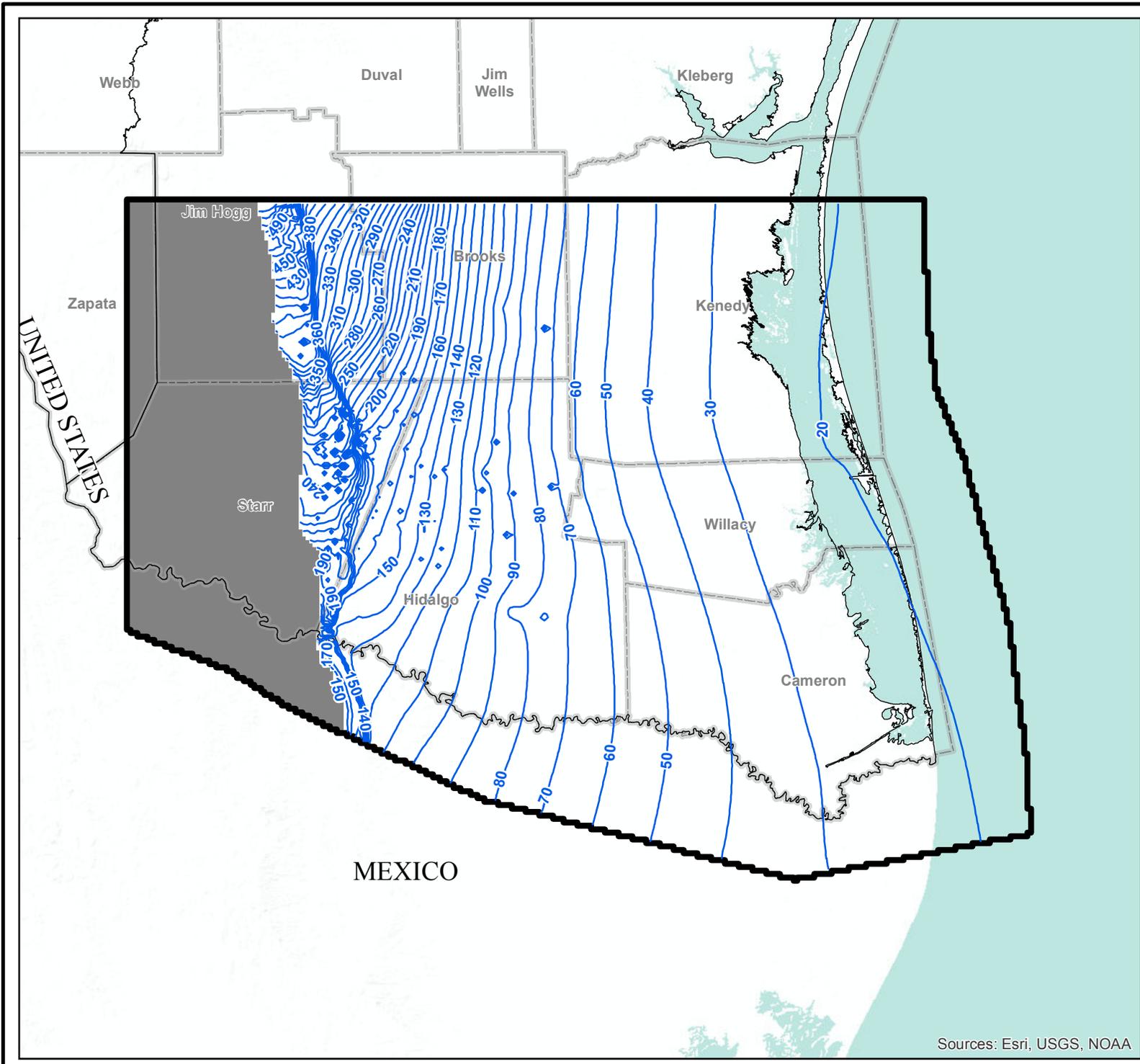
LEGEND

— Modeled Water Level Contour (Feet AMSL)

Texas County

Model Boundary

Layer Pinchout

Notes:

1) Basemap provided by Montgomery & Associates December 2016.
2) AMSL = Above Mean Sea Level.

Scale in Miles

0   10   20

Projected Coordinate System Datum: NAD 1983 Albers Equal Area

GSI ENVIRONMENTAL

SIMULATED WATER LEVELS IN MODEL LAYER 7 (MIDDLE LAGARTO FORMATION OF BURKEVILLE CONFINING UNIT) FOR 2013
Lower Rio Grande Valley

GSI Job No. 4276	Drawn By: AV
Issued: 21-Jun-2017	Chk'd By: KER
Map ID: LRGV_SWLML7_2013	Appv'd By: SP

FIGURE 4.3.12

Sources: Esri, USGS, NOAA

LEGEND

— Modeled Water Level Contour (Feet AMSL)

Texas County

Model Boundary

Layer Pinchout

Notes:

1) Basemap provided by Montgomery & Associates December 2016.
2) AMSL = Above Mean Sea Level.

Scale in Miles

0   10   20

Projected Coordinate System Datum: NAD 1983 Albers Equal Area

GSI ENVIRONMENTAL

SIMULATED WATER LEVELS IN MODEL LAYER 8 (LOWER LAGARTO FORMATION OF JASPER AQUIFER) FOR 2013

Lower Rio Grande Valley

GSI Job No.	Drawn By:
4276	AV
Issued:	Chk'd By:
21-Jun-2017	KER
Map ID:	Appv'd By:
LRGV_SWLML8_2013	SP

Sources: Esri, USGS, NOAA

FIGURE 4.3.13

LEGEND

Modeled Water Level Contour (Feet AMSL)	
Texas County	
Model Boundary	
Layer Pinchout	

Notes:

1) Basemap provided by Montgomery & Associates December 2016.
2) AMSL = Above Mean Sea Level.

Scale in Miles
0   10   20

Projected Coordinate System
Datum: NAD 1983
Albers Equal Area

GSI ENVIRONMENTAL

SIMULATED WATER LEVELS IN MODEL LAYER 9 (OAKVILLE FORMATION OF JASPER AQUIFER) FOR 2013
Lower Rio Grande Valley

GSI Job No. 4276	Drawn By: AV
Issued: 21-Jun-2017	Chk'd By: KER
Map ID: LRGV_SWLML9_2013	Appv'd By: SP
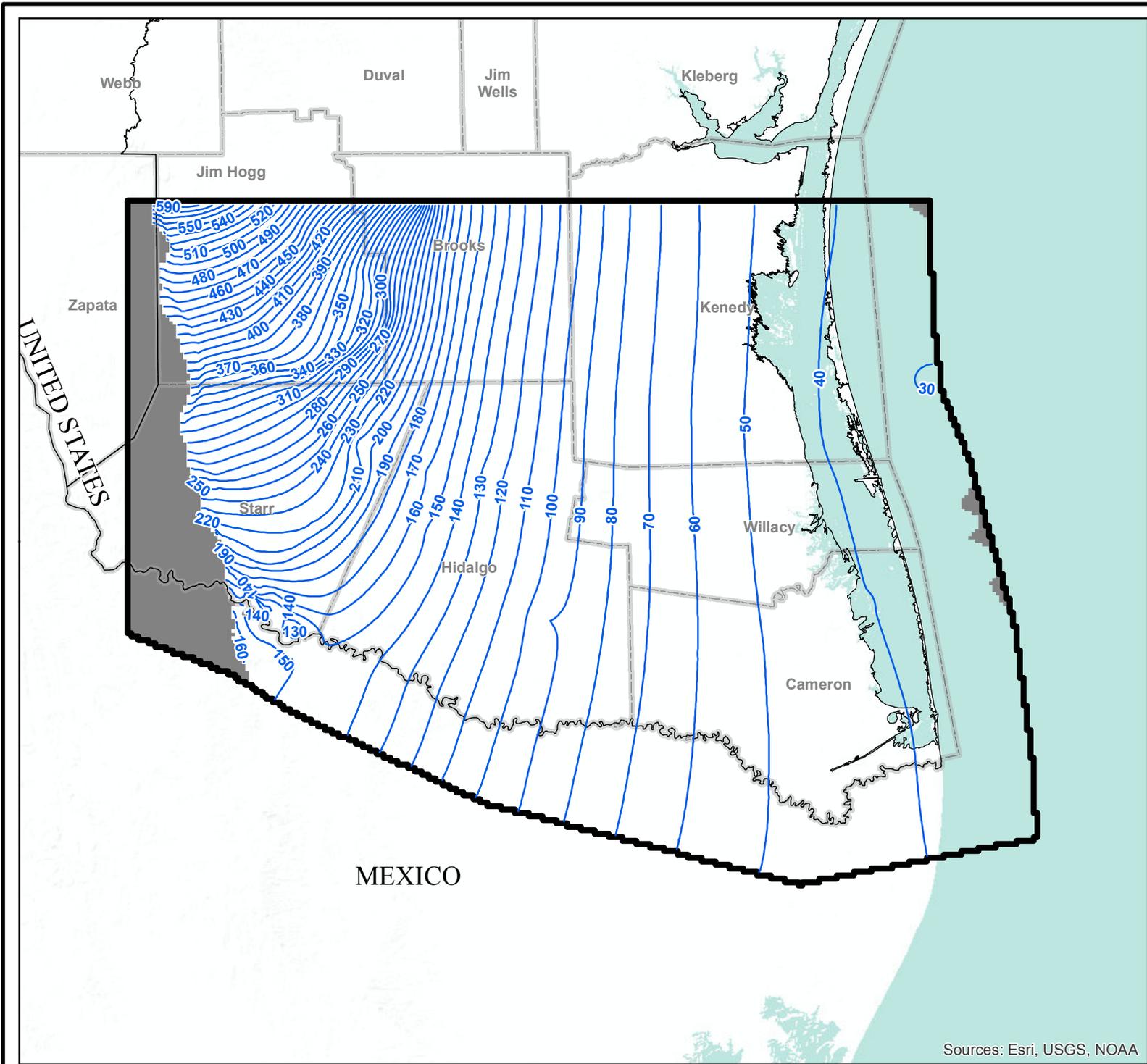
Sources: Esri, USGS, NOAA

FIGURE 4.3.14

LEGEND

— Modeled Water Level Contour (Feet AMSL)

Texas County

Model Boundary

Layer Pinchout

Notes:

1) Basemap provided by Montgomery & Associates December 2016.
2) AMSL = Above Mean Sea Level.

Scale in Miles

0   10   20

Projected Coordinate System Datum: NAD 1983 Albers Equal Area

GSI ENVIRONMENTAL

SIMULATED WATER LEVELS IN MODEL LAYER 10 (UPPER CATAHOULA FORMATION OF JASPER AQUIFER) FOR 2013
Lower Rio Grande Valley

GSI Job No. 4276	Drawn By: AV
Issued: 21-Jun-2017	Chk'd By: KER
Map ID: LRGV_SWLML10_2013	Appv'd By: SP

FIGURE 4.3.15
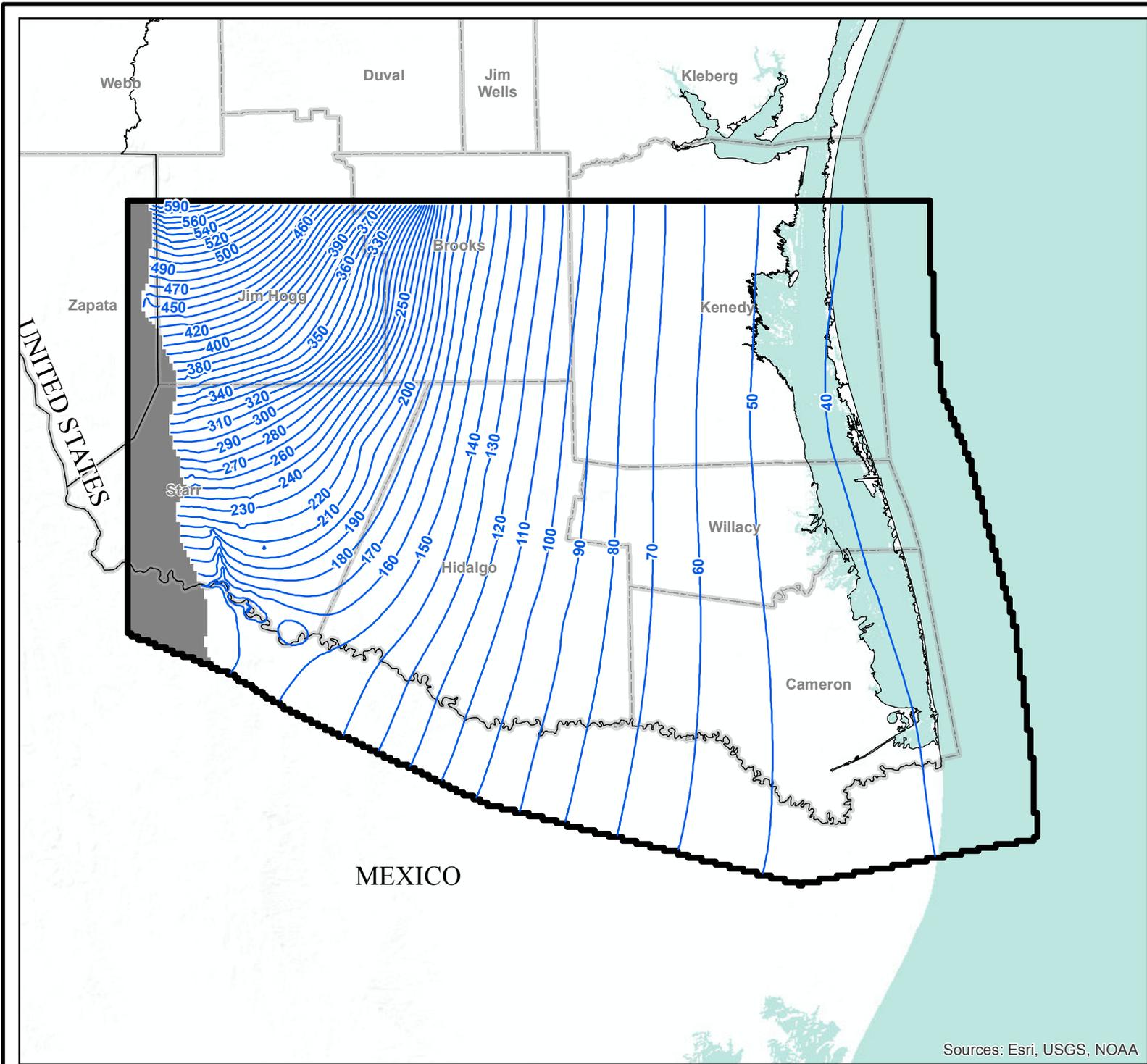
Sources: Esri, USGS, NOAA

LEGEND

— Modeled Water Level Contour (Feet AMSL)

☐ Texas County

☐ Model Boundary

▨ Layer Pinchout

Notes:

1) Basemap provided by Montgomery & Associates December 2016.
2) AMSL = Above Mean Sea Level.

Scale in Miles

0   10   20

Projected Coordinate System Datum: NAD 1983 Albers Equal Area

GSI ENVIRONMENTAL

SIMULATED WATER LEVELS IN MODEL LAYER 11 (CATAHOULA CONFINING SYSTEM) FOR 2013

Lower Rio Grande Valley

GSI Job No. 4276	Drawn By: AV
Issued: 21-Jun-2017	Chk'd By: KER
Map ID: LRGV_SWLML11_2013	Appv'd By: SP

FIGURE 4.3.16
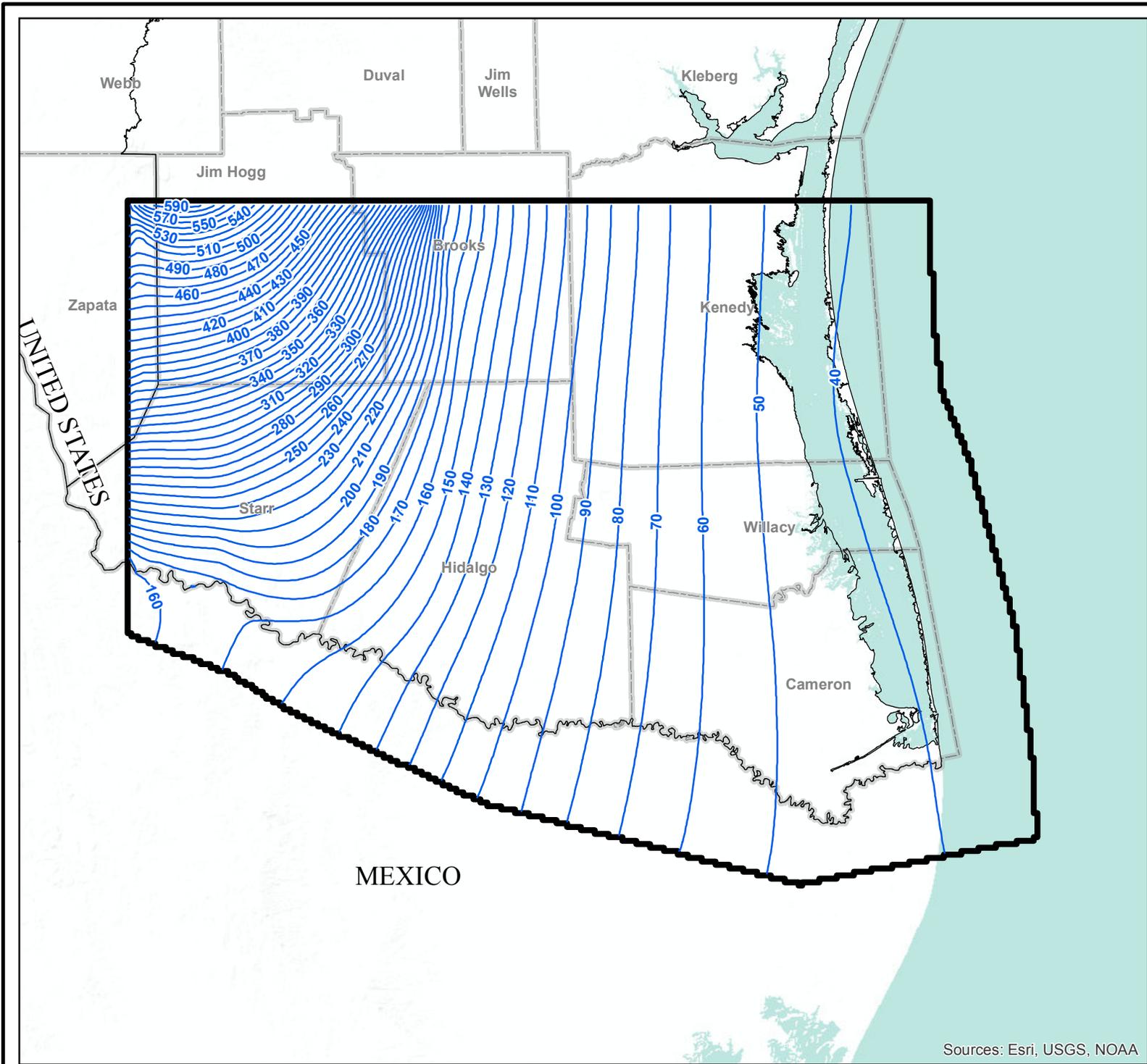
Sources: Esri, USGS, NOAA

LEGEND

— Modeled Water Level Contour (Feet AMSL)

☐ Texas County

☐ Model Boundary

Notes:

1) Basemap provided by Montgomery & Associates December 2016.
2) AMSL = Above Mean Sea Level.

Scale in Miles

0   10   20

Projected Coordinate System Datum: NAD 1983 Albers Equal Area

GSI ENVIRONMENTAL
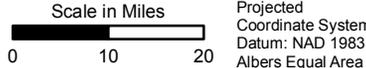
SIMULATED WATER LEVELS IN MODEL LAYER 12 (YEGUA-JACKSON AQUIFER) FOR 2013

Lower Rio Grande Valley

GSI Job No. 4276	Drawn By: AV
Issued: 21-Jun-2017	Chk'd By: KER
Map ID: LRGV_SWLML12_2013	Appv'd By: SP

FIGURE 4.3.17
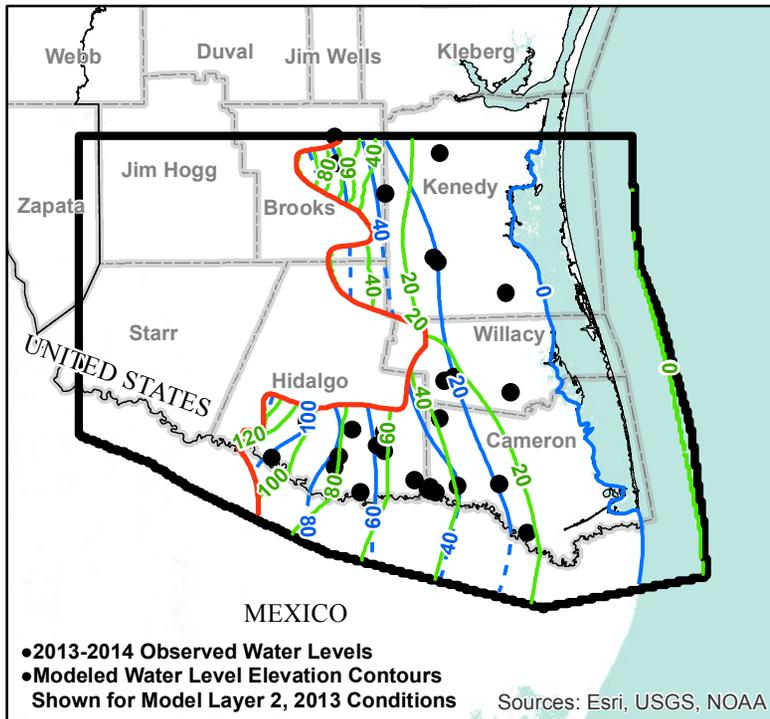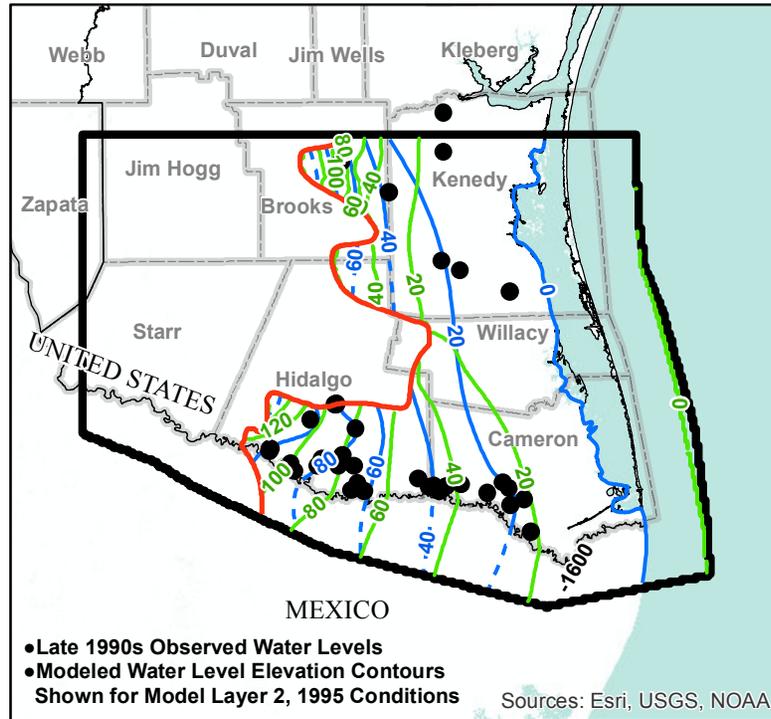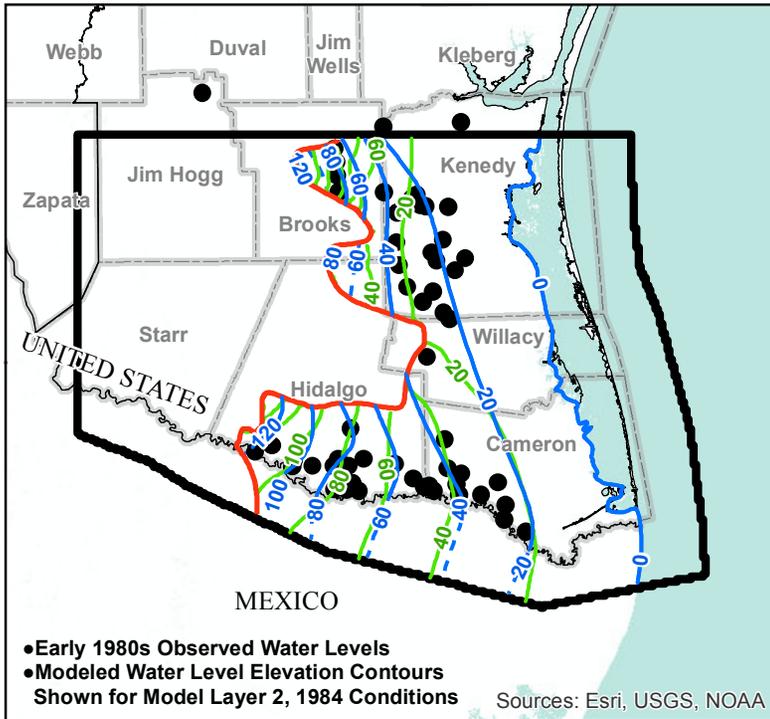
Sources: Esri, USGS, NOAA

Early 1980s Observed Water Levels
Modeled Water Level Elevation Contours
  Shown for Model Layer 2, 1984 Conditions

Sources: Esri, USGS, NOAA

Late 1990s Observed Water Levels
Modeled Water Level Elevation Contours
  Shown for Model Layer 2, 1995 Conditions

Sources: Esri, USGS, NOAA

2013-2014 Observed Water Levels
Modeled Water Level Elevation Contours
  Shown for Model Layer 2, 2013 Conditions

Sources: Esri, USGS, NOAA

LEGEND

● Location of Measurement

Observed Groundwater Level
Elevation Contour (dashed
where inferred)

Modeled Groundwater Level
Elevation Contour

Western Extent of Chicot
Aquifer

Texas County

Model Boundary

Notes:

1) Presented in the "Conceptual Model Report:
Lower Rio Grande Valley Groundwater
Transport Model" prepared by Montgomery &
Associates, January 2017 as Figure 4.2.5.
2) Elevations are in feet above mean sea level.
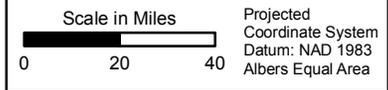
Scale in Miles

0   20   40

Projected
Coordinate System
Datum: NAD 1983
Albers Equal Area

GSI
ENVIRONMENTAL

**OBSERVED AND MODELED
GROUNDWATER LEVEL
ELEVATION CONTOURS
FOR CHICOT AQUIFER**
Lower Rio Grande Valley

GSI Job No. 4276	Drawn By: GM
Issued: 21-Jun-2017	Chk'd By: KER
Map ID: LRGV_Fig_4_2_5	Appv'd By: SP

FIGURE 4.3.18

OBSERVED AND MODELED GROUNDWATER LEVEL ELEVATION CONTOURS FOR EVANGELINE AQUIFER
Lower Rio Grande Valley

FIGURE 4.3.19

Early 1980s Observed Water Levels
Modeled Water Level Elevation Contours Shown for Model Layer 9, 1984 Conditions

Sources: Esri, USGS, NOAA

Late 1990s Observed Water Levels
Modeled Water Level Elevation Contours Shown for Model Layer 2, 1995 Conditions

Sources: Esri, USGS, NOAA

2013-2014 Observed Water Levels
Modeled Water Level Elevation Contours Shown for Model Layer 9, 2013 Conditions

Sources: Esri, USGS, NOAA

LEGEND

● Location of Measurement

—— Observed Groundwater Level Elevation Contour (dashed where inferred)

—— Modeled Groundwater Level Elevation Contour

—— Western Extent of Jasper Aquifer

Texas County

Model Boundary

Notes:

1) Presented in the "Conceptual Model Report: Lower Rio Grande Valley Groundwater Transport Model" prepared by Montgomery & Associates, January 2017 as Figure 4.2.7.

2) Elevations are in feet above mean sea level.

Scale in Miles
0   20   40

Projected Coordinate System
Datum: NAD 1983
Albers Equal Area

GSI ENVIRONMENTAL

OBSERVED AND MODELED GROUNDWATER LEVEL ELEVATION CONTOURS FOR JASPER AQUIFER
Lower Rio Grande Valley

GSI Job No. 4276	Drawn By: AV
Issued: 22-Jun-2017	Chk'd By: KER
Map ID: LRGV_Fig_4_2_7	Appv'd By: SP

FIGURE 4.3.20
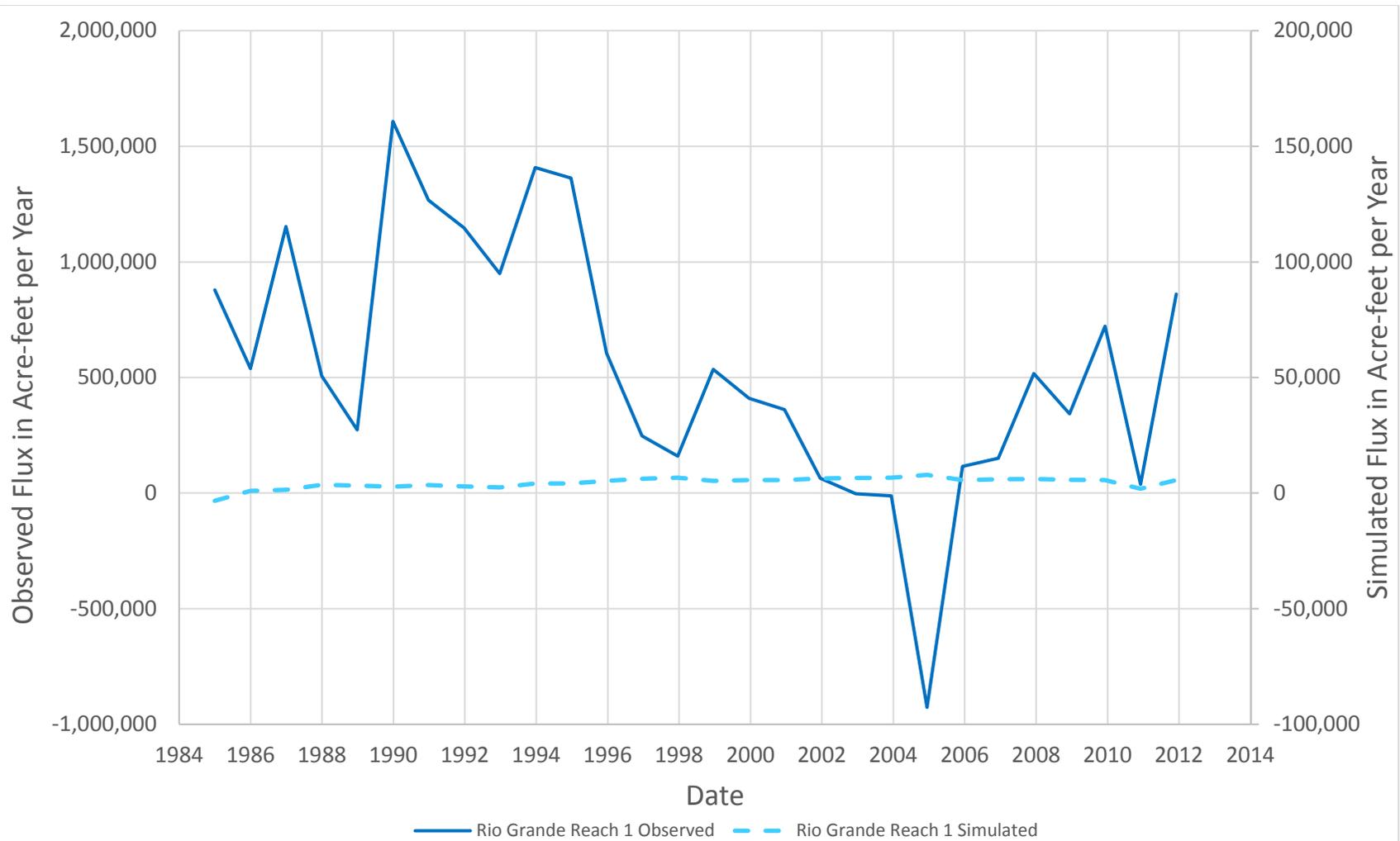
Note:
Rio Grande Reach 1 = Rio Grande reach from the western model boundary to Anzalduas Dam.

GSI Job No. 4276	Drawn By: GM	SIMULATED AND ESTIMATED GROUNDWATER INTERACTION FLUXES
Issued: 21-Jun-2017	Chk'd By: KER	
Revised:	Aprv'd By: SP	Lower Rio Grande Valley
Figure No. 4.3.21-A		
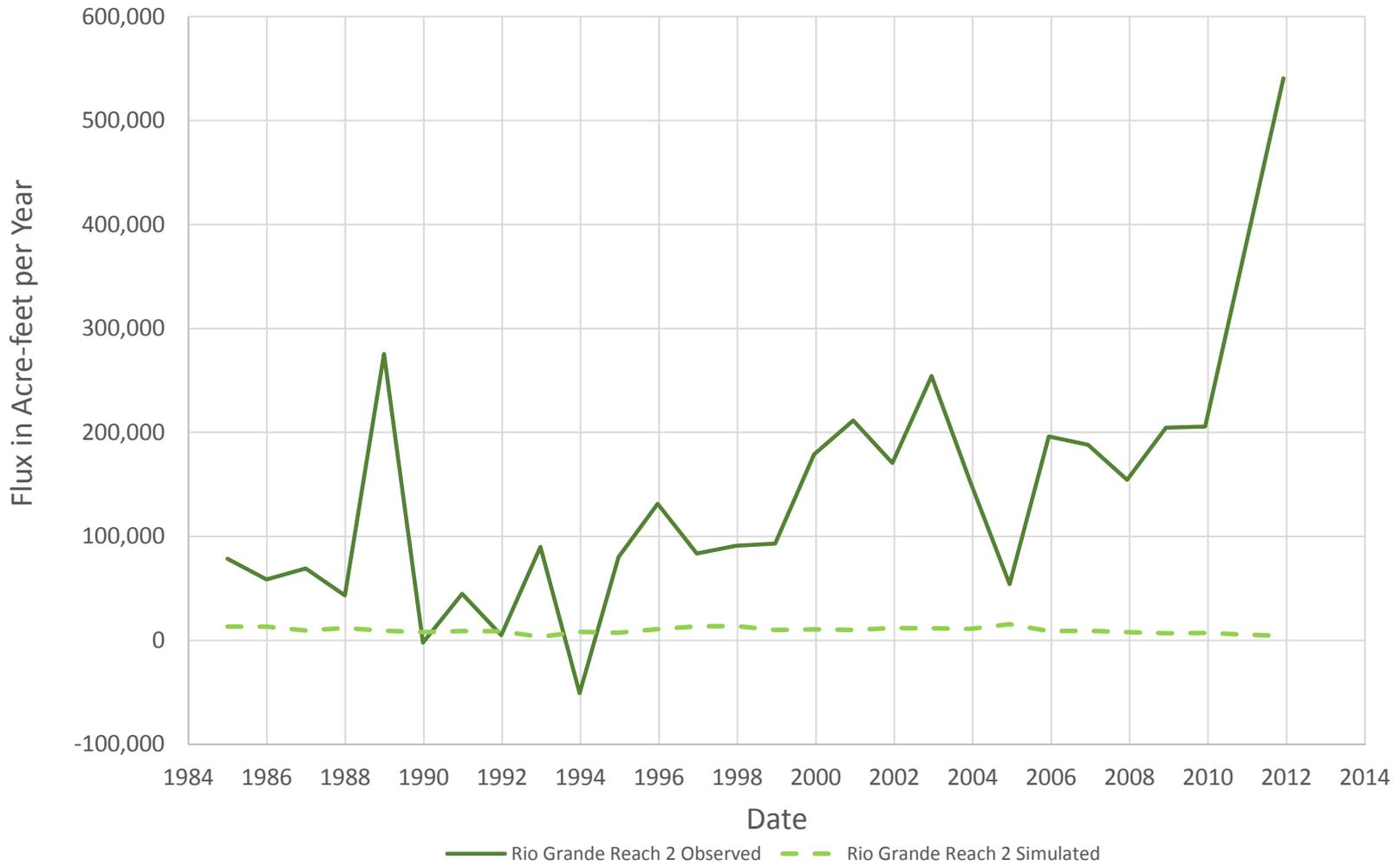
Note:
Rio Grande Reach 2 = Rio Grande reach from Anzalduas Dam to Brownsville Gage.

GSI Job No. 4276	Drawn By: GM	**SIMULATED AND ESTIMATED GROUNDWATER**
Issued: 21-Jun-2017	Chk'd By: KER	**INTERACTION FLUXES**
Revised:	Aprv'd By: SP	
Figure No. 4.3.21-B		Lower Rio Grande Valley

GSI ENVIRONMENTAL

SIMULATED AND ESTIMATED GROUNDWATER INTERACTION FLUXES

Lower Rio Grande Valley
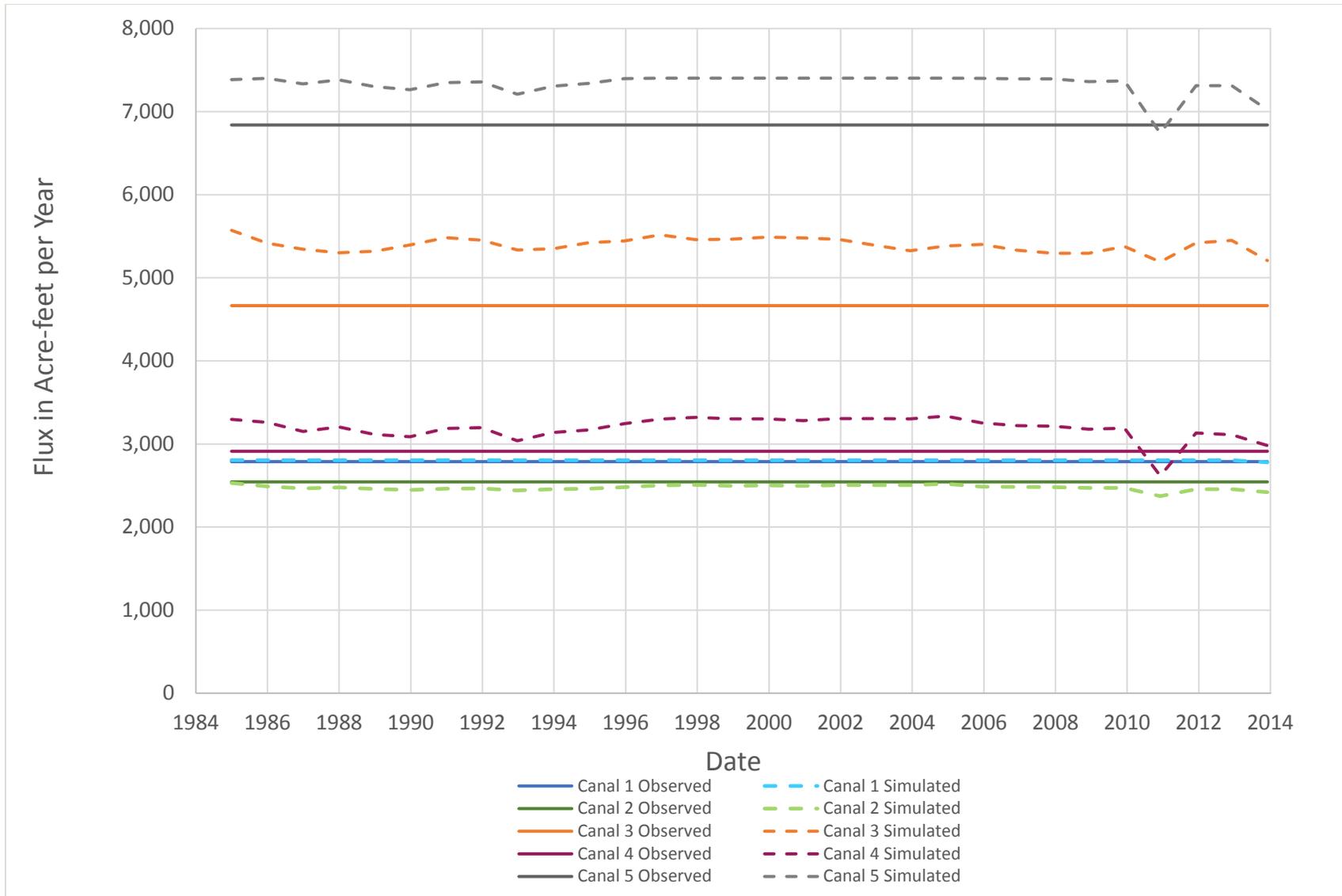
GSI Job No.	4276	Drawn By:	GM
Issued:	21-Jun-2017	Chk'd By:	KER
Revised:		Aprv'd By:	SP
Figure No.	4.3.21-C		

SIMULATED AND ESTIMATED GROUNDWATER
INTERACTION FLUXES
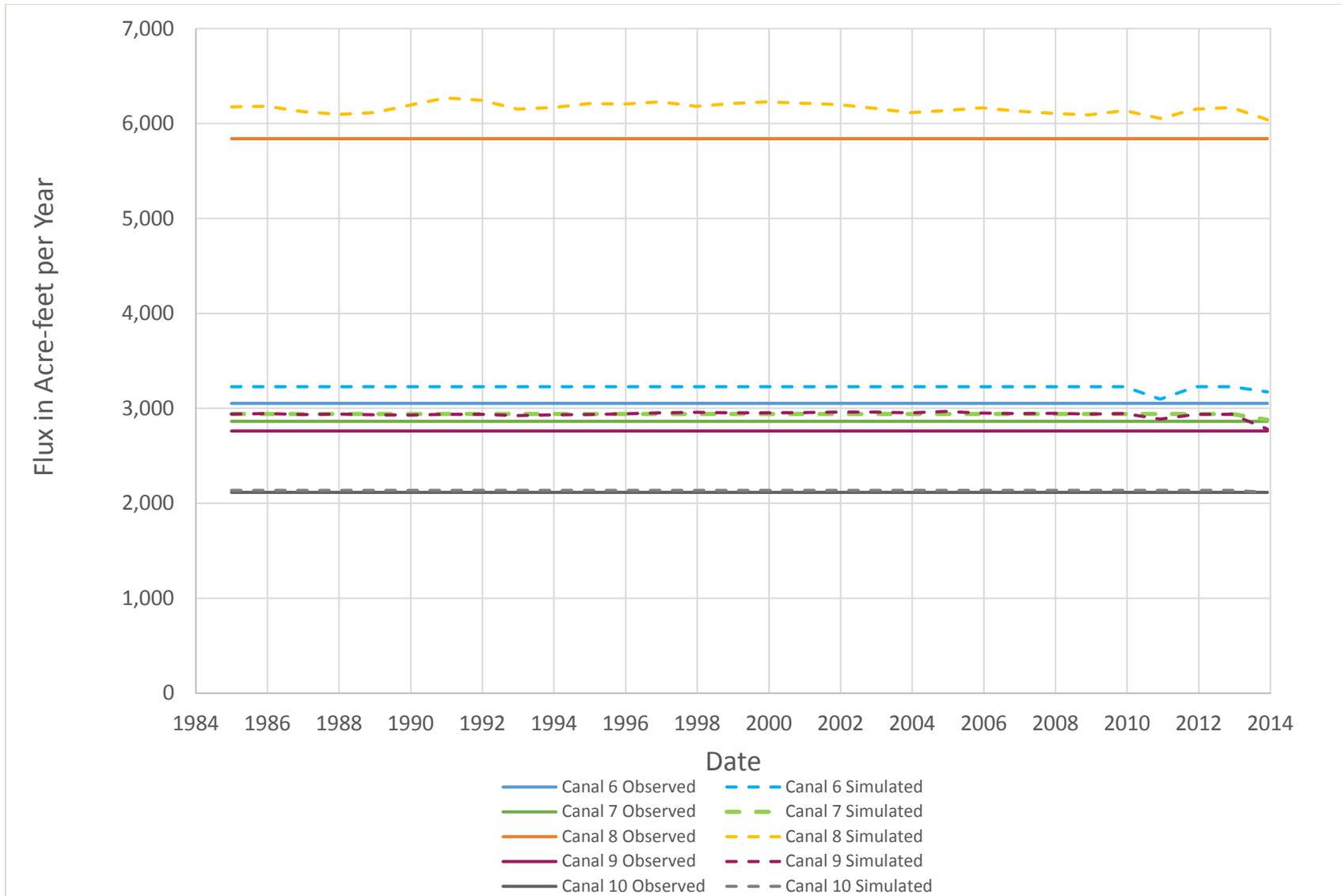
Lower Rio Grande Valley

GSI Job No.	4276	Drawn By:	GM
Issued:	21-Jun-2017	Chk'd By:	KER
Revised:		Aprv'd By:	SP
Figure No.	4.3.21-D		

Chart title: Flux in Acre-feet per Year vs Date

Legend — Model Water Budget:
- In: Storage
- In: LRG River Storage
- In: Coastal Constant Head
- In: LRG River Inflow
- In: Canal Leakage to GW
- In: GHB Inflow
- In: Recharge
- In: Return Flow
- Out: Storage
- Out: LRG River Storage
- Out: Coastal Constant Head
- Out: Wells
- Out: Baseflow to Canals
- Out: Head Dependent Boundary
- Out: Evapotranspiration
- Out: Diversions from LRG River
- Out: LRG River Outflow
- Error
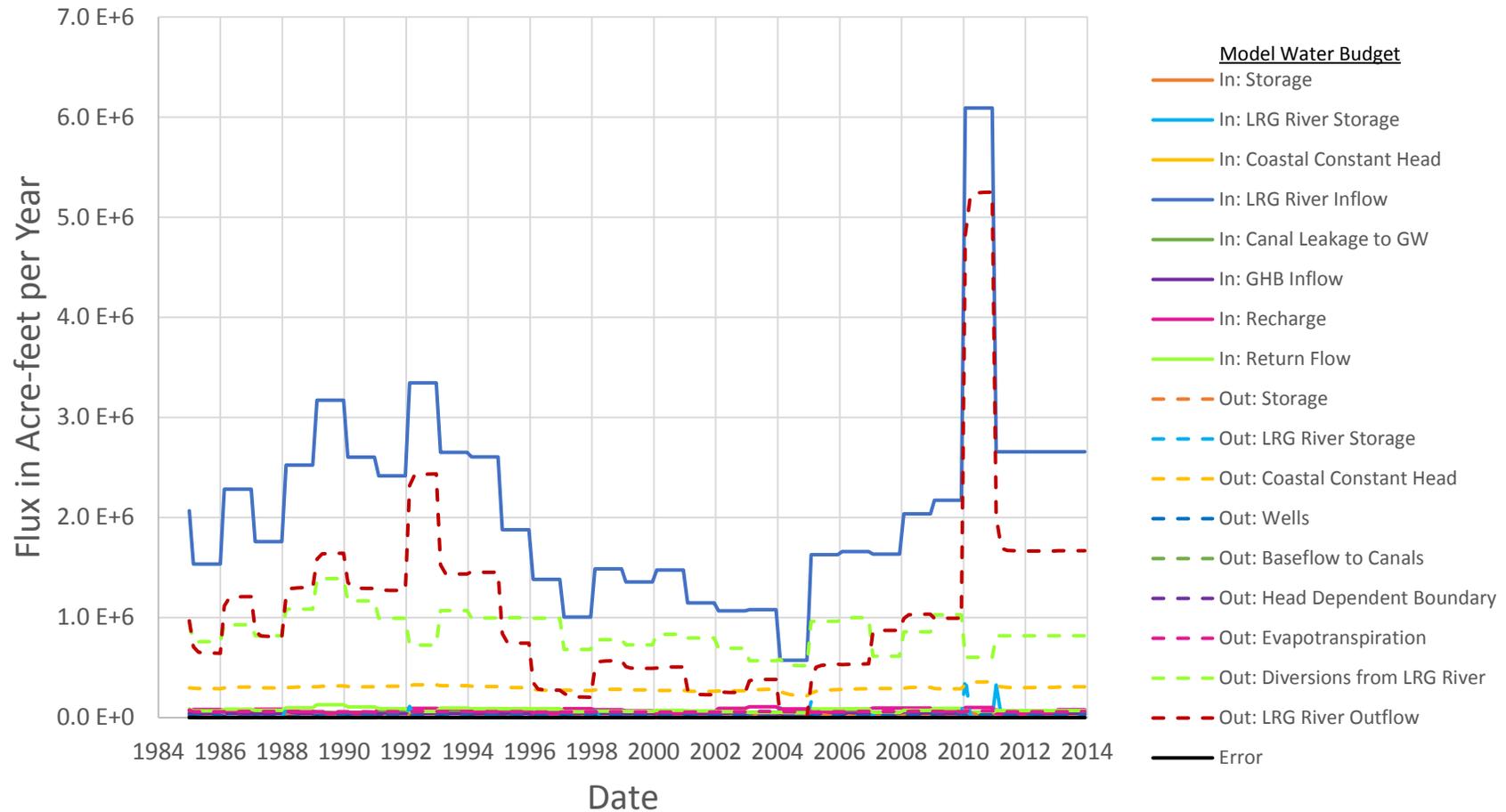
Notes:
LRG = Lower Rio Grande
GW = Groundwater
GHB = General Head Boundary

GSI Job No.	4276	Drawn By:	GM
Issued:	21-Jun-2017	Chk'd By:	KER
Revised:		Aprv'd By:	SP
Figure No.	4.3.22		

GSI ENVIRONMENTAL

WATER BUDGET FOR THE 1984-2013 CALIBRATION SIMULATION

Lower Rio Grande Valley

Model Water Budget

- In: Storage
- In: Coastal Constant Head
- In: Canal Leakage to GW
- In: GHB Inflow
- In: Recharge
- In: Return Flow
- Out: Storage
- Out: Coastal Constant Head
- Out: Wells
- Out: Baseflow to Canals
- Out: GHB
- Out: Evapotranspiration
- Error

Notes:
LRG = Lower Rio Grande
GW = Groundwater
GHB = General Head Boundary
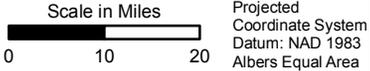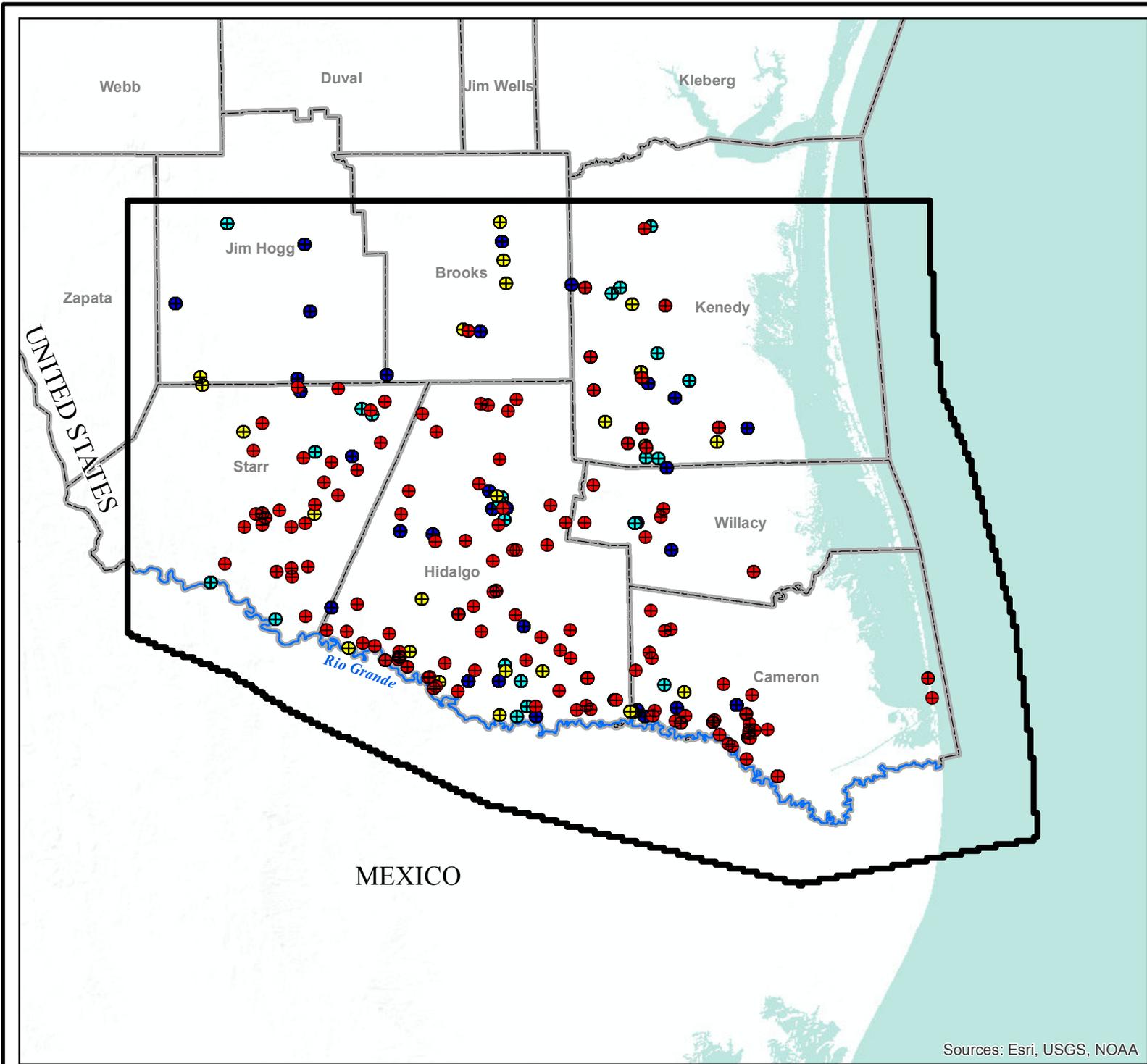
Sources: Esri, USGS, NOAA

LEGEND

Number of Years of Available Data at Each Well Location

- 🔴 <5
- 🟡 5 - 9
- 🔵 10 - 19
- 🔵 ≥20
- ── Rio Grande
- ☐ Texas County
- ▢ Model Boundary

Note:

Basemap provided by Montgomery & Associates December 2016.

Scale in Miles

0   10   20

Projected Coordinate System Datum: NAD 1983 Albers Equal Area

GSI
ENVIRONMENTAL

LOCATION OF GROUNDWATER LEVEL OBSERVATION WELLS AND AVAILABILITY OF ANNUAL WATER LEVEL DATA

Lower Rio Grande Valley

GSI Job No. 4276	Drawn By: AV
Issued: 23-Jun-2017	Chk'd By: KER
Map ID: LRGV_WellLocs	Appv'd By: SP

FIGURE 3.1.1

Webb Duval Jim Wells Kleberg

Zapata Jim Hogg Brooks Kenedy

UNITED STATES

Starr Hidalgo Willacy

Rio Grande

Cameron

MEXICO

Sources: Esri, USGS, NOAA

ANNUAL WATER LEVEL HYDROGRAPHS FOR WELLS WITH MOST AVAILABLE DATA

Lower Rio Grande Valley

FIGURE 3.1.2-A

ANNUAL WATER LEVEL
HYDROGRAPHS FOR WELLS
WITH MOST AVAILABLE DATA

Lower Rio Grande Valley

FIGURE 3.1.2-B

ANNUAL WATER LEVEL HYDROGRAPHS FOR WELLS WITH MOST AVAILABLE DATA

Lower Rio Grande Valley

FIGURE 3.1.2-C

ANNUAL WATER LEVEL HYDROGRAPHS FOR WELLS WITH MOST AVAILABLE DATA

Lower Rio Grande Valley

FIGURE 3.1.2-D

RIO GRANDE FLOW IN MODEL DOMAIN

Lower Rio Grande Valley

GSI Job No.	4276	Drawn By:	AV
Issued:	19-Jun-2017	Chk'd By:	KER
Revised:		Aprv'd By:	SP
Figure No.	3.2.1		
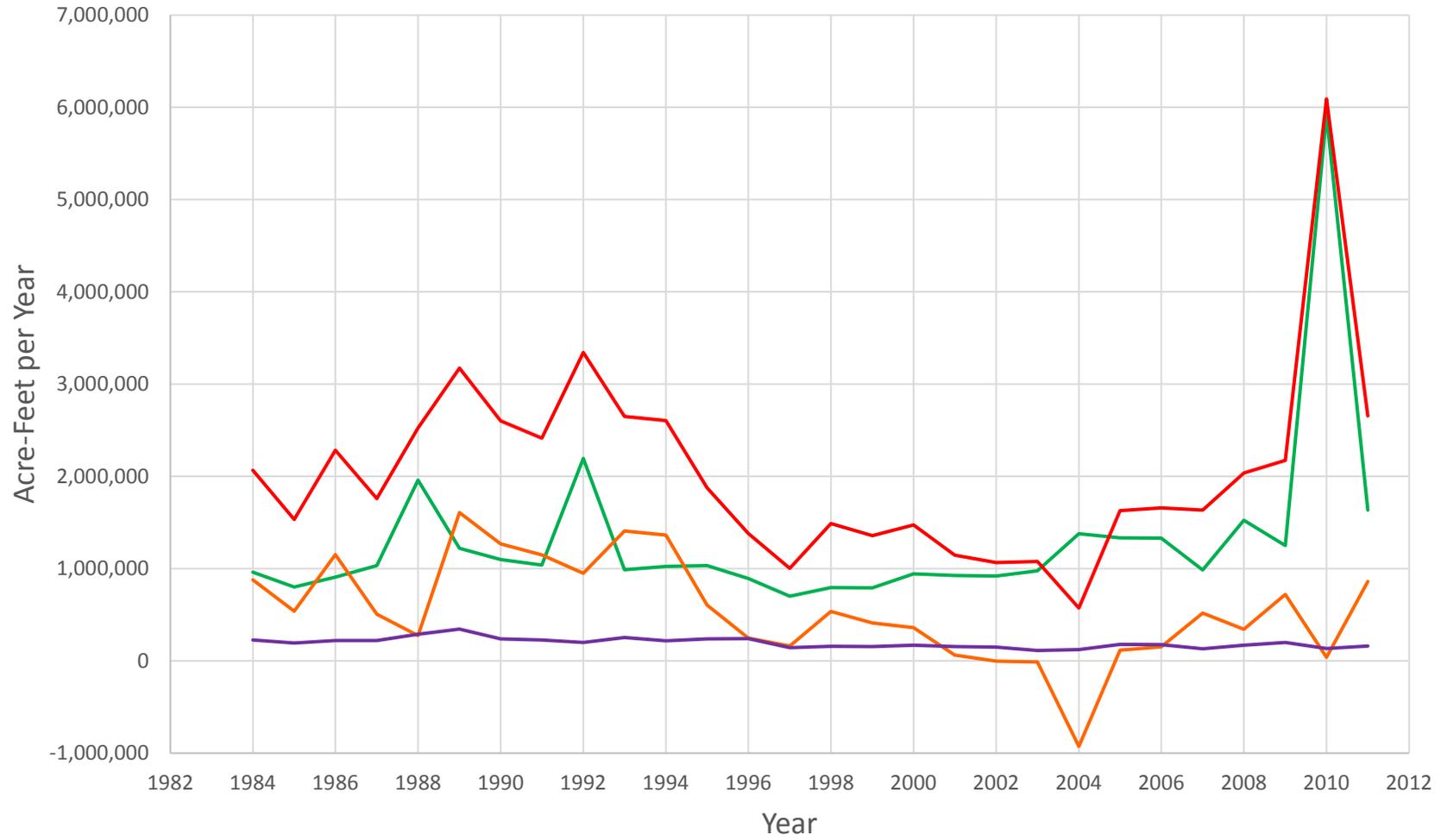
Measured Flow Below Anzalduas Dam   Estimated Rio Grande Inflow
Estimated Groundwater Interaction   Estimated Sum Canals 1 through 4

Y-axis: Acre-feet per Year

X-axis: Year
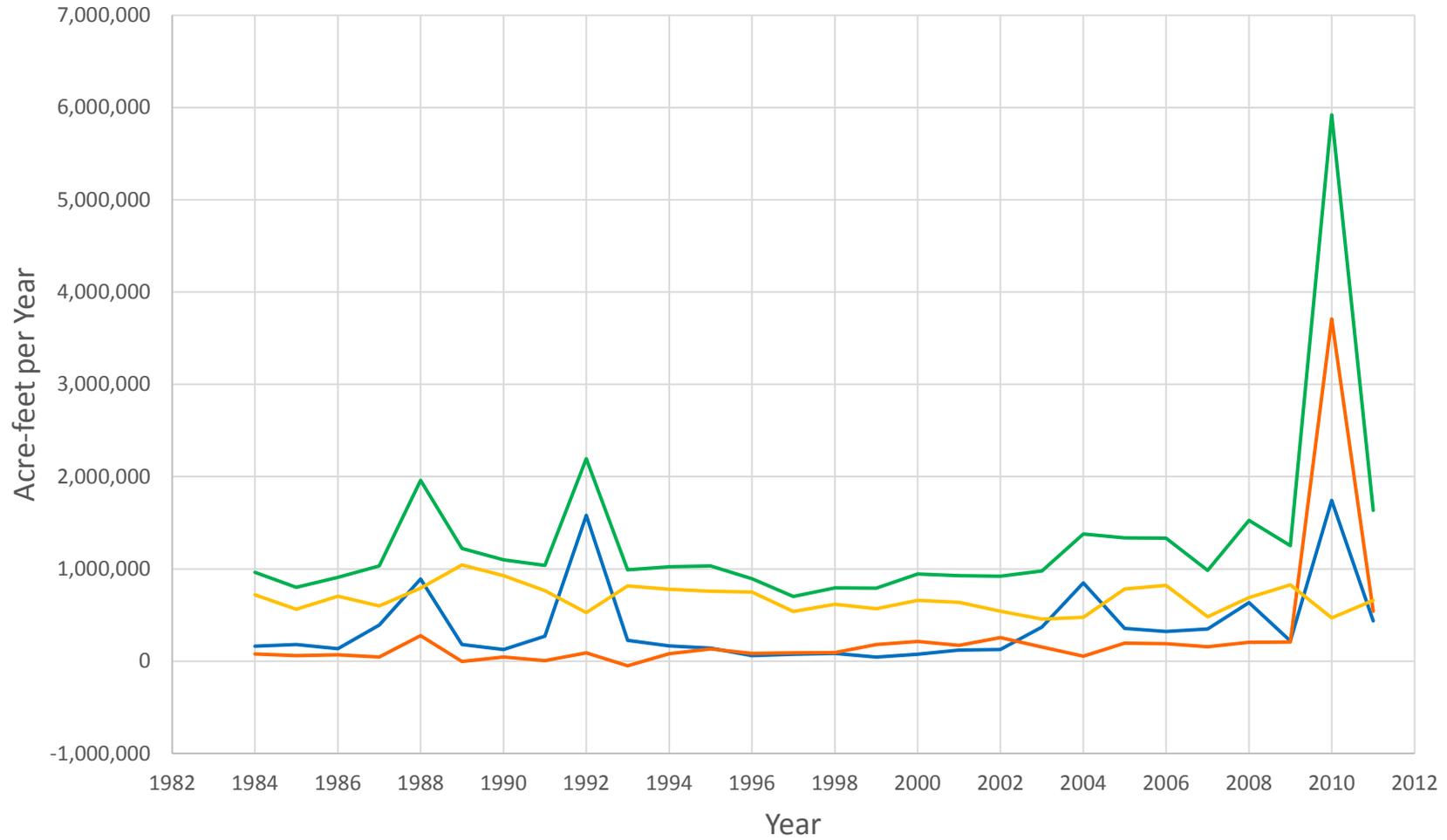
Legend:
- Measured Flow Below Anzalduas Dam
- Measured Flow Near Brownsville
- Estimated Groundwater Interaction
- Estimated Sum Canals 5 through 15

MEASURED AND SIMULATED WATER LEVEL HYDROGRAPHS FOR SELECT WELLS FOR SENSITIVITY TO STORAGE PARAMETERS
Lower Rio Grande Valley

FIGURE 5.1.1-A

MEASURED AND SIMULATED WATER LEVEL HYDROGRAPHS FOR SELECT WELLS FOR SENSITIVITY TO STORAGE PARAMETERS
Lower Rio Grande Valley

FIGURE 5.1.1-B

MEASURED AND SIMULATED WATER LEVEL HYDROGRAPHS FOR SELECT WELLS FOR SENSITIVITY TO STORAGE PARAMETERS
Lower Rio Grande Valley

FIGURE 5.1.1-C

MEASURED AND SIMULATED WATER LEVEL HYDROGRAPHS FOR SELECT WELLS FOR SENSITIVITY TO STORAGE PARAMETERS
Lower Rio Grande Valley

FIGURE 5.1.1-D

SENSITIVITY OF MEAN HEAD ERROR TO THE
HYDRAULIC CONDUCTIVITY VALUE OF SAND
FOR THE VARIOUS GEOLOGIC UNITS

Lower Rio Grande Valley

GSI Job No.	4276	Drawn By:	CSS
Issued:	21-Jun-2017	Chk'd By:	KER
Revised:		Aprv'd By:	SP
Figure No.	5.2.1		

Legend:
- Beaumont [Layer 1]
- Lizzie [Layer 2]
- Willis [Layer 3]
- Upper Goliad [Layer 4]
- Lower Goliad [Layer 5]
- Upper Lagarto [Layer 6]
- Middle Lagarto [Layer 7]
- Lower Lagarto [Layer 8]
- Oakville [Layer 9]
- (upper) Catahoula [Layer 10]
- Catahoula Confining System [Layer 11]
- Yegua-Jackson Aquifer [Layer 12]

Y-axis: Root Mean Squared Head Error (feet)
X-axis: Multiplying Factor

GSI Job No.	4276	Drawn By:	CSS
Issued:	21-Jun-2017	Chk'd By:	KER
Revised:		Aprv'd By:	SP
Figure No.	5.2.2		

SENSITIVITY OF RMS HEAD ERROR TO THE HYDRAULIC CONDUCTIVITY VALUE OF SAND FOR THE VARIOUS GEOLOGIC UNITS

Lower Rio Grande Valley

GSI ENVIRONMENTAL

	12	
Mean Head Error (feet)	11	
	10	

Legend:
- Beaumont [Layer 1]
- Lizzie [Layer 2]
- Willis [Layer 3]
- Upper Goliad [Layer 4]
- Lower Goliad [Layer 5]
- Upper Lagarto [Layer 6]
- Middle Lagarto [Layer 7]
- Lower Lagarto [Layer 8]
- Oakville [Layer 9]
- (upper) Catahoula [Layer 10]
- Catahoula Confining System [Layer 11]
- Yegua-Jackson Aquifer [Layer 12]

X-axis: Multiplying Factor
Y-axis: Mean Head Error (feet)

SENSITIVITY OF MEAN HEAD ERROR TO THE HYDRAULIC CONDUCTIVITY VALUE OF CLAY FOR THE VARIOUS GEOLOGIC UNITS
Lower Rio Grande Valley

GSI ENVIRONMENTAL

SENSITIVITY OF RMS HEAD ERROR TO THE
HYDRAULIC CONDUCTIVITY VALUE OF CLAY
FOR THE VARIOUS GEOLOGIC UNITS
Lower Rio Grande Valley

GSI Job No.	4276	Drawn By:	CSS
Issued:	21-Jun-2017	Chk'd By:	KER
Revised:		Aprv'd By:	SP
Figure No.	5.2.4		

MEAN ERROR SENSITIVITY GRAPH

Lower Rio Grande Valley

Axis labels:
- Y-axis: Root Mean Squared Head Error (feet)
- X-axis: Multiplying Factor

Legend:
- Recharge
- ET Max
- Groundwater pumping
- Return Flow Fraction

GSI ENVIRONMENTAL

ROOT MEAN SQUARED HEAD ERROR SENSITIVITY GRAPH

Lower Rio Grande Valley

Map Labels

Counties: Webb, Duval, Jim Wells, Kleberg, Jim Hogg, Brooks, Zapata, Kenedy, Starr, Hidalgo, Willacy, Cameron

Other labels: UNITED STATES, MEXICO, Rio Grande

LEGEND

——	Contour (Feet)
——	Rio Grande
⬚	Texas County
▪	Model Boundary

Notes:

1) Basemap provided by Montgomery & Associates December 2016.
2) Contours show the change in simulated groundwater elevation between the calibrated model and fault sensitivity model.
3) Contours indicate simulated water levels with faults minus simulated water levels without faults.

Scale in Miles

Projected Coordinate System Datum: NAD 1983 Albers Equal Area

0   10   20

GSI
ENVIRONMENTAL

IMPACT OF HFBs IN MODEL LAYER 12 (YEGUA-JACKSON AQUIFER)

Lower Rio Grande Valley

GSI Job No. 4276	Drawn By: AV
Issued: 23-Jun-2017	Chk'd By: KER
Map ID: LRGV_HFB_L12	Appv'd By: SP

FIGURE 5.4.2

Sources: Esri, USGS, NOAA

LEGEND

— Contour (Feet)
— Rio Grande
Texas County
Model Boundary

Notes:
1) Basemap provided by Montgomery & Associates December 2016.
2) Contours show the change in simulated groundwater elevation between the calibrated model and fault sensitivity model.
3) Contours indicate simulated water levels with faults minus simulated water levels without faults.

Scale in Miles

0   10   20

Projected Coordinate System
Datum: NAD 1983
Albers Equal Area

GSI ENVIRONMENTAL

IMPACT OF HFBs IN MODEL LAYER 6 (UPPER LAGARTO FORMATION OF EVANGELINE AQUIFER)
Lower Rio Grande Valley

GSI Job No. 4276	Drawn By: AV
Issued: 23-Jun-2017	Chk'd By: KER
Map ID: LRGV_HFB_L6	Appv'd By: SP

FIGURE 5.4.3

Sources: Esri, USGS, NOAA

Beaumont Formation (Model Layer 1)

Sources: Esri, USGS, NOAA

Lissie Formation (Model Layer 2)

Sources: Esri, USGS, NOAA

Willis Formation (Model Layer 3)

Sources: Esri, USGS, NOAA

LEGEND

Estimated Initial TDS Concentration (mg/L)

- 0 - 1,000 (freshwater)
- 1,000 - 3,000 (slightly saline)
- 3,000 - 10,000 (moderately saline)
- 10,000 - 35,000 (very saline)
- \>35,000 (brine)
- Layer Pinchout
- Rio Grande
- Texas County
- Model Boundary

Notes:

1) Basemap provided by Montgomery & Associates December 2016.
2) TDS = Total Dissolved Solids.
3) mg/L = milligrams per liter.

Scale in Miles

0   20   40

Projected Coordinate System
Datum: NAD 1983
Albers Equal Area

GSI ENVIRONMENTAL

ESTIMATED TDS DISTRIBUTION FOR CHICOT AQUIFER (MODEL LAYERS 1, 2, 3)
Lower Rio Grande Valley

GSI Job No. 4276	Drawn By: GM
Issued: 23-Jun-2017	Chk'd By: KER
Map ID: LRGV_TDS_CA_L123	Appv'd By: SP

FIGURE 6.1.1
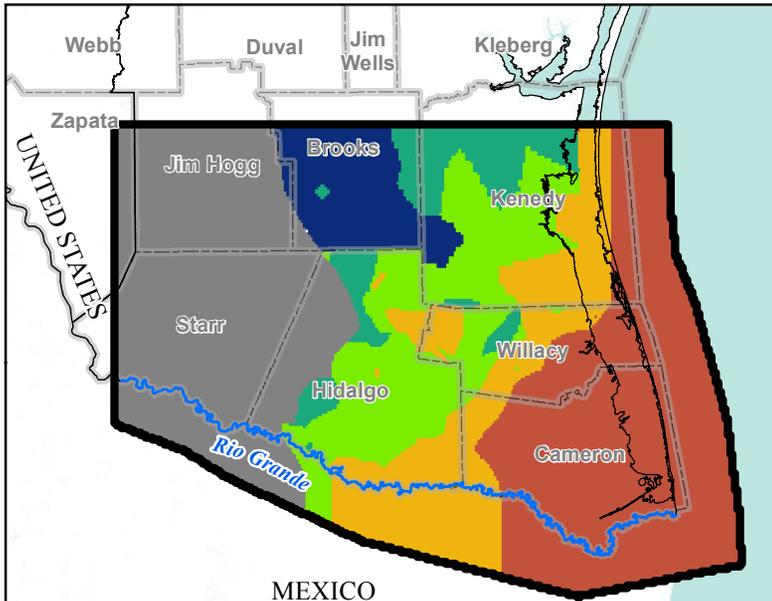
Upper Goliad Formation (Model Layer 4)
Sources: Esri, USGS, NOAA
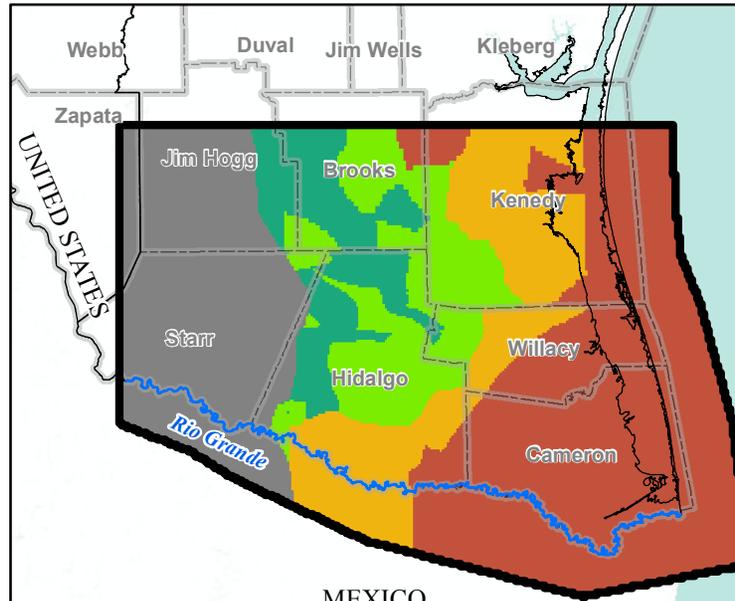
Lower Goliad Formation (Model Layer 5)
Sources: Esri, USGS, NOAA
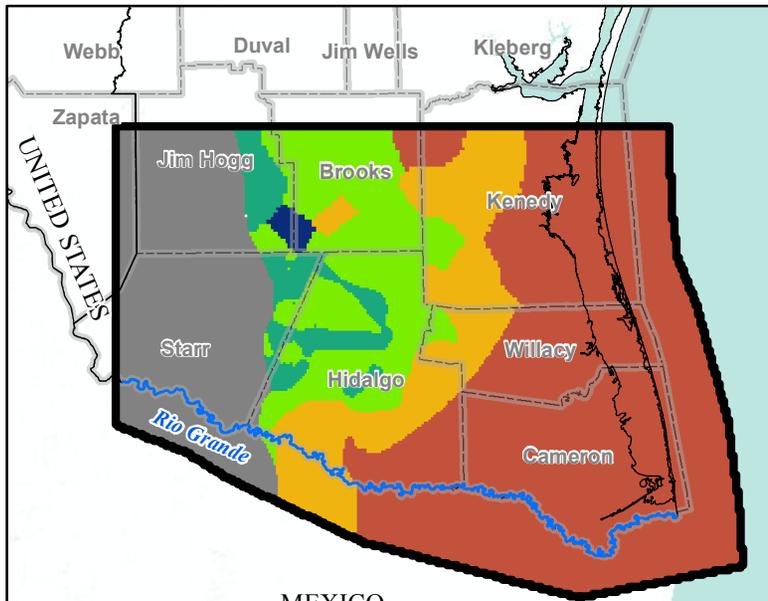
Upper Lagarto Formation (Model Layer 6)
Sources: Esri, USGS, NOAA

LEGEND

Estimated Initial TDS Concentration (mg/L)

- 0 - 1,000 (freshwater)
- 1,000 - 3,000 (slightly saline)
- 3,000 - 10,000 (moderately saline)
- 10,000 - 35,000 (very saline)
- >35,000 (brine)
- Layer Pinchout
- Rio Grande River
- Texas County
- Model Boundary

Notes:

1) Basemap provided by Montgomery & Associates December 2016.
2) TDS = Total Dissolved Solids.
3) mg/L = milligrams per liter.

Scale in Miles
0   20   40

Projected Coordinate System
Datum: NAD 1983
Albers Equal Area

GSI ENVIRONMENTAL
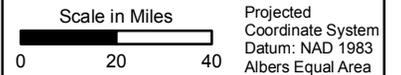
ESTIMATED TDS DISTRIBUTION FOR EVANGELINE AQUIFER (MODEL LAYERS 4, 5, 6)
Lower Rio Grande Valley

GSI Job No. 4276	Drawn By: GM
Issued: 23-Jun-2017	Chk'd By: KER
Map ID: LRGV_TDS_EA_L456	Appv'd By: SP

FIGURE 6.1.2
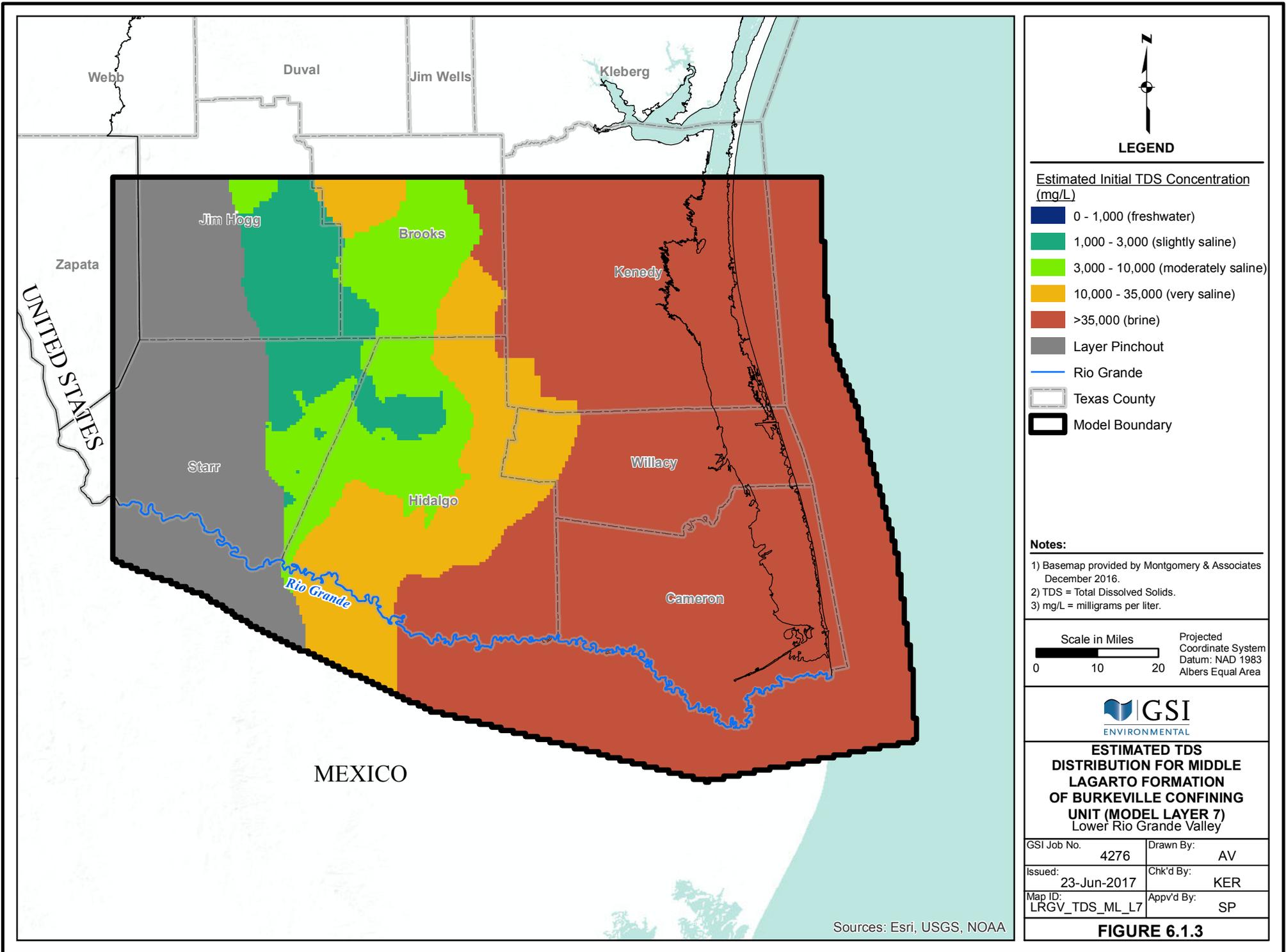
LEGEND

Estimated Initial TDS Concentration (mg/L)

- ■ 0 - 1,000 (freshwater)
- ■ 1,000 - 3,000 (slightly saline)
- ■ 3,000 - 10,000 (moderately saline)
- ■ 10,000 - 35,000 (very saline)
- ■ >35,000 (brine)
- ■ Layer Pinchout
- — Rio Grande
- ☐ Texas County
- ▢ Model Boundary

Notes:

1) Basemap provided by Montgomery & Associates December 2016.
2) TDS = Total Dissolved Solids.
3) mg/L = milligrams per liter.

Scale in Miles
0   10   20

Projected Coordinate System Datum: NAD 1983 Albers Equal Area

GSI ENVIRONMENTAL

ESTIMATED TDS DISTRIBUTION FOR MIDDLE LAGARTO FORMATION OF BURKEVILLE CONFINING UNIT (MODEL LAYER 7)
Lower Rio Grande Valley

GSI Job No. 4276	Drawn By: AV
Issued: 23-Jun-2017	Chk'd By: KER
Map ID: LRGV_TDS_ML_L7	Appv'd By: SP

FIGURE 6.1.3

Sources: Esri, USGS, NOAA
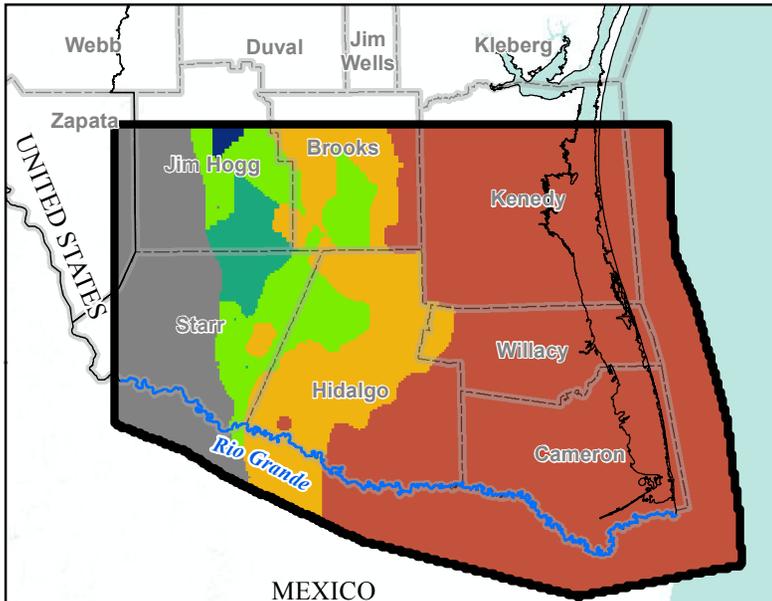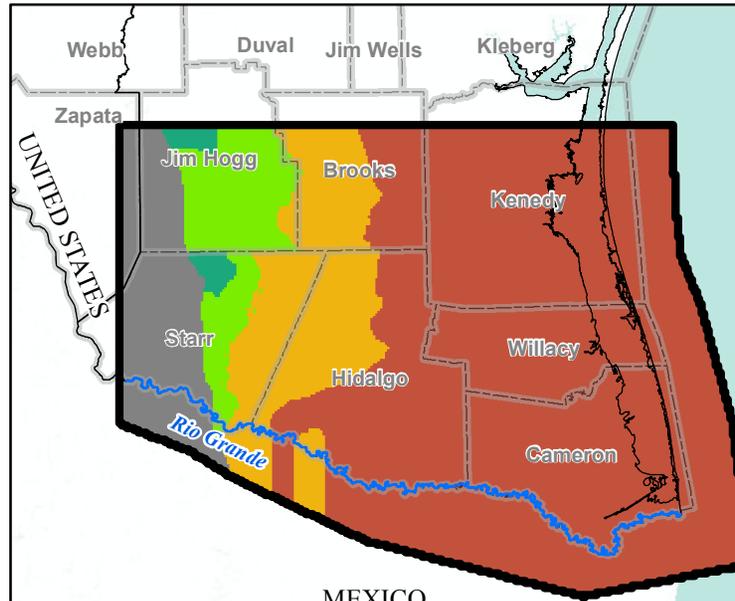
**Lower Lagarto Formation
(Model Layer 8)**

Sources: Esri, USGS, NOAA

**Oakville Formation
(Model Layer 9)**

Sources: Esri, USGS, NOAA

**Upper Catahoula Formation
(Model Layer 10)**

Sources: Esri, USGS, NOAA

LEGEND

Estimated Initial TDS Concentration
(mg/L)

- 0 - 1,000 (freshwater)
- 1,000 - 3,000 (slightly saline)
- 3,000 - 10,000 (moderately saline)
- 10,000 - 35,000 (very saline)
- >35,000 (brine)
- Layer Pinchout
- Rio Grande
- Texas County
- Model Boundary

Notes:

1) Basemap provided by Montgomery & Associates December 2016.
2) TDS = Total Dissolved Solids.
3) mg/L = milligrams per liter.

Scale in Miles

0   20   40

Projected
Coordinate System
Datum: NAD 1983
Albers Equal Area

GSI ENVIRONMENTAL
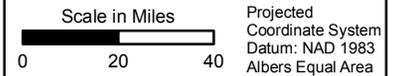
**ESTIMATED TDS
DISTRIBUTION FOR
JASPER AQUIFER
(MODEL LAYERS 8, 9, 10)**
Lower Rio Grande Valley

GSI Job No. 4276	Drawn By: GM
Issued: 23-Jun-2017	Chk'd By: KER
Map ID: LRGV_TDS_JA_L8910	Appv'd By: SP

FIGURE 6.1.4
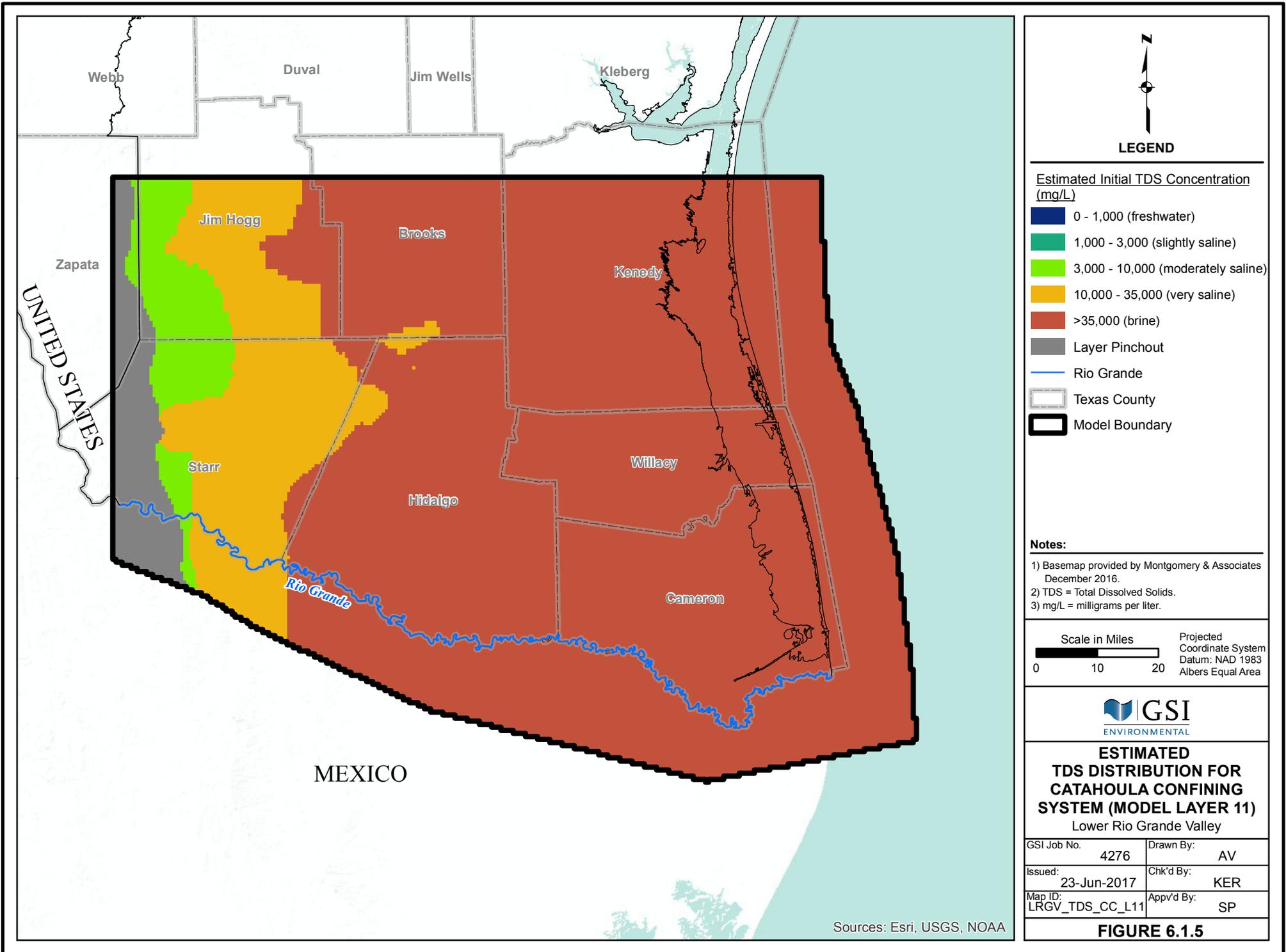
LEGEND

Estimated Initial TDS Concentration (mg/L)

- 0 - 1,000 (freshwater)
- 1,000 - 3,000 (slightly saline)
- 3,000 - 10,000 (moderately saline)
- 10,000 - 35,000 (very saline)
- >35,000 (brine)
- Layer Pinchout
- Rio Grande
- Texas County
- Model Boundary

Notes:

1) Basemap provided by Montgomery & Associates December 2016.
2) TDS = Total Dissolved Solids.
3) mg/L = milligrams per liter.

Scale in Miles

0   10   20

Projected Coordinate System Datum: NAD 1983 Albers Equal Area

GSI ENVIRONMENTAL

ESTIMATED TDS DISTRIBUTION FOR CATAHOULA CONFINING SYSTEM (MODEL LAYER 11)

Lower Rio Grande Valley

GSI Job No. 4276	Drawn By: AV
Issued: 23-Jun-2017	Chk'd By: KER
Map ID: LRGV_TDS_CC_L11	Appv'd By: SP

FIGURE 6.1.5
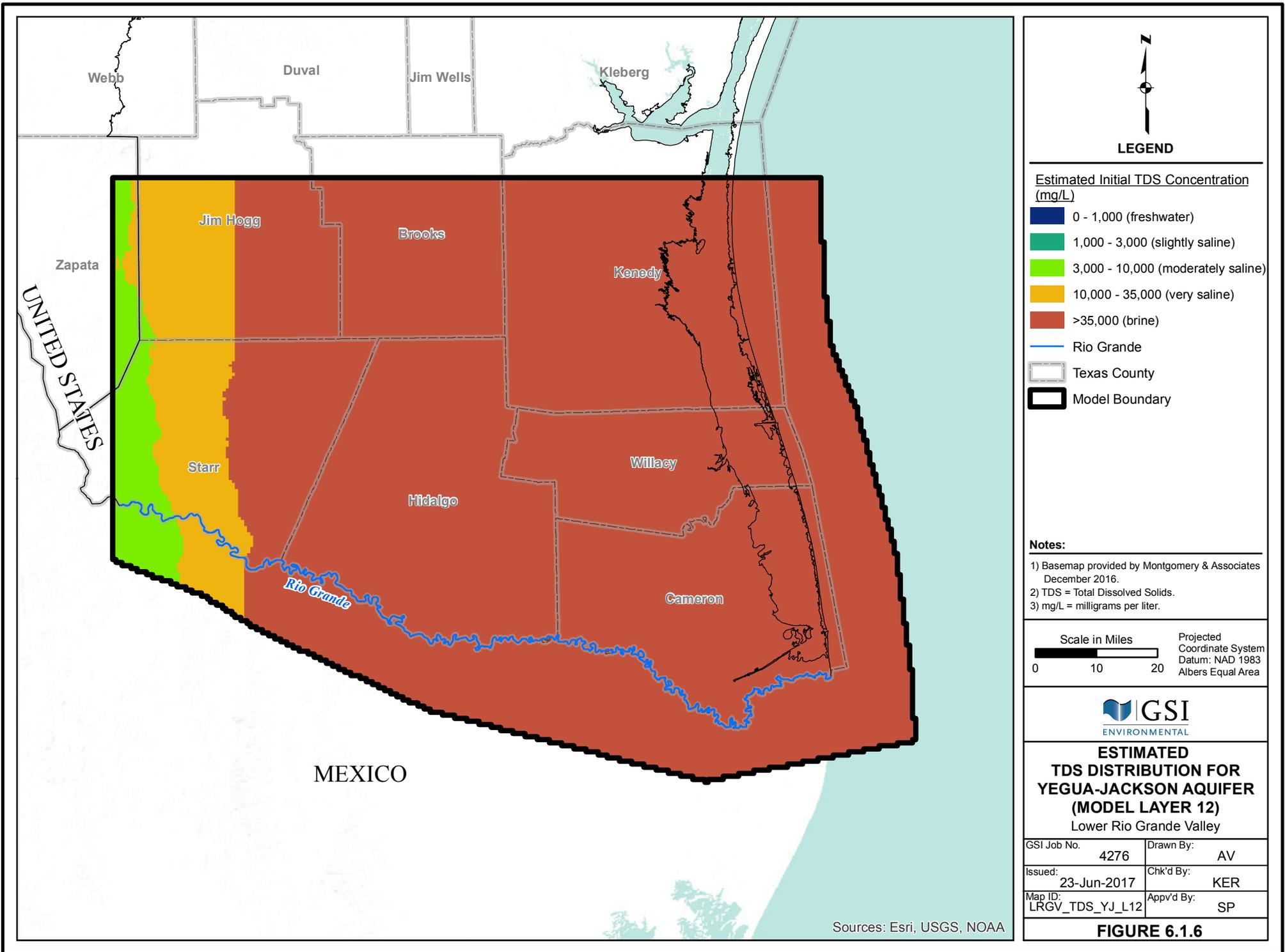
LEGEND

Estimated Initial TDS Concentration (mg/L)

- ■ 0 - 1,000 (freshwater)
- ■ 1,000 - 3,000 (slightly saline)
- ■ 3,000 - 10,000 (moderately saline)
- ■ 10,000 - 35,000 (very saline)
- ■ >35,000 (brine)
- — Rio Grande
- ▢ Texas County
- ▢ Model Boundary

Notes:

1) Basemap provided by Montgomery & Associates December 2016.
2) TDS = Total Dissolved Solids.
3) mg/L = milligrams per liter.

Scale in Miles
0   10   20

Projected Coordinate System Datum: NAD 1983 Albers Equal Area

GSI ENVIRONMENTAL

ESTIMATED TDS DISTRIBUTION FOR YEGUA-JACKSON AQUIFER (MODEL LAYER 12)
Lower Rio Grande Valley

GSI Job No. 4276	Drawn By: AV
Issued: 23-Jun-2017	Chk'd By: KER
Map ID: LRGV_TDS_YJ_L12	Appv'd By: SP

FIGURE 6.1.6

Sources: Esri, USGS, NOAA

County labels on map: Webb, Duval, Jim Wells, Kleberg, Zapata, Jim Hogg, Brooks, Kenedy, Starr, Hidalgo, Willacy, Cameron

UNITED STATES
MEXICO
Rio Grande

LEGEND

Texas County

Model Boundary

Estimated Effective Porosity

- ≤ 0.01
- 0.01 - 0.05
- 0.05 - 0.1
- 0.1 - 0.15
- 0.15 - 0.2
- 0.2 - 0.25
- 0.25 - 0.3
- Layer Pinchout

Note:

Basemap provided by Montgomery & Associates December 2016.

Scale in Miles

0   10   20

Projected Coordinate System Datum: NAD 1983 Albers Equal Area

GSI ENVIRONMENTAL

EFFECTIVE POROSITY DISTRIBUTION IN MODEL LAYER 1 (BEAUMONT FORMATION OF CHICOT AQUIFER)

Lower Rio Grande Valley

GSI Job No. 4276	Drawn By: AV
Issued: 21-Jun-2017	Chk'd By: KER
Map ID: LRGV_EPD_L1	Appv'd By: SP

FIGURE 6.3.1

Sources: Esri, USGS, NOAA

LEGEND

▢	Texas County
▢	Model Boundary

Estimated Effective Porosity

■ (blue)	≤ 0.01
■ (medium blue)	0.01 - 0.05
■ (cyan)	0.05 - 0.1
■ (green)	0.1 - 0.15
■ (yellow)	0.15 - 0.2
■ (orange)	0.2 - 0.25
■ (red)	0.25 - 0.3
■ (gray)	Layer Pinchout

Note:

Basemap provided by Montgomery & Associates December 2016.

Scale in Miles

0   10   20

Projected Coordinate System Datum: NAD 1983 Albers Equal Area

GSI ENVIRONMENTAL

EFFECTIVE POROSITY DISTRIBUTION IN MODEL LAYER 2 (LISSIE FORMATION OF CHICOT AQUIFER)
Lower Rio Grande Valley

GSI Job No. 4276	Drawn By: AV
Issued: 21-Jun-2017	Chk'd By: KER
Map ID: LRGV_EPD_L2	Appv'd By: SP

FIGURE 6.3.2

Sources: Esri, USGS, NOAA

LEGEND

| | Texas County |
| | Model Boundary |

Estimated Effective Porosity

Color	Value
	≤ 0.01
	0.01 - 0.05
	0.05 - 0.1
	0.1 - 0.15
	0.15 - 0.2
	0.2 - 0.25
	0.25 - 0.3
	Layer Pinchout

Note:

Basemap provided by Montgomery & Associates December 2016.

Scale in Miles

0   10   20

Projected Coordinate System
Datum: NAD 1983
Albers Equal Area

GSI
ENVIRONMENTAL
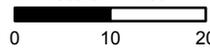
EFFECTIVE POROSITY DISTRIBUTION IN MODEL LAYER 3 (WILLIS FORMATION OF CHICOT AQUIFER)
Lower Rio Grande Valley

GSI Job No. 4276	Drawn By: AV
Issued: 21-Jun-2017	Chk'd By: KER
Map ID: LRGV_EPD_L3	Appv'd By: SP

FIGURE 6.3.3

LEGEND

▢	Texas County
▢	Model Boundary

Estimated Effective Porosity

■ (blue)	≤ 0.01
■ (light blue)	0.01 - 0.05
■ (cyan)	0.05 - 0.1
■ (light green)	0.1 - 0.15
■ (yellow)	0.15 - 0.2
■ (orange)	0.2 - 0.25
■ (red)	0.25 - 0.3
■ (gray)	Layer Pinchout

Note:

Basemap provided by Montgomery & Associates December 2016.

Scale in Miles
0   10   20

Projected Coordinate System Datum: NAD 1983 Albers Equal Area

GSI ENVIRONMENTAL

EFFECTIVE POROSITY DISTRIBUTION IN MODEL LAYER 4 (UPPER GOLIAD FORMATION OF EVANGELINE AQUIFER)

Lower Rio Grande Valley

GSI Job No. 4276	Drawn By: AV
Issued: 21-Jun-2017	Chk'd By: KER
Map ID: LRGV_EPD_L4	Appv'd By: SP

FIGURE 6.3.4

Sources: Esri, USGS, NOAA

LEGEND

☐	Texas County
☐	Model Boundary

Estimated Effective Porosity

🟦	≤ 0.01
🟦	0.01 - 0.05
🟦	0.05 - 0.1
🟩	0.1 - 0.15
🟨	0.15 - 0.2
🟧	0.2 - 0.25
🟥	0.25 - 0.3
⬛	Layer Pinchout

Note:

Basemap provided by Montgomery & Associates December 2016.

Scale in Miles

0   10   20

Projected Coordinate System Datum: NAD 1983 Albers Equal Area

GSI ENVIRONMENTAL

EFFECTIVE POROSITY DISTRIBUTION IN MODEL LAYER 5 (LOWER GOLIAD FORMATION OF EVANGELINE AQUIFER)

Lower Rio Grande Valley

GSI Job No. 4276	Drawn By: AV
Issued: 21-Jun-2017	Chk'd By: KER
Map ID: LRGV_EPD_L5	Appv'd By: SP

FIGURE 6.3.5

Sources: Esri, USGS, NOAA

LEGEND

Texas County

Model Boundary

Estimated Effective Porosity

- ≤ 0.01
- 0.01 - 0.05
- 0.05 - 0.1
- 0.1 - 0.15
- 0.15 - 0.2
- 0.2 - 0.25
- 0.25 - 0.3
- Layer Pinchout

Note:

Basemap provided by Montgomery & Associates December 2016.

Scale in Miles

0   10   20

Projected Coordinate System Datum: NAD 1983 Albers Equal Area

GSI
ENVIRONMENTAL

EFFECTIVE POROSITY DISTRIBUTION IN MODEL LAYER 6 UPPER LAGARTO FORMATION OF EVANGELINE AQUIFER

Lower Rio Grande Valley

GSI Job No. 4276	Drawn By: AV
Issued: 21-Jun-2017	Chk'd By: KER
Map ID: LRGV_EPD_L6	Appv'd By: SP

FIGURE 6.3.6

Sources: Esri, USGS, NOAA

N

LEGEND

☐ Texas County

■ Model Boundary

Estimated Effective Porosity

■ ≤ 0.01

■ 0.01 - 0.05

■ 0.05 - 0.1

■ 0.1 - 0.15

■ 0.15 - 0.2

■ 0.2 - 0.25

■ 0.25 - 0.3

■ Layer Pinchout

Note:

Basemap provided by Montgomery & Associates December 2016.

Scale in Miles

0   10   20

Projected Coordinate System Datum: NAD 1983 Albers Equal Area

GSI ENVIRONMENTAL

EFFECTIVE POROSITY DISTRIBUTION IN MODEL LAYER 7 (MIDDLE LAGARTO FORMATION OF BURKEVILLE CONFINING UNIT)

Lower Rio Grande Valley

GSI Job No. 4276	Drawn By: AV
Issued: 21-Jun-2017	Chk'd By: KER
Map ID: LRGV_EPD_L7	Appv'd By: SP

FIGURE 6.3.7

Sources: Esri, USGS, NOAA

LEGEND

☐	Texas County
▢	Model Boundary

Estimated Effective Porosity

■ (blue)	≤ 0.01
■ (blue)	0.01 - 0.05
■ (cyan)	0.05 - 0.1
■ (light green)	0.1 - 0.15
■ (yellow)	0.15 - 0.2
■ (orange)	0.2 - 0.25
■ (red)	0.25 - 0.3
■ (gray)	Layer Pinchout

Note:

Basemap provided by Montgomery & Associates December 2016.

Scale in Miles
0   10   20

Projected Coordinate System
Datum: NAD 1983
Albers Equal Area

GSI ENVIRONMENTAL

EFFECTIVE POROSITY DISTRIBUTION IN MODEL LAYER 8 (LOWER LAGARTO FORMATION OF JASPER AQUIFER)

Lower Rio Grande Valley

GSI Job No. 4276	Drawn By: AV
Issued: 21-Jun-2017	Chk'd By: KER
Map ID: LRGV_EPD_L8	Appv'd By: SP

FIGURE 6.3.8

Sources: Esri, USGS, NOAA

LEGEND

☐	Texas County
☐	Model Boundary

Estimated Effective Porosity

■	≤ 0.01
■	0.01 - 0.05
■	0.05 - 0.1
■	0.1 - 0.15
■	0.15 - 0.2
■	0.2 - 0.25
■	0.25 - 0.3
■	Layer Pinchout

Note:

Basemap provided by Montgomery & Associates December 2016.

Scale in Miles
0   10   20

Projected Coordinate System
Datum: NAD 1983
Albers Equal Area

GSI ENVIRONMENTAL

EFFECTIVE POROSITY DISTRIBUTION IN MODEL LAYER 9 (OAKVILLE FORMATION OF JASPER AQUIFER)

Lower Rio Grande Valley

GSI Job No. 4276	Drawn By: AV
Issued: 21-Jun-2017	Chk'd By: KER
Map ID: LRGV_EPD_L9	Appv'd By: SP

FIGURE 6.3.9

Sources: Esri, USGS, NOAA

Beaumont Formation (Chicot Aquifer)

Lissie Formation (Chicot Aquifer)

Willis Formation (Chicot Aquifer)

Sources: Esri, USGS, NOAA

LEGEND

Simulated TDS Concentration (mg/L)

- 0 - 1,000 (freshwater)
- 1,000 - 3,000 (slightly saline)
- 3,000 - 10,000 (moderately saline)
- 10,000 - 35,000 (very saline)
- >35,0000 (brine)
- Layer Pinchout
- Rio Grande
- Texas County
- Model Boundary

Notes:

1) Basemap provided by Montgomery & Associates December 2016.
2) TDS = Total Dissolved Solids.
3) mg/L = milligrams per liter.

Scale in Miles

0   20   40

Projected Coordinate System Datum: NAD 1983 Albers Equal Area

GSI ENVIRONMENTAL

SIMULATED TDS CONCENTRATIONS IN CHICOT AQUIFER (MODEL LAYERS 1, 2, 3) FOR 2013

Lower Rio Grande Valley

GSI Job No. 4276	Drawn By: AV
Issued: 21-Jun-2017	Chk'd By: KER
Map ID: LRGV_STDS_L123	Appv'd By: SP

FIGURE 6.6.1

**Upper Goliad Formation
(Evangeline Aquifer)**

Sources: Esri, USGS, NOAA

**Lower Goliad Formation
(Evangeline Aquifer)**

Sources: Esri, USGS, NOAA

**Upper Lagarto Formation
(Evangeline Aquifer)**

Sources: Esri, USGS, NOAA

LEGEND

Simulated TDS Concentration (mg/L)

- 0 - 1,000 (freshwater)
- 1,000 - 3,000 (slightly saline)
- 3,000 - 10,000 (moderately saline)
- 10,000 - 35,000 (very saline)
- >35,0000 (brine)
- Layer Pinchout
- Rio Grande
- Texas County
- Model Boundary

Notes:

1) Basemap provided by Montgomery & Associates December 2016.
2) TDS = Total Dissolved Solids.
3) mg/L = milligrams per liter.

Scale in Miles

0   20   40

Projected
Coordinate System
Datum: NAD 1983
Albers Equal Area

GSI ENVIRONMENTAL

**SIMULATED TDS
CONCENTRATIONS IN
EVANGELINE AQUIFER (MODEL)
LAYERS 4, 5, 6) FOR 2013**

Lower Rio Grande Valley

GSI Job No. 4276	Drawn By: AV
Issued: 21-Jun-2017	Chk'd By: KER
Map ID: LRGV_STDS_L456	Appv'd By: SP

FIGURE 6.6.2

LEGEND

Simulated TDS Concentration (mg/L)
- 0 - 1,000 (freshwater)
- 1,000 - 3,000 (slightly saline)
- 3,000 - 10,000 (moderately saline)
- 10,000 - 35,000 (very saline)
- >35,0000 (brine)
- Layer Pinchout
- Rio Grande
- Texas County
- Model Boundary

Notes:

1) Basemap provided by Montgomery & Associates December 2016.
2) TDS = Total Dissolved Solids.
3) mg/L = milligrams per liter.

Scale in Miles

0   10   20

Projected
Coordinate System
Datum: NAD 1983
Albers Equal Area

GSI
ENVIRONMENTAL

**SIMULATED TDS
CONCENTRATIONS IN MIDDLE
LAGARTO FORMATION OF
BURKEVILLE CONFINING UNIT
(MODEL LAYER 7) FOR 2013**
Lower Rio Grande Valley

GSI Job No. 4276	Drawn By: AV
Issued: 21-Jun-2017	Chk'd By: KER
Map ID: LRGV_STDS_L7	Appv'd By: SP

FIGURE 6.6.3

Sources: Esri, USGS, NOAA

Lower Lagarto Formation
(Jasper Aquifer)

Sources: Esri, USGS, NOAA

Oakville Formation
(Jasper Aquifer)

Sources: Esri, USGS, NOAA

Upper Catahoula Formation
(Jasper Aquifer)

Sources: Esri, USGS, NOAA

LEGEND

Simulated TDS Concentration (mg/L)

- 0 - 1,000 (freshwater)
- 1,000 - 3,000 (slightly saline)
- 3,000 - 10,000 (moderately saline)
- 10,000 - 35,000 (very saline)
- >35,0000 (brine)
- Layer Pinchout
- Rio Grande
- Texas County
- Model Boundary

Notes:

1) Basemap provided by Montgomery & Associates December 2016.
2) TDS = Total Dissolved Solids.
3) mg/L = milligrams per liter.

Scale in Miles

0   20   40

Projected
Coordinate System
Datum: NAD 1983
Albers Equal Area

GSI ENVIRONMENTAL

SIMULATED TDS CONCENTRATIONS IN JASPER AQUIFER (MODEL LAYERS 8, 9, 10) FOR 2013

Lower Rio Grande Valley

GSI Job No. 4276	Drawn By: AV
Issued: 21-Jun-2017	Chk'd By: KER
Map ID: LRGV_STDS_L8910	Appv'd By: SP

FIGURE 6.6.4

LEGEND

Simulated TDS Concentration (mg/L)

- 0 - 1,000 (freshwater)
- 1,000 - 3,000 (slightly saline)
- 3,000 - 10,000 (moderately saline)
- 10,000 - 35,000 (very saline)
- >35,0000 (brine)
- Layer Pinchout
- Rio Grande
- Texas County
- Model Boundary

Notes:

1) Basemap provided by Montgomery & Associates December 2016.
2) TDS = Total Dissolved Solids.
3) mg/L = milligrams per liter.

Scale in Miles

0   10   20

Projected
Coordinate System
Datum: NAD 1983
Albers Equal Area

GSI ENVIRONMENTAL

SIMULATED TDS CONCENTRATIONS IN CATAHOULA CONFINING SYSTEM (MODEL LAYER 11) FOR 2013
Lower Rio Grande Valley

GSI Job No. 4276	Drawn By: AV
Issued: 21-Jun-2017	Chk'd By: KER
Map ID: LRGV_STDS_L11	Appv'd By: SP

FIGURE 6.6.5

Sources: Esri, USGS, NOAA

LEGEND

Simulated TDS Concentration (mg/L)

- 0 - 1,000 (freshwater)
- 1,000 - 3,000 (slightly saline)
- 3,000 - 10,000 (moderately saline)
- 10,000 - 35,000 (very saline)
- >35,0000 (brine)
- Rio Grande
- Texas County
- Model Boundary

Notes:

1) Basemap provided by Montgomery & Associates December 2016.
2) TDS = Total Dissolved Solids.
3) mg/L = milligrams per liter.

Scale in Miles

0   10   20

Projected Coordinate System Datum: NAD 1983 Albers Equal Area

GSI ENVIRONMENTAL

SIMULATED TDS CONCENTRATIONS IN YEGUA-JACKSON AQUIFER (MODEL LAYER 12) FOR 2013

Lower Rio Grande Valley

GSI Job No. 4276	Drawn By: AV
Issued: 21-Jun-2017	Chk'd By: KER
Map ID: LRGV_STDS_L12	Appv'd By: SP

FIGURE 6.6.6

Sources: Esri, USGS, NOAA
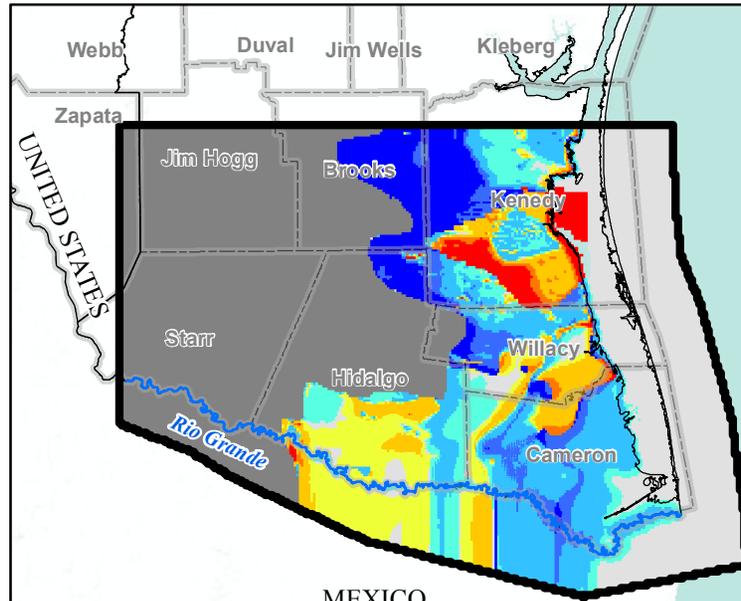
Beaumont Formation (Chicot Aquifer)

Sources: Esri, USGS, NOAA

Lissie Formation (Chicot Aquifer)

Sources: Esri, USGS, NOAA

Willis Formation (Chicot Aquifer)

Sources: Esri, USGS, NOAA

LEGEND

TDS Concentration Difference (mg/L)

- ≤ -10,000
- -10,000 - -5,000
- -5,000 - -1,000
- -1,000 - -100
- -100 - 100
- 100 - 1,000
- 1,000 - 5,000
- 5,000 - 10,000
- ≥ 10,000
- Layer Pinchout
- Rio Grande
- Texas County
- Model Boundary

Notes:

1) Basemap provided by Montgomery & Associates December 2016.
2) TDS = Total Dissolved Solids.
3) mg/L = milligrams per liter.

Scale in Miles

0   20   40

Projected Coordinate System Datum: NAD 1983 Albers Equal Area

GSI ENVIRONMENTAL
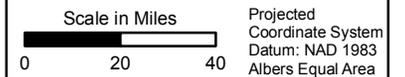
CHANGE IN SIMULATED TDS CONCENTRATIONS IN CHICOT AQUIFER (MODEL LAYERS 1, 2, 3) FROM 1984 TO 2013

Lower Rio Grande Valley

GSI Job No. 4276	Drawn By: AV
Issued: 21-Jun-2017	Chk'd By: KER
Map ID: LRGV_CSTDS_L123	Appv'd By: SP

FIGURE 6.6.7
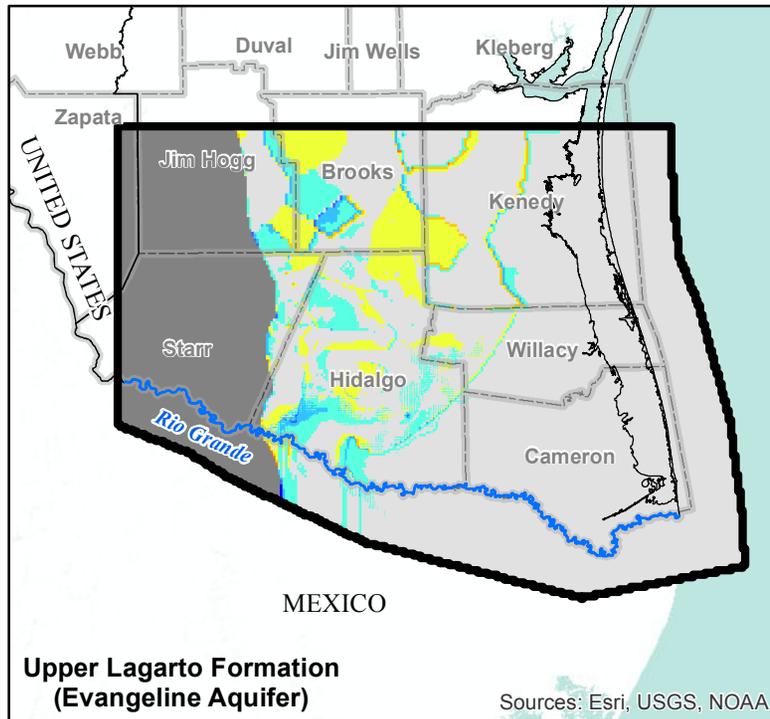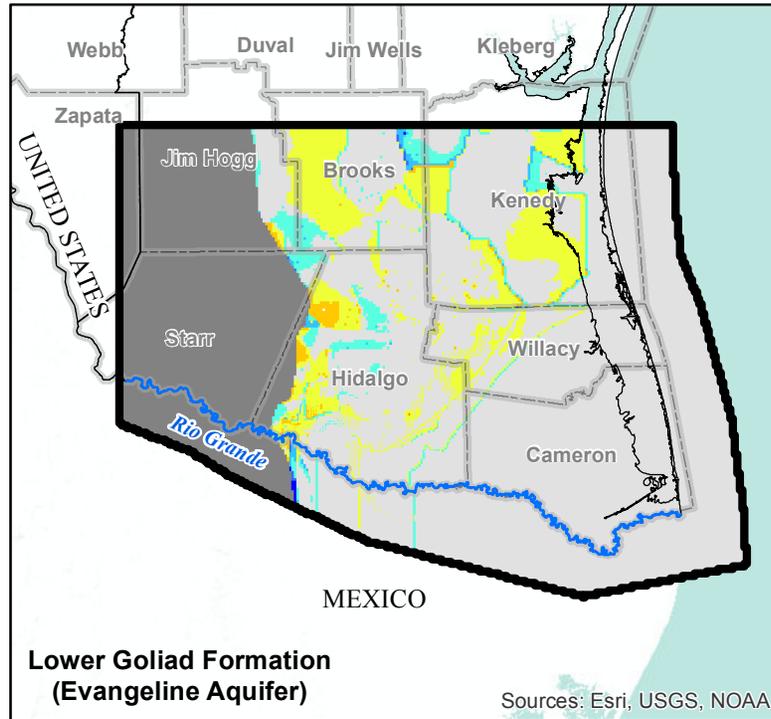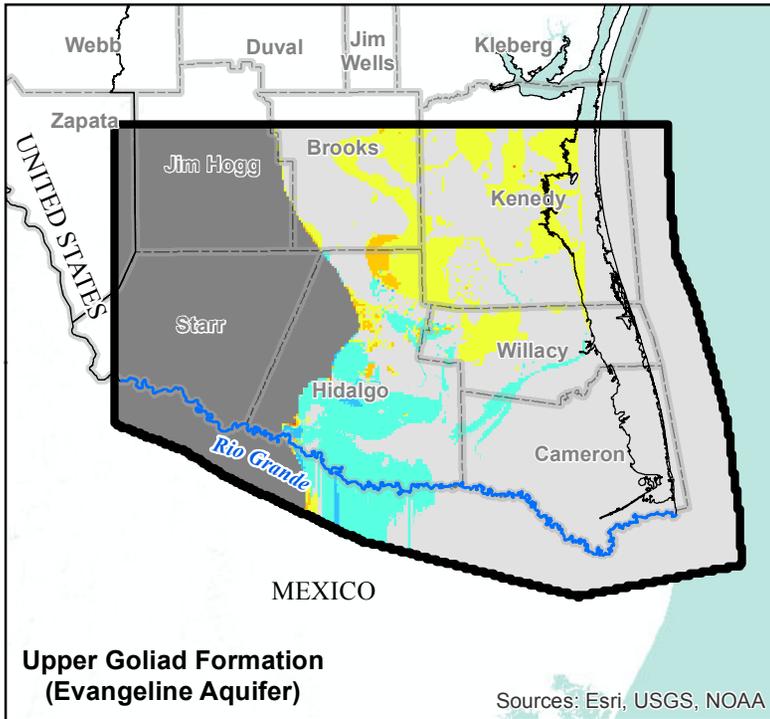
**Upper Goliad Formation
(Evangeline Aquifer)**

Sources: Esri, USGS, NOAA

**Lower Goliad Formation
(Evangeline Aquifer)**

Sources: Esri, USGS, NOAA

**Upper Lagarto Formation
(Evangeline Aquifer)**

Sources: Esri, USGS, NOAA

LEGEND

TDS Concentration Difference (mg/L)

- ≤ -10,000
- -10,000 - -5,000
- -5,000 - -1,000
- -1,000 - -100
- -100 - 100
- 100 - 1,000
- 1,000 - 5,000
- 5,000 - 10,000
- ≥ 10,000
- Layer Pinchout
- Rio Grande
- Texas County
- Model Boundary

Notes:

1) Basemap provided by Montgomery & Associates December 2016.
2) TDS = Total Dissolved Solids.
3) mg/L = milligrams per liter.

Scale in Miles

0   20   40

Projected
Coordinate System
Datum: NAD 1983
Albers Equal Area

GSI ENVIRONMENTAL

**CHANGE IN SIMULATED TDS
CONCENTRATIONS IN
EVANGELINE AQUIFER (MODEL
LAYERS 4, 5, 6) FROM 1984 TO 2013**

Lower Rio Grande Valley

GSI Job No. 4276	Drawn By: AV
Issued: 27-Jun-2017	Chk'd By: KER
Map ID: LRGV_CSTDS_L456	Appv'd By: SP

FIGURE 6.6.8
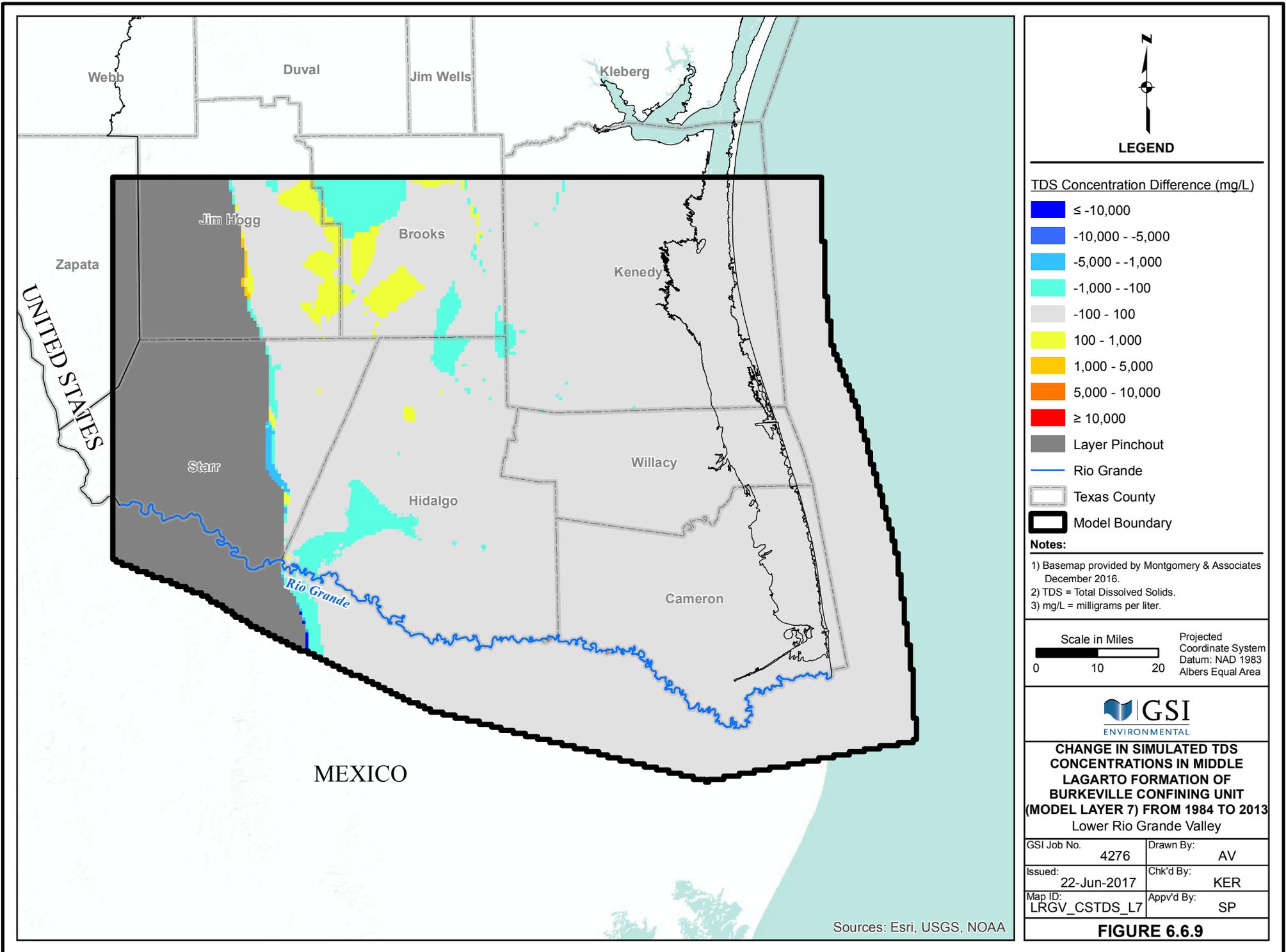
LEGEND

TDS Concentration Difference (mg/L)

- ≤ -10,000
- -10,000 - -5,000
- -5,000 - -1,000
- -1,000 - -100
- -100 - 100
- 100 - 1,000
- 1,000 - 5,000
- 5,000 - 10,000
- ≥ 10,000
- Layer Pinchout
- Rio Grande
- Texas County
- Model Boundary

Notes:

1) Basemap provided by Montgomery & Associates December 2016.
2) TDS = Total Dissolved Solids.
3) mg/L = milligrams per liter.

Scale in Miles

0   10   20

Projected
Coordinate System
Datum: NAD 1983
Albers Equal Area

GSI ENVIRONMENTAL

CHANGE IN SIMULATED TDS CONCENTRATIONS IN MIDDLE LAGARTO FORMATION OF BURKEVILLE CONFINING UNIT (MODEL LAYER 7) FROM 1984 TO 2013

Lower Rio Grande Valley

GSI Job No. 4276	Drawn By: AV
Issued: 22-Jun-2017	Chk'd By: KER
Map ID: LRGV_CSTDS_L7	Appv'd By: SP

FIGURE 6.6.9

Sources: Esri, USGS, NOAA
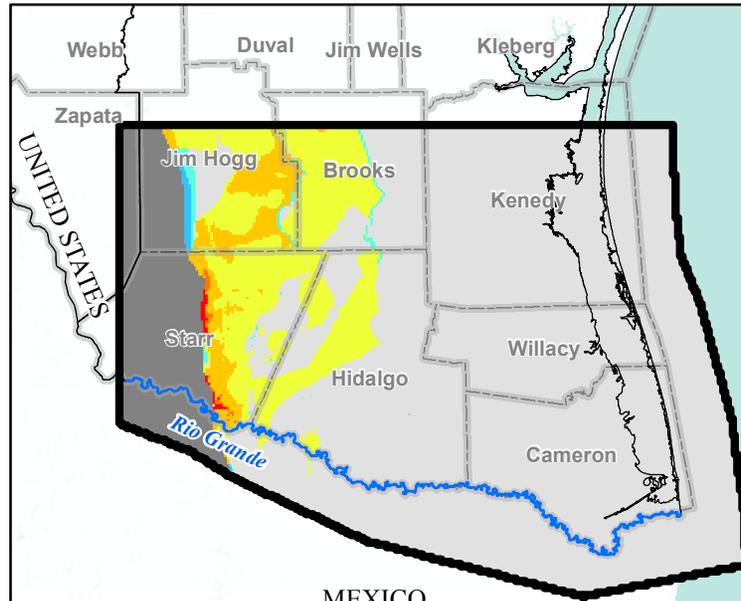
**Lower Lagarto Formation
(Jasper Aquifer)**

Sources: Esri, USGS, NOAA

**Oakville Formation
(Jasper Aquifer)**

Sources: Esri, USGS, NOAA

**Upper Catahoula Formation
(Jasper Aquifer)**

Sources: Esri, USGS, NOAA

LEGEND

TDS Concentration Difference (mg/L)

- ≤ -10,000
- -10,000 - -5,000
- -5,000 - -1,000
- -1,000 - -100
- -100 - 100
- 100 - 1,000
- 1,000 - 5,000
- 5,000 - 10,000
- ≥ 10,000
- Layer Pinchout
- Rio Grande
- Texas County
- Model Boundary

Notes:

1) Basemap provided by Montgomery & Associates December 2016.
2) TDS = Total Dissolved Solids.
3) mg/L = milligrams per liter.

Scale in Miles

0   20   40

Projected
Coordinate System
Datum: NAD 1983
Albers Equal Area

GSI
ENVIRONMENTAL
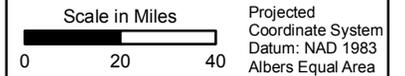
**CHANGE IN SIMULATED TDS
CONCENTRATIONS IN JASPER
AQUIFER (MODEL LAYERS
8, 9, 10) FROM 1984 TO 2013**

Lower Rio Grande Valley

GSI Job No. 4276	Drawn By: AV
Issued: 21-Jun-2017	Chk'd By: KER
Map ID: LRGV_CSTDS_L8910	Appv'd By: SP

FIGURE 6.6.10
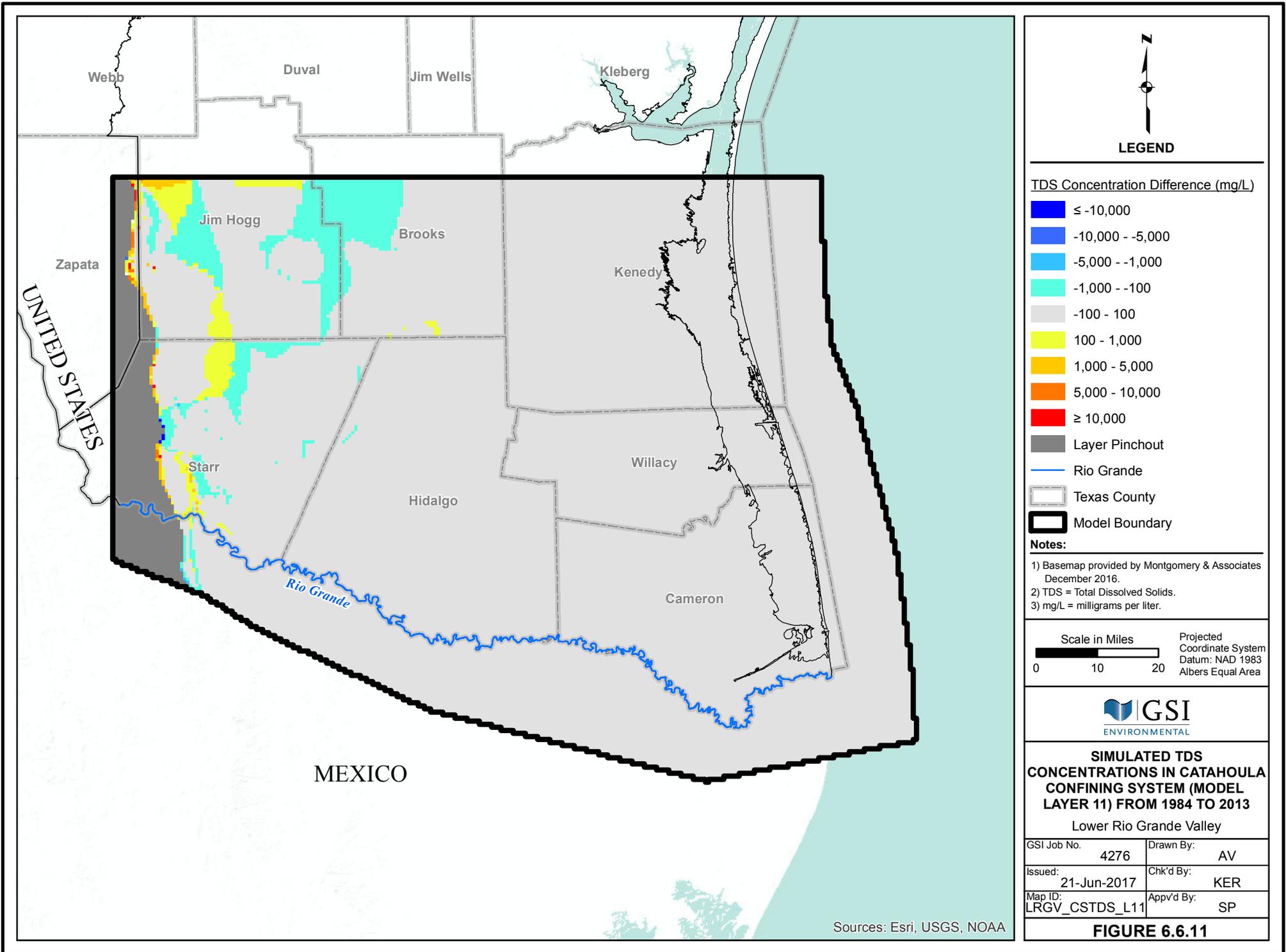
LEGEND

TDS Concentration Difference (mg/L)

- ≤ -10,000
- -10,000 - -5,000
- -5,000 - -1,000
- -1,000 - -100
- -100 - 100
- 100 - 1,000
- 1,000 - 5,000
- 5,000 - 10,000
- ≥ 10,000
- Layer Pinchout
- Rio Grande
- Texas County
- Model Boundary

Notes:

1) Basemap provided by Montgomery & Associates December 2016.
2) TDS = Total Dissolved Solids.
3) mg/L = milligrams per liter.

Scale in Miles

0   10   20

Projected Coordinate System
Datum: NAD 1983
Albers Equal Area

GSI ENVIRONMENTAL

SIMULATED TDS CONCENTRATIONS IN CATAHOULA CONFINING SYSTEM (MODEL LAYER 11) FROM 1984 TO 2013

Lower Rio Grande Valley

GSI Job No. 4276	Drawn By: AV
Issued: 21-Jun-2017	Chk'd By: KER
Map ID: LRGV_CSTDS_L11	Appv'd By: SP

FIGURE 6.6.11

Sources: Esri, USGS, NOAA
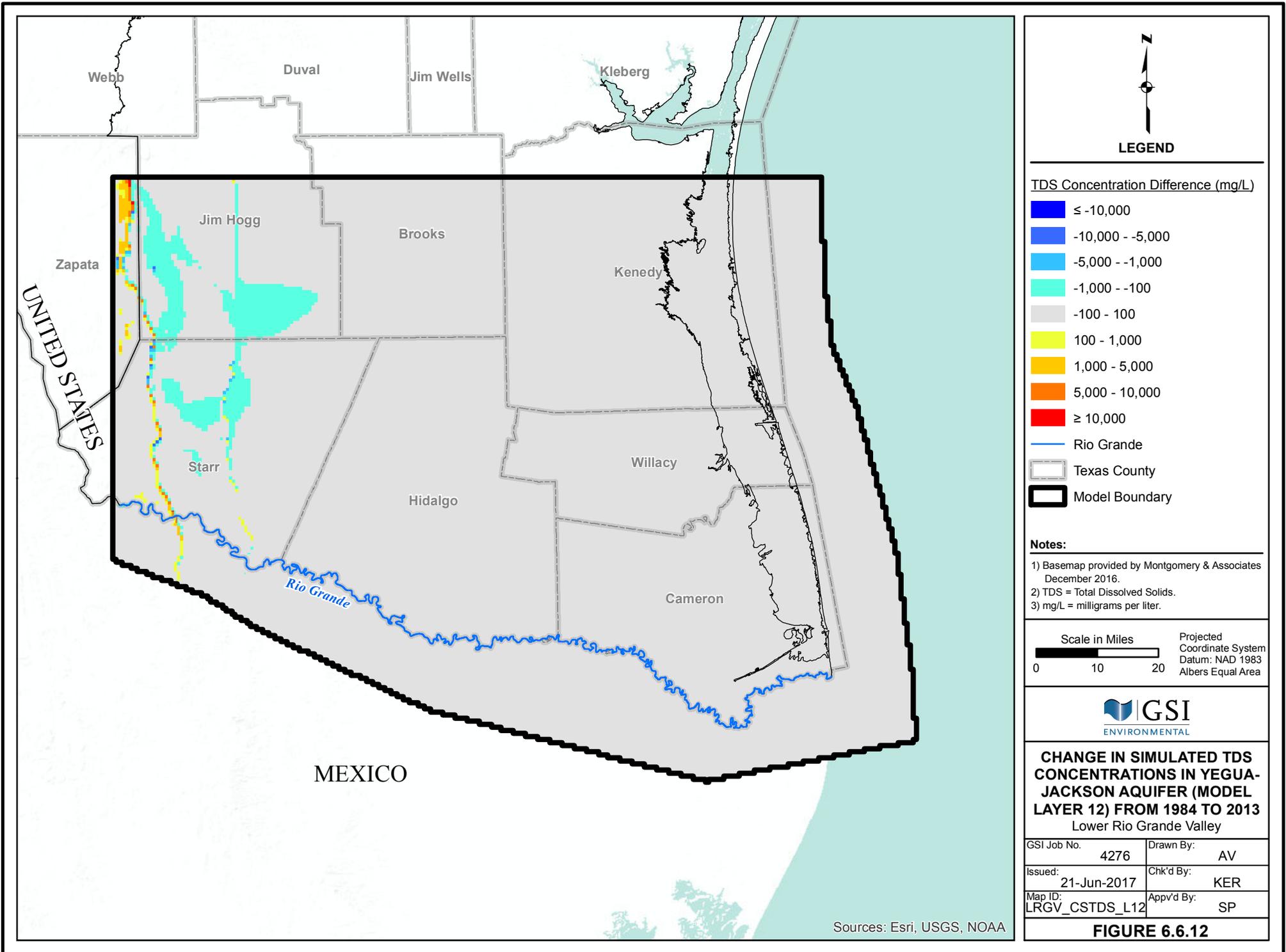
LEGEND

TDS Concentration Difference (mg/L)

- ≤ -10,000
- -10,000 - -5,000
- -5,000 - -1,000
- -1,000 - -100
- -100 - 100
- 100 - 1,000
- 1,000 - 5,000
- 5,000 - 10,000
- ≥ 10,000
- Rio Grande
- Texas County
- Model Boundary

Notes:

1) Basemap provided by Montgomery & Associates December 2016.
2) TDS = Total Dissolved Solids.
3) mg/L = milligrams per liter.

Scale in Miles
0   10   20

Projected Coordinate System Datum: NAD 1983 Albers Equal Area

GSI ENVIRONMENTAL

CHANGE IN SIMULATED TDS CONCENTRATIONS IN YEGUA-JACKSON AQUIFER (MODEL LAYER 12) FROM 1984 TO 2013
Lower Rio Grande Valley

GSI Job No. 4276	Drawn By: AV
Issued: 21-Jun-2017	Chk'd By: KER
Map ID: LRGV_CSTDS_L12	Appv'd By: SP

FIGURE 6.6.12
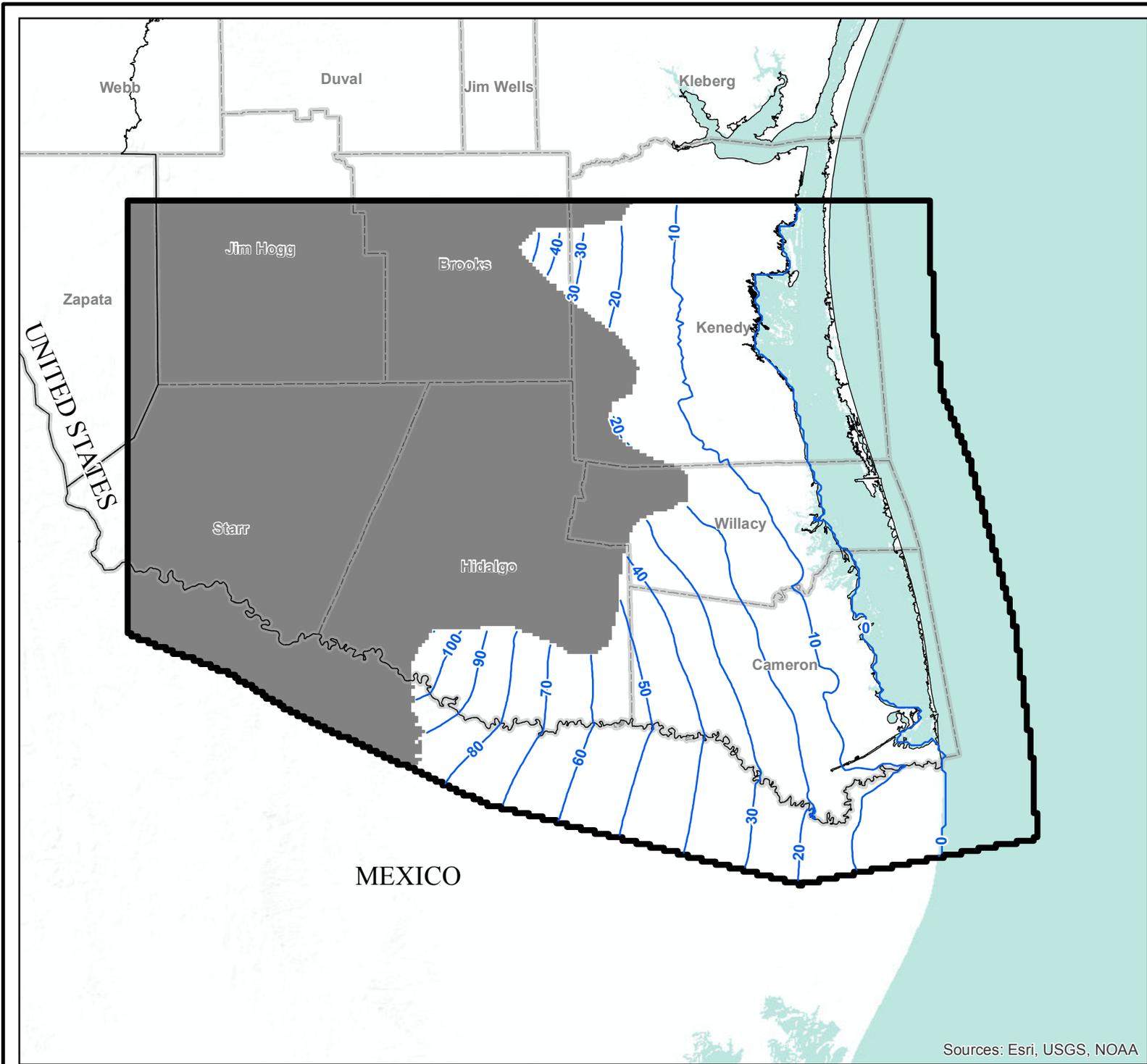
Map labels: Webb, Duval, Jim Wells, Kleberg, Jim Hogg, Brooks, Kenedy, Zapata, UNITED STATES, Starr, Hidalgo, Willacy, Cameron, Rio Grande, MEXICO

Sources: Esri, USGS, NOAA

LEGEND

— Water Level Contour (Feet AMSL)

▭ Texas County

▭ Model Boundary

▭ Layer Pinchout

Notes:

1) Basemap provided by Montgomery & Associates December 2016.
2) AMSL = Above Mean Sea Level.

Scale in Miles

0   10   20

Projected Coordinate System Datum: NAD 1983 Albers Equal Area

GSI ENVIRONMENTAL

SIMULATED WATER LEVELS IN MODEL LAYER 1 (BEAUMONT FORMATION OF CHICOT AQUIFER) FOR 2013 FOR DENSITY DEPENDENT FLOW

Lower Rio Grande Valley

GSI Job No. 4276	Drawn By: AV
Issued: 21-Jun-2017	Chk'd By: KER
Map ID: LRGV_SDDF_L1	Appv'd By: SP

FIGURE 6.6.13

Sources: Esri, USGS, NOAA

LEGEND

— Water Level Contour (Feet AMSL)

▢ Texas County

▢ Model Boundary

▢ Layer Pinchout

Notes:

1) Basemap provided by Montgomery & Associates December 2016.
2) AMSL = Above Mean Sea Level.

Scale in Miles

0   10   20

Projected Coordinate System
Datum: NAD 1983
Albers Equal Area

GSI ENVIRONMENTAL

SIMULATED WATER LEVELS IN MODEL LAYER 2 (LISSIE FORMATION OF CHICOT AQUIFER) FOR 2013 FOR DENSITY DEPENDENT FLOW
Lower Rio Grande Valley

GSI Job No. 4276	Drawn By: AV
Issued: 21-Jun-2017	Chk'd By: KER
Map ID: LRGV_SDDF_L2	Appv'd By: SP

FIGURE 6.6.14
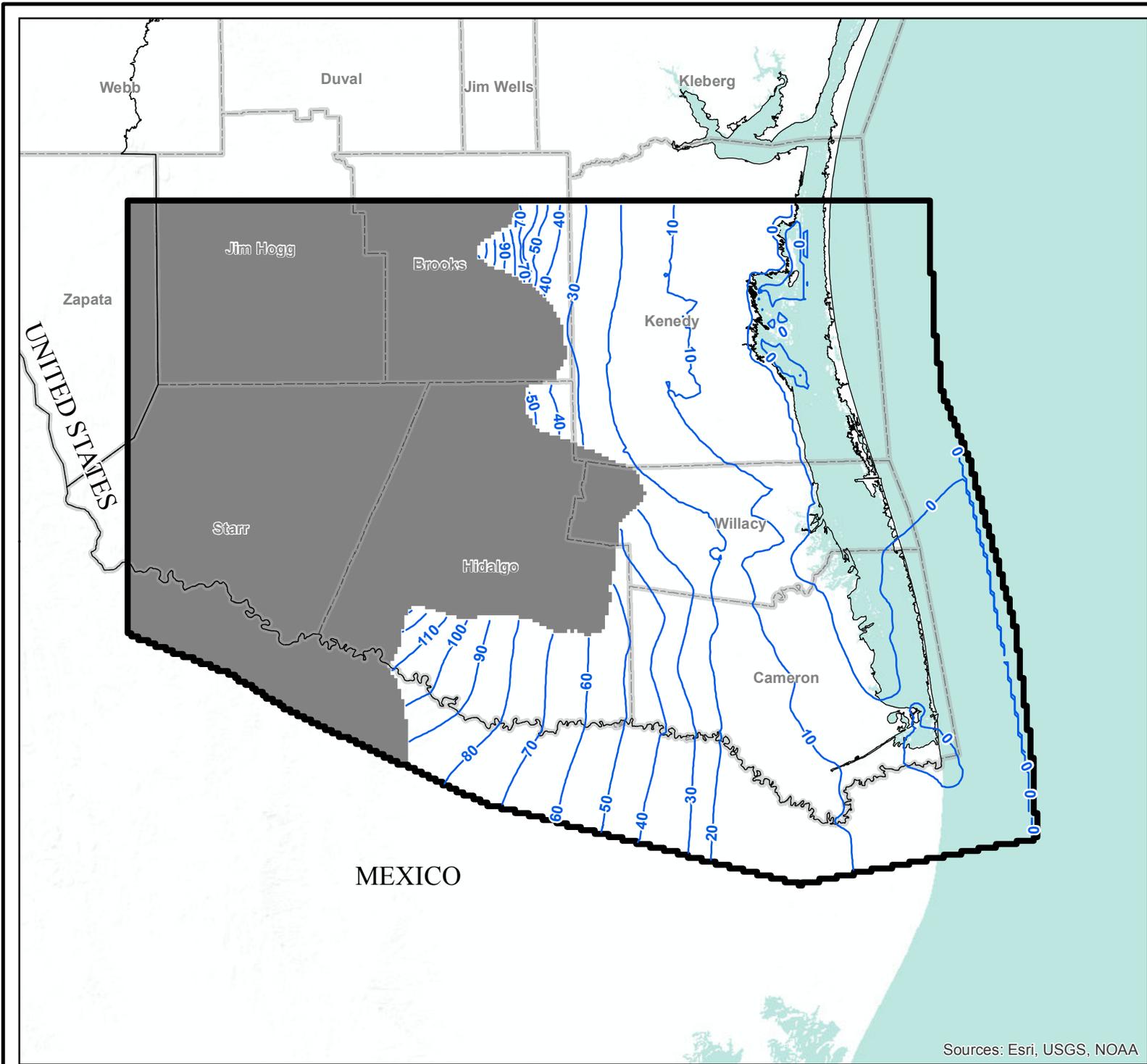
Sources: Esri, USGS, NOAA

LEGEND

— Water Level Contour (Feet AMSL)

▭ Texas County

▭ Model Boundary

▬ Layer Pinchout

Notes:

1) Basemap provided by Montgomery & Associates December 2016.
2) AMSL = Above Mean Sea Level.

Scale in Miles

0   10   20

Projected Coordinate System Datum: NAD 1983 Albers Equal Area

GSI ENVIRONMENTAL

SIMULATED WATER LEVELS IN MODEL LAYER 3 (WILLIS FORMATION OF CHICOT AQUIFER) FOR 2013 FOR DENSITY DEPENDENT FLOW
Lower Rio Grande Valley

GSI Job No. 4276	Drawn By: AV
Issued: 21-Jun-2017	Chk'd By: KER
Map ID: LRGV_SDDF_L3	Appv'd By: SP

FIGURE 6.6.15
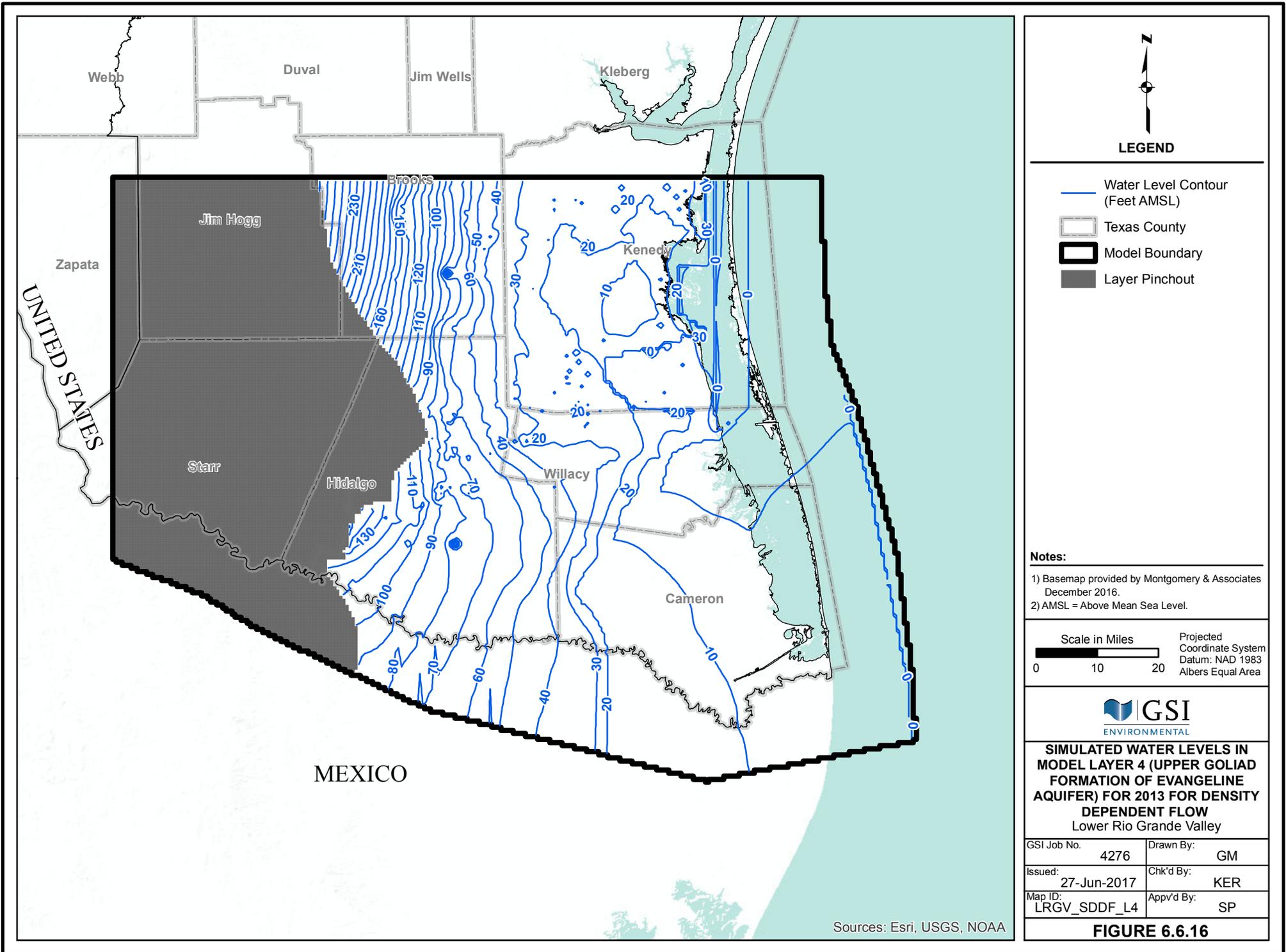
Sources: Esri, USGS, NOAA

Webb • Duval • Jim Wells • Kleberg

Jim Hogg • Brooks

Zapata

Kenedy

Starr

Willacy

Hidalgo

Cameron

UNITED STATES

MEXICO

LEGEND

— Water Level Contour (Feet AMSL)

▢ Texas County

▢ Model Boundary

▢ Layer Pinchout

Notes:

1) Basemap provided by Montgomery & Associates December 2016.
2) AMSL = Above Mean Sea Level.

Scale in Miles

0   10   20

Projected Coordinate System Datum: NAD 1983 Albers Equal Area

GSI ENVIRONMENTAL

SIMULATED WATER LEVELS IN MODEL LAYER 4 (UPPER GOLIAD FORMATION OF EVANGELINE AQUIFER) FOR 2013 FOR DENSITY DEPENDENT FLOW
Lower Rio Grande Valley

GSI Job No. 4276	Drawn By: GM
Issued: 27-Jun-2017	Chk'd By: KER
Map ID: LRGV_SDDF_L4	Appv'd By: SP

FIGURE 6.6.16

Sources: Esri, USGS, NOAA

LEGEND

— Water Level Contour
(Feet AMSL)

☐ Texas County

☐ Model Boundary

☐ Layer Pinchout

Notes:

1) Basemap provided by Montgomery & Associates December 2016.
2) AMSL = Above Mean Sea Level.

Scale in Miles

0   10   20

Projected
Coordinate System
Datum: NAD 1983
Albers Equal Area

GSI
ENVIRONMENTAL

**SIMULATED WATER LEVELS IN
MODEL LAYER 5 (LOWER GOLIAD
FORMATION OF EVANGELINE
AQUIFER) FOR 2013 FOR DENSITY
DEPENDENT FLOW**
Lower Rio Grande Valley

GSI Job No. 4276	Drawn By: GM
Issued: 21-Jun-2017	Chk'd By: KER
Map ID: LRGV_SDDF_L5	Appv'd By: SP

FIGURE 6.6.17

Sources: Esri, USGS, NOAA

LEGEND

— Water Level Contour (Feet AMSL)

Texas County

Model Boundary

Layer Pinchout

Notes:

1) Basemap provided by Montgomery & Associates December 2016.
2) AMSL = Above Mean Sea Level.

Scale in Miles

0   10   20

Projected Coordinate System Datum: NAD 1983 Albers Equal Area

GSI ENVIRONMENTAL

SIMULATED WATER LEVELS IN MODEL LAYER 7 (MIDDLE LAGARTO FORMATION OF BURKEVILLE CONFINING UNIT) FOR 2013 FOR DENSITY DEPENDENT FLOW
Lower Rio Grande Valley

GSI Job No. 4276	Drawn By: GM
Issued: 21-Jun-2017	Chk'd By: KER
Map ID: LRGV_SDDF_L7	Appv'd By: SP

FIGURE 6.6.19
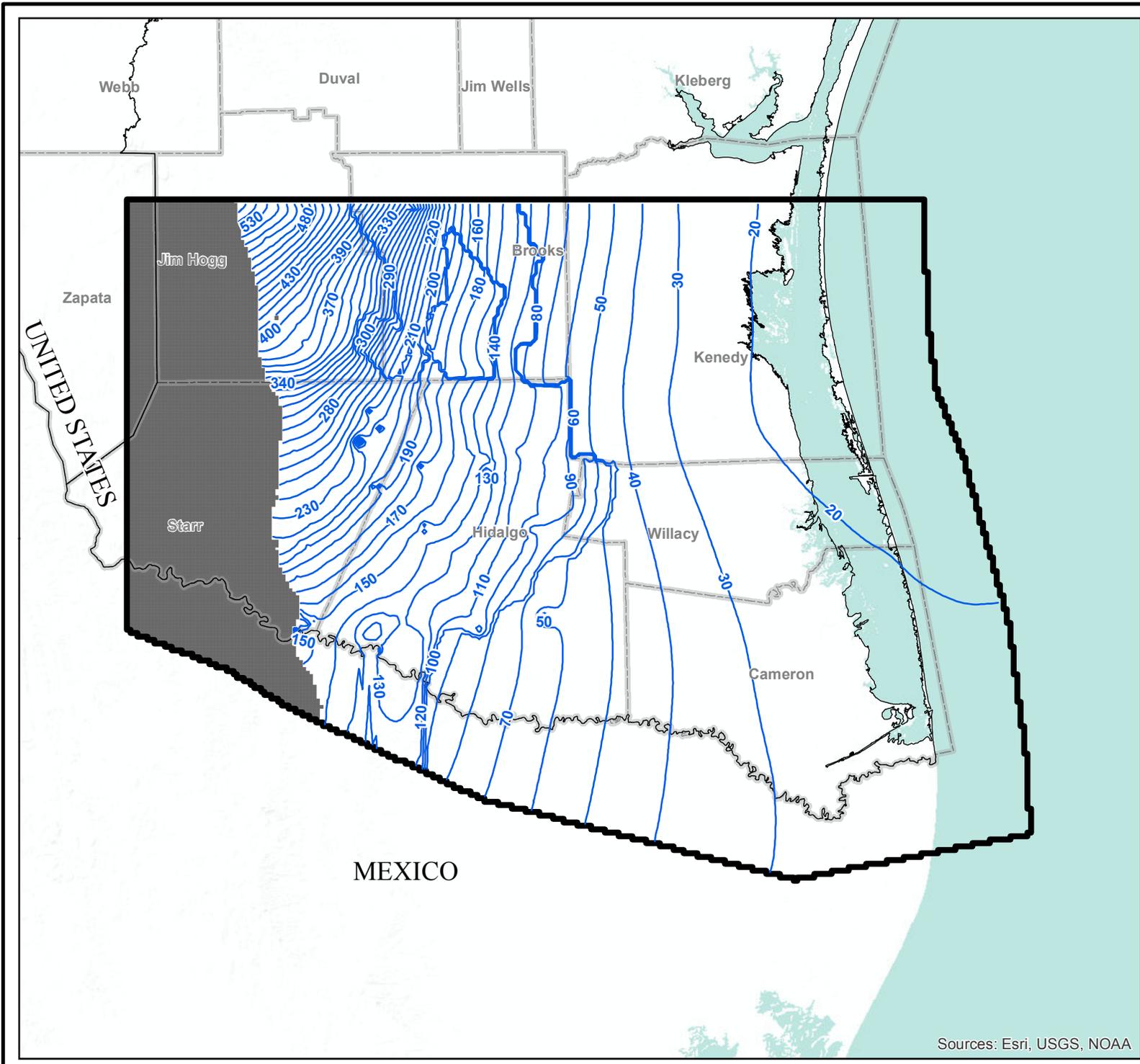
Sources: Esri, USGS, NOAA

LEGEND

— Water Level Contour (Feet AMSL)

Texas County

Model Boundary

Layer Pinchout

Notes:

1) Basemap provided by Montgomery & Associates December 2016.
2) AMSL = Above Mean Sea Level.

Scale in Miles

0   10   20

Projected Coordinate System
Datum: NAD 1983
Albers Equal Area

GSI ENVIRONMENTAL

SIMULATED WATER LEVELS IN MODEL LAYER 8 (LOWER LAGARTO FORMATION OF JASPER AQUIFER) FOR 2013 FOR DENSITY DEPENDENT FLOW
Lower Rio Grande Valley

GSI Job No. 4276	Drawn By: GM
Issued: 21-Jun-2017	Chk'd By: KER
Map ID: LRGV_SDDF_L8	Appv'd By: SP

FIGURE 6.6.20
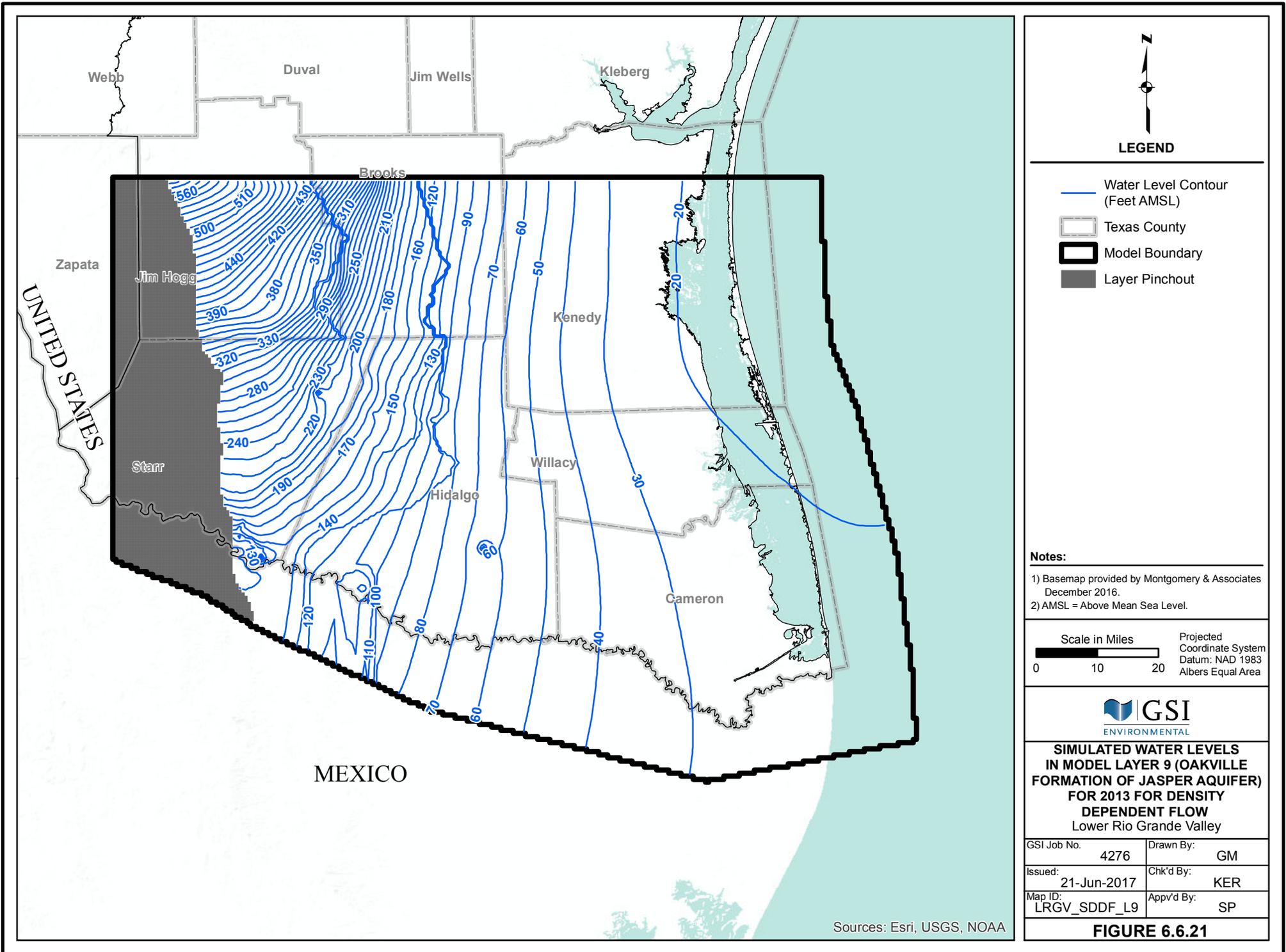
Sources: Esri, USGS, NOAA

LEGEND

— Water Level Contour (Feet AMSL)

☐ Texas County

☐ Model Boundary

■ Layer Pinchout

Notes:

1) Basemap provided by Montgomery & Associates December 2016.
2) AMSL = Above Mean Sea Level.

Scale in Miles

0   10   20

Projected Coordinate System Datum: NAD 1983 Albers Equal Area

GSI ENVIRONMENTAL

SIMULATED WATER LEVELS IN MODEL LAYER 9 (OAKVILLE FORMATION OF JASPER AQUIFER) FOR 2013 FOR DENSITY DEPENDENT FLOW
Lower Rio Grande Valley

GSI Job No. 4276	Drawn By: GM
Issued: 21-Jun-2017	Chk'd By: KER
Map ID: LRGV_SDDF_L9	Appv'd By: SP

FIGURE 6.6.21

Sources: Esri, USGS, NOAA
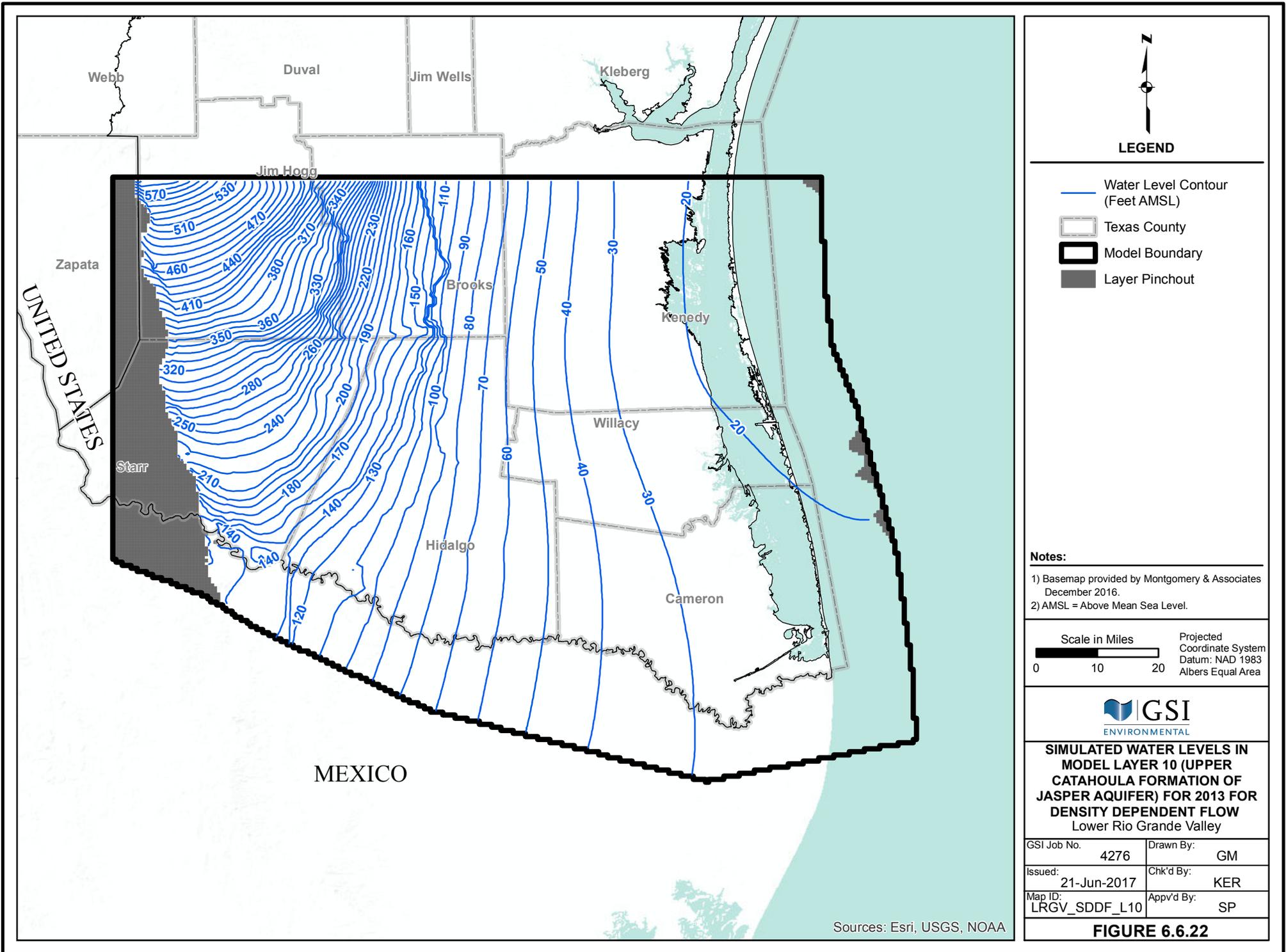
LEGEND

— Water Level Contour (Feet AMSL)

☐ Texas County

▬ Model Boundary

▨ Layer Pinchout

Notes:

1) Basemap provided by Montgomery & Associates December 2016.
2) AMSL = Above Mean Sea Level.

Scale in Miles

0   10   20

Projected Coordinate System Datum: NAD 1983 Albers Equal Area

GSI ENVIRONMENTAL

SIMULATED WATER LEVELS IN MODEL LAYER 10 (UPPER CATAHOULA FORMATION OF JASPER AQUIFER) FOR 2013 FOR DENSITY DEPENDENT FLOW
Lower Rio Grande Valley

GSI Job No. 4276	Drawn By: GM
Issued: 21-Jun-2017	Chk'd By: KER
Map ID: LRGV_SDDF_L10	Appv'd By: SP

FIGURE 6.6.22

Sources: Esri, USGS, NOAA
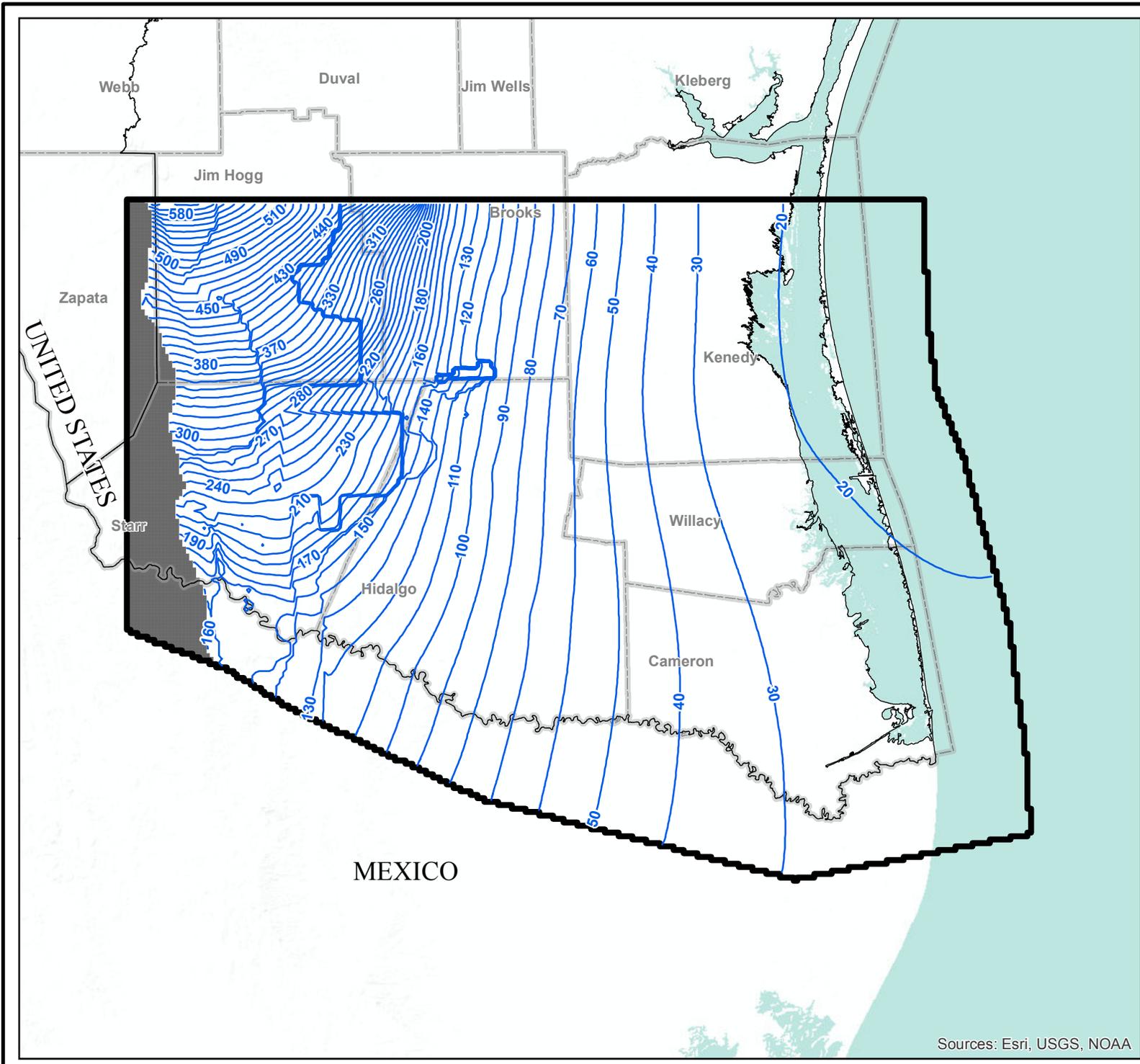
LEGEND

— Water Level Contour (Feet AMSL)

▢ Texas County

▢ Model Boundary

▮ Layer Pinchout

Notes:

1) Basemap provided by Montgomery & Associates December 2016.
2) AMSL = Above Mean Sea Level.

Scale in Miles

0   10   20

Projected Coordinate System
Datum: NAD 1983
Albers Equal Area

GSI ENVIRONMENTAL

SIMULATED WATER LEVELS IN MODEL LAYER 11 (CATAHOULA CONFINING SYSTEM) FOR 2013 FOR DENSITY DEPENDENT FLOW

Lower Rio Grande Valley

GSI Job No. 4276	Drawn By: GM
Issued: 21-Jun-2017	Chk'd By: KER
Map ID: LRGV_SDDF_L11	Appv'd By: SP

FIGURE 6.6.23
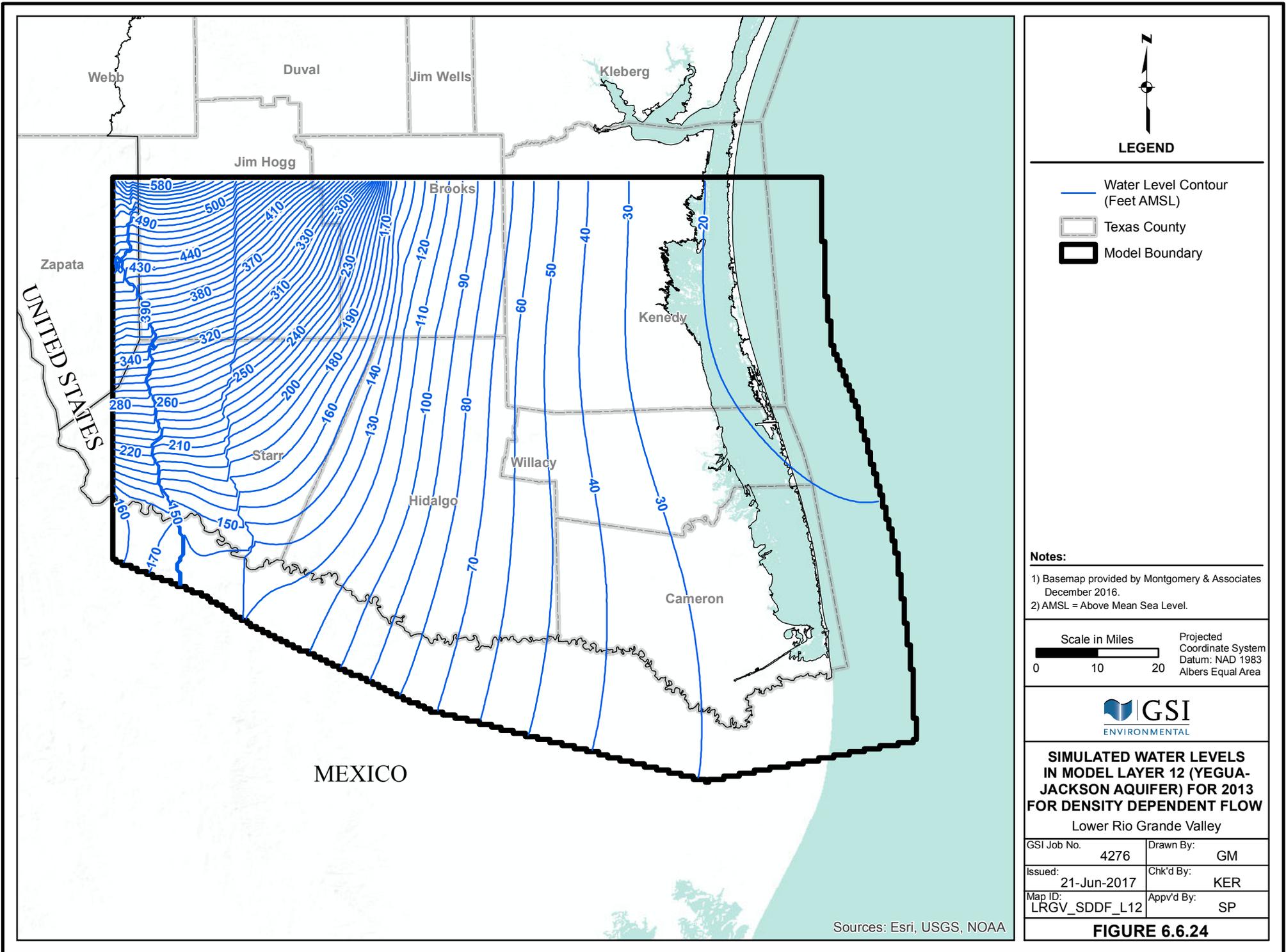
Sources: Esri, USGS, NOAA

LEGEND

— Water Level Contour (Feet AMSL)

Texas County

Model Boundary

Notes:

1) Basemap provided by Montgomery & Associates December 2016.
2) AMSL = Above Mean Sea Level.

Scale in Miles

0   10   20

Projected Coordinate System Datum: NAD 1983 Albers Equal Area

GSI ENVIRONMENTAL

SIMULATED WATER LEVELS IN MODEL LAYER 12 (YEGUA-JACKSON AQUIFER) FOR 2013 FOR DENSITY DEPENDENT FLOW

Lower Rio Grande Valley

GSI Job No. 4276	Drawn By: GM
Issued: 21-Jun-2017	Chk'd By: KER
Map ID: LRGV_SDDF_L12	Appv'd By: SP

FIGURE 6.6.24

Sources: Esri, USGS, NOAA
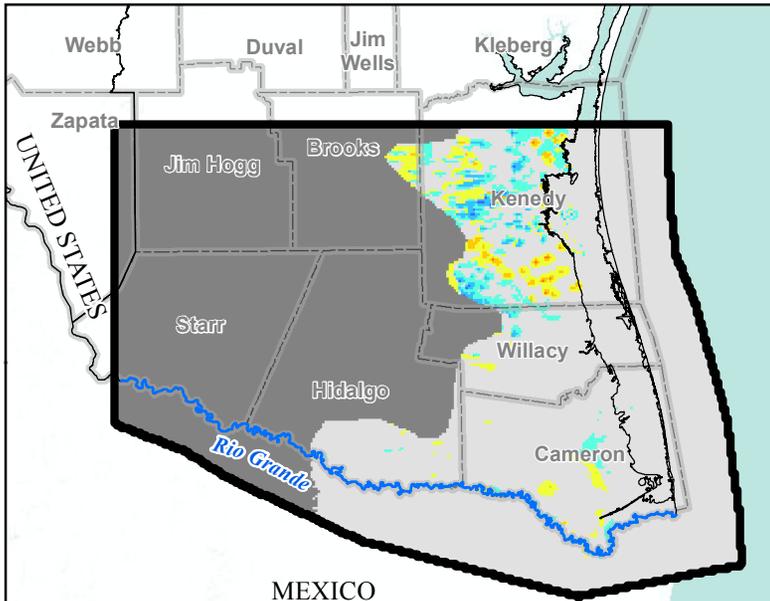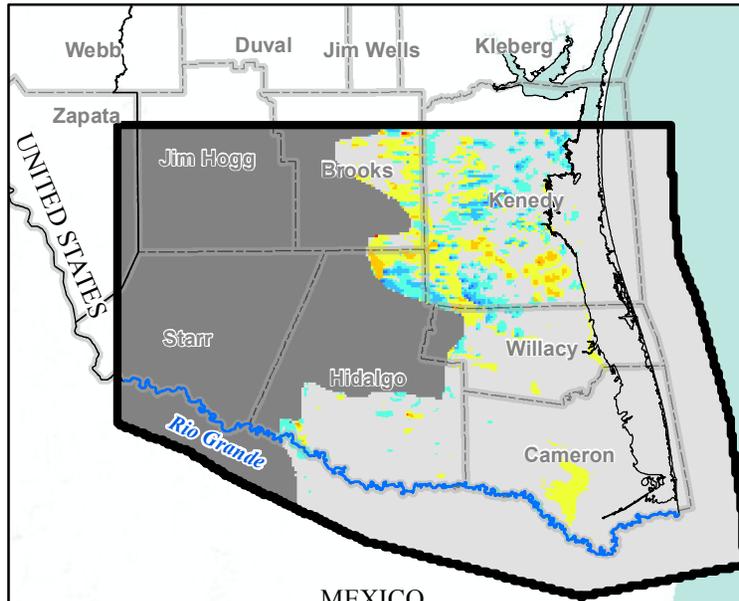
**Beaumont Formation
(Model Layer 1)**

Sources: Esri, USGS, NOAA

**Lissie Formation
(Model Layer 2)**

Sources: Esri, USGS, NOAA

**Willis Formation
(Model Layer 3)**

Sources: Esri, USGS, NOAA

LEGEND

Modeled TDS Concentration
Difference (mg/L)

≤ -10,000	
-10,000 - -5,000	
-5,000 - -1,000	
-1,000 - -100	
-100 - 100	
100 - 1,000	
1,000 - 5,000	
5,000 - 10,000	
≥ 10,000	
Layer Pinchout	
Rio Grande	
Texas County	
Model Boundary	

Scale in Miles

0   20   40

Projected
Coordinate System
Datum: NAD 1983
Albers Equal Area

GSI
ENVIRONMENTAL

**CONCENTRATION DIFFERENCE
BETWEEN DENSITY DEPENDENT
SIMULATIONS WITH AND WITHOUT
WELLS IN CHICOT AQUIFER
(MODEL LAYERS 1, 2, 3) FOR 2013**
Lower Rio Grande Valley

GSI Job No.	Drawn By:
4276	AV
Issued:	Chk'd By:
22-Jun-2017	KER
Map ID:	Appv'd By:
LRGV_CDDDS_L123	SP

FIGURE 6.7.1

Notes:

1) Basemap provided by Montgomery & Associates
   December 2016.
2) TDS = Total Dissolved Solids.
3) mg/L = milligrams per liter.
4) The difference in TDS is the TDS concentration
   for the base case simulation with pumping wells
   minus the TDS concentration for the simulation
   without pumping wells.
5) Negative values shows the TDS concentration
   decreased with pumping compared to no pumping
   and positive values shows the TDS concentration
   increased with pumping compared to no pumping.

Upper Goliad Formation (Model Layer 4)
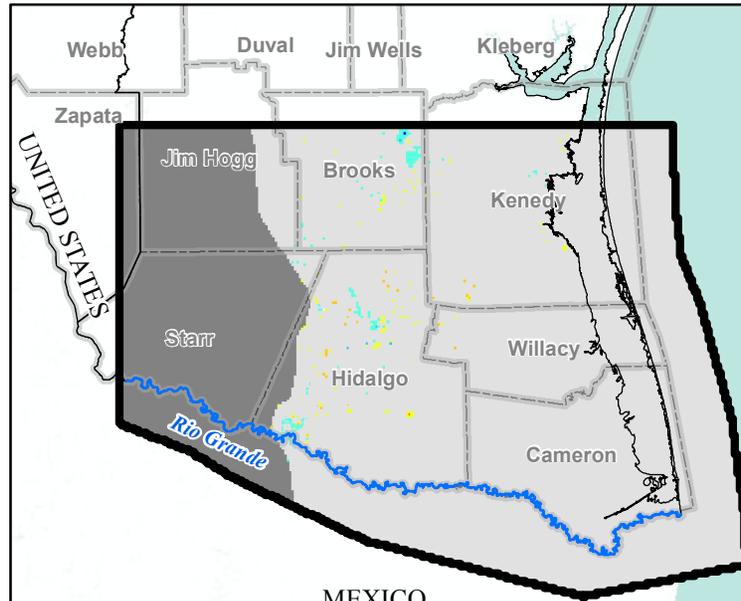
Sources: Esri, USGS, NOAA

Lower Goliad Formation (Model Layer 5)

Sources: Esri, USGS, NOAA

Upper Lagarto Formation (Model Layer 6)

Sources: Esri, USGS, NOAA

LEGEND

Modeled TDS Concentration Difference (mg/L)

- ≤ -10,000
- -10,000 - -5,000
- -5,000 - -1,000
- -1,000 - -100
- -100 - 100
- 100 - 1,000
- 1,000 - 5,000
- 5,000 - 10,000
- ≥ 10,000
- Layer Pinchout
- Rio Grande
- Texas County
- Model Boundary

Scale in Miles

0   20   40

Projected Coordinate System Datum: NAD 1983 Albers Equal Area

GSI ENVIRONMENTAL
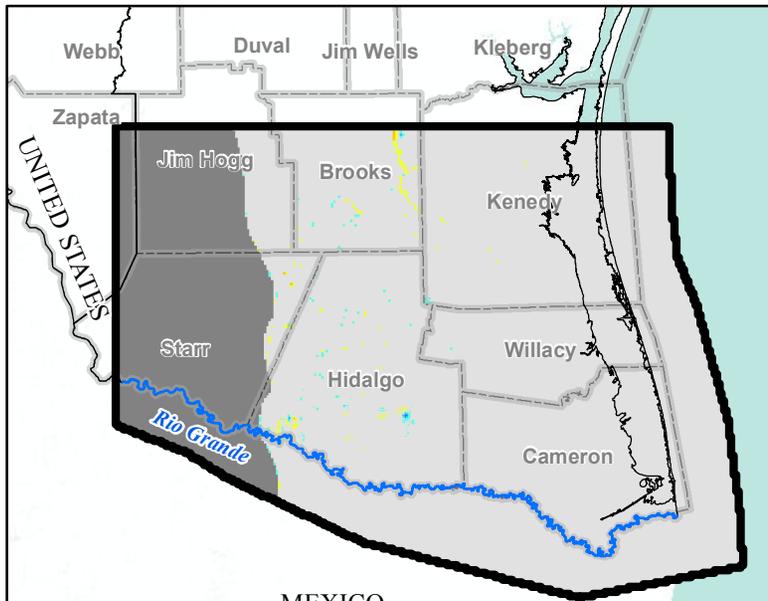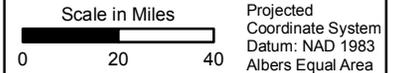
CONCENTRATION DIFFERENCE BETWEEN DENSITY DEPENDENT SIMULATIONS WITH AND WITHOUT WELLS IN EVANGELINE AQUIFER (MODEL LAYERS 4, 5, 6) FOR 2013
Lower Rio Grande Valley

GSI Job No. 4276	Drawn By: AV
Issued: 22-Jun-2017	Chk'd By: KER
Map ID: LRGV_CDDDS_L456	Appv'd By: SP

FIGURE 6.7.2

Notes:

1) Basemap provided by Montgomery & Associates December 2016.
2) TDS = Total Dissolved Solids.
3) mg/L = milligrams per liter.
4) The difference in TDS is the TDS concentration for the base case simulation with pumping wells minus the TDS concentration for the simulation without pumping wells.
5) Negative values shows the TDS concentration decreased with pumping compared to no pumping and positive values shows the TDS concentration increased with pumping compared to no pumping.

Webb   Duval   Jim Wells   Kleberg

Jim Hogg

Brooks

Zapata

Kenedy

UNITED STATES

Starr

Willacy

Hidalgo

Rio Grande

Cameron

MEXICO

LEGEND

Modeled TDS Concentration Difference (mg/L)

- ≤ -10,000
- -10,000 – -5,000
- -5,000 – -1,000
- -1,000 – -100
- -100 – 100
- 100 – 1,000
- 1,000 – 5,000
- 5,000 – 10,000
- ≥ 10,000
- Layer Pinchout
- ──── Rio Grande
- Texas County
- Model Boundary

Scale in Miles
0   10   20

Projected Coordinate System
Datum: NAD 1983
Albers Equal Area

GSI ENVIRONMENTAL

CONCENTRATION DIFFERENCE BETWEEN DENSITY DEPENDENT SIMULATIONS WITH AND WITHOUT WELLS IN MIDDLE LAGARTO FORMATION OF BURKEVILLE CONFINING UNIT (MODEL LAYER 7) FOR 2013
Lower Rio Grande Valley

GSI Job No. 4276	Drawn By: AV
Issued: 22-Jun-2017	Chk'd By: KER
Map ID: LRGV_CDDDS_L7	Appv'd By: SP

FIGURE 6.7.3

Sources: Esri, USGS, NOAA

Notes:
1) Basemap provided by Montgomery & Associates December 2016.
2) TDS = Total Dissolved Solids.
3) mg/L = milligrams per liter.
4) The difference in TDS is the TDS concentration for the base case simulation with pumping wells minus the TDS concentration for the simulation without pumping wells.
5) Negative values shows the TDS concentration decreased with pumping compared to no pumping and positive values shows the TDS concentration increased with pumping compared to no pumping.

**Lower Lagarto Formation
(Model Layer 8)**

Sources: Esri, USGS, NOAA

**Oakville Formation
(Model Layer 9)**

Sources: Esri, USGS, NOAA

**Upper Catahoula Formation
(Model Layer 10)**

Sources: Esri, USGS, NOAA

LEGEND

Modeled TDS Concentration
Difference (mg/L)

☐	≤ -10,000
☐	-10,000 - -5,000
☐	-5,000 - -1,000
☐	-1,000 - -100
☐	-100 - 100
☐	100 - 1,000
☐	1,000 - 5,000
☐	5,000 - 10,000
☐	≥ 10,000
☐	Layer Pinchout
—	Rio Grande
☐	Texas County
☐	Model Boundary

Scale in Miles

0   20   40

Projected
Coordinate System
Datum: NAD 1983
Albers Equal Area

GSI
ENVIRONMENTAL

**CONCENTRATION DIFFERENCE
BETWEEN DENSITY DEPENDENT
SIMULATIONS WITH AND WITHOUT
WELLS IN JASPER AQUIFER
(MODEL LAYERS 8, 9, 10) FOR 2013**
Lower Rio Grande Valley

GSI Job No. 4276	Drawn By: AV
Issued: 22-Jun-2017	Chk'd By: KER
Map ID: LRGV_CDDDS_L8910	Appv'd By: SP

FIGURE 6.7.4

Notes:

1) Basemap provided by Montgomery & Associates December 2016.
2) TDS = Total Dissolved Solids.
3) mg/L = milligrams per liter.
4) The difference in TDS is the TDS concentration for the base case simulation with pumping wells minus the TDS concentration for the simulation without pumping wells.
5) Negative values shows the TDS concentration decreased with pumping compared to no pumping and positive values shows the TDS concentration increased with pumping compared to no pumping.

LEGEND

Modeled TDS Concentration Difference (mg/L)

- ≤ -10,000
- -10,000 - -5,000
- -5,000 - -1,000
- -1,000 - -100
- -100 - 100
- 100 - 1,000
- 1,000 - 5,000
- 5,000 - 10,000
- ≥ 10,000
- 0.3
- Rio Grande
- Texas County
- Model Boundary

Scale in Miles
0   10   20

Projected Coordinate System
Datum: NAD 1983
Albers Equal Area

GSI ENVIRONMENTAL

CONCENTRATION DIFFERENCE BETWEEN DENSITY DEPENDENT SIMULATIONS WITH AND WITHOUT WELLS IN CATAHOULA CONFINING SYSTEM (MODEL LAYER 11) FOR 2013
Lower Rio Grande Valley

GSI Job No. 4276	Drawn By: AV
Issued: 22-Jun-2017	Chk'd By: KER
Map ID: LRGV_CDDDS_L11	Appv'd By: SP

FIGURE 6.7.5

Notes:

1) Basemap provided by Montgomery & Associates December 2016.
2) TDS = Total Dissolved Solids.
3) mg/L = milligrams per liter.
4) The difference in TDS is the TDS concentration for the base case simulation with pumping wells minus the TDS concentration for the simulation without pumping wells.
5) Negative values shows the TDS concentration decreased with pumping compared to no pumping and positive values shows the TDS concentration increased with pumping compared to no pumping.

Sources: Esri, USGS, NOAA
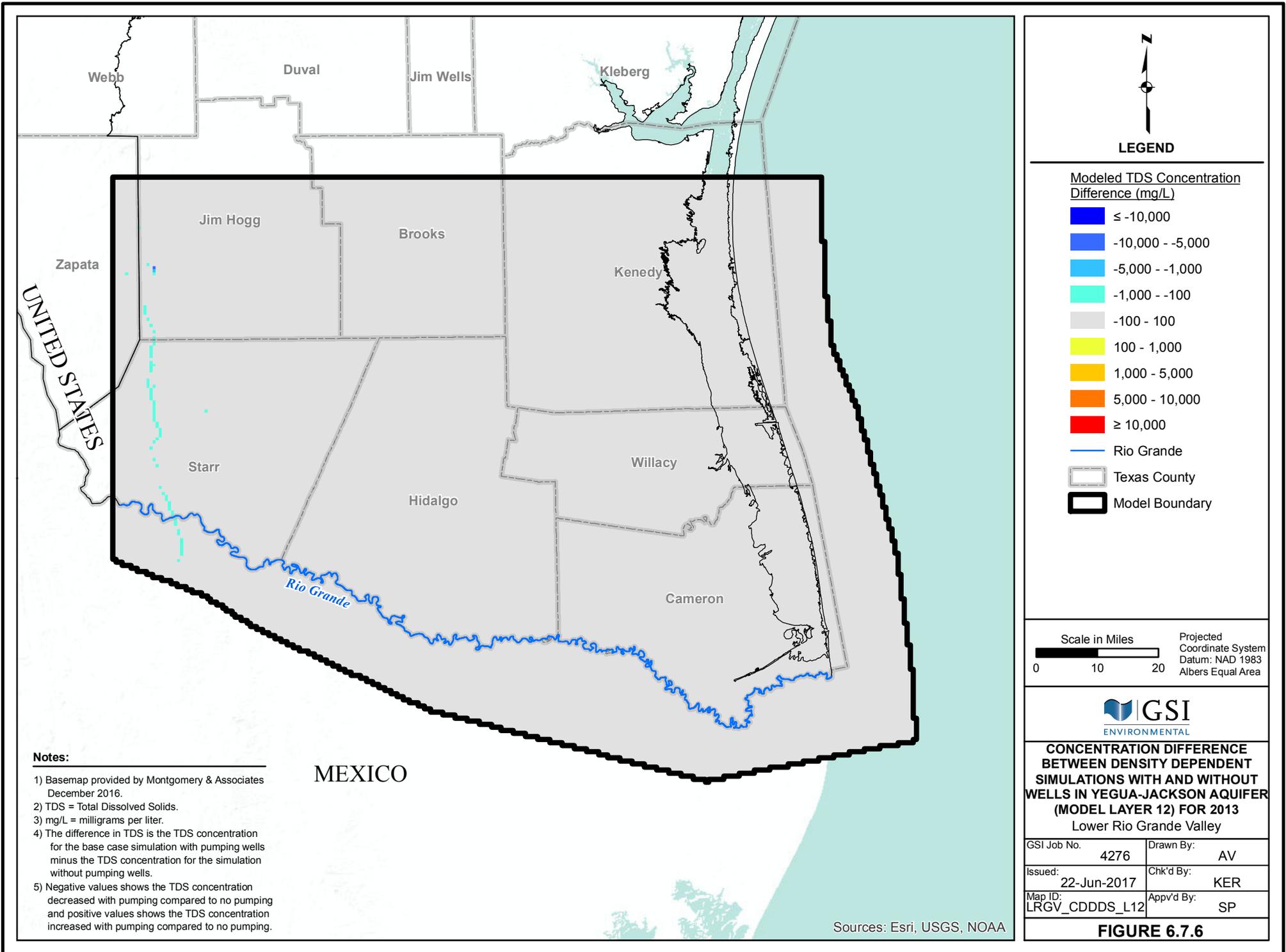
LEGEND

Modeled TDS Concentration Difference (mg/L)

- ≤ -10,000
- -10,000 - -5,000
- -5,000 - -1,000
- -1,000 - -100
- -100 - 100
- 100 - 1,000
- 1,000 - 5,000
- 5,000 - 10,000
- ≥ 10,000
- Rio Grande
- Texas County
- Model Boundary

Scale in Miles
0   10   20

Projected Coordinate System
Datum: NAD 1983
Albers Equal Area

GSI ENVIRONMENTAL

CONCENTRATION DIFFERENCE BETWEEN DENSITY DEPENDENT SIMULATIONS WITH AND WITHOUT WELLS IN YEGUA-JACKSON AQUIFER (MODEL LAYER 12) FOR 2013
Lower Rio Grande Valley

GSI Job No. 4276	Drawn By: AV
Issued: 22-Jun-2017	Chk'd By: KER
Map ID: LRGV_CDDDS_L12	Appv'd By: SP

FIGURE 6.7.6

Notes:

1) Basemap provided by Montgomery & Associates December 2016.
2) TDS = Total Dissolved Solids.
3) mg/L = milligrams per liter.
4) The difference in TDS is the TDS concentration for the base case simulation with pumping wells minus the TDS concentration for the simulation without pumping wells.
5) Negative values shows the TDS concentration decreased with pumping compared to no pumping and positive values shows the TDS concentration increased with pumping compared to no pumping.

Webb   Duval   Jim Wells   Kleberg

Jim Hogg   Brooks   Kenedy

Zapata

UNITED STATES

Starr   Hidalgo   Willacy

Rio Grande   Cameron

MEXICO

Beaumont Formation (Model Layer 1)

Sources: Esri, USGS, NOAA

Lissie Formation (Model Layer 2)

Sources: Esri, USGS, NOAA

Willis Formation (Model Layer 3)

Sources: Esri, USGS, NOAA

LEGEND

Modeled TDS Concentration Difference (mg/L)

- ≤ -10,000
- -10,000 - -5,000
- -5,000 - -1,000
- -1,000 - -100
- -100 - 100
- 100 - 1,000
- 1,000 - 5,000
- 5,000 - 10,000
- ≥ 10,000
- Layer Pinchout
- Rio Grande
- Texas County
- Model Boundary

Scale in Miles

0   20   40

Projected Coordinate System Datum: NAD 1983 Albers Equal Area

GSI ENVIRONMENTAL

CONCENTRATION DIFFERENCE BETWEEN TRANSPORT SIMULATIONS WITH AND WITHOUT DENSITY IN CHICOT AQUIFER (MODEL LAYERS 1, 2, 3) FOR 2013
Lower Rio Grande Valley

GSI Job No. 4276	Drawn By: AV
Issued: 22-Jun-2017	Chk'd By: KER
Map ID: LRGV_CDTS_L123	Appv'd By: SP

FIGURE 6.7.7

Notes:

1) Basemap provided by Montgomery & Associates December 2016.
2) TDS = Total Dissolved Solids.
3) mg/L = milligrams per liter.
4) The difference in TDS is the TDS concentration for the base case simulation with density minus the TDS concentration for the simulation without density.
5) Negative values shows the TDS concentration decreased with density simulated compared to no density simulated and positive values shows the TDS concentration increased with density simulated compared to no density simulated.

**Upper Goliad Formation
(Model Layer 4)**

Sources: Esri, USGS, NOAA

**Lower Goliad Formation
(Model Layer 5)**

Sources: Esri, USGS, NOAA

**Upper Lagarto Formation
(Model Layer 6)**

Sources: Esri, USGS, NOAA

LEGEND

Modeled TDS Concentration
Difference (mg/L)

≤ -10,000
-10,000 - -5,000
-5,000 - -1,000
-1,000 - -100
-100 - 100
100 - 1,000
1,000 - 5,000
5,000 - 10,000
≥ 10,000
Layer Pinchout
Rio Grande
Texas County
Model Boundary

Scale in Miles

0   20   40

Projected
Coordinate System
Datum: NAD 1983
Albers Equal Area

GSI ENVIRONMENTAL

**CONCENTRATION DIFFERENCE
BETWEEN TRANSPORT
SIMULATIONS WITH AND WITHOUT
DENSITY IN EVANGELINE AQUIFER
(MODEL LAYERS 4, 5, 6) FOR 2013**
Lower Rio Grande Valley

GSI Job No.	Drawn By:
4276	AV
Issued:	Chk'd By:
22-Jun-2017	KER
Map ID:	Appv'd By:
LRGV_CDTS_L456	SP

FIGURE 6.7.8

Notes:

1) Basemap provided by Montgomery & Associates
December 2016.
2) TDS = Total Dissolved Solids.
3) mg/L = milligrams per liter.
4) The difference in TDS is the TDS concentration
for the base case simulation with density minus the
TDS concentration for the simulation without density.
5) Negative values shows the TDS concentration
decreased with density simulated compared to no
density simulated and positive values shows the
TDS concentration increased with density simulated
compared to no density simulated.

LEGEND

Modeled TDS Concentration Difference (mg/L)

- ≤ -10,000
- -10,000 - -5,000
- -5,000 - -1,000
- -1,000 - -100
- -100 - 100
- 100 - 1,000
- 1,000 - 5,000
- 5,000 - 10,000
- ≥ 10,000
- Layer Pinchout
- Rio Grande
- Texas County
- Model Boundary

Scale in Miles
0   10   20

Projected Coordinate System
Datum: NAD 1983
Albers Equal Area

GSI ENVIRONMENTAL

CONCENTRATION DIFFERENCE BETWEEN TRANSPORT SIMULATIONS WITH AND WITHOUT DENSITY IN MIDDLE LAGARTO FORMATION OF BURKEVILLE CONFINING UNIT (MODEL LAYER 7) FOR 2013
Lower Rio Grande Valley

GSI Job No. 4276	Drawn By: AV
Issued: 22-Jun-2017	Chk'd By: KER
Map ID: LRGV_CDTS_L7	Appv'd By: SP

FIGURE 6.7.9

Notes:

1) Basemap provided by Montgomery & Associates December 2016.
2) TDS = Total Dissolved Solids.
3) mg/L = milligrams per liter.
4) The difference in TDS is the TDS concentration for the base case simulation with density minus the TDS concentration for the simulation without density.
5) Negative values shows the TDS concentration decreased with density simulated compared to no density simulated and positive values shows the TDS concentration increased with density simulated compared to no density simulated.

Sources: Esri, USGS, NOAA

**Lower Lagarto Formation
(Model Layer 8)**

Sources: Esri, USGS, NOAA

**Oakville Formation
(Model Layer 9)**

Sources: Esri, USGS, NOAA

**Upper Catahoula Formation
(Model Layer 10)**

Sources: Esri, USGS, NOAA

LEGEND

Modeled TDS Concentration
Difference (mg/L)

≤ -10,000
-10,000 - -5,000
-5,000 - -1,000
-1,000 - -100
-100 - 100
100 - 1,000
1,000 - 5,000
5,000 - 10,000
≥ 10,000
Layer Pinchout
Rio Grande
Texas County
Model Boundary

Scale in Miles
0   20   40

Projected
Coordinate System
Datum: NAD 1983
Albers Equal Area

GSI ENVIRONMENTAL

**CONCENTRATION DIFFERENCE
BETWEEN TRANSPORT
SIMULATIONS WITH AND WITHOUT
DENSITY IN JASPER AQUIFER
(MODEL LAYERS 8, 9, 10) FOR 2013**
Lower Rio Grande Valley

GSI Job No. 4276	Drawn By: AV
Issued: 22-Jun-2017	Chk'd By: KER
Map ID: LRGV_CDTS_L8910	Appv'd By: SP

FIGURE 6.7.10

Notes:

1) Basemap provided by Montgomery & Associates December 2016.
2) TDS = Total Dissolved Solids.
3) mg/L = milligrams per liter.
4) The difference in TDS is the TDS concentration for the base case simulation with density minus the TDS concentration for the simulation without density.
5) Negative values shows the TDS concentration decreased with density simulated compared to no density simulated and positive values shows the TDS concentration increased with density simulated compared to no density simulated.

LEGEND

Modeled TDS Concentration Difference (mg/L)

- ≤ -10,000
- -10,000 - -5,000
- -5,000 - -1,000
- -1,000 - -100
- -100 - 100
- 100 - 1,000
- 1,000 - 5,000
- 5,000 - 10,000
- ≥ 10,000
- Layer Pinchout
- Rio Grande
- Texas County
- Model Boundary

Scale in Miles
0   10   20

Projected Coordinate System
Datum: NAD 1983
Albers Equal Area

GSI ENVIRONMENTAL

CONCENTRATION DIFFERENCE BETWEEN TRANSPORT SIMULATIONS WITH AND WITHOUT DENSITY IN CATAHOULA CONFINING SYSTEM (MODEL LAYER 11) FOR 2013
Lower Rio Grande Valley

GSI Job No. 4276	Drawn By: AV
Issued: 22-Jun-2017	Chk'd By: KER
Map ID: LRGV_CDTS_L11	Appv'd By: SP

FIGURE 6.7.11

Notes:

1) Basemap provided by Montgomery & Associates December 2016.
2) TDS = Total Dissolved Solids.
3) mg/L = milligrams per liter.
4) The difference in TDS is the TDS concentration for the base case simulation with density minus the TDS concentration for the simulation without density.
5) Negative values shows the TDS concentration decreased with density simulated compared to no density simulated and positive values shows the TDS concentration increased with density simulated compared to no density simulated.

Sources: Esri, USGS, NOAA

LEGEND

Modeled TDS Concentration Difference (mg/L)

- ≤ -10,000
- -10,000 - -5,000
- -5,000 - -1,000
- -1,000 - -100
- -100 - 100
- 100 - 1,000
- 1,000 - 5,000
- 5,000 - 10,000
- ≥ 10,000
- Rio Grande
- Texas County
- Model Boundary

Scale in Miles

0   10   20

Projected Coordinate System
Datum: NAD 1983
Albers Equal Area

GSI ENVIRONMENTAL

CONCENTRATION DIFFERENCE BETWEEN TRANSPORT SIMULATIONS WITH AND WITHOUT DENSITY IN YEGUA-JACKSON AQUIFER (MODEL LAYER 12) FOR 2013

Lower Rio Grande Valley

GSI Job No. 4276	Drawn By: AV
Issued: 22-Jun-2017	Chk'd By: KER
Map ID: LRGV_CDTS_L12	Appv'd By: SP

FIGURE 6.7.12

Notes:

1) Basemap provided by Montgomery & Associates December 2016.
2) TDS = Total Dissolved Solids.
3) mg/L = milligrams per liter.
4) The difference in TDS is the TDS concentration for the base case simulation with density minus the TDS concentration for the simulation without density.
5) Negative values shows the TDS concentration decreased with density simulated compared to no density simulated and positive values shows the TDS concentration increased with density simulated compared to no density simulated.

Sources: Esri, USGS, NOAA

TDS CONCENTRATIONS IN GROUNDWATER AT EXISTING DESALINATION PLANT WELLS FOR 1984-2013
Lower Rio Grande Valley

Map I.D.	Plant Name
1	North Alamo Supply Corporation (Donna)
2	North Alamo Supply Corporation (Doolittle)
3	North Alamo Supply Corporation (Lasara)
4	North Alamo Supply Corporation (Owassa)
5	North Cameron/Hidalgo Water Authority
6	Southmost Regional Water Authority
7	Valley MUD #2

LEGEND

Existing Desalination Plant
Rio Grande
Urban Area, as defined by USGS Border Environmental Health Initiative
Texas County
Model Boundary

Notes:
1) Basemap provided by Montgomery & Associates December 2016.
2) mg/L = milligrams per liter.
3) The colors represent different Y-axis scales:
   Green is 1,000 to 2,000
   White is 3,000 to 4,000
   Blue is 10,000

Scale in Miles
0   10   20

Projected Coordinate System
Datum: NAD 1983
Albers Equal Area

GSI ENVIRONMENTAL

GSI Job No. 4276	Drawn By: AVR
Issued: 21-Jun-2017	Chk'd By: KER
Map ID: LRGV_TDS_GWDP	Appv'd By: SP

FIGURE 6.7.13

Sources: Esri, USGS, NOAA

Job: 4276
Issued: 17 February 2017
Page 1

**Appendix A - Water Level
Observations Used for Model Calibration**

GSI
ENVIRONMENTAL

Well	Date	Layer	Water Level Elevation	Model Weight
15274_8747607	12/25/2008	5	74	1
15275_8860811	12/28/1999	1	19	1
33608_8850902	12/31/1985	1	33.46	1
	12/31/1986	1	32.67	1
	12/31/1987	1	32.71	1
	12/30/1988	1	32.6	1
	12/30/1989	1	32.79	1
	12/30/1990	1	32.7	1
	12/30/1991	1	30.2	1
	12/29/1992	1	30.9	1
	12/29/1993	1	29.8	1
	12/29/1995	1	30.7	1
	12/28/1997	1	30.4	1
33618_8904602	12/31/1985	1	23.12	1
	12/31/1986	1	21.72	1
	12/31/1987	1	21.3	1
	12/30/1988	1	21.57	1
	12/30/1989	1	19.6	1
	12/30/1991	1	17.3	1
	12/29/1992	1	18.3	1
	12/29/1993	1	22	1
	12/29/1995	1	18.1	1
	12/28/1996	1	21.9	1
	12/28/1997	1	21.92	1
	12/28/1998	1	20.95	1
	12/28/1999	1	19.65	1
	12/27/2001	1	19.11	1
	12/27/2002	1	15.1	1
	12/27/2003	1	20.57	1
	12/26/2004	1	22.24	1
	12/26/2005	1	17.55	1
	12/26/2006	1	16.09	1
	12/26/2007	1	20.1	1
	12/25/2008	1	21.48	1
	12/25/2010	1	18.72	1
	12/25/2011	1	20.4	1
	12/24/2012	1	17.8	1
	12/24/2014	1	17.35	1
33626_8859102	12/31/1985	1	36.5	1
	12/31/1986	1	32	1
	12/30/1988	1	33.58	1
	12/30/1989	1	33.49	1
	12/30/1990	1	31.75	1

Job: 4276
Issued: 17 February 2017
Page 2

**Appendix A - Water Level
Observations Used for Model Calibration**

GSI
ENVIRONMENTAL

Well	Date	Layer	Water Level Elevation	Model Weight
	12/30/1991	1	33.7	1
	12/29/1992	1	34.75	1
	12/29/1993	1	36	1
40029_8904634	12/28/1996	1	22	1
42502_8747208	12/27/2000	5	78.3	1
42503_8747209	12/27/2000	5	61.99	1
42860_8834301	12/24/2014	4	2.85	1
42998_-99999	12/27/2001	2	86	1
43196_8860725	12/26/2004	1	21	1
43199_8860812	12/24/2014	1	-6.2	1
43204_8860726	12/26/2004	1	22.1	1
43214_8860410	12/26/2004	1	22	1
43227_8740407	12/25/2011	5	37	1
	12/24/2014	5	55.03	1
43237_8842508	12/24/2012	1	34	1
43314_8731503	12/31/1985	4	69.55	1
	12/31/1986	4	68.96	1
	12/31/1987	4	66.07	1
	12/30/1988	4	71.83	1
	12/30/1989	4	68.82	1
	12/30/1990	4	64.4	1
	12/30/1991	4	62.8	1
	12/29/1992	4	60.4	1
	12/29/1993	4	61.2	1
	12/29/1994	4	68.4	1
	12/29/1995	4	63.88	1
	12/28/1996	4	68.68	1
	12/28/1997	4	60.6	1
	12/28/1998	4	61.2	1
	12/28/1999	4	59.6	1
	12/27/2000	4	60.7	1
	12/27/2001	4	60.86	1
	12/27/2002	4	55.98	1
	12/27/2003	4	55.76	1
	12/26/2004	4	62.43	1
	12/26/2005	4	68.62	1
	12/26/2006	4	59.99	1
	12/26/2007	4	71.22	1
	12/25/2008	4	73.75	1
	12/25/2010	4	71.28	1
	12/25/2011	4	72.04	1
	12/24/2012	4	68.33	1
	12/24/2013	4	64.5	1
	12/24/2014	4	63.14	1

Appendix A - Water Level
Observations Used for Model Calibration

GSI
ENVIRONMENTAL

Well	Date	Layer	Water Level Elevation	Model Weight
43320_8731601	12/31/1985	4	66.75	1
	12/31/1986	4	64.42	1
	12/30/1988	4	65.35	1
	12/30/1989	4	58.72	1
	12/30/1990	4	55	1
43329_8731903	12/31/1985	4	59.43	1
	12/31/1987	4	53.41	1
	12/30/1988	4	55.11	1
	12/30/1989	4	54	1
	12/30/1990	4	50	1
	12/30/1991	4	46	1
	12/29/1992	4	44.5	1
	12/29/1993	4	45.5	1
	12/29/1994	4	44.2	1
	12/28/1996	4	47.1	1
	12/28/1997	4	50.65	1
	12/27/2002	4	46.1	1
43333_8731917	12/31/1985	4	63.8	1
	12/31/1987	4	61.08	1
	12/30/1988	4	63.43	1
	12/30/1989	4	59.72	1
	12/30/1990	4	52.7	1
	12/30/1991	4	51.1	1
	12/29/1992	4	48.5	1
	12/29/1993	4	51.4	1
	12/29/1994	4	56.3	1
	12/29/1995	4	54.5	1
	12/28/1996	4	54.8	1
43346_8721211	12/31/1987	7	186	1
43365_8728705	12/29/1995	8	199	1
43370_8737301	12/31/1985	7	141	1
	12/31/1986	7	142.09	1
	12/31/1987	7	144.18	1
	12/30/1988	7	142.79	1
	12/30/1989	7	141.8	1
	12/30/1990	7	147	1
	12/30/1991	7	144.7	1
	12/29/1992	7	147	1
	12/29/1993	7	147.5	1
	12/29/1994	7	139	1
	12/29/1995	7	146.9	1
	12/28/1996	7	148.35	1
	12/28/1997	7	147.4	1
	12/28/1998	7	143.02	1

**Appendix A - Water Level
Observations Used for Model Calibration**

GSI
ENVIRONMENTAL

Well	Date	Layer	Water Level Elevation	Model Weight
	12/28/1999	7	142.55	1
	12/27/2000	7	143.35	1
	12/27/2001	7	138.07	1
	12/27/2002	7	139.6	1
	12/27/2003	7	139.81	1
	12/26/2004	7	141.67	1
	12/26/2005	7	139.33	1
	12/26/2006	7	138.22	1
	12/26/2007	7	135.13	1
	12/25/2008	7	135.55	1
	12/25/2010	7	134.8	1
	12/25/2011	7	136.58	1
	12/24/2012	7	135.15	1
	12/24/2013	7	134.78	1
	12/24/2014	7	134.64	1
43373_8738201	12/31/1985	6	122.4	1
	12/31/1986	6	121.12	1
	12/31/1987	6	123.82	1
	12/30/1988	6	124.9	1
	12/30/1989	6	125.3	1
	12/30/1990	6	125	1
	12/30/1991	6	118	1
	12/29/1992	6	125.8	1
	12/29/1993	6	126.5	1
	12/29/1994	6	126	1
	12/29/1995	6	125.39	1
	12/28/1996	6	126.7	1
	12/28/1997	6	125.85	1
	12/28/1998	6	123.8	1
	12/28/1999	6	121.52	1
	12/27/2000	6	120.05	1
	12/27/2001	6	116.6	1
	12/27/2002	6	118	1
	12/27/2003	6	117.4	1
	12/26/2004	6	118.54	1
	12/26/2005	6	117.16	1
	12/26/2006	6	116.65	1
	12/26/2007	6	115.99	1
	12/25/2008	6	115.74	1
	12/25/2010	6	138.7	1
	12/25/2011	6	135.98	1
	12/24/2012	6	131.74	1
	12/24/2013	6	130.7	1
	12/24/2014	6	124.79	1

**Appendix A - Water Level
Observations Used for Model Calibration**

Well	Date	Layer	Water Level Elevation	Model Weight
43387_8744501	12/31/1985	7	189.89	1
	12/31/1986	7	188.81	1
	12/31/1987	7	189.8	1
	12/30/1988	7	186.34	1
	12/30/1989	7	190.6	1
	12/30/1990	7	190.8	1
	12/30/1991	7	187.9	1
	12/29/1992	7	184.5	1
	12/29/1993	7	184.4	1
	12/29/1994	7	183.9	1
	12/28/1997	7	185.2	1
	12/27/2001	7	186.06	1
	12/27/2002	7	186.8	1
	12/27/2003	7	188.93	1
	12/26/2004	7	190.02	1
	12/26/2005	7	189.92	1
	12/26/2006	7	190.31	1
	12/25/2008	7	182.65	1
	12/25/2010	7	181.7	1
	12/24/2012	7	185.1	1
	12/24/2013	7	192.9	1
43418_8753205	12/28/1996	4	105	1
43420_8753302	12/28/1999	4	90.5	1
43427_8753503	12/31/1986	4	109.88	1
	12/30/1989	4	109	1
	12/30/1990	4	106.5	1
	12/30/1991	4	107.3	1
43430_8753606	12/28/1999	3	99	1
43432_8753608	12/28/1999	4	88.6	1
43434_8753610	12/28/1999	4	92.9	1
43439_8754104	12/31/1985	4	107.78	1
	12/31/1986	4	116.72	1
	12/31/1987	4	113.79	1
	12/30/1988	4	114.83	1
	12/30/1989	4	103.98	1
43444_8754517	12/28/1997	1	97	1
43470_8755405	12/28/1999	2	83	1
43481_8755602	12/28/1998	2	78.2	1
	12/27/2000	2	78.85	1
	12/27/2002	2	76.95	1
	12/27/2003	2	84	1
	12/26/2004	2	82.12	1
	12/26/2005	2	80.81	1
	12/26/2006	2	81.31	1

**Appendix A - Water Level
Observations Used for Model Calibration**

Well	Date	Layer	Water Level Elevation	Model Weight
	12/26/2007	2	81.4	1
	12/25/2008	2	79.36	1
	12/25/2010	2	80.28	1
	12/25/2011	2	81.24	1
	12/24/2012	2	75.75	1
43492_8756404	12/28/1997	3	84	1
43493_8756501	12/31/1985	2	82.28	1
	12/31/1986	2	83.21	1
	12/30/1988	2	82.07	1
	12/30/1989	2	82.6	1
	12/30/1990	2	81	1
	12/30/1991	2	81.5	1
	12/29/1992	2	83.5	1
	12/29/1995	2	83.35	1
	12/28/1996	2	83.5	1
43541_8857110	12/31/1986	1	43	1
43542_8857112	12/28/1999	1	33	1
43553_8858101	12/31/1985	1	49.3	1
	12/31/1986	1	47.39	1
	12/31/1987	1	49.75	1
	12/30/1988	1	49.2	1
	12/30/1989	1	47.88	1
	12/30/1990	1	48.2	1
	12/30/1991	1	47.2	1
	12/29/1992	1	49	1
	12/29/1993	1	51	1
	12/28/1996	1	49.82	1
	12/28/1998	1	47.95	1
	12/28/1999	1	33.8	1
	12/27/2000	1	30	1
	12/27/2001	1	38.73	1
	12/27/2003	1	39.11	1
	12/26/2004	1	37.78	1
	12/26/2005	1	48.49	1
	12/26/2006	1	48.12	1
	12/26/2007	1	50.92	1
	12/25/2008	1	51.87	1
	12/25/2011	1	54.59	1
	12/24/2012	1	53.72	1
	12/24/2013	1	52.5	1
	12/24/2014	1	54.12	1
43564_8858302	12/31/1985	1	41.74	1
	12/31/1986	1	40.15	1
	12/31/1987	1	38.46	1

**Appendix A - Water Level
Observations Used for Model Calibration**

GSI
ENVIRONMENTAL

Well	Date	Layer	Water Level Elevation	Model Weight
	12/30/1988	1	41.58	1
	12/30/1989	1	40.9	1
	12/30/1990	1	40.9	1
	12/30/1991	1	40.4	1
	12/29/1992	1	41.8	1
	12/29/1993	1	42.5	1
	12/29/1995	1	40.75	1
	12/28/1996	1	41.7	1
	12/28/1997	1	38.15	1
	12/28/1998	1	39.65	1
	12/28/1999	1	36.6	1
	12/27/2000	1	42.2	1
	12/27/2001	1	39.6	1
	12/27/2002	1	30.3	1
	12/27/2003	1	37.63	1
	12/26/2004	1	38.2	1
	12/26/2005	1	38.12	1
	12/26/2006	1	37.92	1
	12/26/2007	1	39.52	1
	12/25/2008	1	39.91	1
	12/25/2010	1	42.49	1
	12/25/2011	1	42.2	1
	12/24/2012	1	40.53	1
	12/24/2013	1	39.1	1
	12/24/2014	1	39.56	1
43577_8858402	12/31/1985	1	50.88	1
	12/31/1986	1	49.79	1
	12/31/1987	1	51.15	1
	12/30/1988	1	50.94	1
	12/30/1989	1	50.1	1
	12/30/1990	1	50.1	1
	12/30/1991	1	49.7	1
	12/29/1992	1	47.4	1
	12/29/1993	1	42	1
	12/28/1996	1	51.42	1
	12/28/1997	1	28.65	1
	12/28/1998	1	44.6	1
	12/28/1999	1	39.7	1
	12/27/2000	1	33.8	1
	12/27/2002	1	18.15	1
	12/27/2003	1	41.28	1
	12/26/2004	1	38.26	1
	12/26/2005	1	48.64	1
	12/26/2006	1	46.68	1

Appendix A - Water Level
Observations Used for Model Calibration

GSI ENVIRONMENTAL

Well	Date	Layer	Water Level Elevation	Model Weight
	12/26/2007	1	49.67	1
	12/25/2008	1	50.73	1
	12/25/2010	1	44.99	1
	12/25/2011	1	53.43	1
	12/24/2012	1	52.63	1
	12/24/2013	1	51.1	1
	12/24/2014	1	49.94	1
43581_8858502	12/31/1985	1	48.95	1
	12/31/1986	1	45.18	1
	12/31/1987	1	49.32	1
	12/30/1988	1	49.93	1
	12/30/1989	1	46.9	1
	12/30/1990	1	45.9	1
	12/30/1991	1	48.5	1
	12/29/1992	1	51.2	1
	12/29/1993	1	50.5	1
	12/29/1995	1	50.85	1
	12/28/1996	1	50.6	1
	12/28/1997	1	31.7	1
	12/28/1999	1	31.5	1
	12/27/2000	1	26.08	1
	12/27/2001	1	29.6	1
	12/27/2002	1	12.1	1
	12/27/2003	1	25.05	1
	12/26/2004	1	36.85	1
	12/26/2005	1	43.37	1
	12/26/2006	1	44.75	1
	12/26/2007	1	46.29	1
	12/25/2008	1	45.92	1
	12/25/2010	1	51.39	1
	12/25/2011	1	51.35	1
	12/24/2012	1	50.11	1
	12/24/2014	1	48.7	1
43584_8858608	12/30/1989	1	9	1
43607_8859401	12/31/1985	1	43.51	1
	12/31/1986	1	41.8	1
	12/30/1989	1	41.72	1
43615_8859502	12/31/1985	1	36.11	1
	12/31/1986	1	34.83	1
	12/31/1987	1	36.53	1
	12/30/1988	1	36.51	1
43628_8859917	12/31/1985	1	20	1
43629_8860101	12/31/1985	1	26.23	1
	12/31/1987	1	24.69	1

**Appendix A - Water Level
Observations Used for Model Calibration**

GSI
ENVIRONMENTAL

Well	Date	Layer	Water Level Elevation	Model Weight
	12/30/1988	1	25.37	1
	12/30/1989	1	24.85	1
	12/30/1990	1	23.8	1
	12/29/1992	1	25.8	1
	12/29/1993	1	26.6	1
	12/29/1995	1	25.07	1
	12/28/1996	1	25.5	1
	12/28/1997	1	19	1
	12/28/1998	1	25.15	1
	12/28/1999	1	18.95	1
	12/27/2000	1	21.9	1
	12/27/2001	1	19.99	1
	12/27/2002	1	20.05	1
	12/27/2003	1	21.84	1
	12/26/2004	1	23.52	1
	12/26/2005	1	20.36	1
	12/26/2006	1	15.19	1
	12/26/2007	1	16.12	1
	12/25/2008	1	16.63	1
	12/25/2010	1	17.65	1
	12/25/2011	1	17.52	1
	12/24/2012	1	15.25	1
	12/24/2013	1	13.67	1
	12/24/2014	1	14.8	1
43632_8860408	12/28/1999	1	20	1
43685_8849703	12/31/1986	1	54	1
43697_-99999	12/26/2006	5	64	1
43702_-99999	12/26/2004	10	209	1
43705_-99999	12/24/2012	2	55	1
43722_-99999	12/26/2006	7	158	1
43723_-99999	12/25/2009	7	58	1
43728_8721204	12/28/1998	7	188.4	1
	12/28/1999	7	182.5	1
	12/27/2000	7	184.3	1
	12/27/2001	7	179.71	1
	12/27/2002	7	181.67	1
	12/26/2005	7	186.6	1
	12/26/2007	7	158.65	1
	12/25/2011	7	186.51	1
	12/24/2012	7	186.02	1
	12/24/2013	7	183.45	1
	12/24/2014	7	185.19	1
43736_8857206	12/30/1991	1	35	1
43763_8754947	12/27/2000	3	51.88	1

Appendix A - Water Level
Observations Used for Model Calibration

GSI ENVIRONMENTAL

Well	Date	Layer	Water Level Elevation	Model Weight
43782_-99999	12/25/2010	5	-4	1
43784_-99999	12/26/2007	5	17	1
43785_-99999	12/26/2007	5	-21	0.01
43787_-99999	12/26/2006	4	-6	1
43801_-99999	12/26/2004	1	46	1
43802_-99999	12/26/2006	1	37	1
43809_8756604	12/24/2014	2	59.2	1
43811_-99999	12/25/2010	1	69	1
43815_-99999	12/24/2012	2	58	1
43819_-99999	12/26/2006	3	-44	0.01
43824_-99999	12/24/2012	5	28	1
43830_-99999	12/24/2012	5	21	1
43836_-99999	12/25/2008	5	34	1
43840_-99999	12/25/2009	5	57	1
43842_-99999	12/25/2009	4	63	1
43844_-99999	12/25/2008	6	96	1
43847_-99999	12/26/2007	6	47	1
43851_-99999	12/25/2009	6	144	1
43856_-99999	12/25/2008	7	141	1
43857_-99999	12/25/2009	6	72	1
43861_-99999	12/26/2006	6	116	1
43868_-99999	12/25/2008	7	113	1
43873_-99999	12/26/2004	10	305	1
43874_-99999	12/26/2005	10	298	1
43876_-99999	12/26/2005	9	195	1
43877_-99999	12/25/2008	10	125	1
43879_-99999	12/27/2003	8	174	1
43881_-99999	12/26/2004	9	271	0.2
43884_-99999	12/25/2008	9	237	1
43886_-99999	12/26/2004	6	354	1
43887_-99999	12/26/2005	10	447	0.2
43891_-99999	12/25/2009	9	359	1
43892_-99999	12/26/2005	8	181	1
43895_-99999	12/27/2003	8	335	1
43896_-99999	12/26/2006	7	298	1
43900_-99999	12/27/2001	3	88	1
43902_-99999	12/27/2002	3	86	1
43908_-99999	12/26/2004	1	35	1
43909_-99999	12/26/2004	4	67	1
43912_-99999	12/26/2005	1	49	1
43914_-99999	12/26/2006	7	176	1
43925_-99999	12/25/2009	1	21	1
43929_-99999	12/25/2010	3	82	1
43932_-99999	12/25/2010	4	46	1

Appendix A - Water Level
Observations Used for Model Calibration

GSI ENVIRONMENTAL

Well	Date	Layer	Water Level Elevation	Model Weight
43933_-99999	12/25/2008	4	97	1
43934_-99999	12/25/2009	1	20	1
43936_-99999	12/26/2006	1	18	1
43949_-99999	12/27/2003	2	36	1
43969_8748702	12/31/1985	2	83.76	1
	12/31/1986	2	83.73	1
	12/31/1987	2	82.71	1
	12/30/1988	2	82.95	1
	12/30/1989	2	83.1	1
	12/30/1990	2	82.6	1
	12/30/1991	2	81.4	1
	12/29/1994	2	83.4	1
	12/29/1995	2	82.9	1
	12/28/1996	2	82.9	1
	12/28/1997	2	81.95	1
	12/28/1998	2	82.44	1
	12/28/1999	2	81.8	1
	12/27/2000	2	80.95	1
	12/27/2001	2	81.3	1
	12/27/2002	2	81.9	1
	12/27/2003	2	84.2	1
	12/26/2004	2	83.65	1
	12/26/2005	2	82.72	1
	12/26/2006	2	81.3	1
	12/26/2007	2	83.17	1
	12/25/2008	2	83.15	1
	12/25/2010	2	80.22	1
	12/25/2011	2	78.9	1
	12/24/2012	2	78.15	1
	12/24/2013	2	77.8	1
	12/24/2014	2	78.66	1
43974_-99999	12/26/2007	8	195	1
43977_-99999	12/26/2007	9	86	1
43978_-99999	12/26/2007	8	233	1
44714_-99999	12/26/2005	5	80	1
44715_-99999	12/26/2006	4	59	1
44718_-99999	12/26/2007	4	27	1
44719_-99999	12/25/2011	4	38	1
44725_8727805	12/25/2011	9	237	1
4800_8747207	12/27/2000	4	77.3	1
4812_8860723	12/27/2002	1	19	1
48138_-99999	12/26/2005	5	111	1
-99999_8358201	12/27/2001	3	4.75	1
-99999_8358202	12/27/2000	3	7.32	1

**Appendix A - Water Level
Observations Used for Model Calibration**

GSI ENVIRONMENTAL

Well	Date	Layer	Water Level Elevation	Model Weight
	12/27/2002	3	1.2	1
	12/27/2003	3	4.22	1
	12/26/2004	3	4.76	1
	12/26/2005	3	5.08	1
	12/26/2006	3	-1.15	1
	12/26/2007	3	-1.18	1
	12/25/2008	3	-4.76	1
	12/25/2010	3	-2.18	1
	12/25/2011	3	-0.35	1
	12/24/2012	3	-1.3	1
	12/24/2013	3	-0.62	1
	12/24/2014	3	1.04	1
-99999_8458301	12/31/1986	9	541.8	1
	12/31/1987	9	543.67	1
	12/30/1988	9	532.48	1
	12/30/1989	9	524.8	1
	12/30/1990	9	546.3	1
	12/30/1991	9	553.3	1
	12/29/1992	9	524.5	1
	12/29/1993	9	529.2	1
	12/29/1994	9	531.8	1
	12/29/1995	9	549.16	1
	12/28/1996	9	535.35	1
	12/28/1997	9	553.3	1
-99999_8460402	12/31/1985	7	347.4	1
	12/31/1986	7	341.86	1
	12/31/1987	7	350.69	1
	12/30/1988	7	336.4	1
	12/30/1989	7	312.5	1
	12/30/1990	7	347	1
	12/30/1991	7	327.9	1
	12/29/1992	7	352.8	1
	12/29/1993	7	353.8	1
	12/29/1994	7	350.8	1
	12/29/1995	7	346.4	1
	12/28/1996	7	350.6	1
	12/28/1997	7	337.7	1
	12/28/1998	7	337.02	1
	12/28/1999	7	334.2	1
	12/27/2000	7	299	1
	12/27/2001	7	331.4	1
	12/27/2002	7	335.35	1
	12/27/2003	7	296.77	1
	12/26/2004	7	337.6	1

**Appendix A - Water Level
Observations Used for Model Calibration**

GSI ENVIRONMENTAL

Well	Date	Layer	Water Level Elevation	Model Weight
	12/26/2005	7	341.95	1
	12/26/2007	7	344.05	1
	12/25/2008	7	344.58	1
	12/25/2010	7	346.39	1
	12/25/2011	7	341.32	1
	12/24/2012	7	342.7	1
	12/24/2013	7	336.6	1
	12/24/2014	7	338.43	1
-99999_8463301	12/31/1985	4	64.98	1
	12/31/1986	4	67.15	1
	12/31/1987	4	72.26	1
	12/30/1989	4	90.8	1
	12/30/1990	4	66.66	1
	12/30/1991	4	64.99	1
-99999_8463602	12/31/1985	4	74.3	1
	12/31/1986	4	74.96	1
	12/31/1987	4	76.11	1
	12/30/1989	4	75.53	1
	12/30/1990	4	72.65	1
	12/30/1991	4	70.7	1
	12/29/1992	4	68.86	1
	12/29/1993	4	70.35	1
	12/29/1994	4	69.5	1
	12/29/1995	4	70.45	1
	12/28/1996	4	71.12	1
	12/28/1997	4	68.8	1
	12/28/1998	4	70.62	1
	12/28/1999	4	59.6	1
	12/27/2000	4	59.6	1
	12/27/2002	4	66.35	1
	12/27/2003	4	66.14	1
	12/26/2004	4	69.54	1
	12/26/2005	4	70.61	1
	12/26/2006	4	68.36	1
	12/26/2007	4	68.41	1
	12/25/2008	4	69.82	1
	12/25/2010	4	67.51	1
	12/25/2011	4	40.2	1
	12/24/2012	4	68.61	1
	12/24/2013	4	66.78	1
	12/24/2014	4	61.95	1
-99999_8463901	12/31/1985	4	92.28	1
	12/31/1986	4	91.85	1
	12/31/1987	4	91.66	1

**Appendix A - Water Level
Observations Used for Model Calibration**

GSI
ENVIRONMENTAL

Well	Date	Layer	Water Level Elevation	Model Weight
	12/30/1989	4	91.06	1
	12/30/1990	4	88.21	1
	12/30/1991	4	86.1	1
	12/29/1992	4	85.43	1
-99999_8701601	12/31/1986	1	391.45	1
	12/31/1987	1	402.8	1
	12/30/1989	1	397.8	1
	12/30/1991	1	400.6	1
	12/29/1992	1	406.2	1
	12/29/1993	1	376.9	1
	12/29/1994	1	384.95	1
	12/29/1995	1	404.58	1
	12/28/1996	1	455.8	1
	12/28/1997	1	400.2	1
	12/28/1998	1	383.21	1
	12/28/1999	1	396.8	1
	12/27/2001	1	393.65	1
	12/27/2002	1	401	1
	12/27/2003	1	405.35	1
	12/26/2004	1	410.5	1
	12/26/2005	1	406.1	1
	12/24/2012	1	401.27	1
	12/24/2013	1	407.9	1
	12/24/2014	1	410.45	1
-99999_8704402	12/31/1985	8	417.15	1
	12/31/1986	8	417.71	1
	12/31/1987	8	415.18	1
	12/30/1988	8	399.32	1
	12/30/1989	8	413.6	1
	12/30/1990	8	399.4	1
	12/30/1991	8	409.7	1
	12/29/1992	8	409.4	1
	12/29/1993	8	407.6	1
	12/29/1994	8	410.5	1
	12/29/1995	8	407.52	1
	12/28/1996	8	406.7	1
	12/28/1997	8	406.2	1
	12/28/1998	8	404.18	1
	12/28/1999	8	405.1	1
	12/27/2001	8	403.7	1
	12/27/2002	8	403.18	1
	12/27/2003	8	406.56	1
	12/26/2004	8	408.4	1
	12/26/2005	8	409.65	1

Well	Date	Layer	Water Level Elevation	Model Weight
	12/26/2007	8	408.34	1
	12/25/2008	8	408.38	1
	12/25/2010	8	407.65	1
	12/25/2011	8	410.61	1
	12/24/2012	8	408.55	1
	12/24/2013	8	407.35	1
	12/24/2014	8	403.25	1
-99999_8707302	12/31/1985	4	84.11	1
	12/31/1986	4	82.73	1
	12/31/1987	4	84.75	1
	12/30/1989	4	84.74	1
	12/30/1990	4	81.16	1
	12/30/1991	4	78.24	1
	12/29/1992	4	79.11	1
-99999_8707703	12/31/1985	4	133.12	1
	12/31/1986	4	134.37	1
-99999_8707704	12/31/1985	4	107.56	1
	12/31/1986	4	109.75	1
	12/31/1987	4	109.3	1
	12/30/1989	4	109.16	1
	12/30/1990	4	105.5	1
	12/30/1991	4	106.92	1
	12/28/1997	4	103.05	1
-99999_8707802	12/31/1985	4	105.17	1
	12/31/1986	4	106.3	1
	12/31/1987	4	106	1
	12/30/1989	4	103.86	1
	12/30/1990	4	97.79	1
	12/30/1991	4	96.8	1
	12/29/1992	4	108.15	1
	12/29/1993	4	108.31	1
	12/29/1994	4	105.28	1
	12/28/1996	4	106.5	1
	12/28/1997	4	97.1	1
	12/28/1998	4	100.3	1
	12/27/2002	4	96.9	1
	12/27/2003	4	96.44	1
	12/26/2004	4	100.81	1
	12/26/2005	4	101.69	1
	12/26/2006	4	96.06	1
	12/26/2007	4	98.98	1
	12/25/2008	4	99.45	1
	12/25/2010	4	101.18	1
	12/24/2012	4	101.1	1

**Appendix A - Water Level
Observations Used for Model Calibration**

GSI ENVIRONMENTAL

Well	Date	Layer	Water Level Elevation	Model Weight
	12/24/2013	4	100.7	1
	12/24/2014	4	98.4	1
-99999_8710402	12/31/1986	10	414.7	1
	12/30/1988	10	413.93	1
	12/30/1989	10	414	1
	12/30/1990	10	416.2	1
	12/29/1994	10	417.8	1
	12/28/1996	10	402.9	1
-99999_8710702	12/31/1986	10	404.44	1
	12/31/1987	10	408.33	1
	12/30/1988	10	404.94	1
	12/30/1989	10	410.3	1
	12/30/1990	10	410.5	1
	12/29/1995	10	404.24	1
-99999_8711601	12/31/1985	7	341.2	1
	12/31/1986	7	298.21	1
	12/31/1987	7	345.78	1
	12/30/1988	7	340.46	1
	12/30/1989	7	322.1	1
	12/30/1990	7	334.7	1
	12/30/1991	7	337.9	1
	12/29/1992	7	337.6	1
	12/29/1993	7	342	1
	12/29/1994	7	321.2	1
	12/29/1995	7	344.93	1
	12/28/1996	7	279	1
	12/28/1997	7	339.4	1
	12/28/1998	7	276.52	1
	12/28/1999	7	336.7	1
	12/27/2000	7	277.9	1
	12/27/2001	7	317.6	1
	12/27/2002	7	305.8	1
	12/26/2004	7	331.39	1
	12/26/2005	7	270.75	1
	12/26/2007	7	331.55	1
	12/25/2008	7	332.35	1
	12/25/2010	7	311.42	1
	12/25/2011	7	336.36	1
	12/24/2012	7	334.87	1
	12/24/2013	7	333.53	1
	12/24/2014	7	334.06	1
-99999_8712701	12/31/1986	8	368.1	1
	12/31/1987	8	369.5	1
	12/30/1988	8	360.97	1

Job: 4276
Issued: 17 February 2017
Page 17

**Appendix A - Water Level
Observations Used for Model Calibration**

GSI
ENVIRONMENTAL

Well	Date	Layer	Water Level Elevation	Model Weight
	12/30/1989	8	364.2	1
	12/30/1990	8	362.4	1
	12/30/1991	8	361	1
	12/29/1992	8	359.9	1
	12/29/1993	8	358.8	1
	12/29/1994	8	357.5	1
	12/29/1995	8	353.1	1
	12/28/1996	8	354.5	1
	12/28/1997	8	353.2	1
	12/28/1998	8	353.2	1
	12/28/1999	8	353.15	1
	12/27/2000	8	353.05	1
	12/27/2001	8	349.87	1
	12/27/2002	8	348.44	1
	12/27/2003	8	343.81	1
	12/26/2005	8	347.85	1
	12/26/2007	8	346.9	1
	12/25/2010	8	348.7	1
	12/25/2011	8	351.28	1
	12/24/2012	8	348.37	1
-99999_8713503	12/31/1985	6	177.95	1
	12/31/1986	6	177.22	1
	12/30/1989	6	178.35	1
	12/30/1990	6	185.83	1
	12/30/1991	6	188.03	1
	12/29/1992	6	188.62	1
	12/29/1994	6	187.85	1
	12/29/1995	6	191.3	1
	12/28/1996	6	191.2	1
	12/28/1997	6	190.22	1
	12/28/1998	6	188.8	1
	12/28/1999	6	186.9	1
	12/27/2000	6	183.84	1
	12/27/2001	6	184.1	1
	12/27/2002	6	174.1	1
	12/27/2003	6	176.93	1
	12/26/2004	6	184.32	1
	12/26/2005	6	183.92	1
	12/26/2006	6	183.2	1
	12/26/2007	6	184	1
	12/25/2008	6	183.65	1
	12/25/2010	6	183.57	1
	12/25/2011	6	184.78	1
	12/24/2012	6	183.63	1

Job: 4276
Issued: 17 February 2017
Page 18

**Appendix A - Water Level
Observations Used for Model Calibration**

GSI
ENVIRONMENTAL

Well	Date	Layer	Water Level Elevation	Model Weight
	12/24/2013	6	183.6	1
	12/24/2014	6	182.7	1
-99999_8718604	12/31/1985	10	227.85	0.2
	12/31/1986	10	290.56	1
	12/31/1987	10	302.41	1
	12/30/1988	10	285.7	1
	12/30/1989	10	286.5	1
	12/30/1990	10	299.3	1
	12/30/1991	10	300.8	1
	12/29/1992	10	298.1	1
	12/29/1993	10	297.2	1
-99999_8720703	12/29/1995	7	257.29	1
	12/28/1996	7	270.6	1
	12/28/1997	7	270.95	1
	12/28/1998	7	269.8	1
	12/28/1999	7	270.35	1
	12/27/2001	7	271.67	1
	12/27/2002	7	268.45	1
	12/27/2003	7	270.7	1
	12/26/2004	7	275.45	1
	12/26/2005	7	268.7	1
	12/26/2007	7	250.5	1
	12/25/2008	7	267.4	1
	12/25/2010	7	263.65	1
	12/25/2011	7	262.19	1
	12/24/2012	7	267.95	1
	12/24/2013	7	268.88	1
	12/24/2014	7	269.06	1
-99999_8720905	12/31/1985	7	197.83	1
	12/31/1987	7	192.84	1
	12/30/1988	7	185.13	1
	12/30/1989	7	195.7	1
	12/30/1990	7	197.8	1
	12/30/1991	7	195.2	1
	12/29/1992	7	188.2	1
	12/29/1993	7	195.8	1
	12/29/1994	7	186.2	1
	12/29/1995	7	165.02	1
	12/28/1996	7	203.4	1
	12/28/1997	7	206.4	1
	12/28/1998	7	192.84	1
	12/28/1999	7	194.8	1
	12/27/2000	7	223.5	1
	12/27/2001	7	229.73	1

Job: 4276
Issued: 17 February 2017
Page 19

**Appendix A - Water Level
Observations Used for Model Calibration**

GSI
ENVIRONMENTAL

Well	Date	Layer	Water Level Elevation	Model Weight
	12/27/2002	7	233.94	1
	12/27/2003	7	237.21	1
	12/26/2004	7	241.3	1
	12/26/2005	7	240.4	1
	12/26/2007	7	245.65	1
-99999_8721105	12/28/1998	6	253.95	1
	12/28/1999	6	254.05	1
	12/27/2000	6	255.48	1
	12/27/2001	6	249.68	1
	12/27/2002	6	253.03	1
	12/27/2003	6	252.06	1
	12/26/2004	6	257.5	1
	12/26/2005	6	253.9	1
	12/26/2007	6	258.1	1
	12/25/2008	6	257.95	1
	12/25/2010	6	260.72	1
	12/25/2011	6	262.79	1
	12/24/2012	6	259.23	1
	12/24/2013	6	257	1
	12/24/2014	6	261.1	1
-99999_8721804	12/26/2007	6	286.71	1
-99999_8724102	12/24/2014	4	30.79	1
-99999_8727703	12/24/2013	1	306.8	1
	12/24/2014	1	315.49	1
-99999_8727704	12/24/2014	1	289.65	1
-99999_8727804	12/24/2013	10	298.65	1
	12/24/2014	10	297.83	1
-99999_8728701	12/29/1995	9	155.4	1
	12/28/1996	9	145.62	1
	12/28/1997	9	139.73	1
	12/28/1998	9	140.5	1
	12/28/1999	9	145.4	1
	12/27/2000	9	141	1
	12/27/2001	9	142.84	1
-99999_8729901	12/31/1985	7	137.4	1
-99999_8731804	12/31/1985	4	76.96	1
	12/31/1986	4	72.94	1
	12/31/1987	4	71.87	1
	12/30/1988	4	77.12	1
	12/30/1989	4	72.2	1
	12/30/1990	4	66.1	1
	12/30/1991	4	60	1
	12/29/1992	4	58.2	1
	12/29/1993	4	58.8	1

GSI
ENVIRONMENTAL

Well	Date	Layer	Water Level Elevation	Model Weight
	12/29/1994	4	62.15	1
	12/29/1995	4	60.9	1
	12/28/1996	4	61.5	1
	12/28/1997	4	61.29	1
	12/28/1998	4	61.6	1
	12/28/1999	4	60.1	1
	12/27/2000	4	61.21	1
	12/27/2001	4	61.82	1
	12/27/2002	4	60.3	1
	12/27/2003	4	59.52	1
	12/26/2004	4	69.7	1
	12/26/2005	4	69.23	1
	12/26/2006	4	65.54	1
	12/26/2007	4	76.71	1
	12/25/2008	4	74.37	1
	12/25/2010	4	75.03	1
	12/25/2011	4	74.77	1
	12/24/2012	4	70.1	1
	12/24/2014	4	75.74	1
-99999_8731907	12/31/1985	4	53.37	1
	12/31/1986	4	53.57	1
	12/31/1987	4	51.9	1
	12/30/1988	4	50.5	1
	12/30/1989	4	51.6	1
	12/30/1990	4	49.3	1
	12/30/1991	4	48.8	1
	12/29/1992	4	46.2	1
	12/29/1993	4	45	1
	12/29/1994	4	45.15	1
	12/29/1995	4	44.32	1
	12/28/1996	4	45.25	1
	12/28/1997	4	43.5	1
	12/28/1998	4	47.35	1
	12/28/1999	4	46.6	1
	12/27/2000	4	45.25	1
	12/27/2001	4	44.97	1
	12/27/2002	4	44.4	1
	12/27/2003	4	43.18	1
	12/26/2004	4	46.72	1
	12/26/2005	4	48.04	1
	12/26/2006	4	45.1	1
	12/26/2007	4	45.6	1
	12/24/2012	4	43.42	1
	12/24/2013	4	43	1

GSI
ENVIRONMENTAL

Well	Date	Layer	Water Level Elevation	Model Weight
	12/24/2014	4	39.35	1
-99999_8734304	12/27/2000	10	273.36	1
-99999_8735806	12/24/2013	9	242.6	1
	12/24/2014	9	236.79	1
-99999_8739301	12/31/1985	4	60.15	1
	12/31/1986	4	59.31	1
	12/31/1987	4	58.17	1
	12/30/1988	4	59.34	1
	12/30/1989	4	57.56	1
	12/30/1990	4	56.5	1
	12/30/1991	4	54.5	1
	12/29/1992	4	54.1	1
	12/29/1993	4	43.01	1
	12/29/1994	4	53.2	1
	12/28/1997	4	53.11	1
-99999_8742103	12/31/1985	11	120.29	1
	12/31/1986	11	120.38	1
	12/30/1989	11	123	1
	12/30/1990	11	123.5	1
	12/30/1991	11	119.8	1
	12/29/1992	11	118.9	1
	12/29/1993	11	119.5	1
	12/29/1995	11	120.9	1
	12/28/1996	11	118.3	1
	12/28/1997	11	117.25	1
	12/28/1998	11	118.4	1
	12/27/2001	11	127.46	1
	12/27/2002	11	116.43	1
	12/27/2003	11	116.2	1
	12/26/2004	11	117.75	1
	12/26/2005	11	117.75	1
	12/25/2008	11	118.54	1
	12/24/2013	11	118.87	1
-99999_8743813	12/31/1985	9	116.66	1
	12/31/1986	9	116.12	1
	12/31/1987	9	111.04	1
	12/30/1989	9	118.9	1
	12/30/1990	9	116.9	1
	12/30/1991	9	114.6	1
	12/29/1992	9	117.5	1
	12/29/1993	9	114.2	1
	12/29/1995	9	116.7	1
	12/28/1996	9	112.35	1
-99999_8746401	12/31/1985	2	171.77	1

Job: 4276
Issued: 17 February 2017
Page 22

**Appendix A - Water Level
Observations Used for Model Calibration**

GSI
ENVIRONMENTAL

Well	Date	Layer	Water Level Elevation	Model Weight
	12/31/1986	2	172.46	1
	12/31/1987	2	166.66	1
	12/30/1988	2	175.52	1
	12/30/1989	2	175.93	1
	12/30/1990	2	175.2	1
	12/29/1992	2	164.1	1
	12/29/1994	2	167.1	1
	12/28/1997	2	162.26	1
-99999_8746608	12/24/2013	4	103.55	1
	12/24/2014	4	102.85	1
-99999_8746609	12/28/1999	4	113	1
	12/24/2013	4	107	1
	12/24/2014	4	106.6	1
-99999_8752306	12/31/1985	1	97.9	1
	12/31/1986	1	99.01	1
	12/31/1987	1	98.37	1
	12/30/1989	1	102.3	1
	12/29/1992	1	101.4	1
	12/29/1993	1	101.3	1
	12/29/1995	1	101.2	1
-99999_8753307	12/28/1996	4	111	1
-99999_8753619	12/24/2013	4	91.1	1
	12/24/2014	4	89.85	1
-99999_8754810	12/31/1985	1	98.66	1
	12/31/1986	1	98	1
	12/30/1988	1	99.38	1
	12/30/1989	1	100.55	1
	12/30/1990	1	100.5	1
-99999_8755601	12/31/1985	3	80.1	1
	12/31/1986	3	83.2	1
	12/31/1987	3	81.13	1
	12/30/1988	3	77.22	1
	12/30/1989	3	74.9	1
-99999_8755701	12/31/1985	2	81.78	1
	12/31/1986	2	83.81	1
	12/31/1987	2	82.68	1
	12/30/1988	2	83.05	1
	12/30/1989	2	82.05	1
	12/30/1990	2	81	1
	12/30/1991	2	81.8	1
	12/29/1992	2	81.9	1
	12/29/1993	2	82.1	1
	12/29/1994	2	80.7	1
	12/29/1995	2	81	1

**Appendix A - Water Level
Observations Used for Model Calibration**

Well	Date	Layer	Water Level Elevation	Model Weight
	12/28/1996	2	82.25	1
	12/28/1997	2	79.2	1
	12/28/1998	2	81.2	1
	12/28/1999	2	80.1	1
	12/27/2001	2	75.97	1
	12/27/2002	2	75.65	1
	12/27/2003	2	78.51	1
	12/26/2004	2	79.33	1
	12/26/2005	2	78.82	1
	12/26/2006	2	75.41	1
	12/26/2007	2	79.82	1
-99999_8755801	12/31/1985	3	78.8	1
	12/31/1986	3	79.56	1
	12/30/1989	3	77.2	1
	12/30/1991	3	74.9	1
	12/29/1992	3	76.7	1
	12/29/1993	3	78.3	1
	12/29/1995	3	75.1	1
	12/28/1996	3	76.25	1
	12/28/1997	3	74.75	1
	12/28/1998	3	75	1
	12/28/1999	3	73.4	1
	12/27/2000	3	75.48	1
	12/27/2001	3	75.33	1
	12/27/2002	3	74.9	1
	12/27/2003	3	76.6	1
	12/26/2004	3	75.88	1
	12/26/2005	3	77.38	1
	12/26/2006	3	74.13	1
	12/26/2007	3	77.47	1
	12/25/2008	3	78.03	1
	12/25/2010	3	76.99	1
	12/24/2012	3	76.07	1
-99999_8756701	12/31/1985	2	77.5	1
	12/31/1986	2	78.25	1
	12/31/1987	2	75.96	1
	12/30/1988	2	76.98	1
	12/30/1989	2	75.3	1
	12/30/1990	2	72.5	1
	12/30/1991	2	72.2	1
	12/29/1992	2	76	1
	12/29/1993	2	81.8	1
	12/29/1995	2	78.5	1
	12/28/1996	2	79.8	1

Job: 4276
Issued: 17 February 2017
Page 24

**Appendix A - Water Level
Observations Used for Model Calibration**

GSI
ENVIRONMENTAL

Well	Date	Layer	Water Level Elevation	Model Weight
	12/28/1998	2	78.1	1
-99999_8763503	12/31/1985	1	75.4	1
	12/31/1986	1	75.17	1
	12/30/1988	1	76.02	1
	12/30/1989	1	78.99	1
	12/30/1990	1	74.1	1
-99999_8763601	12/31/1985	1	66.74	1
	12/31/1986	1	67.36	1
	12/30/1988	1	69.41	1
	12/30/1989	1	70.55	1
	12/30/1990	1	67	1
	12/30/1991	1	68.9	1
	12/29/1992	1	70.3	1
	12/29/1993	1	68.5	1
	12/29/1995	1	68.9	1
	12/28/1996	1	68.72	1
	12/28/1997	1	63.95	1
	12/28/1998	1	65.4	1
-99999_8764101	12/31/1985	1	71.76	1
	12/31/1986	1	71.06	1
	12/30/1989	1	71.97	1
	12/30/1990	1	71	1
	12/30/1991	1	70.2	1
	12/29/1992	1	72.5	1
	12/29/1993	1	71.05	1
	12/29/1995	1	70.05	1
	12/28/1996	1	70.85	1
	12/28/1997	1	67.02	1
	12/28/1998	1	68.95	1
-99999_8764405	12/31/1985	1	66.48	1
	12/31/1986	1	65.71	1
	12/30/1988	1	68.95	1
	12/30/1989	1	70.9	1
	12/30/1990	1	68.1	1
	12/30/1991	1	65.8	1
	12/29/1992	1	71	1
	12/29/1993	1	67	1
	12/28/1996	1	66.95	1
	12/28/1999	1	70.3	1
	12/27/2000	1	63	1
	12/27/2001	1	61.46	1
	12/27/2002	1	57.5	1
	12/27/2003	1	55.2	1
	12/26/2004	1	66.44	1

**Appendix A - Water Level
Observations Used for Model Calibration**

Well	Date	Layer	Water Level Elevation	Model Weight
	12/26/2005	1	67.95	1
	12/26/2006	1	68.66	1
	12/26/2007	1	69.9	1
	12/25/2008	1	69.91	1
	12/25/2010	1	70.68	1
	12/25/2011	1	75.91	1
	12/24/2012	1	69.86	1
-99999_8801101	12/31/1985	4	41.61	1
	12/31/1986	4	39.57	1
	12/31/1987	4	42.16	1
	12/30/1989	4	41.32	1
	12/30/1990	4	40.65	1
	12/30/1991	4	40.26	1
	12/29/1992	4	36.8	1
	12/29/1993	4	35.5	1
	12/29/1994	4	38.21	1
	12/29/1995	4	39.53	1
	12/28/1996	4	39.11	1
	12/28/1997	4	34.68	1
	12/28/1998	4	32.73	1
	12/28/1999	4	34.4	1
	12/27/2000	4	31.7	1
	12/27/2002	4	33.5	1
	12/27/2003	4	31.94	1
	12/26/2004	4	31.44	1
	12/26/2005	4	34.33	1
	12/26/2006	4	32.75	1
	12/26/2007	4	32.45	1
	12/25/2008	4	32.51	1
	12/25/2010	4	31.56	1
	12/25/2011	4	32.15	1
	12/24/2012	4	31.62	1
	12/24/2013	4	28.85	1
	12/24/2014	4	27.45	1
-99999_8801202	12/31/1987	1	33.87	1
	12/30/1989	1	26.77	1
	12/30/1990	1	23.58	1
	12/30/1991	1	32.89	1
-99999_8801302	12/31/1985	4	28.79	1
	12/31/1986	4	26.76	1
	12/31/1987	4	29.72	1
	12/30/1989	4	28.2	1
	12/30/1990	4	29.87	1
	12/30/1991	4	29	1

Job: 4276
Issued: 17 February 2017
Page 26

**Appendix A - Water Level
Observations Used for Model Calibration**

GSI ENVIRONMENTAL

Well	Date	Layer	Water Level Elevation	Model Weight
	12/29/1992	4	27.6	1
	12/29/1993	4	29.22	1
	12/29/1994	4	30.01	1
	12/29/1995	4	26.12	1
	12/28/1996	4	28.8	1
	12/28/1997	4	24.9	1
-99999_8802103	12/31/1985	3	21.34	1
	12/31/1986	3	22.5	1
	12/31/1987	3	23.3	1
	12/30/1989	3	23.15	1
	12/30/1990	3	20.95	1
	12/30/1991	3	21.39	1
	12/29/1992	3	20.19	1
	12/29/1993	3	21.09	1
	12/29/1994	3	21.01	1
	12/29/1995	3	20.71	1
	12/28/1996	3	21.65	1
	12/28/1997	3	19.24	1
	12/28/1998	3	18.7	1
-99999_8802403	12/31/1985	4	24.1	1
	12/31/1986	4	24.05	1
	12/31/1987	4	24.26	1
	12/30/1989	4	24.43	1
	12/30/1990	4	22.5	1
	12/30/1991	4	22.82	1
	12/29/1994	4	23.27	1
-99999_8802603	12/31/1985	2	11.95	1
	12/31/1986	2	15.31	1
	12/31/1987	2	14.71	1
	12/30/1989	2	10.36	1
-99999_8809501	12/31/1985	4	34.79	1
	12/31/1986	4	34.93	1
	12/31/1987	4	35.01	1
	12/30/1991	4	34.28	1
-99999_8809802	12/31/1985	4	27.79	1
	12/31/1986	4	35.97	1
	12/31/1987	4	34.68	1
-99999_8810303	12/31/1985	1	-3.2	1
	12/31/1986	1	2.22	1
	12/31/1987	1	20.29	1
	12/30/1989	1	-5.48	1
	12/30/1990	1	-6.9	1
	12/30/1991	1	-6.97	1
	12/29/1993	1	-5.65	1

Job: 4276
Issued: 17 February 2017
Page 27

**Appendix A - Water Level
Observations Used for Model Calibration**

GSI
ENVIRONMENTAL

Well	Date	Layer	Water Level Elevation	Model Weight
	12/29/1994	1	-2.89	1
	12/29/1995	1	-4.9	1
	12/28/1996	1	-3.82	1
-99999_8810502	12/29/1993	3	30.05	1
	12/29/1994	3	28.28	1
	12/29/1995	3	27.15	1
	12/28/1996	3	27.65	1
	12/28/1997	3	23.15	1
-99999_8810503	12/31/1986	1	26.56	1
	12/30/1989	1	27.8	1
	12/30/1990	1	23.8	1
	12/30/1991	1	24.18	1
	12/29/1992	1	27.4	1
	12/29/1994	1	26.9	1
	12/29/1995	1	22.85	1
	12/28/1997	1	27.06	1
-99999_8810801	12/24/2012	4	22.5	1
	12/24/2013	4	22.5	1
	12/24/2014	4	21.5	1
-99999_8810802	12/31/1985	1	23.12	1
	12/31/1986	1	28.45	1
	12/31/1987	1	28.6	1
	12/30/1989	1	23.57	1
	12/30/1990	1	17.3	1
	12/30/1991	1	23.29	1
	12/29/1992	1	19.29	1
	12/29/1993	1	24.03	1
	12/29/1994	1	25.55	1
	12/29/1995	1	25.1	1
	12/28/1996	1	18.8	1
	12/28/1997	1	23.42	1
	12/28/1998	1	25.32	1
	12/28/1999	1	24.35	1
	12/27/2002	1	16	1
	12/27/2003	1	26.78	1
	12/26/2004	1	22.33	1
	12/26/2005	1	22.76	1
	12/26/2006	1	23.33	1
	12/26/2007	1	22.98	1
	12/25/2008	1	23.82	1
	12/25/2010	1	21.93	1
	12/25/2011	1	22.25	1
	12/24/2012	1	15.02	1
	12/24/2013	1	10.58	1

**Appendix A - Water Level
Observations Used for Model Calibration**

GSI
ENVIRONMENTAL

Well	Date	Layer	Water Level Elevation	Model Weight
	12/24/2014	1	11.3	1
-99999_8811701	12/31/1985	3	15.38	1
	12/31/1986	3	19.8	1
	12/31/1987	3	19.89	1
	12/30/1989	3	19.46	1
	12/30/1990	3	19.5	1
	12/30/1991	3	15.37	1
	12/29/1993	3	17.28	1
	12/29/1994	3	19.7	1
	12/29/1995	3	18.05	1
	12/28/1996	3	17.62	1
	12/28/1997	3	19.7	1
	12/28/1998	3	18.66	1
	12/28/1999	3	17	1
	12/27/2002	3	7	1
	12/27/2003	3	18.38	1
	12/26/2004	3	17.48	1
	12/26/2005	3	16.82	1
	12/26/2006	3	16.6	1
	12/26/2007	3	16.9	1
-99999_8817603	12/31/1985	1	13.82	1
	12/31/1986	1	22.8	1
	12/30/1989	1	22.2	1
	12/30/1990	1	14.5	1
	12/30/1991	1	15.7	1
	12/29/1993	1	20.22	1
	12/29/1994	1	23.66	1
	12/29/1995	1	11.7	1
	12/28/1997	1	9.5	1
-99999_8818403	12/31/1985	4	16	1
	12/31/1987	4	27.13	1
	12/30/1989	4	23.35	1
	12/30/1991	4	11.96	1
-99999_8818504	12/31/1985	4	27.47	1
	12/31/1987	4	28.14	1
	12/30/1989	4	26.06	1
	12/30/1991	4	24.52	1
-99999_8818701	12/31/1985	4	32.98	1
	12/31/1987	4	29.4	1
	12/30/1989	4	28.51	1
	12/30/1991	4	29.13	1
-99999_8818803	12/31/1985	4	25.13	1
	12/31/1987	4	25.84	1
	12/30/1989	4	23.42	1

Job: 4276
Issued: 17 February 2017
Page 29

Appendix A - Water Level
Observations Used for Model Calibration

GSI
ENVIRONMENTAL

Well	Date	Layer	Water Level Elevation	Model Weight
	12/30/1991	4	21.17	1
	12/29/1994	4	23.8	1
-99999_8819101	12/31/1985	3	-5.98	1
	12/31/1986	3	19.8	1
	12/30/1989	3	19.36	1
	12/30/1990	3	8	1
	12/30/1991	3	15.27	1
	12/29/1993	3	15.8	1
	12/29/1994	3	18.6	1
	12/29/1995	3	18.15	1
	12/28/1996	3	6.1	1
	12/28/1997	3	11.25	1
	12/28/1998	3	17.1	1
	12/28/1999	3	15.2	1
	12/27/2002	3	2.5	1
	12/26/2004	3	8.18	1
	12/26/2005	3	7.82	1
	12/26/2006	3	11.77	1
	12/26/2007	3	9.06	1
	12/25/2008	3	6.83	1
	12/25/2010	3	-11.3	1
	12/25/2011	3	0.02	1
	12/24/2012	3	-19.37	0.2
	12/24/2013	3	-19.55	0.2
	12/24/2014	3	-19.55	0.2
-99999_8819602	12/31/1985	1	-14	1
	12/31/1986	1	-12.42	1
	12/31/1987	1	-13.2	1
	12/30/1989	1	-14.87	1
	12/30/1990	1	-16.55	1
	12/30/1991	1	-14.6	1
	12/29/1993	1	-16.2	1
	12/29/1994	1	-14	1
	12/29/1995	1	-16.65	1
	12/28/1996	1	-15.25	1
-99999_8819603	12/24/2013	2	-19.17	0.2
	12/24/2014	2	-19.53	0.2
-99999_8819901	12/31/1985	1	-66.2	0.2
	12/31/1986	1	-8.9	1
	12/30/1989	1	19.61	1
	12/30/1990	1	8.22	1
	12/30/1991	1	18.72	1
-99999_8820501	12/31/1985	3	20.78	1
	12/31/1986	3	20.3	1

Appendix A - Water Level
Observations Used for Model Calibration

GSI
ENVIRONMENTAL

Well	Date	Layer	Water Level Elevation	Model Weight
	12/31/1987	3	23.4	1
	12/30/1989	3	20.73	1
	12/30/1990	3	14.25	1
	12/30/1991	3	20.52	1
	12/29/1993	3	17.1	1
	12/29/1994	3	20.1	1
	12/29/1995	3	24.2	1
	12/28/1996	3	20.6	1
	12/28/1997	3	17.25	1
	12/28/1998	3	21.7	1
	12/28/1999	3	18.95	1
	12/27/2002	3	13.2	1
	12/27/2003	3	16.4	1
	12/26/2004	3	20.15	1
	12/26/2005	3	19.15	1
	12/26/2006	3	17.58	1
	12/26/2007	3	16.26	1
	12/25/2008	3	17.36	1
	12/25/2010	3	15.2	1
	12/25/2011	3	15.96	1
	12/24/2012	3	11.97	1
	12/24/2013	3	8.45	1
	12/24/2014	3	7.25	1
-99999_8826203	12/31/1985	4	21.01	1
	12/31/1986	4	20.8	1
	12/31/1987	4	21.83	1
	12/30/1989	4	22.8	1
	12/30/1990	4	21.3	1
	12/30/1991	4	21.65	1
	12/29/1993	4	20.81	1
	12/29/1994	4	23.56	1
	12/29/1995	4	20.61	1
	12/28/1996	4	23.5	1
	12/28/1997	4	21.73	1
	12/27/2001	4	15.2	1
-99999_8826301	12/31/1985	4	25.33	1
	12/31/1986	4	24.68	1
	12/31/1987	4	25.25	1
	12/30/1989	4	20.67	1
	12/30/1990	4	7.55	1
	12/30/1991	4	19.23	1
	12/29/1993	4	21.49	1
	12/29/1994	4	21.47	1
	12/28/1996	4	21.8	1

Job: 4276
Issued: 17 February 2017
Page 31

**Appendix A - Water Level
Observations Used for Model Calibration**

GSI
ENVIRONMENTAL

Well	Date	Layer	Water Level Elevation	Model Weight
	12/28/1997	4	20.95	1
	12/27/2001	4	15	1
	12/27/2003	4	14.61	1
	12/26/2004	4	15.62	1
	12/26/2005	4	13.56	1
-99999_8826303	12/31/1985	4	21.63	1
	12/31/1986	4	18.48	1
	12/31/1987	4	21.98	1
	12/30/1989	4	19.8	1
	12/29/1993	4	12.16	1
	12/29/1994	4	19.65	1
	12/29/1995	4	18.8	1
	12/28/1996	4	21.7	1
	12/28/1997	4	15.74	1
	12/27/2001	4	11.9	1
	12/27/2002	4	5.9	1
	12/27/2003	4	11.92	1
	12/26/2004	4	13.37	1
	12/26/2005	4	12.19	1
	12/26/2006	4	4.55	1
	12/26/2007	4	5.4	1
	12/25/2008	4	5.4	1
	12/25/2010	4	-0.83	1
	12/25/2011	4	5.11	1
	12/24/2012	4	-30.94	0.2
	12/24/2013	4	-5.13	1
	12/24/2014	4	-3.3	0.2
-99999_8834101	12/31/1985	4	41.43	1
	12/31/1986	4	41.15	1
	12/31/1987	4	41.65	1
	12/30/1989	4	41.35	1
	12/30/1990	4	41	1
	12/30/1991	4	40.7	1
	12/29/1992	4	41	1
	12/29/1993	4	41.32	1
	12/29/1994	4	41.4	1
	12/29/1995	4	40.97	1
	12/28/1996	4	41.38	1
	12/28/1997	4	40.91	1
	12/28/1998	4	40.6	1
	12/28/1999	4	40.15	1
	12/27/2000	4	40.22	1
	12/27/2001	4	40.69	1
	12/27/2002	4	37.7	1

Job: 4276
Issued: 17 February 2017
Page 32

**Appendix A - Water Level
Observations Used for Model Calibration**

GSI
ENVIRONMENTAL

Well	Date	Layer	Water Level Elevation	Model Weight
	12/27/2003	4	37.05	1
	12/26/2004	4	36.96	1
	12/26/2005	4	25.46	1
	12/26/2006	4	5.4	1
	12/26/2007	4	-1.11	1
	12/25/2008	4	-11.11	1
	12/25/2010	4	-14.19	1
	12/25/2011	4	-6.75	1
	12/24/2012	4	-12.58	1
	12/24/2013	4	-7.9	1
-99999_8834102	12/31/1985	4	35.85	1
	12/31/1986	4	35.8	1
	12/31/1987	4	35.8	1
	12/30/1989	4	35.84	1
	12/30/1990	4	35.4	1
	12/30/1991	4	35.6	1
	12/29/1992	4	35.8	1
	12/29/1993	4	35.46	1
	12/29/1994	4	35.5	1
	12/29/1995	4	35.33	1
	12/28/1996	4	35.55	1
	12/28/1997	4	35.32	1
-99999_8834502	12/28/1997	1	31	1
-99999_8834601	12/31/1985	4	40.65	1
	12/31/1986	4	40.32	1
	12/31/1987	4	40.65	1
	12/30/1989	4	40.46	1
	12/30/1990	4	40.2	1
	12/30/1991	4	40.8	1
	12/29/1992	4	40.8	1
	12/29/1993	4	40.4	1
	12/29/1994	4	40.3	1
	12/29/1995	4	40.2	1
	12/28/1996	4	40.8	1
	12/28/1997	4	40.37	1
	12/28/1998	4	40.29	1
	12/28/1999	4	40.55	1
	12/27/2000	4	39.72	1
	12/27/2001	4	40.5	1
	12/27/2002	4	38.3	1
	12/27/2003	4	37.82	1
	12/26/2004	4	37.58	1
	12/26/2005	4	35.81	1
	12/25/2010	4	12.5	1

Job: 4276
Issued: 17 February 2017
Page 33

**Appendix A - Water Level
Observations Used for Model Calibration**

GSI
ENVIRONMENTAL

Well	Date	Layer	Water Level Elevation	Model Weight
	12/25/2011	4	15.53	1
	12/24/2012	4	11.8	1
	12/24/2013	4	13.8	1
	12/24/2014	4	12.6	1
-99999_8844203	12/24/2013	1	4.88	1
	12/24/2014	1	10.9	1
-99999_8849701	12/31/1985	2	62.81	1
	12/31/1986	2	62.9	1
	12/31/1987	2	62.25	1
	12/30/1988	2	62.59	1
	12/30/1989	2	62.85	1
	12/30/1990	2	61	1
	12/30/1991	2	61.3	1
	12/29/1992	2	63.3	1
	12/29/1993	2	65.1	1
	12/29/1995	2	62.35	1
-99999_8849702	12/31/1986	1	55	1
-99999_8855801	12/28/1997	1	-5	1
-99999_8855802	12/28/1997	1	-5	1
-99999_8857301	12/31/1985	1	49.3	1
	12/31/1986	1	49.02	1
	12/31/1987	1	47.38	1
	12/30/1988	1	49.25	1
	12/30/1989	1	48.7	1
	12/30/1990	1	48	1
	12/30/1991	1	48.8	1
	12/29/1992	1	50.2	1
	12/29/1993	1	49.4	1
	12/29/1995	1	47.98	1
	12/28/1996	1	47.09	1
	12/28/1997	1	11.89	1
	12/28/1998	1	46.8	1
	12/28/1999	1	31.9	1
	12/27/2000	1	25.77	1
	12/27/2003	1	37.08	1
	12/26/2004	1	42.32	1
	12/26/2005	1	52.53	1
	12/26/2006	1	44.95	1
	12/26/2007	1	49.5	1
	12/25/2008	1	53.3	1
	12/25/2010	1	54.53	1
	12/25/2011	1	56.1	1
	12/24/2012	1	51.85	1
	12/24/2013	1	50.84	1

**Appendix A - Water Level
Observations Used for Model Calibration**

Well	Date	Layer	Water Level Elevation	Model Weight
	12/24/2014	1	48.3	1
-99999_8857304	12/28/1997	1	36	1
-99999_8858103	12/31/1985	1	48.84	1
	12/31/1986	1	47.9	1
	12/31/1987	1	46.35	1
	12/30/1988	1	48.83	1
	12/30/1989	1	48.57	1
	12/30/1990	1	46.5	1
	12/28/1996	1	46.37	1
	12/28/1998	1	46.52	1
	12/28/1999	1	42.16	1
-99999_8858206	12/28/1999	1	33	1
-99999_8858503	12/28/1997	1	36	1
-99999_8859412	12/28/1997	1	27	1
-99999_8859511	12/28/1999	1	24	1
-99999_8859915	12/31/1985	1	20	1
-99999_8859916	12/31/1985	1	17	1
-99999_8860407	12/28/1997	1	20	1
-99999_8860701	12/31/1985	1	27.26	1
	12/30/1989	1	27.19	1
	12/30/1990	1	27.1	1
	12/30/1991	1	23.6	1
	12/29/1992	1	26.5	1
	12/29/1993	1	28	1
	12/29/1995	1	27	1
	12/28/1996	1	27.41	1
	12/28/1997	1	24.3	1
	12/28/1998	1	26	1
	12/28/1999	1	20.2	1
	12/27/2001	1	22.99	1
-99999_8863301	12/28/1997	1	-5	1
-99999_8904101	12/31/1985	1	27.85	1

Appendix B – Water Level Hydrographs

4800_8747207

4812_8860723

15274_8747607

15275_8860811

33608_8850902

33618_8904602

33626_8859102

40029_8904634

42502_8747208

42503_8747209

42860_8834301

42998_-99999

Appendix B –
Water Level Observations Used for
Model Calibration

Appendix B –
Water Level Observations Used for
Model Calibration

Appendix B –
Water Level Observations Used for
Model Calibration

Appendix B –
Water Level Observations Used for
Model Calibration

Appendix B –
Water Level Observations Used for
Model Calibration

Appendix B –
Water Level Observations Used for
Model Calibration

Appendix B –
Water Level Observations Used for
Model Calibration

Appendix B –
Water Level Observations Used for
Model Calibration

Appendix B –
Water Level Observations Used for
Model Calibration

Appendix B –
Water Level Observations Used for
Model Calibration

Appendix B –
Water Level Observations Used for
Model Calibration

Appendix B –
Water Level Observations Used for
Model Calibration

Appendix B –
Water Level Observations Used for
Model Calibration

Appendix B –
Water Level Observations Used for
Model Calibration

Appendix B –
Water Level Observations Used for
Model Calibration

Appendix B –
Water Level Observations Used for
Model Calibration

Appendix B –
Water Level Observations Used for
Model Calibration

Appendix B –
Water Level Observations Used for
Model Calibration

Appendix C– Water Level Hydrographs for Sensitivity to Storage Parameters

Legend

- • Observed Water Level Elevation (Feet AMSL)
- —— Simulated Water Level Elevation (Feet AMSL)
- —— Sensitivity to Low Storage Parameters
- —— Sensitivity to High Storage Parameters

Appendix C– Water Level Hydrographs for Sensitivity to Storage Parameters

Legend

● Observed Water Level Elevation
  (Feet AMSL)

— Simulated Water Level Elevation
  (Feet AMSL)

— Sensitivity to Low Storage Parameters

— Sensitivity to High Storage Parameters

Appendix C– Water Level Hydrographs for Sensitivity to Storage Parameters

43470_8755405

43481_8755602

43492_8756404

43493_8756501

43541_8857110

43542_8857112

43553_8858101

43564_8858302

43577_8858402

43581_8858502

43584_8858608

43607_8859401

Legend

• Observed Water Level Elevation (Feet AMSL)

— Simulated Water Level Elevation (Feet AMSL)

— Sensitivity to Low Storage Parameters

— Sensitivity to High Storage Parameters

3

# Appendix C– Water Level Hydrographs for Sensitivity to Storage Parameters

Legend

- Observed Water Level Elevation (Feet AMSL)
- Simulated Water Level Elevation (Feet AMSL)
- Sensitivity to Low Storage Parameters
- Sensitivity to High Storage Parameters

Appendix C– Water Level Hydrographs for Sensitivity to Storage Parameters


Legend

● Observed Water Level Elevation (Feet AMSL)

— Simulated Water Level Elevation (Feet AMSL)

— Sensitivity to Low Storage Parameters

— Sensitivity to High Storage Parameters

Appendix C– Water Level Hydrographs for Sensitivity to Storage Parameters


Legend

● Observed Water Level Elevation (Feet AMSL)

— Simulated Water Level Elevation (Feet AMSL)

— Sensitivity to Low Storage Parameters

— Sensitivity to High Storage Parameters

Appendix C– Water Level Hydrographs for Sensitivity to Storage Parameters

Legend

- Observed Water Level Elevation (Feet AMSL)
- Simulated Water Level Elevation (Feet AMSL)
- Sensitivity to Low Storage Parameters
- Sensitivity to High Storage Parameters

Appendix C– Water Level Hydrographs for Sensitivity to Storage Parameters

Appendix C– Water Level Hydrographs for Sensitivity to Storage Parameters

Legend

- Observed Water Level Elevation (Feet AMSL)
- Simulated Water Level Elevation (Feet AMSL)
- Sensitivity to Low Storage Parameters
- Sensitivity to High Storage Parameters

Appendix C– Water Level Hydrographs for Sensitivity to Storage Parameters

Legend

- Observed Water Level Elevation (Feet AMSL)
- Simulated Water Level Elevation (Feet AMSL)
- Sensitivity to Low Storage Parameters
- Sensitivity to High Storage Parameters

# Appendix C– Water Level Hydrographs for Sensitivity to Storage Parameters

Legend

● Observed Water Level Elevation (Feet AMSL)

— Simulated Water Level Elevation (Feet AMSL)

— Sensitivity to Low Storage Parameters

— Sensitivity to High Storage Parameters

Appendix C– Water Level Hydrographs for Sensitivity to Storage Parameters

Legend
- Observed Water Level Elevation (Feet AMSL)
- Simulated Water Level Elevation (Feet AMSL)
- Sensitivity to Low Storage Parameters
- Sensitivity to High Storage Parameters

Appendix C– Water Level Hydrographs for Sensitivity to Storage Parameters

Legend

● Observed Water Level Elevation (Feet AMSL)

─── Simulated Water Level Elevation (Feet AMSL)

─── Sensitivity to Low Storage Parameters

─── Sensitivity to High Storage Parameters

Appendix C– Water Level Hydrographs for Sensitivity to Storage Parameters

Legend

● Observed Water Level Elevation (Feet AMSL)

— Simulated Water Level Elevation (Feet AMSL)

— Sensitivity to Low Storage Parameters

— Sensitivity to High Storage Parameters

Appendix C– Water Level Hydrographs for Sensitivity to Storage Parameters

Legend

● Observed Water Level Elevation (Feet AMSL)

— Simulated Water Level Elevation (Feet AMSL)

— Sensitivity to Low Storage Parameters

— Sensitivity to High Storage Parameters

Appendix C– Water Level Hydrographs for Sensitivity to Storage Parameters

Legend

• Observed Water Level Elevation (Feet AMSL)

— Simulated Water Level Elevation (Feet AMSL)

— Sensitivity to Low Storage Parameters

— Sensitivity to High Storage Parameters

Appendix C– Water Level Hydrographs for Sensitivity to Storage Parameters

-99999_8855802

-99999_8857301

-99999_8857304

-99999_8858103

-99999_8858206

-99999_8858503

-99999_8859412

-99999_8859511

-99999_8859915

-99999_8859916

-99999_8860407

-99999_8860701

Legend

• Observed Water Level Elevation (Feet AMSL)

— Simulated Water Level Elevation (Feet AMSL)

— Sensitivity to Low Storage Parameters

— Sensitivity to High Storage Parameters

Appendix C– Water Level Hydrographs for Sensitivity to Storage Parameters

-99999_8863301

-99999_8904101

Legend

• Observed Water Level Elevation (Feet AMSL)

—— Simulated Water Level Elevation (Feet AMSL)

—— Sensitivity to Low Storage Parameters

—— Sensitivity to High Storage Parameters

Appendix D - Total groundwater pumping per model stress period for each county.

County	Model stress period								
	1	2	3	4	5	6	7	8	9
Representative Year									
	1984	1985	1986	1987	1988	1989	1990	1991	1992
Brooks	-1,050	-916	-1,173	-833	-947	-913	-735	-790	-818
Cameron	-1,898	-878	-1,233	-1,409	-1,138	-2,103	-1,957	-1,830	-1,626
Duval	0	0	0	0	0	0	0	0	0
Hidalgo	-15,127	-15,294	-6,977	-6,150	-6,695	-17,803	-28,119	-27,523	-15,909
Jim Hogg	-45	-162	-156	-272	-254	-77	-76	-64	-83
Jim Wells	0	0	0	0	0	0	0	0	0
Kenedy	-102	-88	-91	-101	-105	-103	-102	-104	-71
Kleberg	0	0	0	0	0	0	0	0	0
Starr	-1,846	-1,833	-1,648	-1,757	-1,660	-1,531	-1,622	-7,507	-3,832
Webb	0	0	0	0	0	0	0	0	0
Willacy	-59	-40	-30	-32	-33	-34	-34	-41	-37
Zapata	-2	-2	-2	-2	-2	-2	-2	-2	-1
Total Pumping Per Stress Period	-20,129	-19,213	-11,309	-10,556	-10,834	-22,566	-32,646	-37,860	-22,377

Note: Pumping rates are in acre-feet per year

Appendix D - Total groundwater pumping per model stress period for each county.

County	Model stress period						Model stress period		
	10	11	12	13	14	15	16	17	18
	1993	1994	1995	1996	1997	1998	1999	2000	2001
Brooks	-777	-869	-928	-976	-1,407	-1,350	-1,099	-2,055	-2,077
Cameron	-1,596	-1,383	-1,071	-1,616	-3,196	-2,898	-2,981	-7,156	-9,946
Duval	0	0	0	0	0	0	0	0	0
Hidalgo	-20,015	-24,525	-23,476	-21,032	-17,682	-23,577	-21,069	-13,174	-11,667
Jim Hogg	-82	-71	-72	-76	-76	-66	-66	-35	-50
Jim Wells	0	0	0	0	0	0	0	0	0
Kenedy	-83	-69	-65	-71	-63	-81	-85	-192	-188
Kleberg	0	0	0	0	0	0	0	0	0
Starr	-1,330	-1,465	-1,634	-1,664	-1,496	-1,757	-1,681	-1,398	-1,455
Webb	0	0	0	0	0	0	0	0	0
Willacy	-37	-32	-34	-35	-35	-41	-38	-32	-33
Zapata	-1	-1	-1	-1	-1	-1	-1	-1	-3
Total Pumping Per Stress Period	-23,921	-28,416	-27,281	-25,471	-23,956	-29,772	-27,020	-24,043	-25,419

Note: Pumping rates are in acre-feet per y

Appendix D - Total groundwater pumping per model stress period for each county.

County	19	20	21	22	23	24	25	26	27
	2002	2003	2004	2005	2006	2007	2008	2009	2010
Brooks	-1,939	-1,848	-1,794	-2,208	-2,260	-2,020	-2,474	-3,043	-2,332
Cameron	-9,277	-345	-339	-3,744	-5,697	-7,712	-5,032	-27,407	-9,912
Duval	0	0	0	0	0	0	0	0	0
Hidalgo	-11,498	-10,533	-9,795	-10,761	-8,921	-9,211	-11,436	-14,020	-11,168
Jim Hogg	-22	-26	-26	-230	-261	-239	-273	-314	-220
Jim Wells	0	0	0	0	0	0	0	0	0
Kenedy	-182	-63	-65	-432	-434	-360	-742	-603	-702
Kleberg	0	0	0	0	0	0	0	0	0
Starr	-1,578	-1,432	-1,561	-1,861	-1,976	-1,810	-2,135	-2,100	-2,535
Webb	0	0	0	0	0	0	0	0	0
Willacy	-43	-40	-40	-110	-129	-141	-120	-114	-137
Zapata	-1	-1	-1	-8	-8	-8	-70	-46	-21
Total Pumping Per Stress Period	-24,541	-14,288	-13,620	-19,355	-19,686	-21,501	-22,282	-47,648	-27,028

Note: Pumping rates are in acre-feet per y

Appendix D - Total groundwater pumping per model stress period for each county.

County	28	29	30
	2011	2012	2013
Brooks	-2,503	-2,188	-1,997
Cameron	-10,124	-10,390	-9,898
Duval	0	0	0
Hidalgo	-14,910	-13,964	-14,421
Jim Hogg	-205	-174	-236
Jim Wells	0	0	0
Kenedy	-687	-579	-484
Kleberg	0	0	0
Starr	-2,701	-2,102	-1,816
Webb	0	0	0
Willacy	-1,004	-933	-941
Zapata	-17	-6	-7
Total Pumping Per Stress Period	-32,152	-30,337	-29,801

Note: Pumping rates are in acre-feet per y

Appendix D - Total groundwater pumping per model stress period for each county

County	Model Stress period				
	1	2	3	4	5
	Representative Year				
	1984	1985	1986	1987	1988
Brooks	-1.25E+05	-1.09E+05	-1.40E+05	-9.94E+04	-1.13E+05
Cameron	-2.27E+05	-1.05E+05	-1.47E+05	-1.68E+05	-1.36E+05
Duval	0.00E+00	0.00E+00	0.00E+00	0.00E+00	0.00E+00
Hidalgo	-1.81E+06	-1.83E+06	-8.33E+05	-7.34E+05	-7.99E+05
Jim Hogg	-5.37E+03	-1.93E+04	-1.86E+04	-3.24E+04	-3.03E+04
Jim Wells	0.00E+00	0.00E+00	0.00E+00	0.00E+00	0.00E+00
Kenedy	-1.21E+04	-1.05E+04	-1.08E+04	-1.21E+04	-1.25E+04
Kleberg	0.00E+00	0.00E+00	0.00E+00	0.00E+00	0.00E+00
Starr	-2.20E+05	-2.19E+05	-1.97E+05	-2.10E+05	-1.98E+05
Webb	0.00E+00	0.00E+00	0.00E+00	0.00E+00	0.00E+00
Willacy	-7.01E+03	-4.74E+03	-3.61E+03	-3.84E+03	-3.96E+03
Zapata	-2.80E+02	-2.47E+02	-2.36E+02	-2.27E+02	-2.39E+02
Total Pumping Per Stress Period	-2.40E+06	-2.29E+06	-1.35E+06	-1.26E+06	-1.29E+06

Appendix E – Responses to Comments

Comments shown in italics font. Responses to comments shown in regular font.

Draft Numerical Model Report comments:

General comments to be addressed

1. *In the legend of the figures and in the text of the report: as applicable, please remove "River" after Rio Grande since Rio and River are redundant terms; for example, LRG River or Rio Grande River.*

   This is done.

2. *Please review Exhibit 8 (pages 26 through 32 of 38 pages) of the contract for text, tables and figures to include (as applicable) for adhering to the standardization of numerical model reports for the Groundwater Availability Modeling (GAM) Program. Specific items are requested in comments below.*

   We have standardized the report including accessibility considerations.

3. *In the numerical model report, please focus on the input values and attributes for the numerical model and results obtained. Please provide all numerical model inputs and attributes in model grid format in figures unless a uniform value was used for a layer. In the case of uniform value case, please clearly state the value in the text.*

   All numerical inputs have been provided in figures and uniform values are in tables or clearly stated in the text.

4. *If possible, please overlay modeled water level on observed water level contours using different line colors or styles for selected years to help readers understand how well the numerical model simulated the groundwater flow system.*

   This is done on Figures 4.3.18, 19, and 20.

5. *Please make all figures self-explanatory so the reader does not have to refer to the text to identify the contents. Also, please identify the data presented in the figures as measured, estimated or modeled either in the figure captions (recommended) or text.*

   This is done.

6. *Section 2.0, pages 3 to 4: per Exhibit B of the contract, Section 8.0, pages 26 and 27 of 38, please briefly describe the conceptual model and the associated block diagram from the conceptual model report. If possible, please provide comparative figures so that differences between the numerical model input and conceptual model information may be visualized.*

   Explanation is included in the text and comparative figure is provided.

7. *If changes have been made since the conceptual model report, the contractor must document these changes and provide data and analyses to support the changes. Also, if information from the conceptual model was not directly used to construct the numerical model, please provide justification. For example, measured hydraulic conductivity values as pointed out in #56 below.*

    The conceptual model was used to develop the numerical model and no changes were made unless specifically indicated in the numerical model report. Comment #56 is addressed below.

8. *Please add the hydrogeological unit name for each model layer in the figures. For example, use " ... Model Layer 1 (Beaumont Formation of Chicot Aquifer) ... ".instead of " ... Model Layer 1 ... ".*

    This is done.

9. *We would like to commend the team on an overall well written report and deliverables including database.*

    Thank you.

Specific Comments to be addressed

10. *Please provide justification that natural (recharge, discharge etc.) and anthropogenic conditions (pumping, water diversions etc.) in the year 1984 were representative of steady-state conditions. If necessary, please edit the numerical model and report accordingly.*

    Natural conditions vary seasonally in most climate settings. Steady-state conditions are used in a numerical model to kick-off transient simulations. Average conditions of a year are typically used for this purpose.

11. *Executive Summary, page 1, paragraph 4 and Section 2.0, page 4, paragraphs 1 and 2: the Executive Summary states the steady state was 'based on 1984 conditions and the transient conditions were from 1985 through 2013 and in Section 2.0, the steady state, pre-1985 conditions, was represented by 1984 data and transient conditions were annual from 1985 through 2013. Please update text so dates and assumptions are consistent with the model. For example, the 1984 conditions could be stated as pre-1985 or steady-state conditions consistently throughout the report.*

    Text has been updated to be consistent and refer to 1984 conditions as steady-state.

12. *Section 1.0, page 3: per Exhibit B of the contract, Section 8.0, page 26 of 38, please move and reference Figure 2.4.1 in the Introduction Section of the report.*

    The model domain figure has been introduced in Section 1.

13. *Section 2.0, page 4, paragraphs 1 and 2: please expand text with reasoning for selecting 1984 with supporting documentation for pumping and recharge prior to 1985. Please provide supporting documentation that the steady-state produced reasonable starting heads for the transient calibration.*

    A sentence has been added indicting why this time period was selected. A sentence has been added in Section 4.3.3 indicting that the steady-state 1984 simulation provided reasonable starting heads.

14. *Section 2.1, pages 4 to 5: per Exhibit B of the contract, Section 8.0, page 27 of 38, please add BCT, DDF, CCB, CON packages to Table 2.1.1 and cross-reference discussion of packages in text to this table.*

    BCT and DDF have been added to Table 2.1.1. CON and CCB are output files and have been added to table 2.1.2 for output file names.

15. *Section 2.14 EVT Package, Paragraph 2: please provide reference for Mesquite rooting depths.*

    The reference has been added.

16. *Section 2.4.1, pages 5 to 6: per Exhibit B of the contract, Section 8.0, page 27 of_ 38, please include at least two cross-section figures (perpendicular to each other) showing the numerical layers and related hydrogeologic units.*

    Cross-sections are included.

17. *Figures 2.4.3 to 2.4.20: please note in the legend of the figures (related to base elevations) if the elevation contours are in reference to mean sea level.*

    This has been done.

18. *Section 2.3, page 5 and Section 2.4.1, page 6: Section 2.3 states the model was constructed to eliminate any inactive areas and thus all cells were active for the model; however Section 2.4.1 states there were 744,324 active groundwater cells in the model-out of a total of 1,149,564 cells which included no-flow and pinch-out cells. Please clarify in the referenced text if model cells were eliminated or inactivated.*

    There are no inactive cells in the model and the statement in Section 2.4.2 has been clarified.

19. *Figure 2.5.1 through 2.5.9: sand fraction maps appear to have difference based on county line boundaries. Please clarify in the report and make appropriate adjustments as necessary.*

    As described in Section 4.5.3 of the Conceptual Model report, net sand distributions for the valley come from three sources. A single dataset was not available for the entire study area, so the three source datasets were merged. The BRACS dataset was used for most of the model area, and the outlying areas to the north and west were filled in with data from other

studies. Discrepancies at county lines occur due to 1) discrepancies in net sand values in the different datasets and 2) the BRACS dataset being defined by county lines.

20. *Figure 2.6.3: please simplify values in figures and graphs to whole numbers; for example, please use 8 acre-feet per year instead of 08 (labeling by IBWC stream gages), please use 4,613 instead of 4613.00 (labeling by IBWC stream gages), and in. graphs kindly remove ".000" in the vertical axis labels.*

    This has been done.

21. *Section 2.6.3, page 8: per Exhibit B of the contract, Section 8.0, page 27 of 38, please provide a table of total pumping per county per stress period for each layer in an appendix and reference it in the stated section.*

    Well pumping is from all layers and the pumping adjusts dynamically among layers for each time step in each stress period. We have provided a table of total pumping per county per stress period in Appendix D.

22. *Figure 2.7.1: please clarify in the figure if a no-flow boundary is assumed for the model boundary in Brooks and Kenedy counties (black line indicates model boundary) and in Mexico along the southern extent of the model. Also, the constant head boundary representing the Gulf appears to cover the off-coast areas. Please correct.*

    The constant head representing mean sea levels has also been implemented in the lagoon.

23. *Section 2.8.1, page 9: second to last sentence references Figure 2.8.2. Please clarify if this should be Figure 2.8.1 and adjust the text as needed.*

    The reference to Figure 2.8.2 is correct.

24. *Figure 2.8.4: please correct the word confining in the legend for the Burkeville Confining Unit.*

    This has been done.

25. *Figure 2.8.5: suggest "layering" the pumping amounts such that the highest use is always visible then the second highest pumping is only blocked by the highest, and so forth. It is difficult to see the highest pumping along the Rio Grande discussed in the text on page 10.*

    This has been done.

26. *Section 2.10, page 10: text discusses making a no flow boundary along parts of the northern boundary. Please explain in the stated section or in Section 7.0 Modeling Assumptions and Limitations that such an assumption is reasonable with respect to location of current and/ or proposed desalination plants from the boundary. To provide perspective, please note that the GAM program had developed the alternative Groundwater Management Area 16 model because predictive model simulations and pumping assumptions resulted in boundary issues.*

An explanation is provided in Section 2.10 that the desalination plants are sufficiently far from the boundary to cause an impact.

27. *Section 2.10, page 10: per Exhibit B of the contract, Section 8.0, page 28 of 38, please provide a table of GHB head and conductance values as well as associated model lay/row/column or cell number and hydraulic features.*

This has been provided and referenced in Section 2.10.

28. *Section 2.13, pages 11to12 and Figure 2.13.2: please clarify the zoning of recharge in Laguna Madre between Padre Island and the coastline. Please discuss the reasoning for applying recharge since Figure 2.7.1 indicates Laguna Madre and Padre Island have a constant head boundary.*

Recharge applied to the model is shown on Figure 4.1.1 and it does not overlap with the constant head boundary. Figure 2.13.2 shows the recharge distribution from the conceptual model. This has been made more explicit in the figure titles and legends.

29. *Section 2.13, pages 11to12 and Figure 2.13.2: please label Arroyo Colorado Floodway on the figure since it is discussed in the text.*

We have removed the reference to lakes and the floodway from the document instead.

30. *Figure 2.14.1: please explain why the maximum evapotranspiration (ET) rate is zero outside surface water bodies and canals.*

The ET distribution shown on the figure represents ET from mesquite and oak woodlands, as shown in Figure 2.2.2 of the Conceptual Model report. A rate of zero is specified for crop and urban areas because the groundwater table is below the root zone of crops and other vegetation. The groundwater model was developed to simulate only groundwater losses from ET and a net recharge was applied in the irrigated areas near to the River.

31. *Figures 3.1.1, Figures 3.1.2-A through 3.1.2-D: information in these figures is also presented in Figures 4.3.5-A through 4.3.5-D. Please try to eliminate redundant information.*

Figures 3.1.2 discuss the available data while Figures 4.3.5 depict calibration against observed data. Both are therefore kept for completeness.

32. *Figure 4.2.1: please explain and if necessary, edit the anomalous high hydraulic conductivity values present in the Gulf (red dots).*

    The red dots in the Gulf are where the sand fraction was unity. A constant head boundary condition is provided in the Gulf on layer 1 so these isolated occurrences do not impact the model.

33. *Section 4.3.1page17 and Table 4.3.1: please update text or table so terms agree and are consistent; for example text states absolute residual while table lists this as residual mean.*

    Terms have been made consistent in the report.

34. *Figure 4.3.2: please consider splitting figure into multiple figures and using symbols. It is difficult to review the fit of the various water levels per layer when stacked.*

    The figure has been shown whole as well as split up to show the different layers in different graphs.

35. *Figures 4.3.6 to 4.3.17 (simulated water levels in 2013): please overlay 2013 measured water level contours (in different color or different line symbol) or if data is sparse, please include targets with water level measurement.*

    We have instead put the simulated values on Figures 4.3.18, 4.3.19 and 4.3.20 for the middle of the aquifer units for comparison.

36. *Figure 4.3.22 and Figure 4.3.23: recommend the use of negative values for outflow components to make the figures easier to understand.*

    We had done this initially but it was then difficult to compare the inflow and outflow component magnitudes. All inflow components are in solid line and outflow components are dashed lines to help distinguish them.

37. *Figures 4.3.13 to 4.3.15 (Simulated Water Levels in Model layers 8, 9, and 10): please clarify the reasoning for the 30 foot contour along the eastern extent of the model located under the Gulf of Mexico (unlikely to be caused by pumping) and the appearance of "pinch out" cells in layer 10 along the eastern model extent.*

    The 30 foot contour along the eastern extent of the model under the Gulf of Mexico is simulated because the Burkeville Confining Unit (layer 7) extends into the Gulf of Mexico causing resistance to upward flow thus raising the heads.

38. *Section 4.3.4, page 18, paragraph 2: text states that figures 4.3.8, 4.3.18 and 4.3.11, 4.3.19 compare well. Please clarify this statement as the contours appear somewhat aligned in the south although the ones in the north are steeper near the outcrop for the simulated water levels.*

    Figures 4.3.18, 4.3.19 and 4.3.20 now include both simulated and estimated water levels so that a direct comparison can be made.

39. *Section 4.3.6, page 19, last paragraph: please expand discussion on possible reasoning for the 8 wells with flow reduction such as insufficient screening information or pumping was estimated.*

Explanation has been extended in the report.

40. *Figures 5.1.1-A to 5.1.1-D: please update hydrographs with model layer/geologic unit.*

The model layer is now shown in color on the well symbol.

41. *Section 5.2, Page 20, Paragraph 1: please provide reference to the analysis or graph where it is shown that water levels do not indicate long-term trends.*

Figures 3.1.2 show the data indicating generally stable water levels. However, some wells are noted to increase and some decline. The explanation has been extended in the text in Section 5.2.

42. *Table 5.3.1: for consistency, please use whole numbers in the value column.*

This is done.

43. *Section 5.3, Page 21, Paragraph 2: please provide reference for the statement that "In general, errors in recharge and other boundary fluxes are in the order of 30% with maximum errors .... ".*

This was a professional judgement call. The statement has been removed.

44. *Please explain how the head residual was calculated and use that consistently through the documentation.*

This is done in Section 4.3.1 where the residuals are first discussed. A clarifying sentence is included: "All residuals are computed as observed minus simulated metrics thus positive residuals indicate that simulated water levels are lower than observed, while negative residuals indicate that simulated water levels are higher than observed. ".

45. *Figures 6.3.1 through 6.3.9: porosity distribution between Kenedy County and Willacy County to the south appears to change abruptly at the county line. This is also observed in many of the figures between Brooks and Hidalgo counties and Jim Hogg and Starr counties. Please review and, if applicable, edit distribution of porosity or explain this apparent anomaly in the text.*

This results from abrupt changes in sand fractions that were provided to us. The anomaly has been explained in the text.

46. *Section 6.3, page 25, 2ⁿᵈ to last paragraph: text references Burke County. Please update text as appropriate.*

This has been corrected to Brooke County.

47. *Section 6.6, Page 27, Paragraph 2: "The sharp concentration zones of Figures 6.1.1 through 6.1.6 produced sharp horizontal gradients ... " Please provide justification of inclusion of sharp concentration zones in the model in relation with conditions in the natural space. If necessary, please make changes to the model report and the numerical model as applicable.*

These sharp zones of concentration were provided in the BRAC database and were used in the model. This has been noted further in Section 6.1 where initial conditions are discussed.

48. *Section 6.7: please describe, using a table or detailed text, the differences between the various simulations with respect to pumping, recharge, transport, density coupling or not.*

The first paragraph of section 6.7 now includes text discussing the various scenario simulations.

49. *Section 6.7, Page 28, Paragraph 3: "The no-density case deviated significantly from the base-case and no-pumping cases for these locations indicating that the density term had a considerable impact ... ", and Paragraph 4: "Considering the small difference in results between running transport with and without density, future predictive simulations may be performed using the non-density version ... ". These two statements in the same section appear to be contradictory. Please update the report and clarify whether including transport in the simulations is important or not while distinguishing between coupled and non-coupled transport simulations.*

This has been reworded.

50. *Figure 6.7.13: the initial salinity distribution map in the area of Southmost Regional Water Authority (plant #6 on the graph) appears to be inaccurate. The raw water ranges in total dissolved solids values of 1,839-5,032 parts per thousand for the wells feeding this plant. The input salinity map may contain the inaccuracies perhaps due to the way BRACS data was processed for the study. Please clarify the referenced error in Figure 6.7.13.*

The BRACS LRGV salinity dataset and the methods used for model input both introduce inaccuracies to the model. As described in Section 4.8.1 of the Conceptual Model report, a vertical weighted average TDS value was determined for each model grid cell based on the BRACS LRGV salinity datasets. The averaging method was needed because the model layers are thicker than the BRACS salinity zones in most areas of the model domain. Furthermore, in order to assign numerical TDS values to the model grid, the qualitative description of each BRACS zone (ie, "moderately saline") had to be converted to a numerical value. The numerical value assigned to an entire zone is equal to the mean concentration of the corresponding TDS range established by TWDB for each salinity category. For example, a value of 6500 mg/L was assigned to "moderately saline" zones, which has a TDS range of 3000-10000 mg/L. The BRACS zones do not represent heterogeneity of TDS concentrations within each zone.

51. *Section 7.0, Page 29, Paragraph 1: "enabling regional evaluations at long time-scales (of months to decades)." Suggest replacing months with years in the sentence since the model has annual stress periods.*

   That is correct. This has been reworded.

52. *Section 7.0, Page 29, Paragraph 4, bullet 1: suggest replacing the word "accurate" with "detailed".*

   This has been reworded.

Draft Numerical Model comments:

General comments to be addressed

53. *Per Exhibit B, Section 4.4.2, page 35 of 38 of the contract: please provide more documentation for the modeling code. Also, please note that official/published documentation and source code is to be submitted with or referenced in the final deliverable.*

   A brief documentation of the equations being solved for transport is provided. Documentation and source code will be submitted with the final deliverable.

54. *Please provide a readme file in the numerical model folder with documentation of changes made to Groundwater Vistas input options that influences the creation of the LPF package to make the user aware of the change.*

   A readme file has been included in the numerical folder indicating the files and changes made to accommodate the LRGV model.

55. *Please clarify clearly in the numerical model report that due to lack of historical total dissolved solid (TDS) data, calibration was not performed for the transport part of the model after consultation with GAM and BRACS staff at the TWDB due to lack of temporal specificity.*

   A sentence has been added at the end of Section 6.6 indicting this.

Draft Numerical Model comments:

Specific comments to be addressed

56. *Layer Property Flow (LPF) Package: the horizontal hydraulic conductivity (Kx) values for Model Layer 1 (Beaumont of Chicot Aquifer), 2 (Lissie of Chicot Aquifer), and 3 (Willis of Chicot Aquifer) appear too high in comparison with measured data from pumping test and specific capacity test presented in the conceptual model. For example, Kx values of these three model layers range from about 1.6 to 700 feet per day, with a geometric mean of 157 feet per day, while the measured values range from 2 to 5,090 feet per day, with a geometric mean of 28 feet per day. Since the conceptual model does not match the numerical model, please explain the difference and if necessary edit the numerical model. Additionally, please update the model report appropriately since the numerical model is significantly different from the conceptual model.*

    The numerical model has been developed based on the conceptual model. As documented in the report, the model attempted to use sand fraction distributions for hydrogeologic parameterization with values attributed to the sand and non-sand portions that were calibrated using an expert interactive approach along with automatic parameter estimation using PEST. Calibrated hydraulic conductivity values for the Beaumont and Lissie Formations averaged 300-400 feet/day, and that of the Willis Formation averaged 10-50 feet/day. During calibration, PEST suggested that even higher values be used. The values were generally constrained however, to ranges that were evaluated in the conceptual model report (Figure 4.5.1), and further evaluated against values in (Chowdhury and Mace, 2007). It is likely that the sand fraction distributions were not representative throughout the domain causing larger hydraulic conductivity values to the north while trying to calibrate to data in the River valley, causing differences in distributions from the discrete values of Figure 4.5.1. Also, the geometric mean may not represent the distribution of hydraulic conductivities throughout the domain. The Chicot Aquifer data was available from wells that lie mostly in the southern portions of the numerical model domain. The model provided insights into this correlation between sand fraction distributions and hydraulic conductivities and further research is needed to determine sand fraction distributions that also follow hydraulic conductivity trends. This can be done by evaluating the raw sand fraction data along with the model to determine appropriate sand fraction distributions representative of the hydraulic conductivity variations. A further analysis of the data may also reveal differences in material types along the Rio Grande from regions further north which can be used to further categorize the hydraulic conductivity correlations. This has been further discussed in the recommendations within the text.

57. *Layer Property Flow (LPF) Package: the Kx values were calculated based on sand fraction with an assumed sand hydraulic conductivity of 700 feet per day and 100 feet per day for clay as per Table 4.2.1. Please explain the reasoning to choose 100 feet per day for clay and/or if applicable edit the values or headings in the Table and the text.*

    The Beaumont, Lissie and Willis formations act as one aquifer (the Chicot Aquifer) and thus there is not much resistance to flow between them. Modeling efforts in the region also consider them to act as one aquifer unit (Chowdhury and Mace, 2007, Hutchison et al, 2011). The automatic calibration effort using PEST also suggested that a higher value be

used. Thus, providing a 100 feet per day value for the lower end of conductivity used in this aquifer (which dominates vertical conductance) is reasonable.

58. *Layer Property Flow (LPF) Package: because of the method discussed in #57 above, the numerical model appears to ignore the measured hydraulic conductivity values and the spatial trend of the measured values. Please explain how the measured hydraulic conductivity values were honored and if necessary, make appropriate edits to the numerical model and the report.*

    The numerical model does constrain the hydraulic conductivity values to the range of measured values. The sand fraction distribution used to parameterize the model may be inaccurate and may not reflect the spatial distributions of discrete measurements as noted in response to # 61 above.

59. *A storativity of 1.0E-6 and a specific yield of 1.0E-3 were used for all numerical model layers except Layer 7 (Burkeville Confining Unit) where a specific yield of 1.0E-4 was used. Please explain clearly in the report why same or similar values were used for units with significantly different hydrogeological properties.*

    The sensitivity analysis to specific yield and storativity showed that fluctuations were fairly insensitive to these parameters. Even with zero values, the results were not that much different. An additional sensitivity simulation has been conducted with a high value of the specific yield value (equal to the porosity value used in the transport simulation). The sensitivity plots now include hydrographs for this sensitivity run. It is noted that the hydrographs are similar to the modeled values for this sensitivity case. Therefore, it is not an issue whether similar values were used, or if the values were varied.

60. *For the Chicot Aquifer (Layers 1, 2, and 3 in the model), please explain the low specific yield (0.001) value for such a permeable unit and if necessary, make appropriate edits to the numerical model and the report.*

    The sensitivity analysis to specific yield and storativity showed that water levels were insensitive to these parameters. Simulated water levels showed little fluctuation considering the annual stress period time scale and therefore use of even larger values would not impact the results.

61. *Evapotranspiration (EVT) Package: please edit or explain the EVT surface along or within the Gulf that appears to contain negative values.*

    The EVT surface is set along the top of the model domain. Negative values in the Gulf (up to 0.66 feet) are not significant to the model results as EVT is zero in this location.

62. *Discretization (DISU) Package: please change the length unit from meter to feet.*

    This is done.

63. *Block-Centered Transport (BCT) Package: the effective porosity for the transport simulation followed the horizontal hydraulic conductivity distribution. However, the effective porosity values in the BCT package are very different from specific yield in the Layer Property Flow (LPF) package. Please explain why and make edits to the numerical model and report, if necessary.*

   The effective porosity was computed from the porosity values in the Vistas file and not from the specific yield. It was generated from sand fraction distributions using the equation shown in Section 6.3. That is why it is different from the porosity or specific yield values in the Vistas file. A sentence has been added in Section 6.3 to further clarify this. Also, the sensitivity analysis to specific yield shows that the impact of higher specific yield values to flow is small.

64. *Sink with Return Flow Boundary (QRT) Package: please explain if the return flow taken from the Rio Grande River was accounted for in water balance calculation of the river.*

   The flow extracted from the Rio Grande is accounted for in the water balance calculation of the river.

General Suggestions for Draft Geodatabase

65. *Please include all data sets used in the development of the conceptual model including changes or updates to the conceptual model during the numerical model development.*

   This is done.

66. *Please include metadata for each feature class and/or raster dataset noted in the Comments to be Addressed section below.*

   This is done.

67. *Please note units of measured values within the metadata descriptions for all applicable fields within each spatial data set (feature classes and raster datasets).*

   This is done.

68. *Please include pumpage values used in the numerical model in the geodatabase.*

   This is done.

Draft Geodatabase Comments to be Addressed

69. *Please include brief metadata descriptive information for Gulf Coast Aquifer_extent polygon feature class within the Boundary feature dataset.*

   Text added.

70. *Please include brief metadata descriptive information for uscb10_blkgrp_lrgv polygon feature class within the Boundary feature dataset and note any applicable units of measured values.*

    Text added.

71. *Please include brief metadata descriptive information for YeguaJackson_extent polygon feature class within the Boundary feature dataset.*

    Text added.

72. *Please note units for measured values within metadata descriptive information of applicable table fields in PrecipGages point feature class within the Climate feature dataset.*

    Text added.

73. *Please note units for measured values within metadata descriptive information of applicable table fields in all BaseElevation_Contours_* line feature classes within the Geology feature dataset.*

    Text added.

74. *Please note units for measured values within metadata descriptive information of applicable table fields in all LeapfrogEast_BaseStructure_* point feature classes within the Geology feature dataset.*

    Text added.

75. *Please note units for measured values within metadata descriptive information of applicable table fields in all Thick_*_contours line feature classes within the Geology feature dataset.*

    Text added.

76. *Please note units for measured values within metadata descriptive information of applicable table fields in T_K_wells point feature class within the SubsurfaceHydro feature dataset.*

    Text added.

77. *Please note units for measured values within metadata descriptive information of applicable table fields in Wells_WLs_lrgv point feature class within the SubsurfaceHydro feature dataset.*

    Text added.

78. *Please note units for measured values within metadata descriptive information of applicable table fields in all WL_*_* line feature classes within the SubsurfaceHydro feature dataset.*

    Text added.

79. *Please note units for measured values within metadata descriptive information of applicable table fields in all WL_CP_*_* point feature classes within the SubsurfaceHydro feature dataset.*

    Text added.

80. *Please substitute the metadata for the SurfaceHydro polygon feature dataset into the Hydro_Soil_Groups feature class within the SurfaceHydro feature dataset.*

    Text relocated.

81. *Please consider renaming the Topology feature dataset to "Topography" or "Surface Elevation" or preferably "Geomorphology" since the term topology is more often used to describe properties of spatial relationships. GAM geodatabases usually use a Geomorphology feature dataset to store topography/surface elevations and physiography feature class themes.*

    Text renamed to topography.

82. *Please note units for measured values within metadata descriptive information of applicable table fields in all TDS_* point feature classes within the WaterQuality feature dataset or provide web link to BRACS Database data dictionary.*

    Text added.

83. *Please note units for measured values within metadata descriptive information of applicable table fields in desal_plants_lrgv_recomended2016 point feature classes within the Wells feature dataset.*

    Text added.

84. *Please note units for measured values within metadata descriptive information of applicable table fields in GWDB_Wells point feature classes within the Wells feature dataset or provide web link to TWDB Groundwater Database data dictionary.*

    Text added.

85. *Please note units for measured values within metadata descriptive information of applicable table fields in PumpWells_lrgv_studyarea point feature classes within the Wells feature dataset or provide web link to TWDB Groundwater Database data dictionary.*

    Text added.

86. *Please consider moving all feature classes within the Wells feature dataset to the SurfaceHydro feature dataset and remove the Wells feature dataset.*

    Features classes moved to the SubsurfaceHydro feature dataset.

87. *Please note units for measured values within metadata descriptive information for all BaseElevation_* raster datasets within the geodatabase.*

Text added.

88. *Please include brief metadata descriptive information and note units of measured values for LandSurface raster dataset.*

Text added.

89. *Please include the point feature class spatial and attribute data for the salt diapirs used for Figure 2.3.1 of the conceptual model report into the Geology feature dataset within the conceptual model geodatabase, including appropriate metatdata.*

Feature class and associated metadata added to geodatabase.

90. *Please include the shape files TPWD_Veg_ET, STR_input, Recharge_node_grid, and PumpWells_lrgv_sa_input_18aug2016 into the appropriate feature datasets within the conceptual model geodatabase, including appropriate metadata. These datasets are considered changes or updates to the conceptual model.*

TPWD_Veg_ET feature class is already in the CM geodatabase delivered in January.

91. *Please include the sand fraction distribution raster datasets depicted in Figures 5.2.1 through 5.2.10 of the numerical model report into the appropriate feature datasets within the conceptual model geodatabase, including appropriate metadata. These datasets are considered changes or updates to the conceptual model.*

Net sand feature class is already in the CM geodatabase delivered in January. We did not create any rasters for net sands

92. *Please include the recharge, hydraulic conductivity, porosity, and TDS distribution raster datasets depicted in the numerical model report into the appropriate feature datasets within the conceptual model geodatabase, including appropriate metadata. These datasets are considered changes or updates to the conceptual model.*

All shapefiles are in the geodatabase LRGV_4276.gdb. A list of shapefiles and their description can be found in Geodatabase tab of the GSI_File_List.xlsx.

Public Comments:

Note: the public comment period ended on May 1, 2017.

93. *Please explain the treatment of subsidence in project area within the numerical model. Please clarify if the project team plans on delivering a tool to estimate subsidence resulting from groundwater pumping in the model area.*

The issue of subsidence is discussed in detail in the predictive simulations report. In summary, the potential for subsidence in the area is high given the geologic setting and the issues in other parts of the Gulf Coast Aquifer where pumping has been high (Houston area). However, pumping in the LRGV is low, and there is no data to calibrate any

predictions of subsidence. Thus, to include a full treatment of subsidence in the calibrated groundwater model would have been speculative since there was no ability to calibrate the estimated parameters needed to simulate subsidence. There is a general correlation with drawdown and subsidence, so data from the Houston area was used to estimate a potential range of subsidence as a result of increased pumping.

94. *The hydrostratigraphic units/model layers to which particular wells, water levels, pumping, and hydraulic testing are assigned are not identified in the Reports. Instead, aquifer and well information is discussed only at the hydrogeologic unit scale shown in Figure 2.4.2 of the Draft Numerical Report. The result is that a reader cannot discern from the Reports how pumping was assigned to a particular hydrostratigraphic unit—such as the Upper Goliad, for example—and how that pumping changes over time. Please make appropriate edits to the report and the numerical model.*

Pumping is assigned to a well in the model. The well may extract water from multiple layers and the pumping was not assigned to any particular hydrostratigraphic unit; rather, pumping was assigned to the well and the amount that was extracted from each hydrostratigraphic unit is solved by the model at each time-step and each stress period.

95. *As part of the contract, the contractor was supposed to include at least four water quality maps for each of the hydrostratigraphic units included in the model:*

- Pre-desalination conditions
- For the beginning of the transient calibration period
- During the transient calibration period (at a time-period chosen in cooperation with the TWDB)
- For the end of the transient calibration period (information on the transient calibration period is included in Section 3.3)

The response to one of the previous related comments—which appears as Item No. 42 in the Response to Comments—was in part that "[a]vailable well data for water levels, hydraulic properties, and TDS are too limited for characterizing each formation comprising the major aquifers." Does this response mean that particular wells and associated data were not assigned to hydrostratigraphic units? Please clarify regarding whether well depth or well screen information was used to associate measurements at well locations with hydrostratigraphic units.

This comment is confusing since it is unclear whether it is a conceptual model issue (data) or a model output issue. Well depths and screen information were indeed used for assigning data to the model layers. Response to Comment 42 of the Conceptual Model report explains that most wells in the valley are constructed with large screened intervals that intersect multiple hydrostratigraphic units. Measurements from these wells represent average values of all intersected units. Depth specific data were not available for individual hydrostratigraphic units. The measured value was assigned to every hydrostratigraphic unit intersected by the well.

96. *Regarding hydraulic conductivity: In the upper two formations in the Chicot aquifer, there are sizeable areas where the Draft Numerical Report shows horizontal hydraulic conductivity values as being between 400 to 700 feet per day; for vertical hydraulic conductivity, the values vary from 100 feet per day to over 400 feet per day for large regions of the Beaumont and Lissie formations. These values appear to be too high and may be rooted in the interpretation of information from wells screened across high permeability alluvial deposits associated with the Rio Grande in parts of Hidalgo, Cameron, and Willacy counties. The majority of the hydraulic tests that indicate hydraulic conductivity values above 100 feet per day are from screens that are less than 50-feet long. These screens have targeted relatively thin, coarse-grained deposits that generally occur above a depth of 260 feet and do not extend into the Kenedy County District and Brush Country District. Our concern with the current model is illustrated by the hydraulic properties used to characterize Kenedy County. In the model, across most of Kenedy County, the Beamount and Lissie formations have vertical hydraulic conductivity values greater than 100 feet per day, which is more than a 1000 times greater than the vertical hydraulic conductivity values used by the GMA 16 Alternative Model in Kenedy County. Based on a review of available pumping tests data, well yields reports to the Districts, and the hydraulic properties in the GMA 16 Alternative Model, it appears the LRGV model may contain unrealistically high values for hydraulic conductivity in the Beaumont and Lissie formations for several counties. Please clarify the high value for hydraulic conductivity used in the conceptual and numerical model.*

The hydraulic conductivity distribution was determined from sand fractions for each of the geological units. Thus, if sand fractions were similar in portions of Kenedy County and Hidalgo County, they would have similar hydraulic conductivity values. Hydraulic conductivity values for each layer were then calibrated using manual calibration assisted by automatic calibration using PEST.

97. *Available data regarding hydraulic properties include the aquifer tests and reports referred to in one of the previous comments, a response to which appears as Item No. 45 in the Response to Comments. It is not entirely clear from the response or the relevant Conceptual Report text whether the public water well tests referenced in the Districts' Conceptual Report Comments were reviewed and utilized (although the reference to TCEQ data in the text implies it). It is also not clear whether the drillers reports referenced in the Districts' Conceptual Report Comments are part of the "new data obtained from the TWDB databases." Please clarify if the existing data was considered and/or utilized and if not, please explain the rationale for omitting it. If the existing data was in fact utilized, please specify whether this data supports or differs from the hydraulic properties currently included in the model.*

Comment 45 of the Conceptual Model report included a summary table for the number of wells with data. It is unknown whether every well included in the summary table was included in the dataset prepared by Chowdhury and Mace (2007) for the existing GAM. Additional specific capacity data were obtained from the TWDB Groundwater database. Individual drillers logs were not reviewed for this study due to time constraints on the project and because the data coverage from other sources was sufficient to guide numerical

model calibration. Simulated aquifer hydraulic properties are within the range of values determined for each aquifer unit and reported in the Conceptual Model report.

98. *Regarding simulation of total dissolved solid concentrations: There appear to be no comparisons of measured and simulated concentration values at groundwater wells. This lack of comparisons or perhaps the lack of documentation makes it difficult to evaluate the model's usefulness in predicting changes in water quality caused by pumping. In order to assist the Districts and other stakeholders in understanding the ability of the LGRV model to accurately predict changes in TDS concentrations, it would be helpful if the Numerical Report contained a comparison (plots) of measured and modeled TDS concentrations (a) at groundwater wells that have at least four measured values of TDS concentrations and (b) at groundwater wells with TDS concentrations near existing and proposed facilities. Please include such an analysis in the numerical model report or clarify why such an analysis cannot be conducted.*

    The suggested analysis could not be conducted because of a lack of data to calibrate the model. Therefore, the transport model simulations were conducted for historical flow conditions but used the current BRACS database for TDS initial conditions. The intent of these simulations was to evaluate the impact and note the behavior of solute movement rather than match historical conditions.

99. *The Draft Numerical Report does not appear to include a reference to the report that documents the development of the groundwater transport code and the algorithms the code uses to simulate transport. The latter report is required in order to demonstrate that the code is working properly by validating it against results from other codes or known solutions. Please include an explanation in the numerical report regarding review and testing of the groundwater transport code and providing reference to or inclusion of the documentation (report) for the transport code.*

    The groundwater transport code documentation will be provided with the final deliverable.

100. *Simulations with and without pumping seem to indicate that initial and boundary concentrations play a larger role than pumping does in the simulated results. This result raises questions regarding the ability of the model to be used as a predictive tool for various pumping scenarios. Moreover, the draft numerical report does not include calibration with respect to transport—in other words, there does not appear to have been any matching of observed salinity concentrations based on steady-state, pre-development conditions. The plots described above in comment #99 could be used to help assess the model's relative usefulness in evaluating changes in water quality due to long-term withdrawal of groundwater (including possible impacts of probable seawater intrusion).*

    TDS concentrations from the BRACS database are the best information available on distribution of chlorides and the model uses this to evaluate transport behavior. The model therefore predicts the response of pumping into the future from this current condition. Improved estimates of current TDS distributions will improve on the model predictions.